

Copyright
by
Brad David Wolaver
2008

**The Dissertation Committee for Brad David Wolaver Certifies that this is the
approved version of the following dissertation:**

Hydrogeology of the Cuatrocienegas Basin, Coahuila, Mexico:

An Integrative Approach to Arid Karst Aquifer Delineation

Committee:

John M. Sharp, Jr., Supervisor

William H. Asquith

Jay L. Banner

Dean A. Hendrickson

Vincent C. Tidwell

Zong-Liang Yang

**Hydrogeology of the Cuatrocienegas Basin, Coahuila, Mexico:
An Integrative Approach to Arid Karst Aquifer Delineation**

by

Brad David Wolaver, B.S.; M.S.

Dissertation

Presented to the Faculty of the Graduate School of
The University of Texas at Austin
in Partial Fulfillment
of the Requirements
for the Degree of

Doctor of Philosophy

**The University of Texas at Austin
August 2008**

Dedication

I dedicate this dissertation to my family: my mother, Peggy S. Wolaver, my father, John A. Wolaver, and my sister, Joanna L. Wolaver. My uncle, Dr. Thomas G. Wolaver, was an early scientific inspiration in my life. My paternal grandparents retired to Scottsdale, Arizona. We would take road trips from Boston through the Southwest U.S. to visit them. On the way, we often visited national parks and outstanding scenery. These early trips were instrumental in developing my appreciation for nature that led me to study geology. Spending vacations at my maternal grandparents' house in Maine also fed my scientific curiosity at an early age and started me down this path. My brother-in-law, Joseph P. Younger, took me out to the mountains more than once when I needed it —on to the next high point! Sally L. Holl has brightened the last year of this doctorate. Thank you to you all for the support and guidance—this dissertation is dedicated to you!

Acknowledgements

First, I want to acknowledge the support the Jackson School of Geosciences has provided me to make this dissertation a reality. In addition, I received gracious support in the form of grants or scholarships from: BHP Billiton, the Geological Society of America, the Gulf Coast Association of Geological Sciences, the Houston Geological Society, the San Antonio Area Foundation, and the Tinker Foundation. The Environmental Science Institute at the Jackson School of Geosciences provided the invaluable support of three of the ESI's summer NSF REU program students (Megan Andring, Laura Merner, and Dawn Saepia).

My committee has provided sound scientific guidance and helped me navigate my way through my doctoral career. The committee includes: Dr. John M. Sharp, Jr. (my primary advisor), Dr. William H. Asquith (U.S. Geological Survey), Dr. Jay L. Banner, Dr. Dean A. Hendrickson (The Section of Integrative Biology at The University of Texas at Austin), Dr. Vincent C. Tidwell (Sandia National Laboratories), and Dr. Zong-Liang Yang.

Many other people have assisted with this research. At The University of Texas at Austin, Dr. Bayani Cardenas has provided guidance on research direction and helped with field work in August 2007. Dr. Phil Bennett assisted with interpretation of geochemistry data. Dr. Stephen Grand served on my examining committee and provided guidance, along with Dr. Clark Wilson on gravity survey methods. Dr. Mark Helper assisted with differential GPS survey procedures and lent me equipment. Dr. Jack Holt participated in a January 2006 geophysics field trip and experimented with using ground penetrating radar to image the subsurface. Dr. Randall Marrett organized and led a field

trip to the Monterrey Salient in March 2007 that clarified northeast Mexico structure and stratigraphy. Dr. Larry Mack assisted with strontium analyses of travertine and water. Roger Gary helped me weld devices to install temperature loggers in several springs.

Dr. Neil Hurley, formerly with the Colorado School of Mines, and now with Schlumberger, provided guidance on structural models used in this research. Dr. Karen Johannesson, formerly of The University of Texas, Arlington, and now with Tulane University, attended an early field trip and has provided guidance. Dr. Thomas Lowry of Sandia National Laboratories provided help during my summer 2005 internship at Sandia.

In Mexico Juan Carlos Ibarra Flores has been an invaluable link with the Cuatrocienegas Reserve. Cristina Vélez is a Peace Corps Volunteer who managed the Cuatrocienegas research station and helped interface with locals. Chris Bradewie, a Peace Corps volunteer formerly in Cuatrocienegas, also assisted with this research project. Dr. Juan Manuel Rodríguez of the Universidad Autónoma de Nuevo León in Monterrey, Mexico has participated in numerous field trips. Dr. Vsevolod Yutsis of the Universidad Autónoma de Nuevo León in Linares, Mexico also has participated in several field trips. I enjoyed our conversations at the old field house. Alma Zertuche, who manages the local nonprofit, Desuvalle, was a great point of contact in the valley and helped with reservations at the old field house and with gaining access locally. Francisco González Felán has granted access to Poza Escobedo on numerous occasions. Arturo Lerma of Pronatura Noreste provided access to the Reserva Privada Pozas Azules for our gravity survey there.

I appreciate all the help I received from fellow graduate and undergraduate students, many of whom visited Cuatrocienegas with me. They include: Ben Andrews, Megan Andring, Jennifer Aschoff, and Sasha Carter. Trevor Budge provided extensive

consultation on geographic information systems analysis. Gareth “Crossy” Cross helped on a February 2008 field trip to Cuatrocienegas that combined structural geology and hydrogeology. Liza Colucci, Laura DeMott, Shanna Evans, Beatrice Garcia-Fresca, Terence Garner, Laura Merner, Kim Nguyen, Philip Reikenberg, Dawn Saepia, Don Slottke, Thomas Wiles, and Corinne Wong have all participated on field trips to Mexico or provided insightful discussions. Marcus Gary graciously loaned me equipment to install pressure transducers in canals. Theresa Diehl of The University of Texas at Austin Institute for Geophysics provided critical and sustained guidance with the gravity geophysics processing.

Dr. Lawrence Lawver of The University of Texas at Austin Institute for Geophysics has provided informal guidance over the years in all things geological. I thank him for his continued efforts and advice that have been invaluable as I have shaped my career.

Abstract

Hydrogeology of the Cuatrocienegas Basin, Coahuila, Mexico:
An Integrative Approach to Arid Karst Aquifer Delineation

Publication No. _____

Brad David Wolaver, Ph.D.
The University of Texas at Austin 2008

Supervisor: John M. Sharp, Jr.

The Cuatrocienegas Basin is located in the Chihuahuan Desert, Coahuila, Mexico. Over 500 springs and groundwater-dependent ecosystems with >70 endemic species flank the 2,600-meter Sierra San Marcos that bisects the 1,200 square kilometer valley. The west sub-basin contains fracture-controlled springs with elevated relative discharge (~85 percent of total), temperature (~31.0°–34.0°C), and total dissolved solids (~90 milligrams/liter chloride) compared to the east sub-basin, that has stratigraphically-controlled springs with lower relative discharge (~15 percent), temperature (~28.0°–30.0°C), and total dissolved solids (~30 milligrams/liter chloride). Canals convey spring discharge out of the formerly closed valley. Groundwater development since the 1980s lowered groundwater levels >10 meters in adjacent basins and caused some springs to cease flowing.

The author hypothesizes that (1) both local and regional recharge are significant, (2) an integrative data approach can delineate recharge zones, and (3) the low-elevation of the Cuatrocienegas Basin, fault-associated secondary carbonate aquifer permeability,

and stratigraphic influences on permeability control spring locations. To test these hypotheses, the research (1) develops hydrogeologic conceptual models of recharge areas using remotely-sensed topography, hydrogeologic data (e.g., spring geochemistry, temperature, and discharge), and geologic mapping; (2) delineates recharge areas by sequentially including upgradient catchments to match observed spring discharge using geographic information system catchment delineation, chloride-balance recharge estimation, and analytical model interbasin flow evaluation; (3) explains spatial variations in spring chloride, discharge, and temperature using environmental tracers (e.g., $\delta^{18}\text{O}$, noble gases, ${}^3\text{H}$) and an elevation-dependent recharge rate; and (4) uses land gravimetry surveys to generate best-fit hydrogeologic cross sections in areas of high spring density.

The author concludes that local precipitation is insufficient to generate observed spring discharge. Waters with <0.1 tritium units indicate regional flow and aquifer residence times of >50 years. Water-budget based catchment delineation suggests west basin fractures tap a (>10,000-square kilometer) regional carbonate aquifer. Thus, groundwater management should be extended outside the Cuatrociénegas Basin. East basin canyons intersect the potentiometric surface of a stratigraphically controlled (local/regional) aquifer recharged in the 500-square kilometer Sierra San Marcos. Sierra La Madera recharge explains Ocampo Valley predevelopment flow and chloride concentration. This approach can be applied to delineate similar developing arid aquifers.

Table of Contents

Dedication.....	iv
Acknowledgements	v
Abstract.....	viii
Table of Contents.....	x
List of Tables.....	xiv
List of Figures	xvi
Chapter 1: Introduction.....	1
Purpose	1
Science Questions.....	2
Hypotheses.....	3
Significance of the Study.....	4
Dissertation Outline	5
Chapter 2: Delineation of Regional Arid Karst Aquifers: An Integrative Data Approach	10
Abstract.....	10
Introduction	11
Background.....	13
Structure and Tectonics.....	15
Topography	15
Hydrostratigraphy	16
Groundwater Resources and Hydrogeology	20
Recharge Processes in the Cuatrocienegas Basin and Analogous Regions.....	21
Recharge in Other Semi-Arid Areas	23
Recharge in the Cuatrocienegas Basin.....	27
Springs: Cuatrocienegas Basin.....	31
Methods	31
A Note on the Organization of this Chapter.....	31
Groundwater Catchment Delineation.....	32
Precipitation Estimation.....	33
Chloride-Balance Approach to Recharge Estimation	40
Spring Discharge Measurement	54
Evaluation of Interbasin Groundwater Flow Using an Analytical Model.....	54
Results	58
Groundwater Catchment Delineation.....	58
Precipitation Estimation.....	59
Recharge Estimation with Chloride-Balance Approach	62
Spring Discharge Measurement	67
Evaluation of Interbasin Groundwater Flow Using an Analytical Model.....	72
Discussion.....	73
Groundwater Catchment Delineation.....	73
Precipitation: PERSIANN Satellite Precipitation Estimates Compared with Gage Rainfall and Mountain Precipitation Extrapolation	77
Recharge Estimation	79

Spring Discharge Measurement	81
Analytical Interbasin Flow Model Evaluation	81
Conclusions	82
Chapter 3: Using Tritium, Oxygen Isotopes, Noble Gases, and Strontium Isotopes to Evaluate Residence Time and Recharge Processes in an Arid Karst Aquifer	85
Abstract.....	85
Introduction	86
Background.....	89
Structure and Tectonics.....	89
Topography.....	90
Hydrostratigraphy	90
Methods	95
Tritium as an Indicator of Aquifer Residence Time.....	95
Oxygen Isotopes to Estimate Precipitation Elevation	96
Noble Gases to Evaluate Recharge Elevation and Investigate Interbasin Flow	99
Strontium Isotopes of Water and Travertine to Identify Aquifer and Flow Paths.....	107
Results	114
Tritium	114
Oxygen Isotopes	117
Dissolved Noble Gases in Spring Water	120
Strontium Isotopes of Spring Water and Travertine	120
Discussion.....	125
Tritium	125
Oxygen Isotopes	127
Dissolved Noble Gases in Spring Water	129
Strontium Isotopes of Spring Water and Travertine	130
Conclusions	133
Chapter 4: GIS-Based Chloride-Balance Modeling to Evaluate Recharge Areas and Understand Differences in Spring Discharge, Chloride Concentration, and Temperature in an Arid Karst Aquifer.....	135
Abstract.....	135
Introduction	137
Background.....	139
Topography	139
Water Resources	142
Precipitation	147
Hydrogeologic Setting and Conceptual Model	149
Methods	153
Hydrogeologic Data	156
Catchment Delineation Approach	161
Geographic Information System Elevation Slices	161
Recharge Using Maxey and Eakin and Chloride Balance Approaches	163
Temperature Model.....	169
Results	170
Hydrogeologic Data	170
Catchment Delineation Approach	174
Geographic Information System Elevation Slices	174
Recharge Using Maxey and Eakin and Chloride Balance Approaches	176
Temperature Model.....	178
Discussion.....	179
Hydrogeologic Data	179

Recharge Using Maxey and Eakin and Chloride Balance Approaches	182
Temperature Model.....	198
Limitations of Analysis.....	199
Summary.....	199
Conclusions	200
Chapter 5: Using Gravity Geophysics to Characterize Geologic Controls on Arid Karst Aquifer Spring Locations.....	203
Abstract.....	203
Introduction	204
Hypotheses, Objectives, and Importance	204
Motivation for Gravity Surveys	208
Background: Survey Area Setting	209
Northeast Mexico Stratigraphy and Tectonics.....	210
Hydrostratigraphy	213
Structure of the Cuatrocienegas Basin	214
Structural and Fracture Models.....	221
Methods	223
Data Collection	223
Data Reduction	229
Free Air Anomaly	234
Digital Elevation Model.....	234
Bouguer Anomaly	235
Complete Bouguer Anomaly	236
Data Modeling	236
Results	237
Raw and Processed Gravity Data.....	237
Best Fit Geological Models.....	237
Discussion.....	253
Conclusions	257
Chapter 6: A Systematic Approach for Characterization of Arid Aquifer Systems	259
Abstract.....	259
Introduction	260
Motivation for Research	260
Cuatrocienegas Basin: Background	261
Research Questions.....	263
Objectives	264
Hypothesis	264
Importance of Study.....	264
An Application of the Approach in Northeast Mexico	265
Human Narratives	265
Remote Sensing	269
Physical Observations.....	272
Geochemistry and Isotopes	276
Conclusions	280
Chapter 7: Conclusions.....	284
Science Questions.....	284
Hypotheses.....	284
Key Findings.....	285
Groundwater Catchment Delineation	286
Water Budget Estimation.....	288

Surface Geophysics Evaluation	289
Conclusions	289
Recommendations for Future Work.....	290
Significance of Study and Applicability to Other Areas Globally.....	293
Un Punto de Partido (A Point of Departure).....	293
Appendix A Thermochron iButton: Limitation of this inexpensive and small-diameter temperature-logger	294
References	298
Vita.....	314

List of Tables

Table 1. GENERALIZED HYDROSTRATIGRAPHIC COLUMN	20
Table 2. PERMEABILITY FOR CARBONATE TERRAINS IN TEXAS, NEVADA, AND MEXICO ...	22
Table 3. RECHARGE AS A PERCENTAGE OF PRECIPITATION IN WEST TEXAS	26
Table 4. RECHARGE AS A PERCENTAGE OF PRECIPITATION IN NEVADA	26
Table 5. PRECIPITATION ESTIMATES FOR THE CUATROCIÉNEGAS BASIN	38
Table 6. CHLORIDE CONCENTRATION OF SPRINGS FEEDING SANTA TECLA CANAL.....	47
Table 7. CHLORIDE CONCENTRATION OF SPRINGS FEEDING SACA SALADA CANAL	48
Table 8. ANALYTICAL MODEL INPUT PARAMETERS.....	58
Table 9. PERSIANN SATELLITE PRECIPITATION ESTIMATES COMPARED WITH GAGE RAINFALL AND MOUNTAIN PRECIPITATION ESTIMATE	61
Table 10. RANGE OF VALUES FOR PERCENT OF PRECIPITATION RESULTING IN RECHARGE	63
Table 11. SACA SALADA AND SANTA TECLA CANAL INSTANTANEOUS DISCHARGE	68
Table 12. POZA LA BECERRA INSTANTANEOUS DISCHARGE	70
Table 13. CUATROCIÉNEGAS BASIN ANNUAL CANAL DISCHARGE.....	72
Table 14. CUATROCIÉNEGAS BASIN FLOW SUMMARY	72
Table 15. GENERALIZED HYDROSTRATIGRAPHIC COLUMN	94
Table 16. HELIUM ISOTOPIC RATIOS FOR THREE EARTH RESERVOIRS	107
Table 17. HYDROGEOLOGIC DATA.....	115
Table 18. RESULTS OF NOBLE GAS ANALYSES FOR WATER	121
Table 19. RESULTS OF STRONTIUM ISOTOPIC ANALYSES FOR WATER AND TRAVERTINE ..	123
Table 20. PERMEABILITY FOR CARBONATE TERRAINS IN TEXAS, NEVADA, AND MEXICO	154
Table 21. GENERALIZED HYDROSTRATIGRAPHIC COLUMN.....	155
Table 22. GROUNDWATER CATCHMENT AREAS	163
Table 23. MAXEY AND EAKIN (1949) PRECIPITATION DEPTH AND RECHARGE RATE RELATIONSHIP FOR THE GREAT BASIN, NEVADA	167
Table 24. SPRING DISCHARGE, CHLORIDE CONCENTRATION, AND TEMPERATURE.....	170
Table 25. ANNUAL RECHARGE ANALYSIS FOR SOUTHEAST FLANK SIERRA SAN MARCOS SPRINGS	183
Table 26. ANNUAL RECHARGE ANALYSIS FOR HISTORIC OCAMPO VALLEY SPRING (RÍO CAÑON)	184
Table 27. ANNUAL RECHARGE ANALYSIS FOR WESTERN AND NORTHERN FLANK SIERRA SAN MARCOS SPRINGS	185
Table 28. RESULTS OF SPATIALLY-DISTRIBUTED RECHARGE ANALYSIS	191
Table 29. MIXING MODEL INPUTS AND RESULTS: LOCAL VERSUS REGIONAL FLOW.....	195
Table 30. SUMMARY HYDROGEOLOGIC DATA FOR CUATROCIÉNEGAS SPRINGS	213
Table 31. GENERALIZED HYDROSTRATIGRAPHIC COLUMN	215
Table 32. GRAVITY METER CALIBRATION TO ABSOLUTE GRAVITY	238
Table 33. BASE STATION DRIFT MEASUREMENTS, JANUARY 2006 SURVEY.....	239
Table 34. BASE STATION DRIFT MEASUREMENTS, MARCH 2006 SURVEY, PART 1 OF 2	240
Table 35. BASE STATION DRIFT MEASUREMENTS, MARCH 2006 SURVEY, PART 2 OF 2	241

Table 36. RAW AND PROCESSED GRAVITY SURVEY DATA, RANCHO POZAS AZULES, JANUARY 2006.....	242
Table 37. RAW AND PROCESSED GRAVITY SURVEY DATA, SANTA TECLA, MARCH 2006	243
Table 38. RAW AND PROCESSED GRAVITY SURVEY DATA, CHURINCE, JANUARY 2006....	244
Table 39. RAW AND PROCESSED GRAVITY SURVEY DATA, CHURINCE, MARCH 2006.....	245
Table 40. A TOOLBOX FOR CHARACTERIZATION OF A DEVELOPING ARID KARST AQUIFER SYSTEM.....	266

List of Figures

Figure 1. CUATROCIÉNEGAS BASIN STUDY AREA	12
Figure 2. CUATROCIÉNEGAS BASIN GEOGRAPHIC FEATURES AND ANALYTICAL MODEL LOCATIONS.....	14
Figure 3. TOPOGRAPHY OF THE CUATROCIÉNEGAS BASIN REGION.....	17
Figure 4. GEOLOGIC CROSS SECTION FROM THE HUNDIDO VALLEY TO THE CUATROCIÉNEGAS BASIN	18
Figure 5. CALICHE LAYER IN AN ALLUVIAL FAN ON THE EAST SIDE OF THE SIERRA SAN MARCOS.....	25
Figure 6. CUATROCIÉNEGAS BASIN GROUNDWATER CATCHMENTS	36
Figure 7. PERSIANN SATELLITE PRECIPITATION ESTIMATION AREAS	41
Figure 8. LOCATION OF CUATROCIÉNEGAS BASIN SOURCE SPRINGS.....	46
Figure 9. BROMIDE VERSUS CHLORIDE OF WATER SAMPLES FROM WELLS AND SPRINGS....	64
Figure 10. RECHARGE AREA VERSUS CUATROCIÉNEGAS BASIN SPRING DISCHARGE	66
Figure 11. RESULTS OF ANALYTICAL MODEL EVALUATING INTERBASIN GROUNDWATER FLOW.....	74
Figure 12. TRAVERTINE DEPOSIT ON THE WEST FLANK OF THE SIERRA SAN MARCOS	76
Figure 13. CUATROCIÉNEGAS BASIN OUTLET CANYON SUGGESTS EROSION IN PAST WETTER CLIMATE.....	78
Figure 14. CUATROCIÉNEGAS BASIN STUDY AREA	87
Figure 15. CUATROCIÉNEGAS BASIN GEOGRAPHIC FEATURES AND ANALYTICAL MODEL LOCATIONS.....	88
Figure 16. TOPOGRAPHY OF THE CUATROCIÉNEGAS BASIN REGION	91
Figure 17. GEOLOGIC CROSS SECTION FROM THE HUNDIDO VALLEY TO THE CUATROCIÉNEGAS BASIN	92
Figure 18. WATER SAMPLE LOCATIONS FOR TRITIUM, NOBLE GAS, AND HELIUM ISOTOPIC ANALYSES	97
Figure 19. PASSIVE DIFFUSION SAMPLER FOR NOBLE GAS SAMPLE COLLECTION	103
Figure 20. PASSIVE DIFFUSION SAMPLER PINCH-OFF TOOL	104
Figure 21. WATER SAMPLE LOCATIONS FOR STRONTIUM ISOTOPIC ANALYSES	109
Figure 22. TRAVERTINE DEPOSIT ON THE WEST FLANK OF THE SIERRA SAN MARCOS	110
Figure 23. TRAVERTINE SAMPLE LOCATIONS FOR STRONTIUM ISOTOPIC ANALYSES	111
Figure 24. ANALYSIS FLOW CHART FOR STRONTIUM ISOTOPES IN WATER AND TRAVERTINE	113
Figure 25. TRITIUM VALUES FOR SPRING WATER AND PRECIPITATION	116
Figure 26. TRITIUM VERSUS CHLORIDE FOR CUATROCIÉNEGAS BASIN SPRINGS	118
Figure 27. INFERRRED PRECIPITATION ELEVATION FROM SPRING WATER STABLE ISOTOPES.....	119
Figure 28. HELIUM ISOTOPE RESULTS FOR CUATROCIÉNEGAS SPRINGS	122
Figure 29. STRONTIUM ISOTOPIC ANALYSIS RESULTS FOR WATER AND TRAVERTINE	124
Figure 30. STRONTIUM ISOTOPIC VALUES OF CUATROCIÉNEGAS BASIN WATER AND TRAVERTINE, THE CRETACEOUS SECULAR SEAWATER CURVE, AND NORTHEAST MEXICO REGIONAL LITHOLOGY.....	126

Figure 31. CUATROCIÉNEGAS BASIN STUDY AREA	140
Figure 32. TOPOGRAPHY OF THE CUATROCIÉNEGAS BASIN REGION	141
Figure 33. CUATROCIÉNEGAS BASIN FEATURES	143
Figure 34. SPRING-FED RÍO CAÑON PRIOR TO OCAMPO VALLEY GROUNDWATER DEVELOPMENT	144
Figure 35. RÍO CAÑON AFTER OCAMPO VALLEY GROUNDWATER DEVELOPMENT	146
Figure 36. ANNUAL PRECIPITATION OF CUATROCIÉNEGAS BASIN VALLEY FLOOR	148
Figure 37. AVERAGE MONTHLY PRECIPITATION OF CUATROCIÉNEGAS BASIN VALLEY FLOOR	150
Figure 38. HYDROGEOLOGIC CONCEPTUAL CROSS-SECTION A-A' THROUGH THE CUATROCIÉNEGAS BASIN	151
Figure 39. HYDROGEOLOGIC CONCEPTUAL CROSS-SECTION B-B' THROUGH THE CUATROCIÉNEGAS BASIN	152
Figure 40. LOCATION OF THE SIERRA SAN MARCOS AND MAJOR SPRINGS	158
Figure 41. CANAL AND SPRING DISCHARGE MEASUREMENT LOCATIONS	159
Figure 42. CATCHMENTS CHLORIDE BALANCE AND WATER BUDGET EVALUATION	162
Figure 43. HYDROGEOLOGIC CONCEPTUAL MODEL FOR RECHARGE AND CHLORIDE FLUX	168
Figure 44. GROUNDWATER RECHARGE AREAS	175
Figure 45. PLAYA LAKE LOCATED IN THE SOBACO VALLEY	188
Figure 46. GROUNDWATER SEEP LOCATED IN THE HUNDIDO VALLEY	189
Figure 47. LOCAL AND REGIONAL GROUNDWATER FLOW PATHS	197
Figure 48. CUATROCIÉNEGAS BASIN STUDY AREA	205
Figure 49. CUATROCIÉNEGAS BASIN	206
Figure 50. POSSIBLE CUATROCIÉNEGAS HYDROGEOLOGIC CROSS SECTIONS	207
Figure 51. SPRING ON WEST FLANK OF SIERRA SAN MARCOS	211
Figure 52. SPRING ON EAST FLANK OF SIERRA SAN MARCOS	212
Figure 53. GENERALIZED STRUCTURE OF THE CUATROCIÉNEGAS BASIN REGION	216
Figure 54. LOCAL AND REGIONAL GROUNDWATER FLOW PATHS	218
Figure 55. GENERALIZED SIERRA SAN MARCOS STRUCTURAL CROSS SECTION	220
Figure 56. FAULT-PROPAGATION FOLD EVOLUTION BY THE TRISHEAR MECHANISM	222
Figure 57. SURVEYING GRAVITY STATION LOCATIONS	224
Figure 58. GRAVITY SURVEY LOCATIONS WITH SHADED DIGITAL ELEVATION MODEL	226
Figure 59. COLLECTING GRAVITY DATA	227
Figure 60. MEASURING BASE STATION GRAVITY	228
Figure 61. BEST FIT GEOLOGIC MODEL AND JANUARY 2006 CHURINCE GRAVITY DATA	247
Figure 62. BEST FIT GEOLOGIC MODEL AND MARCH 2006 CHURINCE GRAVITY DATA	248
Figure 63. BEST FIT GEOLOGIC MODEL AND JANUARY 2006 RANCHO POZAS AZULES GRAVITY DATA	249
Figure 64. BEST FIT GEOLOGIC MODEL AND MARCH 2006 SANTA TECLA GRAVITY DATA	250
Figure 65. SUMMARY GEOLOGIC CROSS SECTION BASED ON LAND GRAVIMETRY	258
Figure 66. CUATROCIÉNEGAS BASIN STUDY AREA	262

Chapter 1: Introduction

“Water is a public resource that all governments should guarantee. We Mexicans know that access to water is a fundamental premise in the fight against poverty and integral to promoting the development of our families and nation.”

*Vicente Fox Quesada, President of Mexico,
World Water Forum, Mexico City, March 16, 2006*

PURPOSE

The purpose of this dissertation is to document the hydrogeology of the Cuatrocienegas Basin. Specifically, approaches presented here augment and expand upon previously described methods to

1. Delineate regional groundwater catchments in the arid, karst Cuatrocienegas Basin region of Coahuila, Mexico using an integrative data approach;
2. Refine delineation of recharge zones and explain spatial variations of spring discharge, chloride concentration, and temperature using elevation-dependent recharge rates and environmental tracers; and
3. Evaluate subsurface controls on spring location with gravity geophysical surveys.

A lack of long-term well data in the Cuatrocienegas Basin complicates recharge area delineation, which is the focus of this research. As population growth and economic expansion in northeast Mexico and similar arid regions globally continues, previously undeveloped aquifer systems likely will be exploited. As a result, there is a need for

techniques to evaluate and manage groundwater resources effectively despite limited hydrogeologic data.

The Comarca Lagunera is an important agricultural region located approximately 200 kilometers southwest of the Cuatrocienegas Basin, around the City of Torreón, Coahuila. Since the 1800s, overexploitation of groundwater depleted shallow aquifers and has caused water quality problems that include elevated arsenic concentration. As a result, agricultural production has declined in the Comarca Lagunera. This led to large-scale agriculture that started in the 1980s in adjacent valleys upgradient to the Cuatrocienegas Basin. This pumping threatens Cuatrocienegas Basin spring discharge that supports locally important downstream agriculture, unique desert groundwater-dependent ecosystems with a host of endemic species, and a growing ecotourism industry. Partly because agricultural development in the Cuatrocienegas Basin is relatively recent, few hydrogeologic data exist. Thus, this research develops procedures for the delineation of regional groundwater flow systems in arid karst aquifers with sparse hydrogeologic data.

SCIENCE QUESTIONS

This research evaluates three primary science questions:

1. What groundwater catchment(s) recharge rainwater and contribute to Cuatrocienegas Basin spring flow,
2. What are the components of the regional water budget, and
3. What subsurface geologic structures influence the spring locations?

HYPOTHESES

The primary science questions are evaluated by testing the following hypotheses:

1. Cuatrociénegas Basin spring outflow originates as precipitation in both local and regional groundwater catchments; thus, groundwater development in adjacent basins will affect spring discharge;
2. An integrative data approach can delineate recharge zones using remotely sensed digital elevation data, geologic information, an analytical model for interbasin flow determination, chloride-balance recharge estimation using a water budget approach, and an evaluation of environmental isotopes; and
3. Spring locations are controlled by the regional low elevation of the Cuatrociénegas Basin, fault-associated fractures causing secondary permeability in a regional carbonate aquifer system, and stratigraphy causing permeability differences.

In order to test the three hypotheses, the author conducts a hydrogeologic characterization of the Cuatrociénegas Basin and the surrounding region to

1. Delineate regional groundwater catchments in arid karst aquifers systems with sparse hydrogeologic data using geologic and remotely sensed topographic data to create maps of regional groundwater flow;
2. Estimate the regional water budget;
3. Evaluate subsurface controls on spring location with gravity geophysical surveys; and

4. Develop an integrative approach for arid, karst groundwater system characterization applicable to analogous locations globally.

Although considered in the context of outstanding research questions or informative applied hydrogeologic investigations, the scope of this research project does not include the following components that might eventually complement the hydrologic understanding of the Cuatrocienegas Basin:

1. Creation of a MODFLOW numerical groundwater model of the Cuatrocienegas Basin region because of the paucity of hydrogeologic data;
2. Execution of “what-if” scenarios using a water budget model;
3. Installation of groundwater monitoring systems because of limited research project funding, limited time, and installation of a shallow monitoring well network by the Mexican government during winter 2008; or
4. Collection of detailed surface water, groundwater, or rock samples for general mineral, physical, temperature, chemical, or isotopic analyses (instead, this dissertation focuses on using values from published literature and focused sample collection by this research project).

SIGNIFICANCE OF THE STUDY

Previous research in the Cuatrocienegas Basin focused on the characterization of biota, stromatolites, and microbiology. This research project makes a scientific contribution by conducting a thorough hydrogeologic assessment of the Cuatrocienegas Basin and surrounding basins. Previous hydrogeologic research, including that conducted by researchers at the Instituto Mexicano del Tecnología de Agua in Jiutepec, Morelos,

Mexico, hypothesized that all Cuatrocienegas Basin spring flow originates as local mountain recharge and that interbasin groundwater flow does not occur (Rodríguez et al., 2005a). The scientific contributions of this research include (1) evaluating a larger region than previous research to understand the regional groundwater flow system, (2) estimating the water budget of this regional flow system, and (3) explaining the different geologic causes of springs in the west and east sub-basins.

Furthermore, this study makes a fundamental contribution to the field of hydrogeology by developing and applying an integrative data approach for arid, karst aquifer characterization. As global population expands into undeveloped arid regions, this approach can be used to develop hydrogeologic conceptual models in support of effective groundwater management.

DISSERTATION OUTLINE

The dissertation is organized into seven Chapters and one Appendix. It is also arranged in a multi-paper format (Chapters 2, 3, 4, 5, and 6). Therefore, each of these chapters stands alone with some inevitable repetition between chapters. The seven chapters in this dissertation are

- Chapter 1 Introduction
- Chapter 2 Delineation of Regional Arid Karstic Aquifers: An Integrative Data Approach
- Chapter 3 Using Tritium, Oxygen Isotopes, Noble Gases, and Strontium Isotopes to Evaluate Residence Time and Recharge Processes in an Arid Karst Aquifer

- Chapter 4 GIS Based Chloride Balance Modeling to Evaluate Recharge Areas and Understand Differences in Spring Discharge, Chloride Concentration, and Temperature in an Arid Karst Aquifer
- Chapter 5 Using Gravity Geophysics to Characterize Geologic Controls on Arid Karst Aquifer Spring Locations
- Chapter 6 A Systematic Approach for Characterization of Developing Arid Aquifer Systems
- Chapter 7 Conclusions

Chapter 1

The **Introduction** outlines research project components and direction.

Chapter 2

Delineation of Regional Arid Karstic Aquifers: An Integrative Data Approach presents an approach for the delineation of catchments contributing to Cuatrocienegas Basin spring flow. A hydrogeologic conceptual model is developed using remotely sensed topography, hydrogeologic data (e.g., spring geochemistry, temperature, and discharge), and geologic mapping. Also presented in the chapter is a delineation of upgradient catchments with calculated recharge. The calculated recharge matches observed spring discharge using catchment delineation based on a geographic information system analysis of topographic data, chloride-balance recharge estimation, and analytical model interbasin flow evaluation.

Chapter 3

Using Tritium, Oxygen Isotopes, Noble Gases, and Strontium Isotopes to Evaluate Residence Time and Recharge Processes in an Arid Karst Aquifer uses tritium, oxygen isotopes, noble gases, and strontium isotopes to evaluate residence time, recharge processes, and spatial extent of the arid karst aquifer of the Cuatrocienegas Basin, Coahuila, Mexico. Tritium is used to determine aquifer residence time. Oxygen isotopes are used to infer precipitation elevation. Dissolved noble gases in spring water are evaluated to assess groundwater recharge elevation. Strontium isotopes in spring water and travertine are used to identify which aquifer discharges into Cuatrocienegas Basin springs. Isotopes of dissolved helium gas in spring water are used to infer the processes affecting groundwater geochemistry and provide insight into the origin of spring water.

Chapter 4

GIS Based Chloride Balance Modeling to Evaluate Recharge Areas and Understand Differences in Spring Discharge, Chloride Concentration, and Temperature in an Arid Karst Aquifer extends and refines the hydrogeologic conceptual model presented in Chapter 2. Spatial variations in hydrogeologic data (e.g., spring chloride, discharge, and temperature) are explained using a temperature model and an integrated chloride and water-balance approach. Instead of the fixed spatially-distributed recharge rate used in Chapter 2, Chapter 4 uses a recharge rate that varies with elevation to delineate Cuatrocienegas Basin recharge catchments. The variable recharge rate more accurately models recharge process in the Cuatrocienegas Basin, where most rain evaporates that falls on the valleys and most recharge occurs in the mountains.

Chapter 5

Using Gravity Geophysics to Characterize Geologic Controls on Arid Karst Aquifer

Spring Locations uses land-based gravimetry to assess subsurface geologic controls on springs in the Cuatrocienegas Basin of Coahuila, Mexico. Land-based gravimetry is used to test the hypothesis that spring locations are controlled by buried anticlines, faulting, or permeability differences.

Chapter 6

A Systematic Approach for Characterization of Developing Arid Aquifer Systems

describes a systematic approach for the characterization of developing arid karst aquifer systems where long-term well data typically used to generate hydrogeologic conceptual models are sparse or even nonexistent. The aquifer characterization approach combines human narratives that include an evaluation of anecdotal evidence gained by “talking to the locals” and groundwater-related data shared through interdisciplinary collaboration. The approach assesses data acquired through remote sensing tools, including satellite or aerial photos, the analysis of digital elevation models often generated through satellite-derived radar altimetry, and geophysical methods. The approach also integrates physical observations, including field observations, evaluation of geologic maps, measurement of groundwater head in wells and springs, and measurement of spring discharge. The interpretation of geochemistry and isotopic data, including chloride in precipitation and groundwater, dissolved noble gases, strontium isotopes, tritium, and oxygen isotopes is also included in the approach.

Chapter 7

Conclusions synthesizes the research project results, proposes future research directions, and makes recommendations for groundwater management in the Cuatrocienegas Basin region.

One **Appendix** follows that is based primarily on Wolaver and Sharp (2007). The appendix discusses an important limitation, not previously recognized, of a small-diameter temperature logger (called an iButton) recently used for hydrogeologic applications.

Chapter 2: Delineation of Regional Arid Karst Aquifers: An Integrative Data Approach

*Because this dissertation is published under a multi-paper format,
this chapter is based primarily upon Wolaver et al., 2008.*

ABSTRACT

This research integrates data analyses for the delineation of regional groundwater flow systems in arid, karst basins with sparse hydrogeologic data using surface topography, geologic mapping, permeability, chloride concentrations of groundwater and precipitation, and measured discharge data. This data analysis framework can be applied to evaluate arid karst aquifer systems globally. The accurate delineation of groundwater recharge areas in developing aquifer systems with sparse hydrogeologic data is essential for their effective long-term development and management. The use of this approach is illustrated in the Cuatrociénegas Basin of Mexico. Aquifers are characterized using geographic information systems for groundwater catchment delineation, an analytical model for interbasin flow evaluation, a chloride-balance approach for recharge estimation, and a water budget for mapping contributing catchments over a large region. The test study area focuses on the Cuatrociénegas Basin of Coahuila, Mexico, a UNESCO World Biosphere Reserve containing >500 springs that support groundwater-dependent ecosystems with >70 endemic species and irrigated agriculture. Recharge areas that contribute local and regional groundwater discharge to springs and the regional flow system are defined. Results show the regional aquifer system follows a topographic gradient that during past pluvial periods may have linked the Río Nazas and the Río Aguanaval of the Sierra Madre Occidental to the Río Grande through the Cuatrociénegas Basin and other large, presently dry, upgradient lakes.

INTRODUCTION

This research develops procedures for delineation of regional groundwater flow systems in arid karst aquifers with sparse hydrogeologic data and estimation of regional arid karst aquifer recharge based on observed spring discharge. This approach is applied to delineate regional groundwater flow systems in the Cuatrocienegas Basin region of northeast Mexico. The study region is shown on **Figure 1**. This framework for aquifer characterization in developing arid regional karst aquifers is important because resource managers must understand the spatial extent of regional groundwater flow systems to utilize these groundwater systems in an effective manner.

This aquifer evaluation approach overlaps with earlier assessment methods, such as those used to delineate regional arid karst aquifer systems in the Great Basin (Maxey and Eakin, 1949; Eakin, 1966; Maxey, 1968; Eakin et al., 1976; Winograd and Thordarson, 1975; Mifflin, 1988). New technologies presented here augment and expand upon previously described approaches. Hall et al. (2005) described the first global high resolution (3-arc second) digital elevation model. This digital elevation model was produced using elevation data from the National Aeronautics and Space Administration shuttle radar topography mission that is available for 80 percent of the surface of the Earth (60° north– 50° south). The shuttle radar topography mission data set is particularly valuable for developing regions where accurate elevation surveys may not be available for regional hydrogeologic evaluations, such as the earlier Great Basin studies.

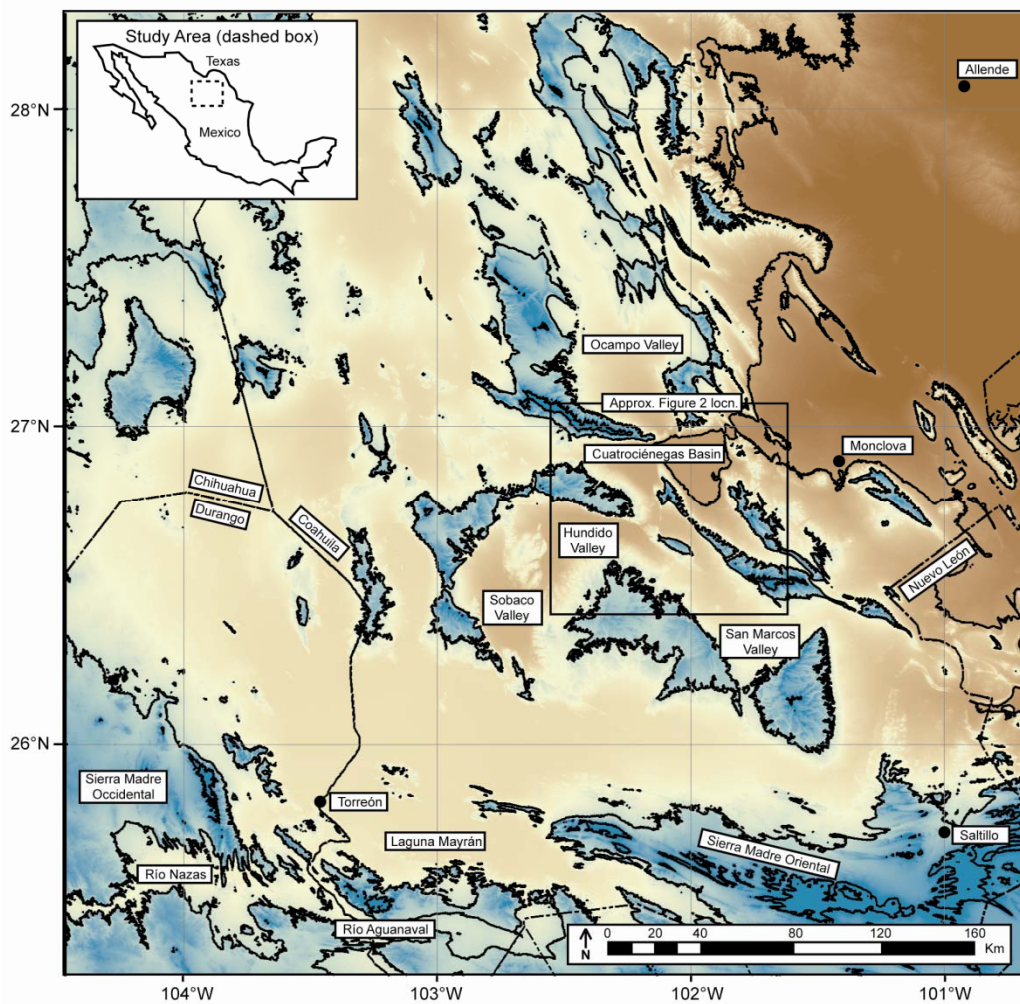


Figure 1. CUATROCIÉNEGAS BASIN STUDY AREA

Contour interval ranges from brown (750-meter) to green (1,500-meter and 2,250-meter). State boundaries (Coahuila, Chihuahua, Durango, Nuevo León) are indicated by dashed lines.

Digital elevation models facilitate the topographic basin analysis approach of Eakin (1966) to delineate groundwater catchments based on surface topography. Also, hydrogeologic parameters, such as precipitation and recharge, can be spatially distributed efficiently using geographic information systems, aiding the recharge evaluation approach of Maxey and Eakin (1949). Geographic information systems also are used to evaluate recharge using Dettinger's (1989) chloride-balance water budget approach.

Using this integrative data approach for arid aquifer characterization, the hypothesis that significant flow to Cuatrocienegas Basin springs originates from recharge from catchments external to the Cuatrocienegas Basin is evaluated. Cuatrocienegas Basin features are shown on **Figure 2**. Groundwater catchments associated with surface water catchments contributing to Cuatrocienegas Basin spring flow are delineated based on surface topography using a combination of remotely sensed digital elevation data of surface topography, geologic information, an analytical model for interbasin flow determination, chloride-balance recharge estimation using a water budget approach, and an evaluation of environmental isotopes. Up-gradient catchments are sequentially included in a regional groundwater flow system until calculated recharge equals observed spring discharge. The results of this research show that Cuatrocienegas Basin spring discharge cannot all be locally derived and a regional flow system provides significant water.

BACKGROUND

The Cuatrocienegas Basin is located in a complex geologic setting. The structural, tectonic, hydrostratigraphic, and hydrogeologic setting of the Cuatrocienegas Basin and surrounding region are discussed below. The Cuatrocienegas Basin is compared with similar regional arid, karst aquifer systems where interbasin flow occurs.

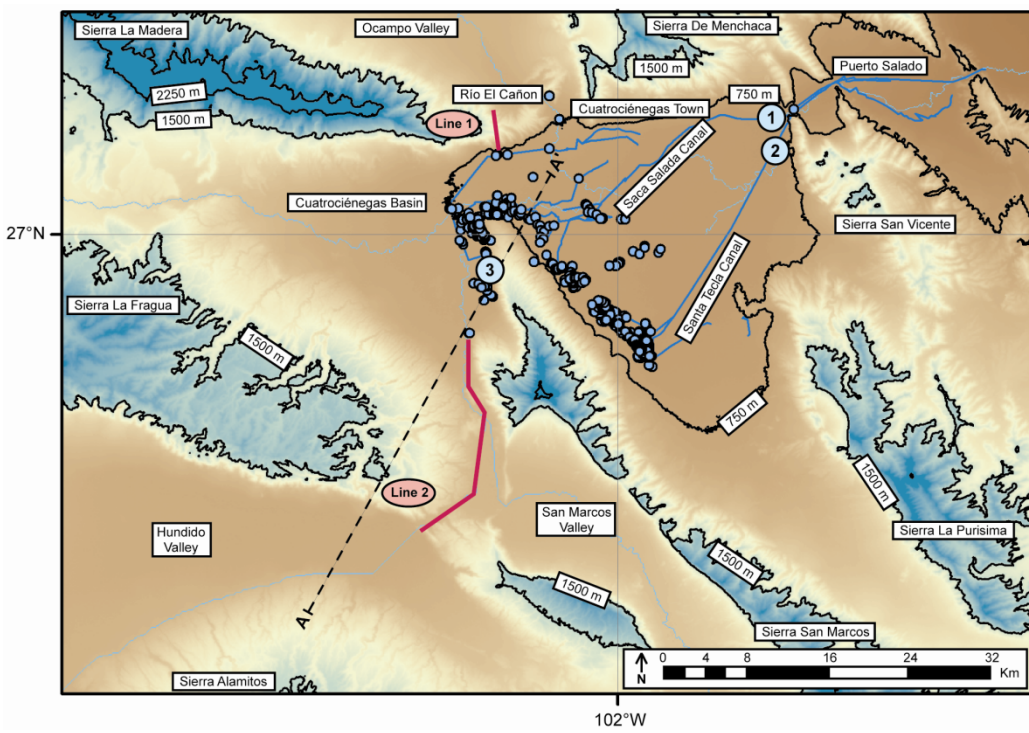


Figure 2. CUATROCIÉNEGAS BASIN GEOGRAPHIC FEATURES AND ANALYTICAL MODEL

LOCATIONS

Explanation: springs (open blue circles), analytical model locations (red lines), canals (light blue lines), discharge measurement locations (light blue numbered open circles), inferred surface drainage network (light blue dashed line), and 750-meter contour intervals (low–high elevation ranges from brown–green, respectively). The location of cross section A-A' (Figure 4) is shown as a dashed black line.

Structure and Tectonics

The Cuatrociénegas Basin is located at the northern edge of the highly folded and faulted Sierra Madre Oriental. Goldhammer (1999) described Upper Triassic–Late Middle Jurassic stratigraphy of northeastern Mexico. Lehmann et al. (1999) correlated Cretaceous carbonate mountain anticlines surrounding the Cuatrociénegas Basin with rocks in Texas. Murillo (1997) noted that the Lower Cretaceous Cupido Formation, which crops out in the Cuatrociénegas Basin, is the equivalent of the Sligo Formation of Texas.

Goldhammer (1999) described rifting in northeast Mexico associated with the opening of the Gulf of Mexico that created basement highs (e.g., Coahuila Platform). These permitted shallow water marine carbonate deposition and lows (e.g., the Sabinas Basin located approximately 125 kilometers northeast of the Cuatrociénegas Basin) that resulted from passive margin accumulation from the Upper Jurassic–the Early Upper Cretaceous.

Eguiluz de Antunano (2001) quantified Sabinas Basin regional marine sediment accumulation >5,000 meters in three supersequences: (1) synriftal sediments of primarily conglomerates and evaporates, (2) high frequency cycles of carbonates, evaporates, and coastal siliciclastics deposited on extensive platforms on a passive margin (144–96 million years ago); and (3) regressive terrigenous clastic facies deposited in a foreland setting (96–39.5 million years ago).

Topography

Elevation in the Cuatrociénegas Basin region ranges from approximately 770 meters in the valley itself to over 3,000 meters in the Sierra La Madera that bounds the Cuatrociénegas Basin to the north. Topography of the Cuatrociénegas region is shown

on **Figure 3**. Elevation increases to the north, west, and south of the Cuatrocienegas Basin, providing a topographic gradient that may also represent a gradient for groundwater flow into the Cuatrocienegas Basin, based on the regional flow principals of Hubbert (1940) and Tóth (1963). Red indicates vegetation in this LANDSAT image and includes irrigated agriculture to the east of the Cuatrocienegas Basin that relies on spring discharge and also thin mountain-top pine forests.

Hydrostratigraphy

Evans (2005) described the stratigraphy in the Cuatrocienegas Basin as primarily Jurassic and Cretaceous carbonates, evaporites, and siliciclastics overlying a basement comprised of Triassic granodiorite. Lesser y Asociados (2001) and Rodríguez et al. (2005a) presented a hydrogeologic conceptual model for the Cuatrocienegas Basin and adjacent valleys that includes parallel mountain anticlines and synclines filled with alluvium and lacustrine sediments. A geologic cross section from the Hundido Valley to the Cuatrocienegas Basin is shown on **Figure 4**.

Highlands are dominated by Cretaceous carbonates and intermontane basins are filled with alluvial fan, playa, and lacustrine sediments. Mountains surrounding the Cuatrocienegas Basin and the valley fill alluvium both display a high degree of karstification (Badino et al., 2004). Wolaver et al. (2005) calculated annual recharge on the 870-square kilometer intra-basin recharge area that both Lesser y Asociados (2001) and Rodríguez et al. (2005a) suggested produces all Cuatrocienegas Basin spring discharge. The annual recharge calculations generated only 215,000 cubic meters/year of discharge compared to an observed discharge of 35,000,000 cubic meters/year. These annual discharge values indicate interbasin groundwater flow occurs. Johannesson et al. (2004) identified high elevation recharge zones from stable isotopes, but did not identify in which catchments recharge likely occurs.

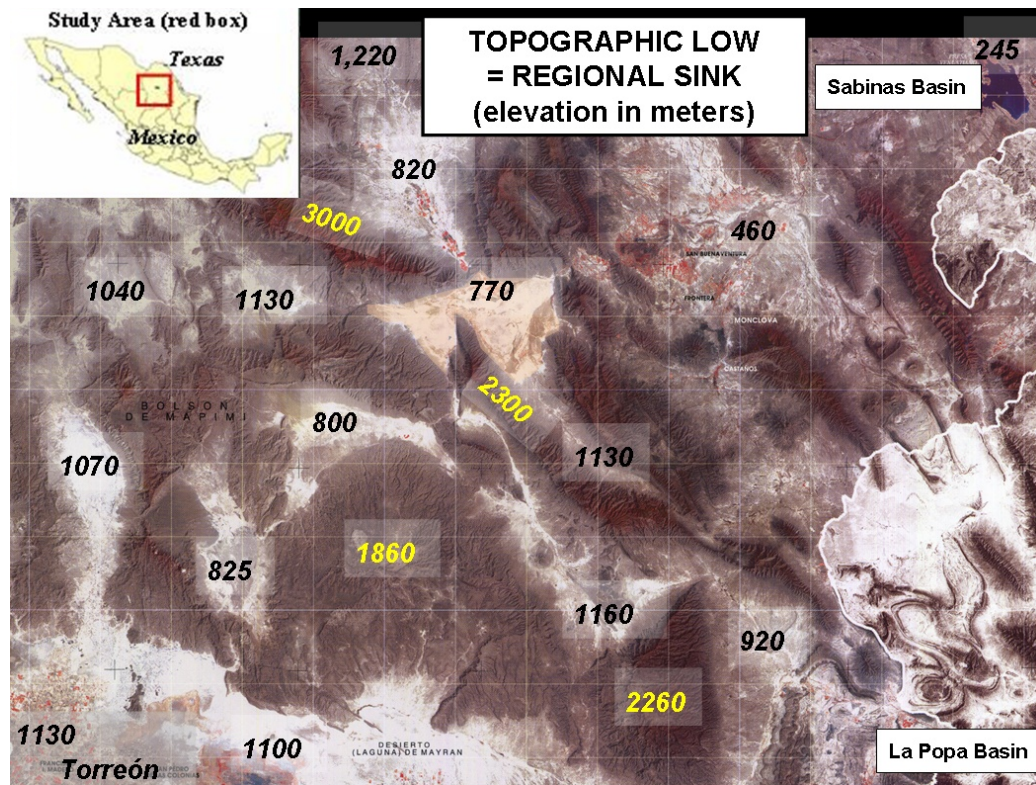


Figure 3. TOPOGRAPHY OF THE CUATROCIÉNEGAS BASIN REGION

Valley-floor elevation is shown in black. Mountain-top elevation is shown in yellow. Red indicates vegetation in this LANDSAT image with 10-kilometer grid marks. The Cuatrocienegas Basin is at a regional low elevation.

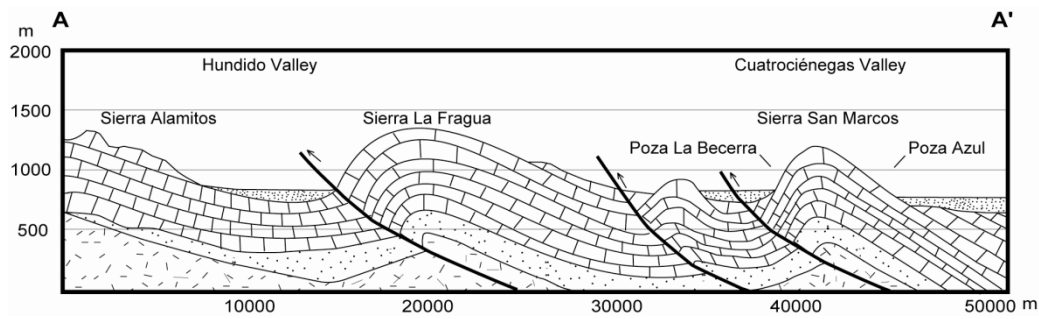


Figure 4. GEOLOGIC CROSS SECTION FROM THE HUNDIDO VALLEY TO THE CUATROCIÉNEGAS BASIN

The cross section passes through the Sierra La Fragua and Sierra San Marcos (after Rodríguez et al., 2005a). The geologic cross section orientation is from south south-west to north north-east crossing the Sierra San Marcos and associated springs. The cross section location is shown on Figure 2. Cretaceous carbonate rocks (block pattern) and Cretaceous terrigenous siliciclastics (coarse stippled pattern) underlie Quaternary valley-fill alluvium (fine stippled pattern) throughout the study region. The regional basement is comprised of Triassic granodiorite (dashed pattern). Arrows indicate the relative motion of multi-reactivated thrust faults that bound many of the anticlinal structures in the region. Geologic structure at depth is based on an extrapolation of structure at the surface.

Lehmann et al. (1999) used strontium isotopes and biostratigraphy to determine that the Cretaceous carbonate rocks that form the uplands and underlie valley-fill alluvium are predominantly late Barremian–late Albian in age (see Chapter 3). Lehmann et al. (1999) also described lime mudstones (Cupido Formation), shale and lime mudstones (La Peña Formation), lime mudstones and intercalated wackestones/packstones, dolomitized grainstones, shallow subtidal to peritidal carbonates, shales, and lime mudstones (Aurora Formation), overlain by more deep-water laminates (Cuesta del Cura Formation) in the nearby Sierra de Parras. Badino et al. (2004) described the highly karstified nature of the carbonate rocks present in the Cuatrociénegas Basin region.

Meyer (1973) collected sediment cores in the Cuatrociénegas Basin. Radiocarbon dating in the groundwater-dependent ecosystems yields dates of at least 30,000 years before present. Alluvial fans are present primarily on the eastern flank of the Sierra San Marcos. Badino et al. (2004) described lacustrine and playa lake valley-fill alluvium; they noted that evaporation of spring water from Poza El Churince precipitates gypsum and has produced the second-largest, white-sand, dune complex in North America, second only to White Sands, New Mexico. Evans (2005) and Minckley (1969) described the valley fill alluvium as highly karstified with sinkholes and re-emergent springs towards the center of the valley. Minckley and Cole (1968) noted that results of water quality analyses of water samples collected at some playa lakes approach 300,000 milligrams/liter total dissolved solids. Prior to the construction of canals which now drain the valley, the Cuatrociénegas Basin was a closed basin with large playa lakes dominating the eastern half of the valley. Miele et al. (2000) used magnetotelluric soundings to determine that mountains comprised of carbonate rocks continue in the subsurface. Rodríguez et al. (2005a) estimated an average Cuatrociénegas Basin alluvium

depth of 200 meters using time domain electromagnetics. A generalized hydrostratigraphic column of the Cuatrocienegas Basin is presented in **Table 1**.

Table 1. GENERALIZED HYDROSTRATIGRAPHIC COLUMN

Stratigraphic nomenclature is modified from McKee et al., 1990; Rodríguez and Sanchez, 2000; Lesser y Asociados, 2001; Evans, 2005.

Age	Formation	Description	Permeability
Quaternary	Alluvium	Sand, gravel, lake deposits, evaporate deposits, travertine	Variable
	Eagle Ford	Limestone, shale	Low
	Buda	Limestone, interbedded sand and gravel	Low
	Del Rio	Clay, sandy limestone	Low
	Georgetown (Cuesta del Cura)	Limestone	Moderate
	Washita Group	Limestone	Moderate
	Kiamichi	Limestone, shale	Low
	Aurora	Lime mudstones and wackestones, gypsum, dolomitized grainstones	High
	La Peña	Dark laminated shale, thin lime mudstone interbeds	Low
	Cupido	Lime mudstone	High
Cretaceous	La Virgen	Gypsum, dolomite, limestone, shale and clay	Low
	La Mula	Shale, sandstone, limestone, conglomerate	Low
	La Padilla	Massive dolomite, interbedded shale, sandstone, and evaporites	Low
	San Marcos	Sandstone, hematitic cement, interbedded conglomerate	Low–Moderate
	Basement	Granodiorite	Low

Groundwater Resources and Hydrogeology

Irrigation pumping of groundwater commenced in the mid-1980s, which caused groundwater level declines of 10s of meters in the neighboring Hundido and Ocampo Valleys (**Figure 1** and **Figure 2**). Interbasin spring-fed stream flow (historically

0.25 cubic meters/second, Minckley, 1969) from the Ocampo Valley has decreased. The Río Cañon now only intermittently flows into the Cuatrocienegas Basin, and interbasin groundwater flow also may have decreased (Hendrickson, 2005; Minckley, 1969; Rodríguez, 2005; and Rodríguez et al., 2005b). Continued regional groundwater resource development may further decrease spring discharge.

Spring discharge generally is too saline in the Cuatrocienegas Basin for potable use, and abundant spring discharge has been conveyed into canals for irrigation in lieu of groundwater production wells. As a result, transmissivity data are sparse. Comparisons of aquifers properties from analogous karst terrains in Texas and Nevada where interbasin groundwater flow is created by high transmissivity carbonate rocks similar to those of the Cuatrocienegas Basin region are shown in **Table 2**.

Recharge Processes in the Cuatrocienegas Basin and Analogous Regions

Possible recharge mechanisms in the Cuatrocienegas Basin include (1) direct recharge on fractured carbonate mountain highlands where precipitation is >400 millimeters/year at the highest elevations in the study area (>3,000 meters; González, 2006, pers. com.), (2) limited recharge of mountain front runoff on calichified alluvial fans, (3) recharge in valley floors where precipitation averages approximately 219 millimeters/year (Rodríguez et al., 2005a), and (4) interbasin flow. Recharge in semi-arid and arid regions (Dettinger, 1989) is typically calculated as

$$R = P - ET - R . \quad (1)$$

Table 2. PERMEABILITY FOR CARBONATE TERRAINS IN TEXAS, NEVADA, AND MEXICO

¹Hydraulic conductivity (meters/day) values from the literature are converted to transmissivity (shown in italics) assuming a saturated thickness of 22.5 meters, based on an average saturated thickness from analytical model inputs below. ²Belcher et al. (2002) reported hydraulic conductivity values as low as 10^{-4} meters/day for unfractured portions of the Lower Carbonate Aquifer of the Death Valley regional flow system. No data is indicated by -- .

Reference	Location & Rock Type	Hydraulic Conductivity [cm/sec]	Hydraulic Conductivity [m/sec]	Hydraulic Conductivity [m/day]	Transmissivity ¹ [m ² /day]
Nielson and Sharp (1985)	West Texas, U.S., Dell City, Bone Spring-Victorio Peak limestone	--	--	--	9×10^2 to 3×10^3
Bedinger et al. (1986)	Great Basin, Southwest U.S., Dense to mod. dense unfractured carbonate ²	6×10^{-7} to 9×10^{-4}	6×10^{-9} to 9×10^{-6}	5×10^{-4} to 8×10^{-1}	1×10^{-2} to 2×10^1
	Great Basin, Southwest U.S., Fractured, karst carbonate	1×10^{-4} to 1×10^1	1×10^{-6} to 1×10^{-1}	1×10^{-1} to 1×10^4	2×10^1 to 2×10^5
Uliana (2000)	West Texas, U.S., Apache Mts., Permian carbonate reef facies	--	--	--	2×10^2 to 2×10^3
Mace et al. (2004)	U.S. and Mexico Edwards-Trinity Aquifer	1×10^{-6} to 3×10^{-1}	1×10^{-8} to 3×10^{-3}	9×10^{-4} to 2×10^2	2×10^{-1} to 3×10^4
Rodríguez et al. (2005)	Cuatrociéneas Basin, Coahuila, México	2×10^{-2}	2×10^{-4}	2×10^1	4×10^2

Where

R = recharge,

P = precipitation,

ET = evapotranspiration, and

R = runoff.

Spatially distributed evapotranspiration is extremely difficult to estimate reliably in arid karst aquifers without an array of meteorological stations. However, insights can be drawn from scientific literature on the estimation of recharge as a function of precipitation in analogous regions (i.e., West Texas and Nevada). Recharge in the Cuatrocienegas Basin region is estimated using the chloride mass balance method (Dettinger, 1989; Anderholm, 2000; Wolaver et al., 2005). The hypothesized regional groundwater catchments are considered verified when measured canal discharge equals calculated recharge.

Recharge in Other Semi-Arid Areas

In West Texas, a complexly-faulted karst aquifer is overlain by alluvium. Gates et al. (1980) estimated recharge from local precipitation ranging from a low of approximately 183 millimeters/year (at an elevation of 1,119 meters at Ysleta, Texas, near El Paso) to a high of approximately 476 millimeters/year (at an elevation of 2,000 meters at Mt. Locke in the Davis Mountains). They suggest that recharge occurs in foothills surrounding valley-fill aquifers, in plateaus where sediments are coarse-grained, and in ephemeral stream channels during high precipitation events. Gates et al. (1980) commented that regardless of the mechanism, recharge probably does not occur unless precipitation is great enough so that surface flow occurs.

Contrary to Gates et al. (1980), Hibbs and Darling (2005) found that low-permeability, late-stage calcic soils like those in alluvial fans of the Cuatrocienegas Basin limit recharge on the fans. A caliche layer in an alluvial fan on the east side of the Sierra San Marcos is shown on **Figure 5**. Based on environmental isotope data (e.g., high radioactive tritium activities from 0.5–3.0 tritium units and 40- to 50-percent modern carbon in carbon-14 in shallow upper mountain wells) originally published by Darling et al. (1994), elevated recharge rates occur on fractured rocks of mountainous areas in west Texas. Van Broekhoven (2002) found that upland fractures contribute significant recharge to valley-fill aquifers. A summary of recharge estimates as a percentage of precipitation in west Texas is shown in **Table 3**.

Maxey and Eakin (1949) and Eakin (1966) assessed recharge and groundwater flow in the White River Valley of Nevada, an aquifer system with interconnected valley-fill basins overlying Paleozoic carbonates. Eakin and Moore (1964) investigated the uniformity of discharge at Muddy River Springs at the end of the White River flow system and noted that large springs with uniform discharge (such as those in the Cuatrocienegas Basin) are indicative of regional flow systems with distant recharge areas. Tyler et al. (1996) analyzed oxygen isotopes and deuterium and soil water chloride to infer that recharge in Nevada occurs only in the mountain fronts and basin margins, not in lower elevation valley fill. Recharge as a percent of precipitation in Nevada is summarized in **Table 4**.

Considering these analogous areas, it is inferred that valley floor recharge in the Cuatrocienegas Basin may be quite low (approaching zero percent of precipitation), whereas mountain recharge potential is elevated (approximately three–seven percent), and results in an overall recharge rate well under five percent (perhaps as low as one percent) of precipitation when regional elevation is considered.

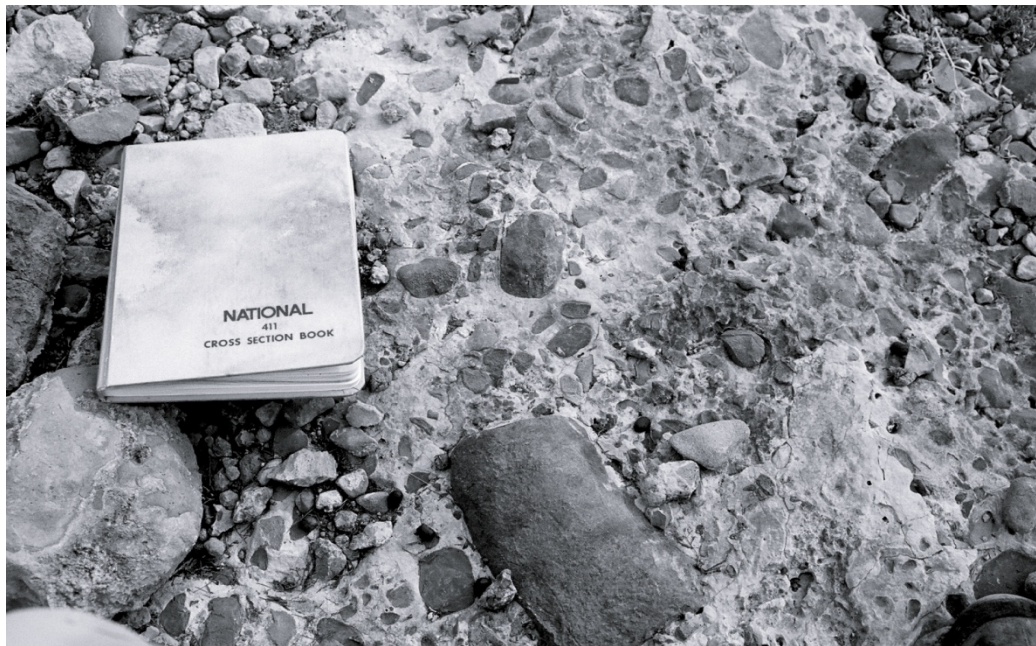


Figure 5. CALICHE LAYER IN AN ALLUVIAL FAN ON THE EAST SIDE OF THE SIERRA SAN MARCOS

Calichified alluvial fans limit groundwater recharge in stream beds draining the mountains surrounding the Cuatrocienegas Basin and other analogous arid regions such as West Texas. In the Cuatrocienegas Basin—especially the larger drainage areas on the east side of the Sierra San Marcos—mountain-front runoff after large storms is diverted to the valley floor, where it is subject to evapotranspiration.

Table 3. RECHARGE AS A PERCENTAGE OF PRECIPITATION IN WEST TEXAS

¹Based on a recharge rate of 0.18 centimeter/year and 0.6 percent of precipitation recharged, limited to a recharge area of only 20 percent of the overall landscape.

²Gates et al. (1980) and Meyer (1976) estimated recharge in West Texas at one percent of annual precipitation for all elevations.

Reference	Location	Elevation [m]	Precipitation ¹ [mm]	Recharge as Percent of Precipitation ²
Gates et al. (1980)	West of Pecos River	--	294	
	Ysleta, Texas	1,119	183	1.00
	Mount Locke, Davis Mts.	2,000	476	
	Hueco Bolson	--	254	1.00
Meyer (1976)	Hueco Bolson	--	254	0.95
Darling (1997)	Red Light Basin	--	225	0.60
Nielson and Sharp (1985)	Wildhorse Flat	--	--	1.00

Table 4. RECHARGE AS A PERCENTAGE OF PRECIPITATION IN NEVADA

¹Tyler et al. (1996) found that recharge at the Nevada Test Site does not occur at valley floor at current arid climatic conditions; it is limited to higher elevations.

Reference	Location	Elevation [m]	Precipitation ¹ [mm]	Recharge as Percent of Precipitation ²
Eakin (1966)	White River Valley	>1,800	>508	25
		<1,800	<508	~0
Eakin et al. (1976)	Great Basin	--	--	5
Tyler et al. (1996) ¹	Nevada Test Site	High	High	Yes ¹
		975	124	No Recharge
		--	>508	25
Maxey and Eakin (1949)	White River Valley	--	381–508	15
		--	305–381	7
		--	204–305	3
		--	<204	0

Recharge in the Cuatrocienegas Basin

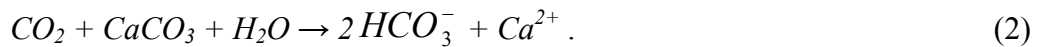
Field observations show that alluvial fans on the slopes of the Sierra San Marcos are heavily calichified. In addition, a caliche layer at a depth of approximately 0.3 meters on the west side of the Sierra San Marcos and in the floor of the unlined Saca Salada canal in the northeast corner of the basin. Canals are shown on **Figure 2**. The presence of caliche layers suggests that recharge is limited in the valley floor by a thick caliche layer similar to that reported in West Texas by Hibbs and Darling (2005).

Rodríguez et al. (2005a) presented carbon-14 relative residence times of groundwater from wells in the Hundido Valley and wells and springs in the Cuatrocienegas Basin. Carbon-14 is naturally formed in the upper atmosphere by interaction of nitrogen-14 with cosmic rays. Because carbon-14 has a half-life of 5,730 years, it is used as an indicator of groundwater residence time of approximately 20,000 years. Water samples were analyzed using liquid scintillation counting for carbon-14 and mass spectrometry for $\delta^{13}\text{C}$. Carbon-14 is reported as percent modern carbon, a ratio of radiocarbon in a groundwater sample to the concentration in an international oxalic acid standard (Tamers, 1975). Values for $\delta^{13}\text{C}$ are reported in ‰ (per mil) and are normalized to the South Carolina Pee Dee Formation belemnite standard (Coplen, 1996).

It should be noted that several uncertainties are associated with the concentration of carbon-14, including dilution of radiocarbon because of carbonate dissolution, isotopic exchange reactions between dissolved carbonate species and calcium carbonate in aquifers, and mixing of groundwaters of different radiocarbon relative residence times. Tamers (1975) also commented that field sampling is a potentially large source of error because carbon dioxide out gassing of a sample occurs immediately after collection and can lead to spurious carbon-13 values. Sampling during the hottest part of the day, or

during warmer summer months can exacerbate this problem. Uncertainties related to the source of carbon dioxide in the soil zone (i.e., atmospheric, plant respiration, decay of organic material, from magma intrusions, or related to petroleum accumulations in the subsurface) presents an additional uncertainty.

Dilution of carbon-14 due to carbonate dissolution may introduce uncertainty into the evaluation of Cuatrocienegas Basin relative groundwater residence time because of the presence of carbonate rocks. Tamers (1975) commented that it is important to account for dilution of radiocarbon activity due to the dilution of carbonate species (e.g., carbonate and bicarbonate) from limestone. Münnich (1957) showed that radiocarbon concentrations are diluted because of dissolved carbon dioxide reacting with limestone to form bicarbonate following the reaction



Thus, half the carbon in a groundwater sample is from dissolved carbon dioxide and has the radiocarbon concentration of the contemporary planet and half is “dead carbon” from the dissolution of limestone. The groundwater relative residence time must be corrected because of the presence of “dead carbon” (in the form of HCO_3^-) from carbonate dissolution. Salem et al. (1980) proposed doing such a correction using the equation

$$A_0 = 1.016 \left(\frac{\delta^{13}C(HCO_3^-) - \delta^{13}C(CaCO_3)}{\delta^{13}C(CO_2) - \delta^{13}C(CaCO_3) + \Sigma} \right). \quad (3)$$

Where

A_0 = the initial concentration of radiocarbon in the groundwater sample (assumed to be 100 percent modern carbon),

$\delta^{13}C = \left(\frac{^{13}C / ^{12}C_{sample}}{^{13}C / ^{12}C_{std}} - 1 \right) \times 1000$ the carbon standard (C_{std}) is the South Carolina

Pee Dee Formation belemnite [Coplen, 1996]),

$\delta^{13}C(HCO_3^-)$ = the value of $\delta^{13}C$ in the water sample,

$\delta^{13}C(CaCO_3)$ = the value of $\delta^{13}C$ in a standard carbonate (assumed to be 0 ‰),

$\delta^{13}C(CO_2)$ = the value of $\delta^{13}C$ in soil (assumed to be -25 ‰), and

Σ = the fractionation factor (assumed to be 8).

The corrected groundwater relative residence time is calculated based on the application of the radioactive decay equation (Salem et al., 1980)

$$t = 8,267 \ln\left(\frac{A_0}{A}\right). \quad (4)$$

Where

t = the calculated relative residence time (in years before present),

8,267 = the decay constant of carbon-14 (the ratio of the half-life of radiocarbon to the natural logarithm of 2.0), and

A = the concentration of radiocarbon (carbon-14) in the sample of groundwater.

Despite the uncertainties in the method, Rodríguez et al. (2005a) presented carbon-14 relative groundwater residence times from approximately 100s of years (at the northern flank of the Sierra Alamitos in the eastern Hundido Valley) to 17,000 years (at the northeastern corner of the Hundido Valley). Many corrected relative residence times in both the Hundido Valley and the Cuatrociénegas Basin range between 7,000 and 10,000 years. One sample from a spring travertine deposit at the southwest corner of the basin has a carbon-14 relative residence time of approximately 17,000 years. One analysis from, Las Playitas, a terminal lake at the end of a surface water drainage from a spring, had a result of 119 percent modern carbon. As discussed previously, many uncertainties are associated with using the carbon-14 method to evaluate the relative aquifer residence time, especially in carbonate aquifers. For example, a percent modern carbon value greater than 100 percent may be an artifact of sample handling, analytical method, or because of evaporative concentration of the sample. However, the interpretation of this anomalous result is outside the scope of this research project.

Carbon-14 relative residence time analyses from well water in the center of the Hundido Valley, spring discharge, and travertine suggest increased recharge may have occurred during a past period of wetter climate. In the eastern Cuatrociénegas Basin at the northern flank of the Sierras Purísima and Vicente and at the base of the Sierra La Madera, percent modern carbon >40 percent suggests moderate to high recharge rates (Hibbs and Darling, 2005). Lower percent modern carbon values from wells in the center of the Hundido valley and most Cuatrociénegas Basin source springs suggest lower recharge rates consistent with the findings of Hibbs and Darling (2005). Thus, direct recharge in mountain highlands (as in Nevada and west Texas) may be the primary recharge mechanism in the Cuatrociénegas Basin with minimal recharge on the valley floors approaching zero percent of precipitation.

Springs: Cuatrocienegas Basin

Adkins (1920) conducted the earliest hydrogeologic assessment of the Cuatrocienegas Basin. He inferred that faults influence the linear trend of dozens of springs on either side of the Sierra San Marcos anticline, as shown on **Figure 2**. Minckley and Cole (1968) described spring water chemistry from an aquatic biology perspective, and Evans (2005) defined groundwater flow paths within the basin from source springs to terminal playa lakes based on hydrochemical facies. Evans (2005) and Minckley and Cole (1968) found spring discharge temperatures ranging from 23.7°–34.7°C and total dissolved solids range from approximately 900–1,600 milligrams/liter (source spring) to >300,000 milligrams/liter (terminal playa lakes). Within the valley, spring water flows on the surface and through subsurface channels in karstified alluvium.

METHODS

From what groundwater catchment(s) does Cuatrocienegas Basin spring flow originate; and what components compose the regional water budget? This section describes the methods used in this research project to conduct groundwater catchment delineation for the Cuatrocienegas Basin region and evaluate the regional water budget.

A Note on the Organization of this Chapter

To complete the goals of the research project, this research project uses the following approaches:

1. A **groundwater catchment delineation** approach using geographic information systems to determine catchments upgradient to the Cuatrocienegas Basin;

2. **Precipitation estimation** using sparse gage measurements and vegetation precipitation requirements to estimate how much precipitation occurs in the study area;
3. **A chloride-balance approach to recharge estimation** to evaluate how much precipitation recharges the aquifer system;
4. **A spring discharge measurement** approach to estimate how much groundwater is leaving the Cuatrocienegas Basin (and therefore at least how much recharge occurs); and
5. **Evaluation of interbasin groundwater flow using an analytical model** to evaluate if interbasin flow is plausible between adjacent groundwater catchments.

Groundwater Catchment Delineation

Digital Elevation Models

Digital elevation data produced by the National Aeronautics and Space Administration shuttle radar topography mission are available from the U.S. Geological Survey Seamless Data Distribution System (<http://seamless.usgs.gov>) at a 3-arc second spatial resolution (approximately 90-square meter at the latitude of northeast Mexico) for an area that encompasses the Cuatrocienegas Basin (Hall et al., 2005). This research project considers an initial study area that extends between approximately 24.9°–28.7° north latitude and 100.7°–104.8° west longitude, as shown on **Figure 1**. The area includes most of Coahuila, easternmost Chihuahua, northeastern Durango (including the eastern Sierra Madre Occidental and the presently internally-draining terminus of the Río Nazas), northern Zacatecas, and western Nuevo León (including the northernmost

Sierra Madre Oriental). The digital elevation models are imported into a geographic information system to create a regional digital elevation model. A spline interpolation routine fills occasional null data points as described by Hall et al. (2005) to create a cleaned digital elevation model.

Geographic Information Systems

The cleaned digital elevation model is used in a geographic information system environment to delineate groundwater catchments based upon surface topography. Tarboton (1997) and Maidment (2002) described a method for the determination of surface water flow directions from digital elevation models in the ArcHydro package of ArcGIS by Environmental Systems Research Institute, Inc. of Redlands, California. The groundwater catchment delineation approach is used to infer regional hydraulic gradient from high elevation recharge areas to low elevation discharge zones. The approach also delineates surface water catchments and associated groundwater catchments based on topography. Groundwater catchments delineated by this approach are used as the spatial domain for precipitation and recharge calculations described below. These calculations are conducted for the area of each groundwater water catchment.

Precipitation Estimation

Spatially-distributed precipitation over the study area is estimated based on a 60-year, valley-floor, precipitation record and high-elevation precipitation inferred from mountain vegetation. Catchments are delineated along the hypothesized regional flow path. In the subsequent section, a chloride mass-balance estimates recharge from precipitation—the recharge for each successive basin is summed until recharge is equal to observed discharge using a water-balance approach.

Lesser y Asociados (2001) and Rodríguez et al. (2005a) postulated that precipitation on the mountains surrounding the Cuatrociénegas Basin (i.e., Sierra San Marcos, Sierra La Fragua, Sierra La Madera, Sierra La Purísima, Sierra Vicente, and Sierra La Menchaca, as shown on **Figure 2**) can provide all groundwater to basin springs. The goal of the recharge evaluation described in the next section is to test if sufficient precipitation falls on the mountains immediately surrounding the Cuatrociénegas Basin to generate measured spring discharge, as hypothesized by Lesser y Asociados (2001) and Rodríguez et al. (2005a). The water budget is

$$R = (P - ET) = Q + GW_{out} . \quad (5)$$

Where

R = recharge,

P = precipitation,

ET = evapotranspiration

Q = canal discharge, and

GW_{out} = interbasin groundwater flow.

The accurate quantification of spatially-distributed rainfall is essential to estimate groundwater recharge. Precipitation is linearly extrapolated using a long-term precipitation record from the floor of the Cuatrociénegas Basin and by estimating precipitation at elevated elevations based on the precipitation requirements of mountain vegetation.

The three groundwater catchments (red lines) delineated using methods described above that are similar in area to those presented by Lesser y Asociados (2001) and Rodríguez et al. (2005a) are shown on **Figure 6**. Precipitation in the catchments that encompass the Cuatrociénegas Basin and Ocampo Valley is hypothesized by Lesser y Asociados (2001) and Rodríguez et al. (2005a) to provide recharge to Cuatrociénegas Basin spring flow. The hypothesis of these authors that no interbasin flow to Cuatrociénegas Basin occurs is tested by this research. The three groundwater catchments that previous researchers think contribute to Cuatrociénegas Basin spring discharge are shown as red lines and labeled on **Figure 6**: (1) the Ocampo Valley (6,650 square kilometers) that fed a spring-fed stream that historically flowed at approximately 0.25 cubic meters/second into the northern end of the Cuatrociénegas Basin (Minckley, 1969), (2) the eastern Cuatrociénegas Basin (1,450 square kilometers), including the Sierra San Marcos and Sierra La Purísima that are hypothesized to provide recharge to the Santa Tecla Canal (**Figure 2**), and (3) the western Cuatrociénegas Basin (2,450 square kilometers) that includes the Sierra La Fragua and southern Sierra La Madera that are hypothesized to discharge to Saca Salada Canal springs (**Figure 2**).

Precipitation: Gage Measurements

Rodríguez et al. (2005a) presented precipitation data measured from 1942–2003 in the Town of Cuatrociénegas at a valley-floor elevation of 740 meters. They calculate annual precipitation by summing monthly precipitation from January to December (i.e., annual precipitation data are not presented using a water year approach). The average annual precipitation depth in this record is 219 millimeters/year and ranges between approximately 100–400 millimeters/year. Precipitation falls primarily during heavy summer rains from May–October. September is the雨iest month (41 millimeters) and March is the driest months (6 millimeters, Rodríguez et al., 2005a).

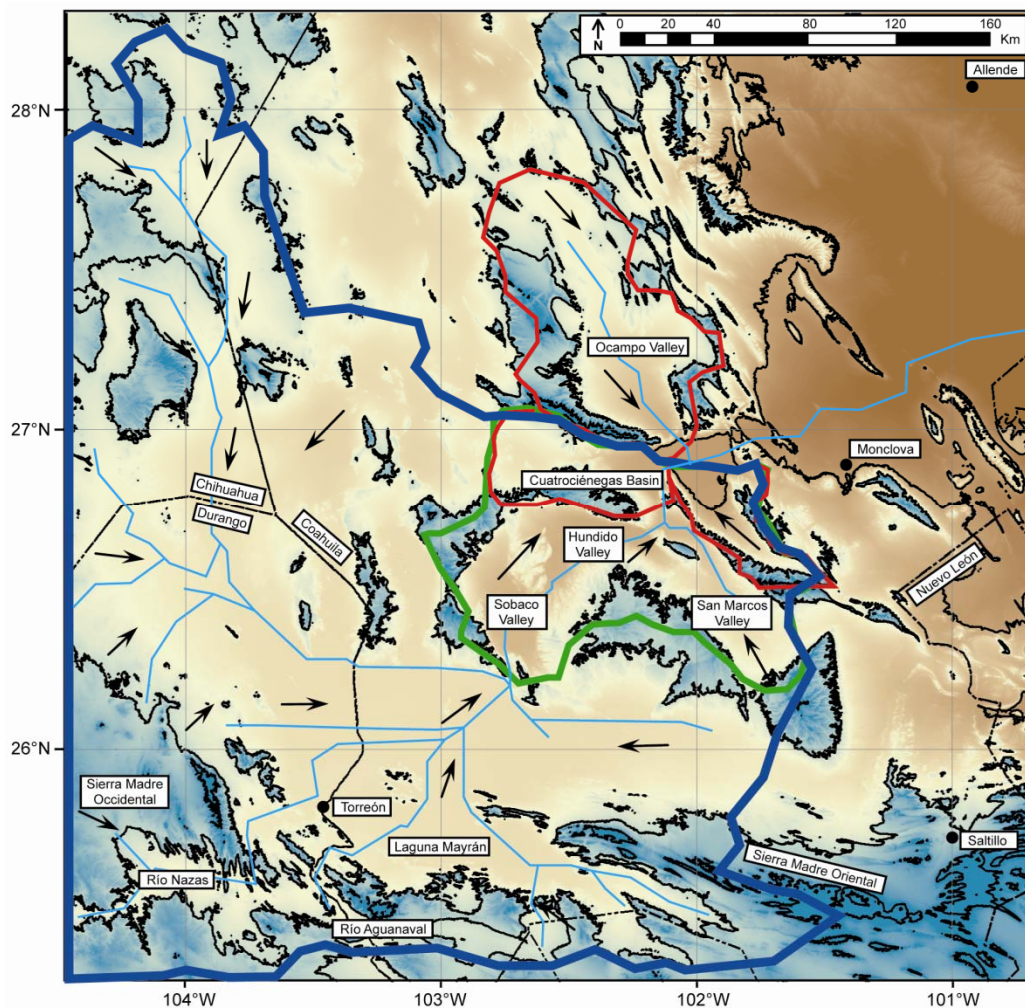


Figure 6. CUATROCIÉNEGAS BASIN GROUNDWATER CATCHMENTS

Groundwater catchments include: Local flow systems of Saca Salada and Santa Tecla Canals and Ocampo Valley (thick red lines), expanded flow system including Sobaco, Hundido, and San Marcos Valleys (thick green line), approximately 91,000-square kilometer regional flow system (thick blue line), hypothesized regional groundwater flow system (black arrows) inferred surface drainage network (light blue line), and 750-meter contour intervals (low–high elevation ranges from brown–green, respectively).

The wettest year on record (421 millimeters), occurred in 1985. Rodríguez et al. (2005a) stated that a station in the Hundido Valley yields a 14-year average precipitation (1991–2004) of 137 millimeters/year. A summary of published Cuatrocienegas Basin area precipitation estimates is presented in **Table 5**.

Precipitation: Spatial Distribution Based on Vegetation Requirements

Precipitation gages are located only in the valley floor areas and are not present in the mountains of the study area, which is a common situation around the globe. Thus, this research project estimates mountain precipitation based on vegetation requirements. Spatially-distributed precipitation estimates are improved by evaluating the precipitation requirements of vegetation that occurs in the Cuatrocienegas Basin region. This evaluation is based on a linear relationship between long-term gage precipitation values and mountain top vegetation precipitation requirements at a 3-arc second spatial resolution in a geographic information systems environment.

A vegetation map (Meyer, 1973) delineates the extent of pine trees in the Sierra San Marcos and Sierra La Madera ranges surrounding the Cuatrocienegas Basin, which occur at approximately 2,000 meters on the northern slopes of the Sierra de la Madera and Sierra San Marcos, and approximately 2,400 meters on the southern slope of the Sierra de la Madera. Kolb (2005) stated that ponderosa pines in Northern Arizona that are similar to the pine trees in the mountains surrounding the Cuatrocienegas Basin thrive when annual precipitation ranges between 450 and 650 millimeters/year. González (2006) commented that approximately 400 millimeters/year precipitation occurs in the highest mountains surrounding the Cuatrocienegas Basin in thin pine tree stands.

Table 5. PRECIPITATION ESTIMATES FOR THE CUATROCIÉNEGAS BASIN

¹The elevation for Cuatrocienegas is not specifically stated.

²Approximate elevation.

³González (2006) estimated that 400 millimeters/year precipitation occurs in the highest mountains surrounding the Cuatrocienegas Basin. The Sierra San Marcos peak is 2,600 meters, and the Sierra La Madera tops out at 3,025 meters.

Source	Precipitation	Elevation	Comments
	[mm/year]	[m]	
	260	740	Cuatrocienegas Town ¹
Badino et al. (2004)		1,500	Sierra San Marcos ²
	350	to 2,000	
Meyer (1973)	<200	740	Cuatrocienegas Valley Floor ¹
Minckley and Cole (1968)	<200	740	References Vivó Escoto (1964) ¹
Minckley (1969)	<200	740	Cuatrocienegas Valley Floor ¹
Rodríguez et al. (2005a)	219	740	Cuatrocienegas Town, 1942–2003
	137	800	Hundido Valley 1991–2004 ²
SEMARNAT (2003)	<200	N/A	Chihuahuan Desert precipitation (Shreve, 1944) ²
González (2006)		2,600	Mountain precipitation ³
	~400	to 3,025	

Because mountain-top precipitation gages do not exist, two precipitation relationships estimate spatially-distributed precipitation for a continuous range of elevations from valley floors to mountain tops throughout the study area to account for uncertainties in actual spatially-distributed precipitation. The research estimates 400 millimeters/years precipitation based on pine forest needs on Cuatrocienegas Basin mountain tops of (1) the Sierra San Marcos (maximum elevation=2,600 meters), and (2) the Sierra La Madera (maximum elevation=3,025 meters).

Precipitation: PERSIANN Satellite Precipitation Estimates Compared with Gage Rainfall and Mountain Precipitation Extrapolation

Commonly, precipitation records are limited in many semi-arid, karst aquifers around the world, and the Cuatrociénegas Basin is no exception. In order to provide accurate precipitation estimates in areas of the globe where precipitation gages are not present, Hsu et al. (1997) and Sorooshian et al. (2000) presented research on the Precipitation Estimation from Remotely Sensed Information using Artificial Neural Networks (PERSIANN). This method estimates precipitation from infrared and daytime visible satellite imagery at a spatial resolution of $0.25^{\circ} \times 0.25^{\circ}$ from 50°S to 50°N globally every half hour using satellite-based measurements (GOES-8, GOES-9/10, GMS-5, Meteosat-6, and Meteosat-7 for infrared images). The method also uses the Tropical Rainfall Monitoring Mission Microwave Imager instantaneous rain product 2A12) from 2002–2007 (precipitation estimates for 2008 are incomplete).

Although satellite derived precipitation estimates might become an adequate means to quantify precipitation where gages are not available, a six-year precipitation record may not be sufficient to make reliable estimates of long-term average annual precipitation. Thus, long-term, low-elevation gage measurements are synthesized with the precipitation inferred from mapped mountain vegetation to estimate precipitation at all elevations throughout the study area. In order to test this approach in the Cuatrociénegas Basin, ground-truth precipitation data (1942–2003 in the Town of Cuatrociénegas at a valley-floor elevation of 740 meters; Rodríguez et al., 2005a) and extrapolated precipitation estimates based on mountain vegetation requirements are compared with PERSIANN satellite-derived precipitation estimates for 2002–2007.

Two areas of interest are investigated: one near the valley-floor gage with the long-term record in the town of Cuatrociénegas and one in the highest elevations of the study area in the Sierra La Madera (where the highest mountain is $>3,000$ meters).

PERSIANN satellite-derived precipitation estimates are obtained for these two areas of interest from The Henry Samueli School of Engineering at The University of California, Irvine. The two areas of interest are defined by name, north latitude, south latitude, west longitude, and east longitude and include (1) the Cuatrocienegas Basin Gage, 27.02° , 27.00° , 102.08° , 102.06° , and (2) the Sierra La Madera, 27.04° , 27.00° , 102.40° , 102.36° where ground-truth data exist.

The two areas of interest are shown on **Figure 7**. The Cuatrocienegas Basin Gage area ($0.02^{\circ} \times 0.02^{\circ}$) is slightly smaller than the Sierra La Madera area ($0.04^{\circ} \times 0.04^{\circ}$) so as to include only valley-floor elevation for the PERSIANN estimate. The average elevation of the two areas of interest is extracted from the digital elevation model of the area (Hall, 2005) in a geographic information systems environment. The average annual precipitation is evaluated using two precipitation extrapolation equations that relate average annual precipitation to the average elevation of the two areas. The average annual precipitation from the precipitation extrapolation equations is then compared to the precipitation estimates derived from the PERSIANN approach and the long-term valley-floor gage record.

Chloride-Balance Approach to Recharge Estimation

In order to determine what percent of precipitation results in groundwater recharge, a chloride-balance approach to recharge estimation is used. This method estimates recharge in semi-arid regions with sparse hydrogeologic data (Dettinger, 1989). Wood (1999) stated that the chloride-balance is attractive due to its low cost and for providing a time-integrated estimate of recharge. It has been used in the Great Basin of Nevada and in other arid and semi-arid regions.

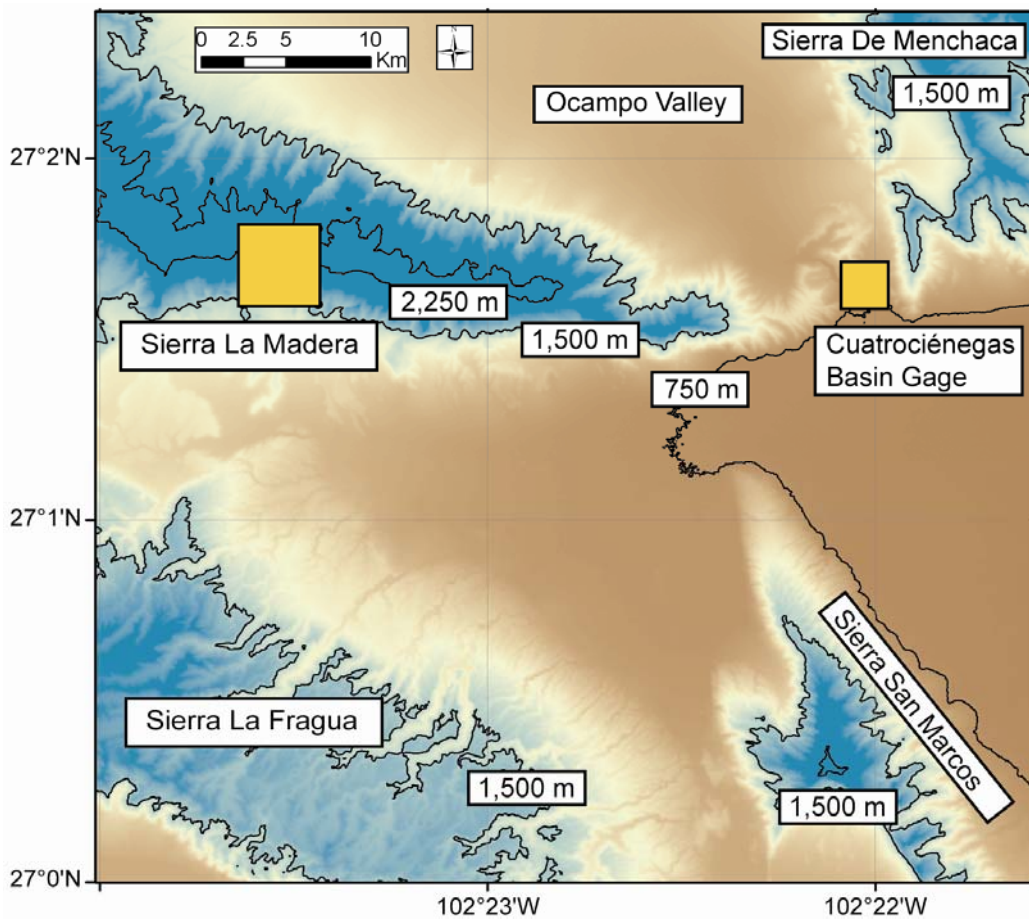


Figure 7. PERSIANN SATELLITE PRECIPITATION ESTIMATION AREAS

PERSIANN (Hsu et al., 1997; Sorooshian et al., 2000) satellite derived precipitation estimates are obtained from The Henry Samueli School of Engineering at The University of California, Irvine for two areas of interest defined by name, north latitude, south latitude, west longitude, and east longitude: (1) Cuatrocíenegas Basin Gage, 27.02°, 27.00°, 102.08°, 102.06°, and (2) Sierra La Madera, 27.04°, 27.00°, 102.40°, 102.36°.

Anderholm (2000) estimated mountain front recharge in the Middle Río Grande Basin of Central New Mexico at <one-fifteen percent of total annual precipitation (approximately 360 millimeter/year). Wilkes et al. (2004) estimated recharge at approximately seven percent of mean annual precipitation in a fractured and weathered granite porphyry aquifer overlain by a shallow sandy aquifer in the Augustus River catchment of Western Australia. Mahlknecht et al. (2004) evaluated recharge in the Independence Basin of the Mexican Altiplano (6,840 square kilometers). In the Independence Basin, recharge primarily occurs in mountainous highlands (>800 millimeters/year) and little recharge occurs in the plains (10 millimeters/year, or approximately two and a half percent of annual precipitation). There, precipitation ranges from <400 millimeters in the plains as low as 1,850 meters to >800 millimeters in highlands up to 2,850 meters (Mahlknecht et al., 2004).

Spatially-distributed recharge is estimated by (Dettinger, 1989; Wood, 1999; Anderholm, 2000) by the equation (where Cl_p/Cl_r is the recharge rate)

$$R_{mf} = P \left(\frac{Cl_p}{Cl_r} \right). \quad (6)$$

Where

R_{mf} = Volume of mountain-front recharge (or spring discharge),

P = Mountain precipitation volume,

Cl_p = Chloride concentration of bulk precipitation (milligrams/liter, Lamb and Bowersox, 2000), and

Cl_r = Chloride concentration of mountain-front recharge (i.e., chloride concentration of spring discharge—assuming chloride is a conservative tracer and no halite dissolution occurs, milligrams/liter, Evans, 2005, Rodríguez et al., 2005a, and Johannesson et al., 2004) .

The method assumes that

1. No significant chloride sinks or changes in chloride storage occur within the system (no halite deposits have been identified in the valley, although Minckley and Cole [1968] measured approximately 10,000 milligrams/liter chloride and approximately 300,000 milligrams/liter total dissolved solids in Laguna Salada, an evaporative pool);
2. Precipitation represents the only chloride source (i.e., it is assumed that dry deposition of chloride over the entire study area from Laguna Salada — or the dunes around Laguna Grande that Minckley and Cole [1968] stated are >95 percent gypsum—is minimal);
3. All groundwater discharges to springs (i.e., no interbasin groundwater outflow from the Cuatrociénegas Basin); and
4. Spring chloride concentrations represent the average chloride concentration of mountain front recharge.

The recharge analyses do not consider the dry deposition contribution of chloride. However, it is possible that chloride, including in the gypsum dunes surrounding Laguna Grande, is deposited by dry deposition in the mountains surrounding the Cuatrociénegas Basin, and dissolved by rainfall. Dry deposition of chloride in the mountains surrounding

the Cuatrocienegas Basin is undocumented, as is re-deflation from the mountain recharge areas.

Kushnir (1980) studied the coprecipitation of chloride with gypsum and found that the concentration of chloride coprecipitated in gypsum crystals formed in the laboratory from a brine, dried, dissolved in distilled water, and analyzed for chloride is negligibly small, with a Cl/Ca $<10^{-4}$ (or <100 parts chloride/million parts of calcium on a molar basis). At a concentration of <100 parts/million, the chloride concentration was below the detection limit of the Gran's Plot method used by Orion (1977). More recently, Lu et al. (1997) also evaluated the abundance of minor and trace elements in gypsum and find that chloride does not occur in the lattice of gypsum and chloride, as postulated by Kushnir (1980), and that chloride is only present in fluid inclusions. Furthermore, Lu et al. (1997) found that the chloride concentration of gypsum (in powdered samples from ten locations) ranges from 18–728 parts/million, as analyzed with a Dionex 2000i Ion Chromatography with a Star-Ion-A300 column and a NaHCO₃-Na₂CO₃ eluent.

In the High Plains of Texas, Scanlon et al. (2007) used the chloride balance approach to estimate recharge, but did not quantify chloride dry deposition. Therefore, Scanlon et al. (2007) double the chloride concentration in precipitation to account for dry fallout based upon total chloride fallout indicated by prebomb ³⁶Cl/Cl ratios of borehole profiles near Amarillo, Texas (Scanlon and Goldsmith, 1997). Chloride dry deposition data do not exist for the mountains of northeast Mexico. In the absence of dry deposition data for Mexico, this research follows the approach of Scanlon et al. (2007).

Precipitation Chloride Concentration

Rodríguez et al. (2005a) collected a rain water sample for stable isotope analyses, but chloride analyses were not conducted (Gallardo, pers. com., 2006). Evans (2005) used an average chloride content of precipitation of 0.13 milligrams/liter (1980–2004)

measured at the closest National Atmospheric Deposition Program station in Big Bend National Park (TX04), located approximately 300 kilometers to the north (Lamb and Bowersox, 2000). Because of uncertainties in actual precipitation chloride, a value of 2.0 milligrams/liter (Drever, 1997, using data presented by Junge and Werby, 1958) also is used to assess recharge resulting from a range of precipitation chloride concentrations.

Spring Water Chloride Concentration

Evans (2005), Rodríguez et al. (2005a), and Johannesson et al. (2004) present chloride analyses for both source springs (i.e., first emergence of spring water from aquifer) and resurgent springs (i.e., springs located far from original source spring) samples. Cuatrocienegas Basin source spring locations are shown on **Figure 8**. Only source springs are considered in the chloride balance analysis to avoid including evaporative effects on chloride concentrations. Andring et al. (2006) used plots of chloride and bromide to show that dissolution of halite does not influence the Cuatrocienegas Basin spring water chloride concentration. Similarly, this research project plots bromide and chloride to determine if chloride sources are present in the study area.

The Cuatrocienegas Basin springs feed two separate canals: Santa Tecla Canal, which drains springs in the east half of the basin, and Saca Salada Canal, which captures western basin spring discharge. The chloride concentrations of these two groups of springs are different and are grouped accordingly in **Table 6** and **Table 7**.

Saca Salada Canal chloride values are used to estimate recharge in the Ocampo Valley (former source of spring-fed Río Cañon). Saca Salada Canal average chloride is approximately 99 milligrams/liter. An average of chloride from wells in the Ocampo Valley (CNA-119B, -161, -162, and -170-B; Rodríguez et al., 2005a) is approximately 170 milligrams/liter. This analysis uses the lower chloride concentration value because some evaporative concentration probably has occurred near agricultural supply wells.

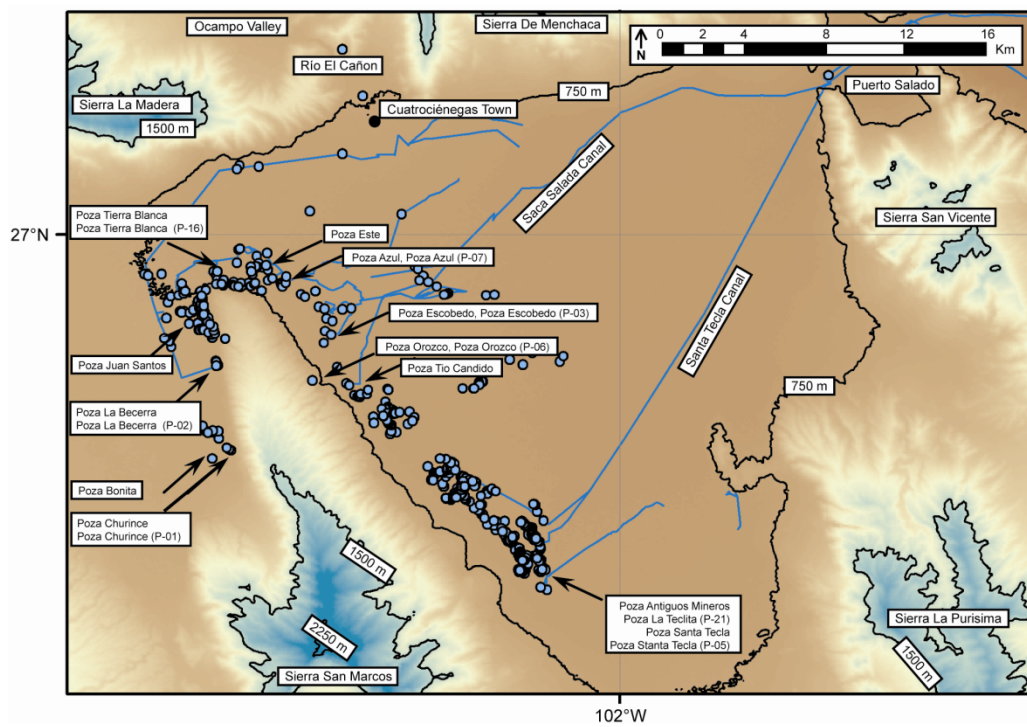


Figure 8. LOCATION OF CUATROCIÉNEGAS BASIN SOURCE SPRINGS

Table 6 and Table 7 show the results of the chloride analyses for springs shown on this figure.

Table 6. CHLORIDE CONCENTRATION OF SPRINGS FEEDING SANTA TECLA CANAL

¹Sample name in parenthesis is Rodríguez et al. (2005a) nomenclature.

²Samples collected by Evans (2005) for spring 2004 do not have a specific sample date.

³Average chloride concentration is not flow-weighted because discharge measurements are not available for all springs. Poza Orozco and Poza Tío Cándido are located in the Santa Tecla (eastern Cuatrocienegas Basin) drainage area, but actually drain to the Saca Salada canal. Because discharge is relatively low, these springs are accounted for in the Santa Tecla Canal calculations.

⁴Johannesson et al. (2004) reported results of analyses conducted on samples collected by Winsborough (1990) in 1983.

⁵Multi-sample average is used for chloride-balance calculations.

Chloride concentrations here are refined in Chapter 4 to 30 milligrams/liter.

Site ¹	Sample Date ²	Chloride Concentration [mg/L]	Average Chloride Concentration (Multi-Sample) ³ [mg/L]	Source ⁴
Poza Antiguos Mineros	Spring 2004	45.63	45.63	Evans, 2005
Poza Santa Tecla (P-05)	May 6, 2004	30.50	29.75	Rodríguez et al., 2005a
Poza Santa Tecla	1983	29.00		Johannesson et al., 2004
Poza Escobedo	Spring 2004	102.40		Evans, 2005
Poza Escobedo	July 1983	107.00	100.30	Johannesson et al., 2004
Poza Escobedo (P-03)	May 5, 2004	91.50		Rodríguez et al., 2005a
Poza La Teclita (P-21)	August 4, 2004	29.60	29.60	Rodríguez et al., 2005a
Poza Orozco (P-06)	May 6, 2004	91.50	91.50	Rodríguez et al., 2005a
Poza Tío Cándido	July 1983	119.00	107.46	Johannesson et al., 2004
Poza Tío Cándido	Spring 2004	95.91		Evans, 2005
Approximate Average ²			67.37	Multi-sample average ⁵

Table 7. CHLORIDE CONCENTRATION OF SPRINGS FEEDING SACA SALADA CANAL

See Table 6 for explanation of notes.

Chloride concentrations here are refined in Chapter 4 to 90 milligrams/liter.

Site ¹	Sample Date ²	Chloride Concentration [mg/L]	Average Chloride Concentration (Multi-Sample) ³ [mg/L]	Source ⁴
Poza Azul	Spring 2004	59.98		Evans, 2005
Poza Azul (P-07)	May 6, 2004	91.50	75.74	Rodríguez et al., 2005a
Poza Becerra	Spring, 2004	101.20		Evans, 2005
Poza Becerra	July 1983	104.00	98.90	Johannesson et al., 2004
Poza Becerra (P-02)	May 4, 2004	91.50		Rodríguez et al., 2005a
Poza Bonita	Spring, 2004	106.40		Evans, 2005
Poza Bonita	July 1983	108.00	107.20	Johannesson et al., 2004
Poza Churince	January 2005	103.55		Evans, 2005
Poza Churince	Spring 2004	104.80	103.95	Evans, 2005
Poza Churince (P-01)	April 30, 2004	103.50		Rodríguez et al., 2005a
Poza Este	Spring 2004	87.81	87.81	Evans, 2005
Poza Juan Santos	Spring 2004	105.30		Evans, 2005
Poza Juan Santos	Spring 2004	92.37	98.84	Evans, 2005
Poza Tierra Blanca	Spring 2004	114.70		Evans, 2005
Poza Tierra Blanca (P-16)	July 29, 2004	101.00	107.85	Rodríguez et al., 2005a
Approximate Average ²			98.75	Multi-sample average ⁵

Chloride Analysis Methods: Spring Water and Precipitation

Chloride concentrations are evaluated by this research from several previous publications. Chloride in spring water samples are evaluated from Minckley and Cole (1968), Winsborough (1990), Johannesson et al. (2004), Evans (2005), Rodríguez et al. (2005a), and Wolaver (unpublished). The chloride concentration of precipitation samples are evaluated using data published by Junge and Werby (1958) and the National Atmospheric Deposition Program (2008).

Johannesson et al. (2004) presented chloride data for thirteen spring water samples collected in 1983 by Winsborough (Winsborough and Golubić, 1987; Winsborough, 1990). Winsborough (1990) collected filtered (0.45 micrometer) water samples in polyethylene bottles previously leached with hot distilled water. Chloride was measured using ion-specific electrodes. Winsborough (1990) did not mention the instrument type, method detection limit, accuracy, precision, or uncertainty associated with the method.

Evans (2005) collected 39 water samples from springs and canals in the Cuatrocienegas Basin from April 2004 to January 2005. Water samples were collected as grab samples in pools at a depth of approximately 0.3 meters approximately 0.3 to 0.5 meters from the side of the spring pool or canal bank. Water for anion analysis (including chloride) was hand-filtered using a syringe with a 0.2 micron filter into an un-acidified bottle. Evans (2005) did not state the bottle type used or volume of sample collected. Chloride analyses were done at The University of Minnesota using a Dionex ICS-2000 ion-exchange chromatography system. Evans (2005) did not discuss if replicates or blanks were analyzed. Evans (2005) did not present accuracy or precision of chloride analyses, mention the method detection limit of the instrument, or comment if standard chloride values were analyzed.

Rodríguez et al. (2005a) collected water samples from wells and springs in April, May, July, and August 2004 for chloride (and other anions and cations) analysis. If a well was equipped with a pump in-situ, it was used to collect water, or else a sampling pump was installed. Rodríguez et al. (2005a) did not state for how long a well was pumped prior to collection of a sample. Rodríguez et al. (2005a) did not discuss how spring water samples were collected (e.g., depth, location within pool). Water samples for chloride analysis were collected in 500 milliliter polyethylene bottles that were pre-washed in the laboratory with hydrochloric acid and rinsed with distilled water. The water samples for chloride analysis were not filtered and were not preserved with nitric acid. Water samples were stored on ice in a cooler until analysis at the Water and Soil Laboratory at the Universidad Autónoma de San Luis Potosí.

Rodríguez et al. (2005a) analyzed chloride in spring water at the Universidad Autónoma de San Luis Potosí using the argentometric method (American Water Works Association, 1998). Ion-exchange chromatography is typically used to analyze common anions. However, because Rodríguez et al. (2005a) mentioned that sulfate and nitrate were measured using spectrophotometric methods and trace elemental analyses were done at Activation Laboratories, Ltd., of Ontario, Canada; it appears that they did not have access to ion-exchange chromatography.

Rodríguez et al. (2005a) did not mention the use of standards in the chloride analyses, so the accuracy of reported chloride concentrations is not stated. Furthermore, Rodríguez et al. (2005a) did not state if replicates or blanks were analyzed. The American Water Works Association (1998) describes the argentometric method for chloride analysis of water samples. Using the argentometric method to analyze a synthetic sample containing 241 milligrams/liter chloride, 41 laboratories found a relative standard deviation of 4.2 percent and a relative error of 1.7 percent (American Water Works

Association, 1998). Rodríguez et al. (2005a) did not discuss chloride analysis precision. Neither the American Water Works Association (1998) nor Rodríguez et al. (2005a) discussed chloride detection limits for the argentometric method. Miller (pers. com., 2008) states that it is probably not possible to determine a detection limit for the chloride analyses published by Rodríguez et al. (2005a), because the argentometric method uses a titration based on the visual identification of a red-colored silver chromate precipitate.

Wolaver (unpublished) evaluated ten spring water samples that were analyzed for chloride at the Chemistry Laboratory of The University of New Mexico Department of Earth and Planetary Sciences. Crossey (2008, pers. com.) stated that a Dionex 500X ion-exchange chromatograph was used to analyze for anion concentrations, including chloride. All chloride concentrations were well above detection. Duplicate samples were not run.

Junge and Werby (1958) analyzed over 60 precipitation samples on a monthly basis from July 1955 to July 1956 and present average monthly chloride concentrations. They calculate chloride concentrations (with an accuracy of \pm ten percent) using a nephelometric method similar to the argentometric silver nitrate titration method used by Rodríguez et al. (2005a). In coastal areas where high accuracy was required, Junge and Werby (1958) used a null method to determine chloride concentration where seawater was diluted and analyzed with a flame photometer until the sodium value was exactly equal to that of the precipitation sample being analyzed.

The National Atmospheric Deposition Program (2008) analyzed precipitation samples for chloride in Big Bend National Park. The National Atmospheric Deposition Program was established in 1981 to understand the causes and effects of acid rain (National Atmospheric Deposition Program, 2008). Precipitation samples are collected weekly if a rain water sample >10 milliliters is available in Big Bend National Park using

60 milliliter high density polyethylene bottles. Samples are maintained at 4°C and sent to the National Atmospheric Deposition Program Central Analytical Laboratory at the University of Illinois at Champaign-Urbana for chloride, pH, sulfate, nitrate, ammonium, and base cation analysis (i.e., calcium, magnesium, potassium and sodium; National Atmospheric Deposition Program, 2008). Since June, 2004, the laboratory has used a Dionex ICS-2000 ion chromatography instrument (National Atmospheric Deposition Program, 2008). Dionex (2003) states that this instrument can determine chloride concentration in rain water with a method detection limit (the minimum chloride concentration that can be reported with a 99 percent confidence that the value exceeds zero based on the standard deviation of seven replicate samples) of 0.010 milligrams/liter (assuming a precipitation chloride concentration from 0.02–2.0 milligrams/liter). Because standards for chloride concentration in precipitation do not exist, bias (a persistent positive or negative deviation of the measured value from the actual value) is estimated by comparing National Atmospheric Deposition Program results to similar networks and by routinely analyzing blind samples of known concentration.

The bias goals for the National Atmospheric Deposition Program are: \pm 100 percent at the method detection limit, \pm 20 percent at ten times the method detection limit, and \pm 10 percent at 100 times the method detection limit. Standardization is instrument specific and a minimum of five standards (based on fifth–99th percentile of the concentration found in the dataset) are used daily. Five blanks/week are analyzed (two 50 milliliter samples of deionized water, one 50 milliliter sample of FR25, and two sample lids leached with 50 milliliters of deionized water and FR25). Replicates are performed with approximately two percent of the samples (if sufficient sample volume is available for a split) and four double blind (blind to the sample receiving staff and the analysis staff) internal quality control samples are run per month (one sample/week) and

analytical bias (estimated from the mean difference between measured and target values) and precision (estimated from the relative standard deviation of the measurements) are calculated. The data are verified by capturing sample results directly using data acquisition software and stroke-verifying the keyboard entry of field forms with two independent data entry staff.

Bromide Analysis Method

Rodríguez et al. (2005a) stated that inductively coupled plasma-mass spectrometry was used to analyze bromide in spring water. Water samples for bromide analysis were collected in 60 milliliter polyethylene bottles that were pre-washed in the laboratory with hydrochloric acid and rinsed with distilled water. The water samples for bromide analysis were filtered with a 0.45 micron acetate filter and were preserved with nitric acid to lower the pH of the sample to less than two pH units. Samples were analyzed using inductively coupled plasma-mass spectrometry at Activation Laboratories, Ltd., of Ontario Canada using a Perkin Elmer SCIEX ELAN 6100 or 9000. Activation Laboratories (2008) used a total digestion of hydrofluoric, nitric, and perchloric acids on a 0.25-gram sample. The heated solution was dried and then brought back into solution using aqua regia. Rodríguez et al. (2005a) stated a detection limit for their bromide analyses of 0.003 milligrams/liter, although Activation Laboratories (2008) stated a detection of 0.005 milligrams/liter for this method. Rodríguez et al. (2005a) did not mention the use of standards in the bromide analyses, so the accuracy of reported chloride concentrations is not stated. The use of replicates or blanks for bromide analyses are not mentioned by Rodríguez et al. (2005a). However, Activation Laboratories (2008) stated that internationally-certified reference materials (i.e., U.S. Geological Survey Geological Reference Samples-1, -2, -4 and -6; Gladney et al., 1984) are analyzed at the beginning and end of each batch of samples. Activation Laboratories (2008) also

analyzed internal control standards by using a duplicate run every ten samples every ten samples.

Spring Discharge Measurement

The goal of this section is to quantify how much groundwater leaves the Cuatrocienegas Basin annually so that annual recharge may be estimated. This research project measures instantaneous spring discharge on the Saca Salada and Santa Tecla Canals using a FlowTracker® hand-held acoustic Doppler velocimeter. U.S. Geological Survey standard methods used by this research project for stream gaging are described in Carter and Davidian (1968) and for using acoustic velocity meter systems in Laenen (1985). Spring discharge is also measured at Poza La Becerra, the largest spring in the Cuatrocienegas Basin. Gaging locations are shown as labeled circles on **Figure 2** (where 1 is the Saca Salada Canal, 2 is the Santa Tecla Canal, and 3 is Poza La Becerra).

Prior to groundwater development in the Cuatrocienegas Basin, spring discharge terminated in an evaporative playa lake in the eastern part of the basin. Because gaging dozens of individual springs is impractical, discharge of these two canals is measured to estimate composite spring discharge. Average annual basin discharge is estimated with a stage-discharge relationship using instantaneous stage data collected by a water-level pressure transducer installed in the Saca Salada Canal (Buchanan and Somers, 1982).

Evaluation of Interbasin Groundwater Flow Using an Analytical Model

The chloride balance recharge model tests if interbasin groundwater flow must occur to generate observed springs discharge. An analytical model (Hermance, 1998; Uliana, 2000; Jacob, 1943) evaluates if interbasin groundwater flow from adjacent valleys to the Cuatrocienegas Basin is possible under topographic divides by calculating hydraulic head given a range of plausible permeability and recharge conditions.

Interbasin Groundwater Flow in Analogous Karst Terrains

Previous studies suggested that interbasin groundwater flow occurs under topographic highs of high permeability carbonate rocks in West Texas (Gates et al., 1980; Nielson and Sharp, 1985; Sharp, 1989; Darling, 1997; Sharp, 1998; Uliana, 2000; Uliana and Sharp, 2001; Hibbs and Darling, 2005) and Nevada (Maxey and Eakin, 1949; Snyder, 1962; Eakin and Moore, 1964; Eakin, 1966; Maxey, 1968; Winograd and Thordarson, 1975; Eakin et al., 1976; Anning and Konieczki, 2005). Snyder (1962) presented a hydrogeologic conceptual model of a closed and drained basin in the Great Basin of the western U.S. Hibbs and Darling (2005) investigated the hydrogeology of basins in west Texas. They found that interbasin groundwater flow occurs in highly permeable, deep, carbonate aquifers that underlie hydrological-closed alluvial basins. Tóth (1963), Back (1966), and Freeze and Witherspoon (1967) showed that regional groundwater flow systems can exist underneath topographic highs.

Evaluation of Interbasin Groundwater Flow in the Cuatrocienegas Basin

The analytical model investigates the possibility of interbasin groundwater flow into the Cuatrocienegas Basin from two adjacent basins: (1) the Ocampo Valley (to the north), and (2) the Hundido Valley (to the south-southwest). The location of the Ocampo and Hundido Valleys are shown on **Figure 2**. The model is used to evaluate whether or not a (numerical) groundwater divide is formed under both the Sierra La Madera and the Sierra La Fragua, based upon selected ranges of recharge rates and hydraulic conductivity values. The systems consist of basin-fill valleys underlain by carbonate rocks and separated by carbonate rock topographic highs (Lesser y Asociados, 2001).

The model calculates hydraulic head at any point [x] in an unconfined aquifer based on the boundary conditions of heads [h_1 and h_2] on either side of a topographic divide separated by length [L] comprised of a porous material with a hydraulic

conductivity [K]. Hydraulic conductivity is calculated by dividing transmissivity by the average saturated aquifer thickness ($h_1 + h_2 / 2$). A constant recharge [W_s] is applied to the top of the topographic divide. The existence of a groundwater divide under a topographic divide is evaluated using the analytical model by varying recharge as a percentage of precipitation on the topographic divide to consider a range of permeability and recharge scenarios. When the calculated head at $x = 1$ meter is greater than h_1 , a groundwater divide exists. When the calculated head at $x = 1$ meter is less than h_1 , groundwater flows down-gradient and interbasin groundwater flow occurs. The equation for the analytical model is

$$h(x) = \sqrt{h_1^2 + \frac{(h_2^2 - h_1^2)}{L}x + \frac{W_s}{K} \left(\frac{L}{2}\right)^2 - \frac{W_s}{K} \left(x - \frac{L}{2}\right)^2} \quad . \quad (7)$$

Where

$h(x)$ = hydraulic head at any point [x] (meters),

x = distance (meters),

h_1 = head at point 1 (meters),

h_2 = head at point 2 (meters),

L = length separating point 1 and point 2 on opposites sides of a topographic divide (meters),

W_s = constant recharge applied to the topographic divide (meters), and

K = hydraulic conductivity of porous material comprising the topographic divide (meters/time).

Head values are assigned for the model boundary conditions using land surface elevation as a proxy for pre-development groundwater level, by assuming (1) predevelopment phreatic playas represent groundwater levels in the Ocampo and Hundido Valleys, and (2) spring elevations represent groundwater elevation in the Cuatrocienegas Basin. Land surface and spring elevations were derived from a regional 3-arc second digital elevation model (Hall et al., 2006).

Two interbasin flow analyses are conducted. The location of these analysis lines are shown on **Figure 2**. Line 1 extends four km from the location of a pre-development phreatic playa at the southern end of the Ocampo Valley to Poza Antejo in the northern end of the Cuatrocienegas Basin. Poza Azul is used instead of the former Río Cañon spring because it is located at the base of the Sierra La Madera and may represent interbasin flow through carbonate rocks. The former Río Cañon spring probably was groundwater discharge from alluvium and not interbasin flow through carbonate rock because the springs used to discharge from alluvium and were relatively fresh (22 milligrams/liter chloride; Minckley and Cole, 1968) compared to other springs in the Cuatrocienegas Basin (that typically have chloride concentration around 90 milligrams/liter). Line 2 extends 21 km from the location of a vadose playa (that was probably phreatic prior to water resource development, given the nearby seep described by Rodríguez, 2005) at the northern end of the Hundido Valley to the Cuatrocienegas Basin. The second elevation on Line 2 is selected at Poza El Churince, because this is the closest spring to the Hundido Valley. Finally, model input parameters are presented in **Table 8**.

Table 8. ANALYTICAL MODEL INPUT PARAMETERS

¹Precipitation presented in Rodríguez et al. (2005a).

²Recharge (W_s) is considered as a percentage of precipitation and is varied from 0.00001–100,000 percent of precipitation to consider a range of precipitation and recharge scenarios.

Model Variable	Ocampo Valley to the Cuatrociénegas Basin (Line 1)	Hundido Valley to the Cuatrociénegas Basin (Line 2)
h_1 [meters]	800	790
h_2 [meters]	730	770
Δh [meters]	70	20
b [meters]	35	10
L [meters]	4,000	21,000
P , Precipitation [mm/year] ¹	230	220
W_s , Recharge [mm] ²	Variable	Variable

RESULTS

Groundwater Catchment Delineation

A regional surface water drainage network would exist during sufficiently wet climatic conditions. The network has a total of 56 catchments (60–5,200 square kilometers) in or upgradient to the Cuatrociénegas Basin. The catchments were generated using geographic information systems based upon surface topography for the study area. The catchments encompass an approximately 91,000-square kilometer area labeled as the thick blue line shown on **Figure 6**. The area determined by the groundwater catchment delineation is used as the spatial extent for the precipitation and recharge calculations described below.

Precipitation Estimation

This section presents the results of spatially distributed precipitation in the Cuatrocienegas Basin regional study area. Precipitation is used to calculate recharge using the chloride-balance method. Precipitation is extrapolated linearly for two different precipitation-elevation relationships. González (2006) specified a maximum precipitation of approximately 400 millimeter/year on the highest mountains, but not a specific elevation or mountain range. Thus, precipitation is linearly extrapolated based on the maximum elevation of two Cuatrocienegas Basin area mountain ranges (Sierra San Marcos, 3,025 meters; and Sierra La Madera, 2,600 meters) to generate spatially distributed precipitation estimates for the study area. For the Sierra San Marcos (3,025 meters), the precipitation estimate is defined by the following equation for a line that describes valley-floor through mountain-top precipitation

$$P = 0.000097 E + 0.15 . \quad (8)$$

Where

P = precipitation (meters/year), and

E = elevation (meters).

For the Sierra La Madera (2,600 meters), the equation is

$$P = 0.000079 E + 0.16 . \quad (9)$$

Where

P = precipitation (meters/year), and

E = elevation (meters).

Both extrapolation equations are used for estimating spatially distributed recharge throughout the study area. Two precipitation extrapolation equations are used to give a range that accounts for uncertainty in spatially-distributed precipitation values.

Precipitation: PERSIANN Satellite Precipitation Estimates Compared with Gage Rainfall and Mountain Precipitation Extrapolation

Satellite-derived precipitation estimates using the PERSIANN data are shown in **Table 9** for the two areas of interest. The table also includes the average elevation of the two areas of interest, long-term valley-floor precipitation gage measurements (1942–2003; Rodríguez et al., 2005a), and the result of interpolated precipitation using long-term valley floor precipitation and mountain-top precipitation estimates based on vegetation requirements. The long-term average annual precipitation from the valley-floor Cuatrociéegas Basin Gage precipitation record (1942–2003) is approximately 220 millimeters/year (Rodríguez et al., 2005a). The valley-floor annual precipitation was 146 millimeters in 2002 and 337 millimeters in 2003 (Rodríguez et al., 2005a). No precipitation gage is installed in the Sierra La Madera.

Table 9. PERSIANN SATELLITE PRECIPITATION ESTIMATES COMPARED WITH GAGE RAINFALL AND MOUNTAIN PRECIPITATION ESTIMATE

Cuatrociéneas Basin Gage precipitation data range from 1942 to 2003 (years with no precipitation data are indicated by --) with a long-term average of approximately 220 millimeters/year (Rodríguez et al., 2005a). No precipitation gage is located in the Sierra La Madera. Extrapolated precipitation is calculated by entering the average elevation for the two areas of interest into the hypsometric curves (Equations 8 and 9) and described above. PERSIANN precipitation data are obtained from The University of California, Irvine by a special data request for the two areas of interest.

Area of Interest	North Latitude	South Latitude	West Longitude	East Longitude	Average Elevation	Year	PERSIANN Precipitation	Cuatro-Ciéneas Basin Gage	Extrapolated Precipitation 1	Extrapolated Precipitation 2
					[m]		[mm]	[mm]	[mm]	[mm]
61 Cuatrociéneas Basin Gage	27.02°	27.00°	102.08°	102.06°	794	2002	208	146		
						2003	664	337		
						2004	318	--		
						2005	223	--	223	224
						2006	472	--		
						2007	203	--		
						Average	348	220		
Sierra La Madera	27.04°	27.00°	102.40°	102.36°	2,125	2002	218			
						2003	656			
						2004	402			
						2005	264	No data	328	353
						2006	489			
						2007	196			
						Average	371			

PERSIANN precipitation estimates for the Cuatrocienegas Basin Gage location for the period of 2002–2007 range from 203–664 millimeters/year ($n=6$, average=348, standard deviation=186) and precipitation is estimated with PERSIANN at 146 millimeters in 2002 and 337 millimeters in 2003 for the Cuatrocienegas Basin Gage location. PERSIANN precipitation estimates for the Sierra La Madera location for the period of 2002–2007 range from 196–656 millimeters/year ($n=6$, average=371, standard deviation=180). Extrapolated precipitation estimates using the two hypsometric curves (based upon average elevations from the areas of interest of 794 meters and 2,125 meters) are 223 and 224 millimeters/year for the Cuatrocienegas Basin Gage location and 328 and 358 millimeters/year for the Sierra La Madera location.

Recharge Estimation with Chloride-Balance Approach

This section discusses the results of the chloride balance recharge estimates on groundwater catchments immediately surrounding the Cuatrocienegas Basin and in the larger regional groundwater catchment. The results of the recharge analysis are shown in **Table 10**.

Because of uncertainties in data, a range of spatially-distributed precipitation (P), spring discharge chloride concentration (Cl_r), and precipitation chloride concentration values (Cl_p) are considered for the chloride-balance recharge analysis. The Mexican government does not have a precipitation chloride monitoring program, so data are used from a precipitation monitoring station in west Texas and also estimated for northeast Mexico. Chloride in precipitation is from Big Bend National Park, Texas (Lamb and Bowersox, 2000; Gay et al., 2008; National Atmospheric Deposition Program, 2008) and also from estimates in northeast Mexico presented in Junge and Werby (1958). Spring water chloride concentration is 67.67 and 98.75 milligrams/liter in this analysis. A refinement of spring chloride concentration is presented in Chapter 4.

Table 10. RANGE OF VALUES FOR PERCENT OF PRECIPITATION RESULTING IN RECHARGE

A range of values are considered to account for data uncertainty in the recharge analysis.

¹Case 1: Precipitation extrapolation equation for the Sierra San Marcos (low P), and spring discharge chloride concentration for springs feeding the Santa Tecla Canal (low Cl_r).

²Precipitation chloride concentration ranges from 0.13 milligrams/liter (low Cl_p) to 2.00 milligrams/liter (high Cl_p)

³Case 2: Precipitation extrapolation equation for the Sierra La Madera (high P), and spring discharge chloride concentration for springs feeding the Saca Salada Canal (high Cl_r).

Chloride in Precipitation [mg/L]	Chloride in Spring Water [mg/L]	Percent Precipitation Resulting in Recharge
Sierra San Marcos Precipitation & Santa Tecla Canal Springs^{1,2}		
0.13	67.67	0.19
2.00	67.67	2.99
Sierra La Madera Precipitation & Saca Salada Canal Springs^{2,3}		
0.13	98.75	0.13
2.00	98.75	2.03

Bromide and Chloride Plot to Understand Chloride Sources or Sinks

The results of bromide and chloride analyses for water samples from wells and springs are shown on **Figure 9**. The bromide and chloride data for wells and springs in the Cuatrocienegas Basin region plot in a straight line suggesting that evaporative concentration of waters is the dominant process. Halite dissolution is not observed in Cuatrocienegas Basin waters — if it were to occur, an enrichment of chloride relative to bromide would be observed. Similarly, halite does not appear to be precipitating out of solution, except at isolated sites, such as Laguna Salada (approximately 10,000 milligrams/liter chloride, with an area of approximately 30,000 square meters; Minckley and Cole, 1968).

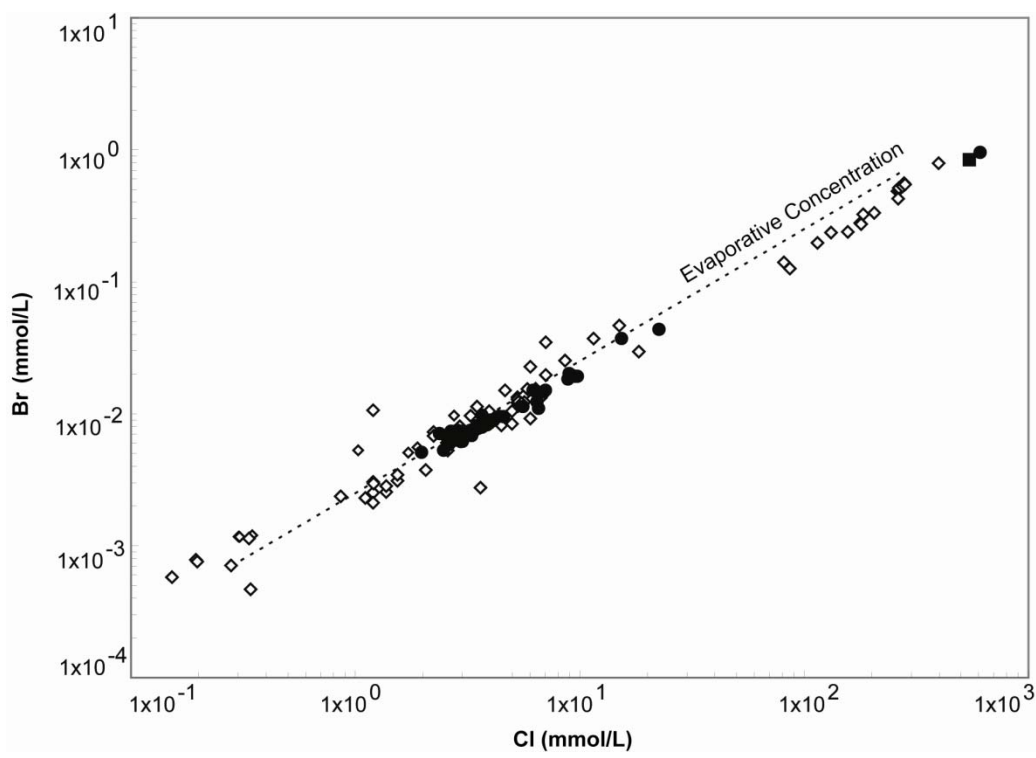


Figure 9. BROMIDE VERSUS CHLORIDE OF WATER SAMPLES FROM WELLS AND SPRINGS

Wells are shown as open diamonds and springs as solid circles. The dashed line represents evaporative concentration and the solid square shows a representative seawater value. If halite dissolution were occurring, the samples would show an enrichment of chloride relative to bromide as the waters evolve; thus, it is assumed that chloride in spring water originates from precipitation. Bromide and chloride data are from water samples collected in springs and wells in the Cuatrocienegas Basin region and are published in Evans (2005), Johannesson et al. (2005), and Rodríguez et al. (2005a).

Minckley and Cole (1968) presented a chloride value of approximately 300 milligrams/liter for Laguna Grande (and approximately 2,900 milligrams/liter for sulfate), an ephemeral lake where gypsum precipitation has developed an extensive gypsum dune complex. At Poza Churince, the source spring for Laguna Grande, Minckley and Cole (1968) reported a chloride concentration of approximately 110 milligrams/liter and a sulfate concentration of approximately 1,250 milligrams/liter. Thus, remobilization of chloride from these dunes probably represents a relatively low flux when the entire study area is considered.

The results of the chloride-balance recharge analysis for four scenarios are summarized on **Figure 10**. A local recharge area of approximately 4,000 square kilometers (Saca Salada and Santa Tecla catchments) produces observed spring discharge with high Cl_p and low P. A combined local and interbasin recharge area of approximately 7,000 square kilometers (the Cuatrocienegas Basin and the Hundido Valley) produces observed spring discharge with high Cl_p and high P. When low Cl_p and low P are considered, a regional interbasin recharge area of approximately 65,000 square kilometers produces observed spring discharge. A regional interbasin recharge area of approximately 91,000 square kilometers (including all catchments upgradient of the Cuatrocienegas Basin to the Sierra Madre Occidental and Sierra Madre Oriental and the Ocampo Valley to the north) produces observed spring discharge when low Cl_p and high P are considered.

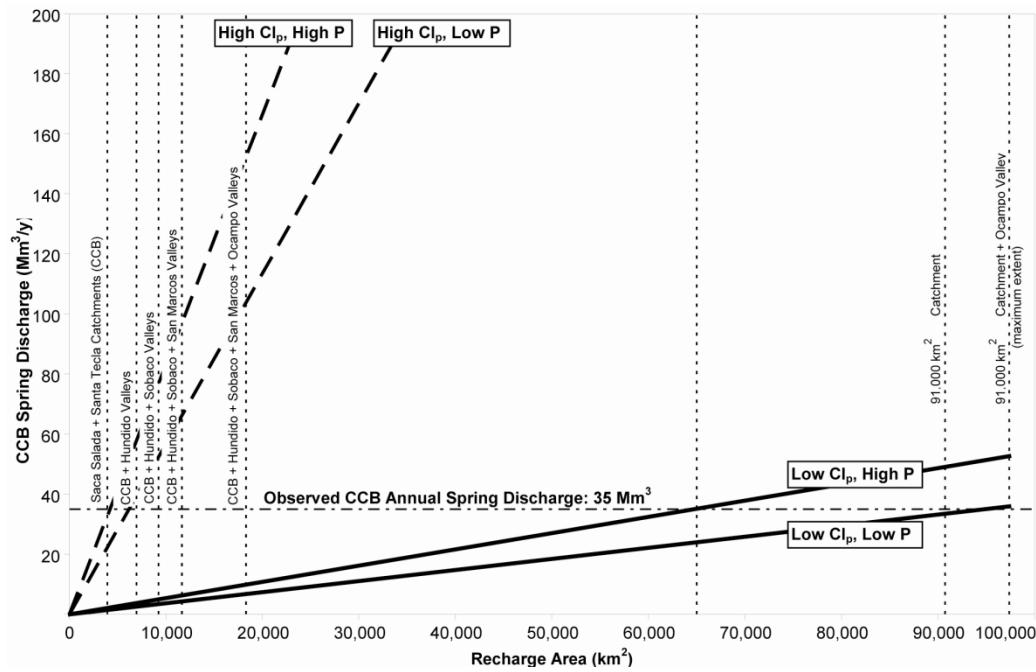


Figure 10. RECHARGE AREA VERSUS CUATROCIÉNEGAS BASIN SPRING DISCHARGE

A recharge analysis calculates the recharge area needed to produce observed Cuatrocienegas Basin annual spring discharge (35,000,000 cubic meters/year). Four cases (two bold dashed lines and two bold solid lines) account for data uncertainty (1. high precipitation chloride concentration and high precipitation; 2. high precipitation chloride and low precipitation; 3. low precipitation chloride and high precipitation; and 4. low chloride and low precipitation). The horizontal dotted and dashed line indicates the observed Cuatrocienegas Basin annual spring discharge volume of 35,000,000 cubic meters/year. The eight dotted vertical lines show incrementally greater summations of plausible recharge catchments. A calculated discharge of 35,000,000 cubic meters/year occurs where the bold solid and dashed lines intersect the dotted and dashed horizontal line for the four different recharge scenarios. For reference, the 91,000-square kilometer catchment corresponds to the thick blue line in Figure 6.

The above analysis assumes the dry deposition of chloride is negligible. However, if we assume a dry deposition of chloride that is equivalent to the chloride concentration in precipitation, following the approach of Scanlon et al. (2007), the recharge analysis changes slightly. The result of adding chloride from dry deposition would be the doubling of the recharge rate. For example, if the chloride input to the system is doubled, the volume of water recharging must also be doubled to maintain the same chloride concentration in spring water.

Spring Discharge Measurement

This section presents discharge measurements for the Saca Salada and Santa Tecla Canals, Poza La Becerra (the largest spring in the Cuatrocienegas Basin), and historic spring discharge from the Ocampo Valley into the Cuatrocienegas Basin via the Río Cañon.

Canal Discharge Measurements

Spring discharge measurements (conducted using a handheld acoustic Doppler velocimeter flow meter) in the two canals draining the Cuatrocienegas Basin are presented in **Table 11** (measurement locations are shown on **Figure 2**). The canal discharge represents integrated flow from dozens of springs that are extremely difficult to measure individually. Saca Salada canal discharge fluctuates seasonally. During summer and fall, irrigation and increased evapotranspiration of riparian vegetation along the unlined canal reduce Saca Salada discharge. Conversely, Santa Tecla Canal discharge has decreased during the study period, during which time the region has experienced a prolonged drought.

Table 11. SACA SALADA AND SANTA TECLA CANAL INSTANTANEOUS DISCHARGE

Refer to locations one (Saca Salada Canal) and two (Santa Tecla Canal) on Figure 2 for canal gaging locations.

¹Discharge measurements from January 2005–June 2006 are used for catchment delineation water budget calculations; however, additional discharge measurements (July 2006–July 2007) are presented that are not included in the calculations in Wolaver et al. (2008).

²The Santa Tecla Canal was closed for repairs during January 2007.

Date	Santa Tecla Discharge [L/sec]	Saca Salada Discharge [L/sec]
January 29, 2005	216	1,243
March 14, 2005	232	1,321
October 29, 2005	170	934
January 9, 2006	176	1,259
March 13, 2006	171	1,258
June 11, 2006	159	885
Average ¹ January 2005–June 2006	187	1,150
Standard Deviation ¹ January 2005–June 2006	29	188
July 29, 2006	153	821
January 27, 2007 ²	--	1,613
July 4, 2007	218	1,147
Average ¹ January 2005–July 2007	187	1,109
Standard Deviation ¹ January 2005–July 2007	30	197

Canal Discharge Gaging Using a Stage Discharge Relationship

In addition to instantaneous discharge measurements, long-term continuous pressure transducer data measuring canal stage were collected in the Saca Salada Canal from January 29, 2005–July 11, 2006. Combined with the instantaneous discharge data, a stage-discharge relationship was constructed for the Saca Salada Canal. The stage-discharge relationship has the following mathematical definition

$$Q = 0.0009 h + 0.89 . \quad (10)$$

Where

Q = discharge (liters/second), and

h = stage (meters).

The equation is used to calculate an average Saca Salada Canal discharge of approximately 930 liters/second.

It is important to note the stage-discharge relationship is generated using a long-term continuous pressure transducer that was not vented to the atmosphere. Changes in atmospheric pressure caused by diurnal temperature fluctuations and weather systems can affect the stage recorded by the pressure transducer. Typically, a weather service barometer can be used to correct pressure transducer measurements. No barometric data are available for the period of record. Thus, a barometric correction cannot be done. This limitation in the data is recognized. However, because this research project considers several measurements taken over the study period, it is considered that the measurements constitute a random suite of values that can effectively estimate discharge. In addition,

plant growth also can affect the readings of a pressure transducer—this research project does not consider any vegetation changes in the stage-discharge relationship.

Poza La Becerra Discharge Measurements

In addition to canal discharge measurements near the Cuatrocienegas Basin outlet, the results of gaging for Poza La Becerra (the largest spring in the Cuatrocienegas Basin) are shown in **Table 12**.

Table 12. POZA LA BECERRA INSTANTANEOUS DISCHARGE

Refer to location three on Figure 2 for canal gaging location.

¹Discharge measurements from January 2006–June 2006 are used for catchment delineation water budget calculations; however, additional discharge measurements (July 2006–July 2007) are presented that are not included in the calculations in Wolaver et al. (2008).

Date	Discharge [L/sec]
January 3, 2006	548
March 17, 2006	592
June 11, 2006	594
Average ¹ January 2006–June 2006	578
Standard Deviation ¹ January 2006–June 2006	26
July 30, 2006	558
January 27, 2007	580
July 2, 2007	504
Average ¹ January 2006–July 2007	563
Standard Deviation ¹ January 2006–July 2007	34

Measurements at Poza La Becerra show constant spring discharge from winter to summer 2006. Over the period of record, Poza La Becerra discharge varies from 504 to 594 L/sec. The difference of readings between winter and summer is approximately 50 L/sec and is within the approximately \pm 5–10 percent uncertainty expected with this method. Thus, discharge is essentially stable during the period of record.

Ocampo Valley Historic Spring Discharge to the Cuatrociénegas Basin

Minckley (1969) presents a historic spring discharge value from the Ocampo Valley into the Cuatrociénegas Basin (measured at the former spring at Río Cañon) of approximately 250 liter/sec. For the recharge analysis, historical inflow from the Ocampo Valley is ignored. Calegari (1997) presents anecdotal evidence that Río Cañon discharge was sufficient to power two wheat mills using water wheels.

Cuatrociénegas Basin Flow Summary

A summary of Cuatrociénegas Basin discharge measurements is presented in **Table 13**. The total present basin discharge is approximately 35,000,000 cubic meters/year (**Table 14**). Historically, the Río Cañon discharged approximately 8,000,000 cubic meters/year into the Cuatrociénegas Basin prior to large-scale groundwater development for agriculture in the Ocampo Valley (**Table 14**).

Canal discharge measurements indicate an annual Cuatrociénegas Basin spring discharge of approximately 35,000,000 cubic meters/year, compared to an approximate canal discharge of approximately 53,000,000 cubic meters/year presented by Lesser y Asociados (2001). Because of a transducer failure in the Saca Salada Canal, actual canal discharge measurement may be closer to those of Lesser y Asociados (2001). However, the more conservative value is used for this study.

Agricultural diversions and increased summer evapotranspiration decrease Saca Salada discharge. Actual composite annual spring discharge may be elevated, supported by the consistent discharge measured at Poza La Becerra.

Table 13. CUATROCIÉNEGAS BASIN ANNUAL CANAL DISCHARGE

Canal	Discharge [m ³ /year]
Saca Salada Canal	29,076,192
Santa Tecla Canal	5,897,232
Total Annual Cuatrocienegas Basin Discharge	34,973,424

Table 14. CUATROCIÉNEGAS BASIN FLOW SUMMARY

¹Prior to groundwater development in the Ocampo Valley, the Río Cañon flowed into the Cuatrocienegas Basin.

Flow	Flow Rate [m ³ /year]	Inflow / Outflow
Saca Salada Canal	29,000,000	Outflow
Santa Tecla Canal	6,000,000	Outflow
Ocampo Valley	8,000,000	Inflow ¹

Evaluation of Interbasin Groundwater Flow Using an Analytical Model

Chloride-balance recharge estimates suggest that a regional groundwater system supplies Cuatrocienegas Basin springs. The results of the analytical model suggest that interbasin flow is possible from the Ocampo and Hundido Valleys to the Cuatrocienegas Basin under a regional precipitation value of approximately 220 millimeters/year (for the location of the two analysis lines), plausible permeability values for carbonate terrains (from approximately 1×10^{-5} to 1×10^5 meters/second), and a conservative one percent of

precipitation recharge rate. Hydraulic conductivity values from carbonate terranes are shown on **Figure 11**.

DISCUSSION

Groundwater Catchment Delineation

Groundwater catchments delineated by this research project are shown on **Figure 6**. This section describes groundwater catchment delineation for the Cuatrocienegas Basin and also the identification of a paleo surface water drainage network in the study area.

Groundwater Catchments: Discharge in the Cuatrocienegas Basin

Local flow dominates in the Santa Tecla Canal spring system with the majority of recharge originating in the Sierra San Marcos. However, some regional groundwater flow probably contributes to these springs. In the springs that feed the Saca Salada Canal, high, steady discharge and elevated chloride concentration dominate, suggesting a predominantly regional flow system that includes the Sobaco Valley, Hundido Valley, and San Marcos Valley. The Saca Salada Canal spring system may also include recharge from a larger regional aquifer system that may include recharge from the Río Nazas or mountains in eastern Chihuahua. During predevelopment conditions, a groundwater-fed surface water system (and perhaps also associated interbasin groundwater system) flowed from the Ocampo Valley to the Cuatrocienegas Basin.

A surface hydraulic connection does not currently exist. However, it is possible that even as northeastern Mexico dried climatically in the late Holocene to the present day (Castiglia and Fawcett, 2006), a regional surface water flow system persisted. This surface water flow system eventually retreated into the subsurface in highly permeable carbonate rocks present throughout the study area.

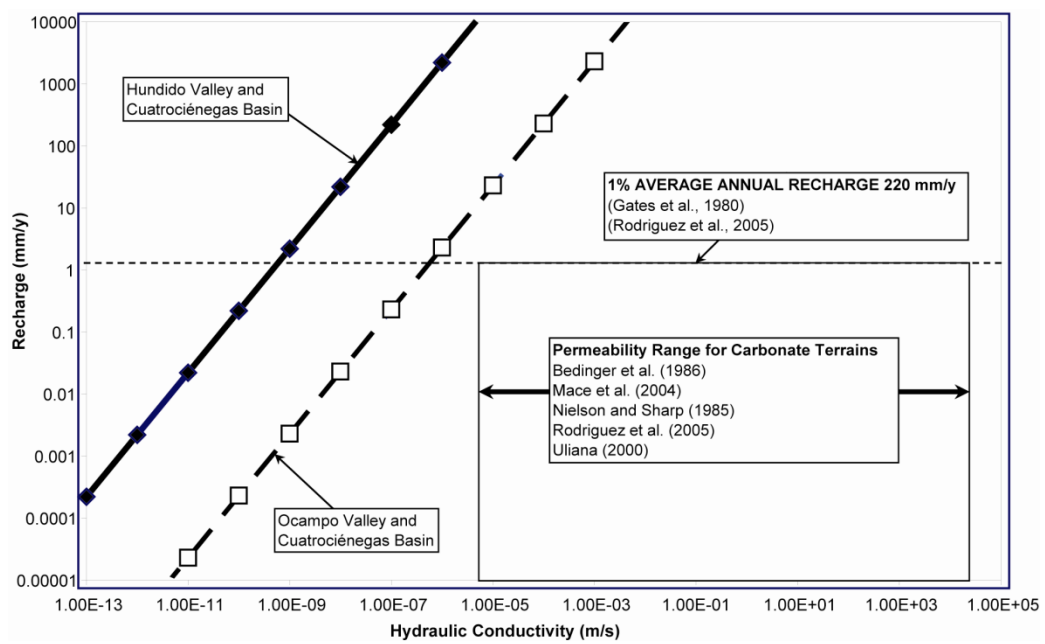


Figure 11. RESULTS OF ANALYTICAL MODEL EVALUATING INTERBASIN GROUNDWATER FLOW

Evidence supporting the hypothesis of a surface water system in a wetter climate that now provides the topographic gradient for an interbasin, regional groundwater flow system includes (1) lacustrine travertine deposits, (2) lacustrine deltaic deposits, (3) deep canyons at the Cuatrocienegas Basin outlet, and (4) large carbonate springs with relatively constant discharge. The model evaluates interbasin groundwater flow between the Ocampo and Hundido Valleys and the Cuatrocienegas Basin. The analytical model shows that interbasin groundwater flow occurs from adjacent valleys to the Cuatrocienegas Basin below the one-percent recharge dotted line and to the right of the two diagonal model solution lines in the shaded box of plausible permeability values. Permeability values for carbonate terrains are shown in **Table 2**. Analytical model input values are shown in **Table 8**.

Minckley (1969) suggested a travertine deposit that rises 30–40 meters above the southwestern valley floor may be evidence of a former lake filling the Cuatrocienegas Basin. Rodríguez et al. (2005a) used carbon-14 to estimate that the travertine deposit formed approximately 17,000 years ago. The possible lacustrine travertine deposit is shown on **Figure 12**. Flat-topped, raised alluvial fans on the eastern flank of the Sierra San Marcos below two large canyons suggest lacustrine alluvial fan/deltaic deposition during a previous wetter climate when the Cuatrocienegas Basin was filled by a lake. Present surface drainage from the canyons bypasses the raised fans, downcutting channels in the older alluvial deposit. Whereas no beach deposits have been noted in the Cuatrocienegas Basin, the ancestral Lake Sacramento of New Mexico did not leave beach deposits in a similar karst terrain (Hawley, 1993).

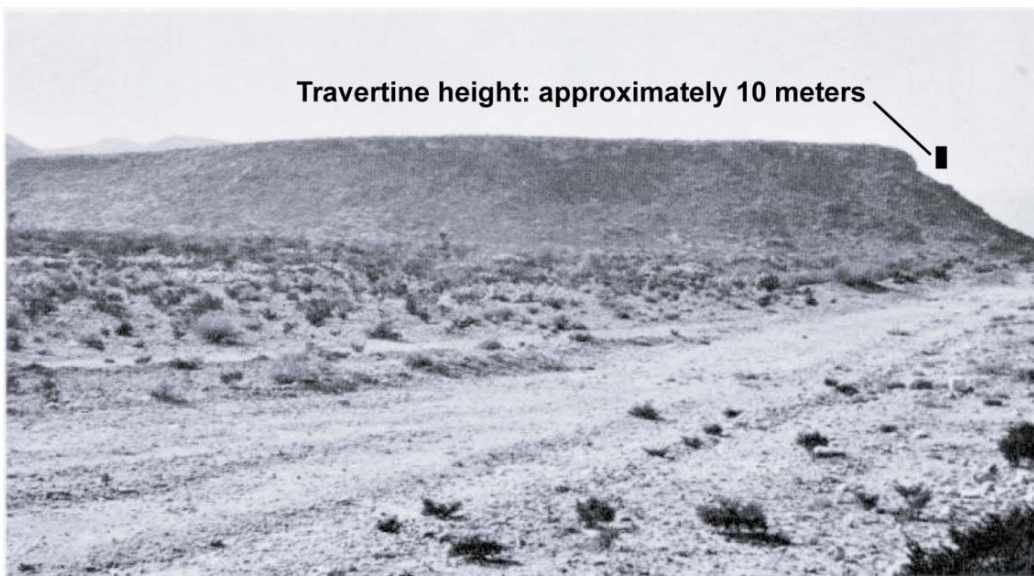


Figure 12. TRAVERTINE DEPOSIT ON THE WEST FLANK OF THE SIERRA SAN MARCOS

This travertine deposit is attributed to deposition in a lacustrine environment. The height of the vertical bar indicates an approximate travertine height of 10 meters. The travertine strata cap the hill and are roughly horizontal. Photo by Minckley, 1969.

Deep canyons exist in the north-south trending ridges that form the eastern boundary of the Cuatrocienegas Basin. Whereas the basin was recently closed, surface water flowing in a previous wetter period most certainly carved these features. The Cuatrocienegas Basin outlet canyon suggests that surface water erosion occurred during past wetter climates and is shown on **Figure 13**. Downcutting of the ridges on the eastern border of the Cuatrocienegas Basin drained the lake that filled the Cuatrocienegas Basin, stranding a travertine deposit and alluvial fans. A canyon also exists where the Río Canyon used to drain the Ocampo Valley, suggesting significant discharge in past wetter climates.

Whereas surface water discharge does not currently occur in this 91,000-square kilometer catchment upgradient to the Cuatrocienegas Basin (other than water from the Río Nazas, which is entirely used for irrigated agriculture in the vicinity of the City of Torreón). This large catchment is inferred to represent the possible extent of a regional carbonate aquifer providing constant discharge to the Cuatrocienegas Basin.

Precipitation: PERSIANN Satellite Precipitation Estimates Compared with Gage Rainfall and Mountain Precipitation Extrapolation

The PERSIANN method of satellite-derived precipitation may become useful for arid, ungaged regions, however, PERSIANN over-estimates valley-floor precipitation. Thus, confidence is low for regional application of PERSIANN precipitation estimates in the arid, ungaged regions of northeast Mexico — particularly in the topographically complex terrain of northeast Mexico. Calibration of PERSIANN needs to be improved using more gage precipitation data for longer periods of record and greater elevation ranges (i.e., use precipitation gage data from valley and mountainous locations).



Figure 13. CUATROCIÉNEGAS BASIN OUTLET CANYON SUGGESTS EROSION IN PAST WETTER CLIMATE.

Stream is fed by the Cuatrocienegas Basin canal discharge. Prior to canal construction in the early and mid-1960s, all Cuatrocienegas Basin spring surface water discharge flowed to large playa lakes and wetlands in the southeast of the basin and surface water flow through this basin outlet canyon did not occur. Photo by Miller (1961).

The long-term average annual precipitation from the valley-floor Cuatrocienegas Basin Gage precipitation record (1942–2003) is approximately 220 millimeters/year (Rodríguez et al., 2005a). PERSIANN precipitation estimates for the Cuatrocienegas Basin Gage location for the period of 2002–2007 range from 203–664 millimeters/year, with an average of 348 millimeters/year. Thus, the PERSIANN precipitation estimate for a six-year average is approximately 1.6 times greater than the long-term (1942–2003) gage record. In addition, PERSIANN overestimates precipitation for the two years that there is valley-floor gage data (i.e., in 2002, 146 vs. 208 millimeters/year, and in 2003, 337 vs. 664 millimeters/year). The PERSIANN precipitation estimates are also higher than the extrapolated precipitation (223 and 224 millimeters/year). PERSIANN precipitation estimates for the Sierra La Madera location for the period of 2002–2007 range from 196–656 millimeters/year with an average of 371 millimeters.

Future studies should consider comparing PERSIANN precipitation with mountain gage precipitation. Extrapolated precipitation estimates using the two hypsometric curves are 328 and 358 millimeters/year for the Sierra La Madera location, values that are close to the PERSIANN six-year average precipitation of 371 millimeters/year. However, it is evident that PERSIANN precipitation estimates must be constrained by ground-truth data in this, and perhaps, similar settings.

Recharge Estimation

For springs that feed the Saca Salada Canal, precipitation on local groundwater catchments on the Sierra La Madera, Sierra La Fragua, and western flank of the Sierra San Marcos are not sufficient to generate observed discharge, which is estimated conservatively low. If conservatively low precipitation chloride values are used, the water budget balances for an approximately 91,000-square kilometer recharge area that stretches to the Sierra Madre Oriental and Occidental, as shown on **Figure 6**. This result

suggests a large, regional aquifer system provides water to Cuatrocienegas Basin springs. If a value of 2.0 milligrams/liter precipitation chloride calculation is applied to a regional recharge area, calculated discharge is about an order of magnitude too large. Alternatively, springs in the Cuatrocienegas Basin may derive groundwater from a regional carbonate aquifer system that was recharged in a past pluvial period of wetter climatic conditions.

A regional groundwater catchment of approximately 10,000 square kilometers is considered that includes the Cuatrocienegas Basin, in addition to the upgradient Hundido, Sobaco, and San Marcos Valleys. These catchments are shown on **Figure 6**. Recharge estimates suggest that groundwater supplying Cuatrocienegas Basin springs is recharged in groundwater catchments located in the intermontane valleys 50–100 kilometers to the south of the Cuatrocienegas Basin. If the pre-development Ocampo Valley is added, the recharge area increases to approximately 18,000 square kilometers.

The analysis assumes chloride dry deposition is negligible. If a dry deposition of chloride equivalent to the chloride concentration in precipitation is assumed, the recharge rate would be double. Data do not exist to show this is occurring and it is therefore an uncertainty of the analysis. If dry deposition of chloride contributed an amount equivalent to precipitation, then it is possible that the recharge area needed to produce observed spring discharge could be less than the 18,000 square kilometers considered in this research.

Spring Discharge Measurement

Canal Discharge Measurements

Santa Tecla Canal discharge has steadily decreased during the study period, during which time the region has experienced a prolonged drought. Thus, decreased Santa Tecla Canal discharge may represent the effects of a combined local and regional groundwater flow system influenced by decreased Sierra San Marcos precipitation. Alternatively, the Santa Tecla canal leaks. Discharge in the Saca Salada Canal varies with time. Possible causes of the change in canal discharge include evapotranspiration of vegetation along the unlined banks of the canal, water diversions for crop irrigation within the basin, and/or variations in spring discharge.

Poza La Becerra Discharge Measurements

Measurements at Poza La Becerra show constant spring discharge from winter to summer 2006. These results support the hypothesis that a regional groundwater flow system discharges to some Cuatrociénegas Basin springs.

Analytical Interbasin Flow Model Evaluation

Referring to **Figure 11**, interbasin flow would occur with recharge and hydraulic conductivity conditions to the right of the lines labeled “Hundido Valley and Cuatrociénegas Basin” and “Ocampo Valley and Cuatrociénegas Basin” (i.e., topographic divides would not represent groundwater divides and that interbasin flow is possible). Conversely, a groundwater divide with an associated local flow system would form on the left of these lines—a condition where interbasin flow would not be possible.

Based on the analytical model, interbasin flow occurs from Hundido and Ocampo Valleys to the Cuatrociénegas Basin under plausible transmissivity and recharge conditions. The model considered recharge rates less than or equal to one percent of

precipitation, (a typical recharge rate suggested by Gates et al., 1980 for arid West Texas) and typical carbonate rock transmissivity values. Local groundwater flow systems would only develop in the study area under conditions of very high recharge rates that might have occurred during past pluvial periods, or in isolated locations with lower than expected permeability values.

CONCLUSIONS

An integrative data approach provides a framework for the evaluation of recharge areas in developing arid karst aquifer systems with sparse hydrogeologic data. In this research, disparate geologic data are integrated, including field observations, historical hydrologic data (that may be anecdotal), and all other available data, including geologic maps, digital elevation models, geographic information systems, analytical models, water quality parameters, environmental isotopes, and spring discharge data, to evaluate recharge areas to support development of effective groundwater management policies.

In northeast Mexico long-term well records are sparse. Delineation of groundwater catchments based upon surface topography and geology reveal an approximately 91,000-square kilometer basin upgradient of the Cuatrociénegas Basin that includes the terminal drainage of the Río Nazas near the City of Torreón, which has headwaters in the Sierra Madre Occidental. A surface water flow system probably existed until the late Pleistocene that linked the Río Nazas to the Río Grande via a series of Chihuahuan Desert lakes, which included the Cuatrociénegas Basin (and Laguna Mayrán near the City of Torreón, as shown on **Figure 1**). As the regional climate dried, surface water drainages became truncated, but a regional aquifer exists, and interbasin groundwater flow occurs under topographic divides between valleys (e.g., the Hundido and Sobaco Valleys). Presently, the Cuatrociénegas Basin represents a low elevation discharge zone of a regional aquifer system.

Regional flow provides groundwater to Cuatrocienegas Basin springs with elevated, nearly constant-discharge (e.g., Poza La Becerra, Poza Azul, Poza Escobedo, Poza Churince, etc.). A mixed local and regional groundwater flow system supplies water to smaller springs at the head of the Santa Tecla Canal on the eastern flank of the Sierra San Marcos which decreases discharge during periods of drought. Recharge estimates in the Ocampo Valley appear to be sufficient to generate historical, pre-development Río Canon discharge (neglecting interbasin groundwater discharge).

Because of the uncertainty of chloride concentration in precipitation, it is unclear what portion of the approximately 91,000-square kilometer regional groundwater catchment currently provides for basin spring flow. However, it is inferred that a regional aquifer system discharges to the larger springs (such as Poza La Becerra, Poza Azul, Poza Escobedo, and Poza El Churince). Given the range of chloride values for precipitation possible, the recharge area may range from a few thousand to >10,000 square kilometers. Either a significant portion of groundwater discharge is presently recharged in the intermontane basins within approximately 100 kilometers to the south and west of the Cuatrocienegas Basin, or groundwater recharged during previous wetter climatic periods flows to the Cuatrocienegas Basin from a portion of a larger 91,000-square kilometer regional carbonate aquifer.

An approximately 18,000-square kilometer hydrogeologic system is considered with groundwater presently flowing from mountain highland recharge areas surrounding the Sobaco, Hundido, Ocampo, and San Marcos Valleys to the Cuatrocienegas Basin. Spring discharge in the Cuatrocienegas Basin may also include paleo groundwater recharged to the larger 91,000-square kilometer regional aquifer system during past pluvial periods. The regional aquifer system follows a topographic gradient that during past pluvial periods may have linked the Río Nazas and the Río Aguanaval of the Sierra

Madre Occidental to the Río Grande via the Cuatrociénegas Basin and other large, presently dry, upgradient lakes.

This study develops procedures to delineate regional groundwater catchments in arid and semi-arid, karst aquifers with sparse hydrogeologic data. The approach is tested in the Cuatrociénegas Basin of northeastern Mexico. The procedures may be used to understand the spatial extent and quantify recharge processes in similar terrains globally.

Chapter 3: Using Tritium, Oxygen Isotopes, Noble Gases, and Strontium Isotopes to Evaluate Residence Time and Recharge Processes in an Arid Karst Aquifer

A revised version of this chapter will be submitted for publication.

ABSTRACT

Tritium, oxygen isotopes, noble gases, and strontium isotopes are used to evaluate residence time and recharge processes in the arid karst aquifer of the Cuatrocienegas Basin, Coahuila, Mexico. This approach is applied to evaluate the spatial extent of the regional aquifer system contributing to the springs of the Cuatrocienegas Basin. Tritium is used to estimate aquifer residence time. Oxygen isotopes are used to infer precipitation elevation. Dissolved noble gases in spring water are evaluated to assess groundwater recharge elevation. Strontium isotopes of spring water and travertine evaluate the source of strontium ions to evaluate the aquifer through which groundwater flows. Isotopes of dissolved helium gas in spring water are used to infer processes affecting groundwater geochemistry and provide insight into the origin of spring water.

The results of tritium in most spring waters is under the detection limit of 0.1 tritium units, suggesting that most precipitation resulting in recharge to Cuatrocienegas Basin springs occurred at least 50 years ago. The results of oxygen isotopic analyses exhibit a $\delta^{18}\text{O}$ value ranges from -8.2 to -5.7‰ with a mean $\delta^{18}\text{O}$ value of $-6.5 \pm 0.82\text{\textperthousand}$, suggesting a precipitation elevation that ranges from 1,170 to 2,350 meters. Noble gas data show that the approximate elevation of the water table at which recharge occurs for the Cuatrocienegas Basin is between approximately 720 and 770 meters (indicated by recharge temperatures ranging from 17.0°–26.0°C). This suggests topographic divides are not groundwater divides and that interbasin groundwater

flow is plausible. The values of helium isotopes, reported as R/R_a , range from a low of 0.9 to high of 1.8, suggesting that some component of mantle-derived helium is leaking up basement-involved faults in the Cuatrocienegas Basin. Strontium isotope results ($^{87}\text{Sr}/^{86}\text{Sr}$) for seventeen water samples and three travertine samples range between approximately 0.707428 to 0.707468 ± 0.000016 , suggesting that the Barremian/Aptian Cupido Formation is the regional carbonate aquifer and that groundwater does not interact significantly with lower Cretaceous siliciclastics of the San Marcos Formation. Thus, a regional carbonate aquifer that does not have appreciable recharge of rapid, locally-derived precipitation contributes to springs in the Cuatrocienegas Basin.

INTRODUCTION

This research uses tritium, oxygen isotopes, noble gases, and strontium isotopes to evaluate residence time and recharge processes to infer the spatial extent of the regional aquifer system contributing to the springs of the Cuatrocienegas Basin (**Figure 14**). This approach is important because resource managers must understand the spatial extent of the Cuatrocienegas Basin regional groundwater flow systems to manage groundwater effectively. This aquifer evaluation approach builds upon that presented by Wolaver et al. (2008). New geochemical and isotopic data augment and expand upon the previous aquifer delineation approach. This approach permits the testing of the hypothesis that significant flow to Cuatrocienegas Basin springs originates from recharge from catchments external to the Cuatrocienegas Basin by providing insights on residence time and recharge processes. Cuatrocienegas Basin features are shown on **Figure 15**.

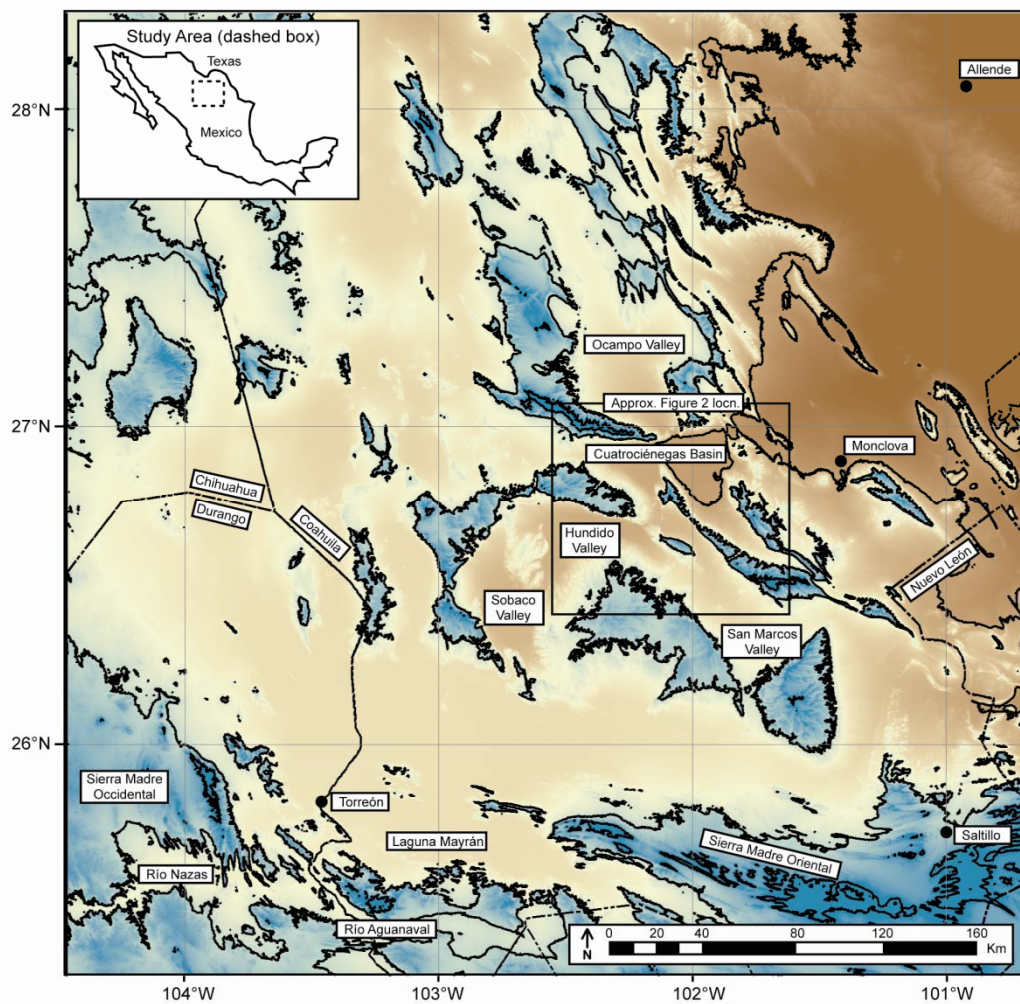


Figure 14. CUATROCIÉNEGAS BASIN STUDY AREA

Contour interval ranges from brown (750-meter) to green (1,500-meter and 2,250-meter). State boundaries are indicated by dashed lines.

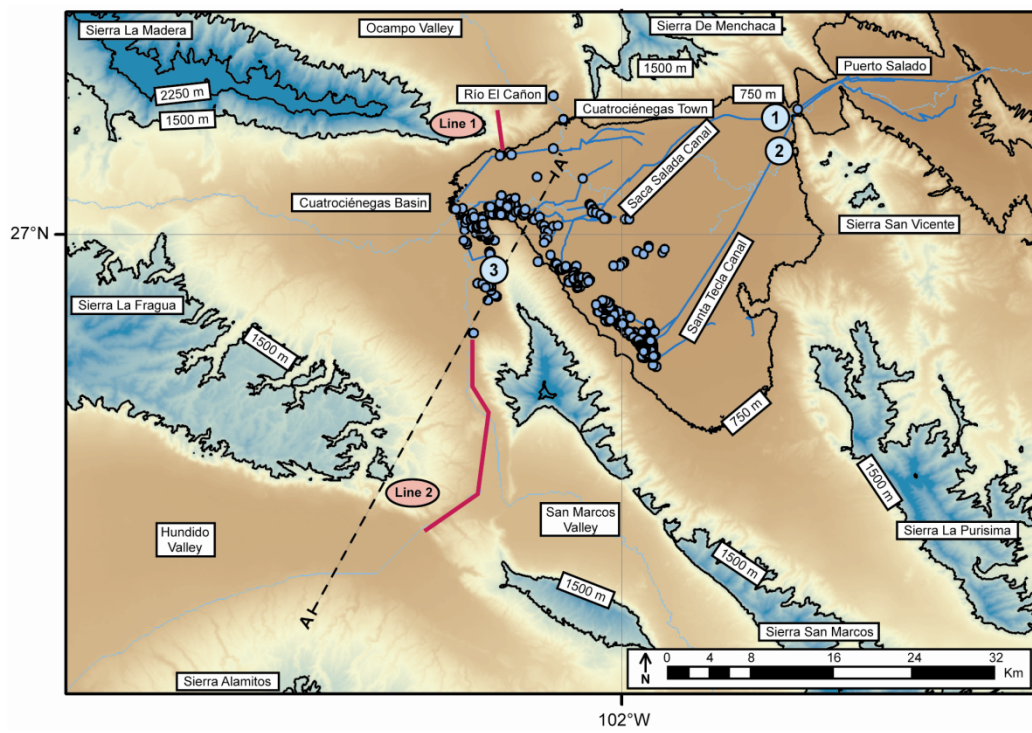


Figure 15. CUATROCIÉNEGAS BASIN GEOGRAPHIC FEATURES AND ANALYTICAL MODEL LOCATIONS

Explanation: springs (blue dots), analytical model locations (red lines), canals (light blue lines), discharge measurement locations (light blue numbered circles), inferred surface drainage network (light blue dashed line), and 750-meter contour intervals (low–high elevation ranges from brown–green, respectively). The location of cross section A-A' (Figure 17) is shown as a dashed black line.

Tritium is used to determine aquifer residence time. Oxygen isotopes are used to infer precipitation elevation. Dissolved noble gases in spring water are evaluated to assess groundwater recharge elevation. Strontium isotopes of spring water and travertine evaluate the source of strontium ions to evaluate the aquifer through which groundwater flows. Isotopes of dissolved helium gas in spring water are used to infer processes affecting groundwater geochemistry and provide insight into the origin of spring water.

BACKGROUND

The Cuatrocienegas Basin is located in a complex geologic setting. The structural, tectonic, hydrostratigraphic, and hydrogeologic setting of the Cuatrocienegas Basin and surrounding region are discussed below. The Cuatrocienegas Basin is compared with similar regional arid, karst aquifer systems where interbasin flow occurs.

Goldhammer (1999) described rifting associated in northeast Mexico associated with the opening of the Gulf of Mexico that created basement highs (e.g., Coahuila Platform). These permitted shallow water marine carbonate deposition and lows (e.g., the Sabinas Basin located approximately 125 kilometers northeast of the Cuatrocienegas Basin) that resulted from passive margin accumulation from the Upper Jurassic–the Early Upper Cretaceous.

Structure and Tectonics

The Cuatrocienegas Basin is located at the northern edge of the highly folded and faulted Sierra Madre Oriental. Goldhammer (1999) described northeastern Mexico Upper Triassic–Middle Jurassic stratigraphy. Lehmann et al. (1999) correlated Cretaceous carbonate mountain anticlines surrounding the Cuatrocienegas Basin with rocks in Texas. Murillo (1997) noted that the Lower Cretaceous Cupido Formation, which crops out in the Cuatrocienegas Basin, is the equivalent of the Sligo Formation of Texas.

Eguiluz de Antunano (2001) quantified Sabinas Basin regional marine sediment accumulation >5,000 meters in three supersequences: (1) synriftal sediments of primarily conglomerates and evaporates, (2) high frequency cycles of carbonates, evaporates, and coastal siliciclastics deposited on extensive platforms on a passive margin (144–96 million years ago); and (3) regressive terrigenous clastic facies deposited in a foreland setting (96–39.5 million years ago).

Topography

Elevation in the Cuatrocienegas Basin region ranges from approximately 770 meters in the valley itself to over 3,000 meters in the Sierra La Madera that is located immediately to the north of the Cuatrocienegas Basin. Regional topography is shown in **Figure 16**. Elevation increases to the north, west, and south of the Cuatrocienegas Basin, providing a topographic gradient that may also represent a gradient for groundwater flow into the Cuatrocienegas Basin, based on the regional flow principals of Hubbert (1940) and Tóth (1963). Red indicates vegetation in this LANDSAT image and includes irrigated agriculture to the east of the Cuatrocienegas Basin that relies on spring discharge and also thin mountain-top pine forests.

Hydrostratigraphy

Evans (2005) described the stratigraphy in the Cuatrocienegas Basin as primarily Jurassic and Cretaceous carbonates, evaporites, and siliciclastics overlying a basement comprised of Triassic granodiorite. Lesser y Asociados (2001) and Rodríguez et al. (2005a) presented a hydrogeologic conceptual model for the Cuatrocienegas Basin and adjacent valleys that includes parallel mountain anticlines and synclines filled with alluvium and lacustrine sediments. A geologic cross section from the Hundido Valley to the Cuatrocienegas Basin is shown on **Figure 17**.

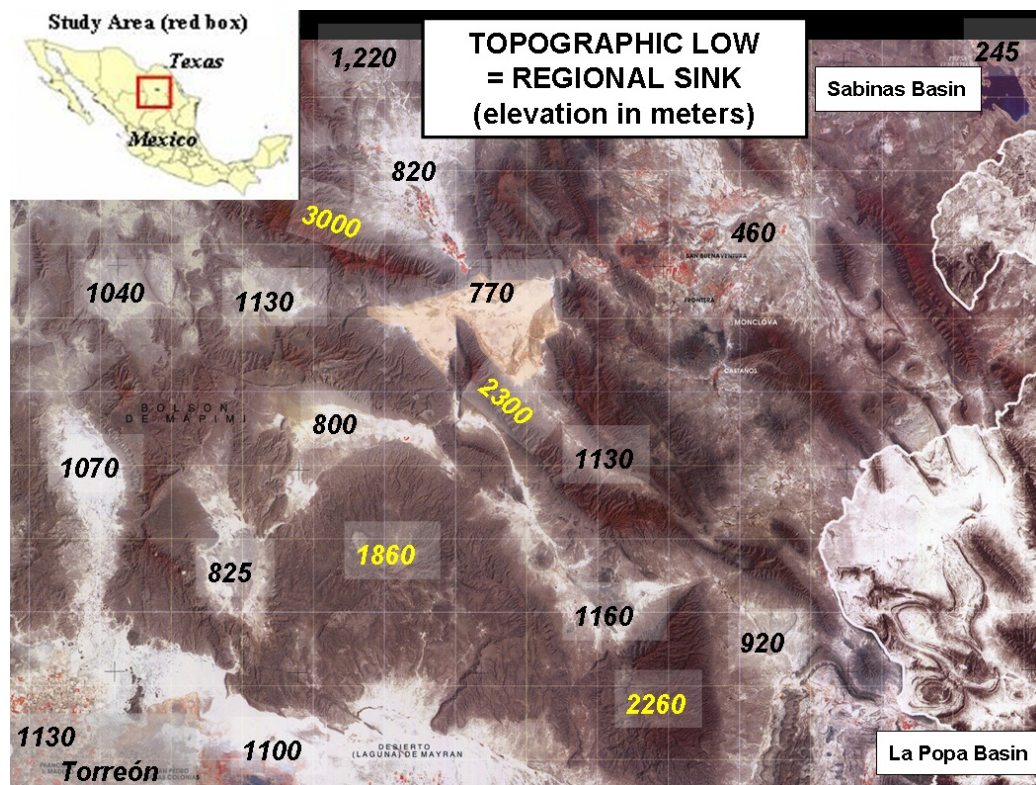


Figure 16. TOPOGRAPHY OF THE CUATROCIÉNEGAS BASIN REGION

Valley-floor elevation is shown in black. Mountain-top elevation is shown in yellow. Red indicates vegetation in this LANDSAT image with 10-kilometer grid marks. The Cuatrocienegas Basin is at a regional low elevation.

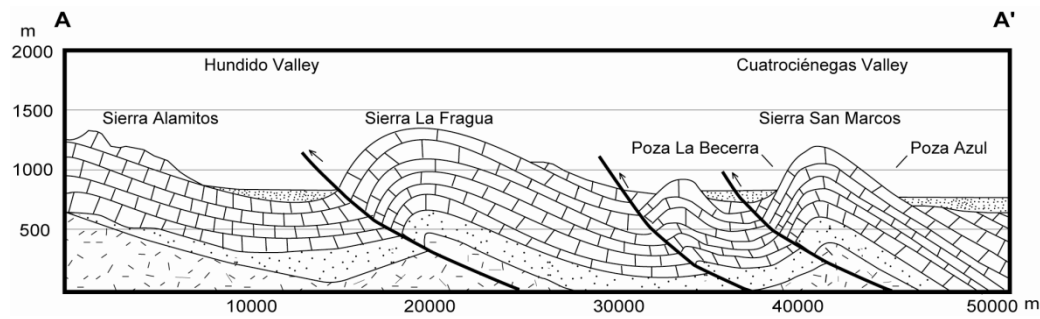


Figure 17. GEOLOGIC CROSS SECTION FROM THE HUNDIDO VALLEY TO THE CUATROCIÉNEGAS BASIN

Cross section passes through the Sierra La Fragua and Sierra San Marcos (after Rodríguez et al., 2005a). Orientation of geologic cross section is from south south-west to north north-east crossing the Sierra San Marcos and associated springs. The location of the cross section is shown on 2. Cretaceous carbonate rocks (block pattern) and Cretaceous terrigenous siliciclastics (coarse stippled pattern) underlie Quaternary valley-fill alluvium (fine stippled pattern) throughout the study region. The regional basement is comprised of Triassic granodiorite (dashed pattern). Arrows indicate the relative motion of multi-reactivated thrust faults that bound many of the anticlinal structures in the region.

Highlands are dominated by Cretaceous carbonates and intermontane basins are filled with alluvial fan, playa, and lacustrine sediments. Mountains surrounding the Cuatrocienegas Basin and the valley fill alluvium both display a high degree of karstification (Badino et al., 2004). Wolaver et al. (2005) calculated annual recharge on the 870-square kilometer intra-basin recharge area that both Lesser y Asociados (2001) and Rodríguez et al. (2005a) suggested produces all Cuatrocienegas Basin spring discharge. The annual recharge calculations generated only 215,000 cubic meters/year of discharge compared to an observed discharge of 35,000,000 cubic meters/year (Wolaver et al., 2008). These annual discharge values indicate interbasin groundwater flow occurs. Johannesson et al. (2004) identified high elevation recharge zones from stable isotopes, but did not identify in which catchments recharge likely occurs.

Lehmann et al. (1999) used strontium isotopes and biostratigraphy to determine that the Cretaceous carbonate rocks forming the uplands and underlying valley-fill alluvium are predominantly late Barremian–late Albian in age. Lehmann et al. (1999) also described lime mudstones (Cupido Formation), shale and lime mudstones (La Peña Formation), lime mudstones and intercalated wackestones/packstones, dolomitized grainstones, shallow subtidal to peritidal carbonates, shales, and lime mudstones (Aurora Formation), overlain by more deep water laminates (Cuesta del Cura Formation) in the nearby Sierra de Parras. Badino et al. (2004) described the highly karstified nature of the carbonate rocks present in the Cuatrocienegas Basin region. A generalized hydrostratigraphic column of the Cuatrocienegas Basin is presented in **Table 15**.

Table 15. GENERALIZED HYDROSTRATIGRAPHIC COLUMN

Stratigraphic nomenclature is modified from McKee et al., 1990; Rodríguez and Sanchez, 2000; Lesser y Asociados, 2001; Evans, 2005.

Age	Formation	Description	Permeability
Quaternary	Alluvium	Sand, gravel, lake deposits, evaporate deposits, travertine	Variable
	Eagle Ford	Limestone, shale	Low
	Buda	Limestone, interbedded sand and gravel	Low
	Del Rio	Clay, sandy limestone	Low
	Georgetown (Cuesta del Cura)	Limestone	Moderate
	Washita Group	Limestone	Moderate
	Kiamichi	Limestone, shale	Low
	Aurora	Lime mudstones and wackestones, gypsum, dolomitized grainstones	High
	La Peña	Dark laminated shale, thin lime mudstone interbeds	Low
	Cupido	Lime mudstone	High
Cretaceous	La Virgen	Gypsum, dolomite, limestone, shale and clay	Low
	La Mula	Shale, sandstone, limestone, conglomerate	Low
	La Padilla	Massive dolomite, interbedded shale, sandstone, and evaporites	Low
	San Marcos	Sandstone, hematitic cement, interbedded conglomerate	Low–Moderate
	Basement	Granodiorite	Low

Meyer (1973) used carbon-14 to date organic material in Cuatrociénegas Basin sediment cores. He found organic material associated with groundwater-dependent ecosystems yields dates of at least 30,000 years before present. Alluvial fans are present primarily on the eastern flank of the Sierra San Marcos. Badino et al. (2004) described lacustrine and playa lake valley-fill alluvium; they noted that evaporation of spring water from Poza El Churince precipitates gypsum and has produced the second-largest, white-sand, dune complex in North America (second only to White Sands, New Mexico).

Evans (2005) and Minckley (1969) described the valley fill alluvium as highly karstified with sinkholes and re-emergent springs towards the center of the valley. Minckley and Cole (1968) noted that results of water quality analyses of water samples collected at terminal lakes approaches 300,000 milligrams/liter total dissolved solids. Prior to the construction of canals, which now drain the valley, the Cuatrocienegas Basin was a closed basin with large playa lakes dominating the eastern half of the valley. Miele et al. (2000) used magnetotelluric soundings to determine that mountains comprised of carbonate rocks continue in the subsurface. Rodríguez et al. (2005a) estimated an average Cuatrocienegas Basin alluvium depth of 200 meters using time domain electromagnetics.

METHODS

Tritium as an Indicator of Aquifer Residence Time

Tritium (${}^3\text{H}$) in spring water is used to estimate aquifer residence time in the Cuatrocienegas Basin. Knowledge of the aquifer residence time can be used to understand the spatial extent of the aquifer system. Tritium is produced naturally in the Earth atmosphere in very low concentration and also in larger amounts during atmospheric nuclear bomb testing during the 1950s and 1960s (Payne, 1972). Because tritium has a half-life of 12.43 years, it can be used to infer recharge pathways and aquifer residence time (Solomon and Cook, 2000). Tritium values are typically expressed in tritium units, which are equal to one tritiated water molecule (${}^3\text{H}^1\text{HO}$) in 10^{18} molecules of ${}^1\text{H}_2\text{O}$. Tritium decays to form ${}^3\text{He}$ (or, so called tritiogenic helium) at the rate of one tritium unit to 2.487×10^{-12} cubic centimeters of ${}^3\text{He}/\text{kilogram}$ of water at standard temperature and pressure (Solomon and Cook, 2000). Solomon and Cook (2000) noted that tritium concentrations greater than 0.5 tritium units indicate there is a significant component of post-bomb (post 1952) recharge in a water sample. Helium-3

also forms from the generation of neutrons through the decay of uranium and thorium within the Earth (Solomon, 2000).

Water samples for tritium analysis were collected in one-liter polyethylene bottles. The samples were analyzed for tritium using the in-growth method (Solomon and Cook, 2000). The tritium in-growth method was used to analyze tritium in spring water with a detection limit of approximately 0.1 tritium units (Clark et al., 1976, Solomon and Cook, 2000). Water sample locations for tritium analyses (as well as noble gas and helium isotopic analyses discussed later in this chapter) are shown on **Figure 18**. To understand the origin of chloride in Cuatrocienegas Basin spring waters, a plot of tritium versus chloride is generated using these data.

Oxygen Isotopes to Estimate Precipitation Elevation

Rodríguez et al. (2005) and Johannesson et al. (2004) collected water samples from springs in the Cuatrocienegas Basin and analyzed them for oxygen and hydrogen isotopes to estimate the elevation at which precipitation that results in spring discharge occurs. Johannesson et al. (2004) collected water samples from six springs on the northern flank of the Sierra San Marcos, one shallow pool, and one canal in January 1999. Water samples were collected in one-liter borosilicate glass bottles with Teflon-lined caps. Bottles were tripled rinsed prior to sample collection with MilliQ water (18 micro Ohms/centimeter), then filled with 50 percent volume/volume solution of reagent-grade hydrochloric acid and MilliQ water. After a six-hour hold time, the bottles were rinsed three times with MilliQ water, dried in a laminar fume hood, and placed in zip-style plastic bags. Water samples were collected by placing the bottle beneath the water surface after conditioning the bottle by rinsing it three times with sample water. The bottles were capped, put in a plastic bag, and stored in a cooler.

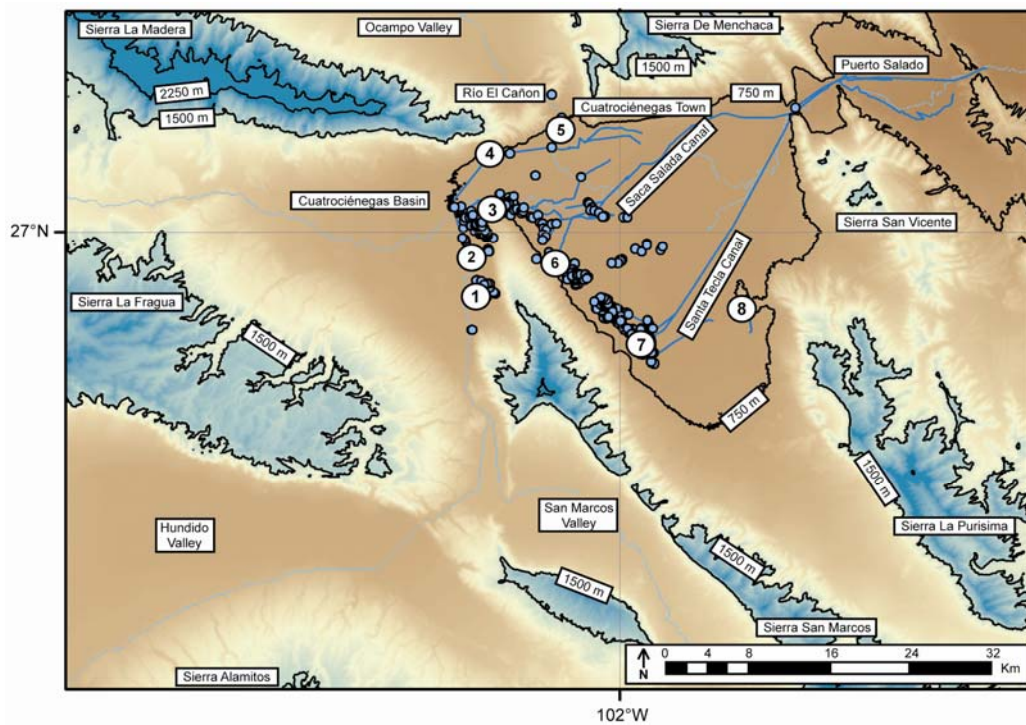


Figure 18. WATER SAMPLE LOCATIONS FOR TRITIUM, NOBLE GAS, AND HELIUM ISOTOPIC ANALYSES

Water samples for tritium and helium isotopic analyses were collected in July 2007. Sample locations are indicated by large, numbered open circles. The numbers correspond to the following features:

- (1) Poza Churince,
- (2) Poza La Becerra,
- (3) Poza Azul,
- (4) Poza Anteojo,
- (5) Cuatrocienegas Town (where Rodríguez et al [2005a] collected a rain sample in 2004 for oxygen isotopic analysis),
- (6) Poza Escobedo,
- (7) Poza Santa Tecla, and
- (8) El Venado.

Johannesson et al. (2004) analyzed the water samples for oxygen and hydrogen isotopes using Geochron Laboratories (of Cambridge, Massachusetts) with a high-precision, dual-inlet, multiple-collector mass spectrometer. The water samples are analyzed for oxygen isotopes using a modification of the carbon dioxide equilibration technique described by Epstein and Mayeda (1953). The water samples were analyzed for stable isotopes of hydrogen using a method similar to Bigeleisen et al. (1952). A VG 903 measured oxygen isotopes and a VG 602 measured stable isotopes of hydrogen. Krueger (2008) stated the analytical precision for these samples (based upon the analyses of laboratory standards and duplicates) is approximately $\pm 0.2\text{‰}$ for oxygen and approximately $\pm 3.0\text{‰}$ for hydrogen. Rodríguez et al. (2005a) collected water samples from wells, springs, pools and canals and analyzed results using an unreported mass spectrometer. They reported that the precision for these samples is less than $\pm 0.1\text{‰}$ for oxygen and less than $\pm 1.0\text{‰}$ for hydrogen. Results are presented relative to Standard Mean Ocean Water (Craig, 1961) and Vienna Standard Mean Ocean Water (Coplen, 1996).

Cortés and Durazo (2001) presented a relationship between $\delta^{18}\text{O}$ and elevation that is used to estimate precipitation elevation of waters that result in spring discharge using the following formula

$$\delta^{18}\text{O} = 2.37 E - 3.2 . \quad (11)$$

Where

$$\delta^{18}\text{O} = \frac{\left(\frac{^{18}\text{O}}{^{16}\text{O}}\right)_{sample} - \left(\frac{^{18}\text{O}}{^{16}\text{O}}\right)_{std}}{\left(\frac{^{18}\text{O}}{^{16}\text{O}}\right)_{std}} \times 1000 \text{ and} \quad (12)$$

E = elevation (meters).

Values for $\delta^{18}\text{O}$ are typically reported in parts/thousand, represented by the symbol ‰ (per mil).

Noble Gases to Evaluate Recharge Elevation and Investigate Interbasin Flow

In order to estimate the elevation at which recharge water enters the water table, dissolved noble gas data were evaluated for Cuatrocienegas Basin springs using gas diffusion samplers (Solomon and Cook, 2000; Manning and Solomon, 2003; Heilweil et al., 2006). During July 24–July 26, 2007, the author collected nine dissolved noble gas samples from springs spatially distributed across the Cuatrocienegas Basin at the same locations as the tritium samples (shown on **Figure 18**). Because noble gases are conservative tracers, the temperature dependency of the solubility concentration of noble gases in recharge areas can be used to infer recharge elevation (Mazor, 1972; Stute et al., 1992; Castro et al., 2007).

Oxygen isotopes correlate with the elevation at which precipitation occurs, but not the elevation at which the recharged waters enter the water table (Heilweil et al., 2006). The solubility of noble gases (e.g., argon, helium, neon, nitrogen, xenon) is a function of altitude, salinity, excess air, and temperature (Stute and Schlosser, 2000; Manning and Solomon, 2003; Castro et al., 2007) and is governed by Henry's Law as a function of temperature and pressure of the gases. The concentration of each noble gas in spring

water is measured. Assuming a lapse rate, the resulting recharge elevation is an optimization of each noble gas recharge elevation.

Manning and Solomon (2003) outlined the theory behind the use of noble gases to estimate recharge elevation. The governing equation for the concentration of noble gas i dissolved in fresh water (C_i) is

$$C_i = C_i^E + C_i^A . \quad (13)$$

Where

C_i^E = component resulting from equilibrium with the atmosphere, and

C_i^A = component resulting from excess air.

Aeschbach-Hertig et al. (2000) commented that noble gas concentration is also affected by the creation of helium isotopes from radioactive decay (e.g., radiogenic helium — ${}^3\text{He}$ from ${}^3\text{H}$, and ${}^4\text{He}$ from U/Th), that must be subtracted by separating the helium component. However, it is assumed that non-atmospheric gas concentration is relatively low. Excess air is comprised of dissolved atmospheric gases above the equilibrium values caused by trapped air bubbles during recharge. C_i^E is defined (Aeschbach-Hertig et al., 2000; Manning and Solomon, 2003) as

$$C_i^E = \frac{X_i P_r}{K_i(T_r)} . \quad (14)$$

Where

X_i = the dry mole fraction of gas i in air,

P_r = the recharge pressure,

K_i = the Henry's Law constant for gas i , and

T_r = a nonlinear function (Manning and Solomon, 2003).

The value for C_i^A is defined as

$$C_i^A = X_i A . \quad (15)$$

Where

A = the total concentration of excess air.

The recharge elevation in meters (H) is related to the recharge pressure by

$$P_r = \exp\left(-\frac{H}{8300}\right) - P_{H_2O} . \quad (16)$$

Where

P_{H_2O} = the partial pressure of water.

Several dissolved noble gases are measured so that a system of equations for C_i can be solved to find the unknown parameters of T_r , H , and A using either the continuous

equilibrium model (Aeschbach-Hertig et al., 2000) or the unfractionated air model (Stute and Schlosser, 1993). This research estimates the recharge elevation using the continuous equilibrium model using of the dependence of C_i on H and T_r and estimating the local lapse rate.

The author collected dissolved noble gas samples at locations shown on **Figure 18** using the passive diffusion gas sampler described by De Gregorio et al. (2005) and shown in **Figure 19**. The passive diffusion samplers were placed directly in the spring orifice for at least 24 hours to ensure the sampler equilibrated with spring water and not the atmosphere. The passive diffusion samplers are retrieved from the spring and cold-soldered within two minutes using the pinch-off tool shown in **Figure 20** and placed in a protective zip-style bag for shipment.

The noble gas samples were processed at The University of Utah Dissolved Gas Laboratory. The abundance (concentration) and isotopic composition of atmospheric gases, including neon, argon, and krypton are determined by isotope dilution using a quadrupole mass spectrometer residual gas analyzer (Stanford Research Systems RGA-300) in static mode to permit relatively small-volume gas samples (e.g., 5.5 cubic centimeter water samples with 7×10^{-7} cubic centimeters of Xe and standard temperature and pressure, Poole et al., 1997). In this process, water samples are degassed and spiked with minor isotopes of each gas (^{36}Ar , ^3He , ^{78}Kr , ^{22}Ne , and ^{136}Xe) of known composition and volume. Nitrogen and oxygen are measured with the quadrupole mass spectrometer dynamically using a leak valve (Manning and Solomon, 2003). The argon, neon, nitrogen, and krypton concentrations are used to calculate a minimum and maximum recharge temperature and resulting recharge elevation. Poole et al. (1997) stated that an accuracy of $\pm 1^\circ\text{C}$ from the air equilibration temperature is possible with this approach.

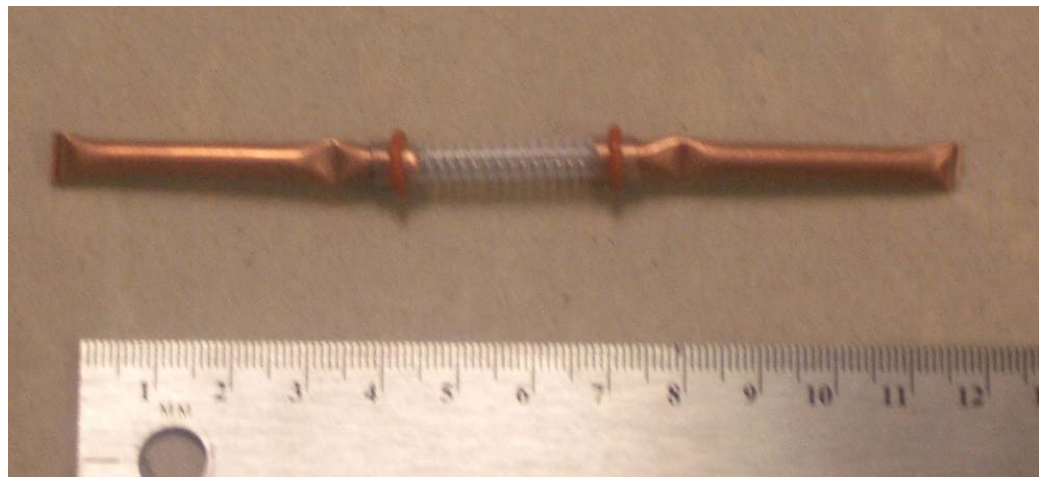


Figure 19. PASSIVE DIFFUSION SAMPLER FOR NOBLE GAS SAMPLE COLLECTION

De Gregorio et al. (2005) describe the sampling device used to collect noble gases dissolved in Cuatrocienegas Basin spring waters. Photo by the University of Utah Dissolved Gas Laboratory.

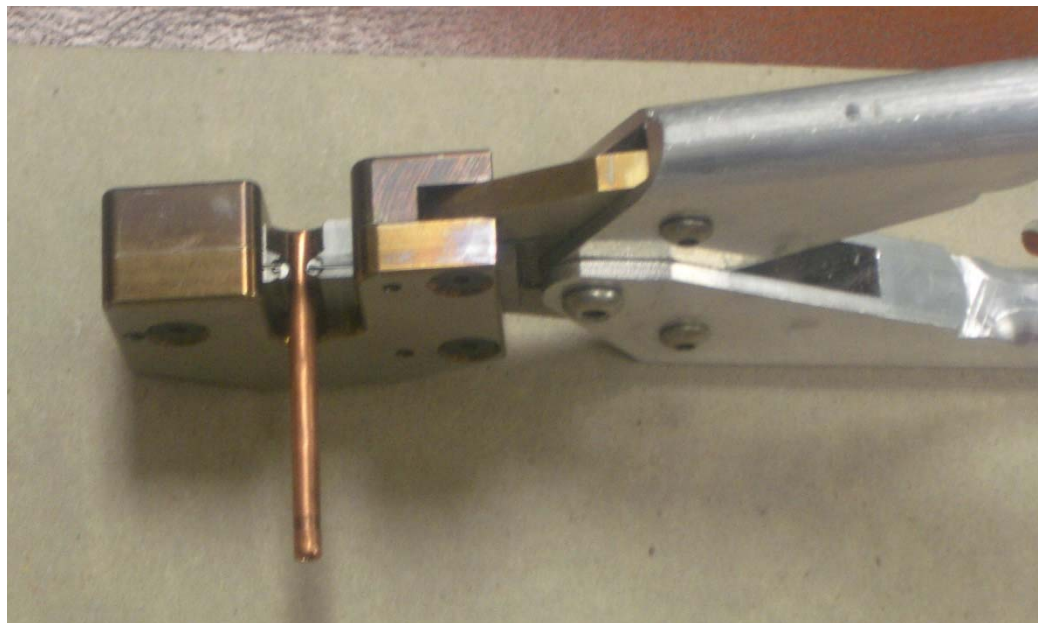


Figure 20. PASSIVE DIFFUSION SAMPLER PINCH-OFF TOOL

Passive diffusion samplers are cold-soldered with a pinch off tube immediately after sampler retrieval. Photo by the University of Utah Dissolved Gas Laboratory.

To complete noble gas sample analyses and calculate the radiogenic component of dissolved gas concentration, a magnetic sector-field linear mass spectrometer (Mass Analyzer Products 215-50) measures ^3He and ^4He . Air and water standards are used for the quadrupole mass spectrometer. The air sample is atmospheric gas run every two–three samples. The water sample is equilibrated with atmospheric gas over a range of ambient temperatures. The University of Utah Dissolved Gas Laboratory (2008) stated that the precision for all other gasses is $\pm 1\text{--}2$ percent of the value and the precision for helium is $\pm 0.5\text{--}1$ percent of the value.

Noble gas thermometry is an attractive tool to characterize recharge elevation based on the temperature at which the noble gases equilibrate. Stute et al. (1992) stated that noble gas thermometry can infer temperature in aquifers with relatively well-understood hydrogeology, simple geochemistry, and low dispersion and mixing rates. However, some uncertainties are associated with noble gas thermometry. Castro et al. (2007) outlined several studies that are unable to reproduce groundwater temperatures at the interface with the unsaturated zone (Stute et al., 1992; Stute and Schlosser, 1993; Aeschbach-Hertig et al., 2000). Stute et al. (1992) used noble gases to infer paleotemperatures in the southwest U.S. and found a bias $>4^\circ\text{C}$ that suggest that noble gas temperature models do not accurately describe mechanisms controlling noble gas concentration (e.g., increased noble gas partial pressure in the unsaturated zone due to O_2 depletion, modification of gas solubility due to reduced soil humidity).

Also, atmospheric temperature changes, a seasonality in recharge, the presence of high heat flow, and (most importantly) a significant variation in water table depth (between long-scale humid and arid climatic changes, or more short-term inter-annual water table fluctuations, resulting in entrapped, or “excess air”) can introduce uncertainty into this method (Castro et al., 2007).

Moreover, Heilweil et al. (2006) commented that uncertainties in atmospheric lapse rate can affect calculations due to changes in solar radiation strength, topography—such as cold air drainages, or differences in relative humidity. Cey (2008) investigated the effects of fractionization of excess air due to incomplete dilution of entrapped air bubbles during recharge, degassing after recharge, and denitrification induced gas stripping in the saturated zone. In terms of the sampling and analytical uncertainties of the method, both leakage of the passive diffusion sampler after collection and pinch-off and incomplete degassing of the sample can lead to erroneous noble gas temperature determinations. Despite the uncertainties associated with the method, Manning and Solomon (2003) and Heilweil et al. (2006) used dissolved noble gas data to estimate recharge elevation.

In addition using noble gases to evaluate recharge elevation, helium isotopes are analyzed to infer what processes affect groundwater geochemistry. Isotopes of helium are present as ^3He (discussed in the tritium section above) and ^4He . Helium-4 is a product of radioactive alpha decay of uranium-238, uranium-235, and thorium-232 within the Earth (Solomon, 2000; Crossey et al., 2006). Solomon (2000) stated the relative abundance of helium-3 to helium-4 is distinct for the three helium reservoirs on the Earth (**Table 16**). Knowledge of this helium isotopic ratio can be used to infer the origin of fluids (Solomon, 2000). Helium gas was collected by the author using the diffusion gas sampler described by De Gregorio et al. (2005) and was processed at The University of Utah Dissolved Gas Laboratory using a magnetic sector-field linear mass spectrometer to measure ^3He and ^4He . The location of the helium gas samples is the same as the tritium and noble gas water sample locations shown on **Figure 18**.

Table 16. HELIUM ISOTOPIC RATIOS FOR THREE EARTH RESERVOIRS

Reservoir	$\frac{^3He}{^4He}$	Reference
Atmosphere	1.384×10^{-6}	Clark et al. 1976
Crust	10^{-9} to 10^{-7}	Mamyrin and Tolstikhin, 1984
Mantle	1.1×10^{-5} to 1.4×10^{-5}	Ozima and Podosek, 1983

The isotopic ratio of helium is examined using the equation

$$\frac{R}{R_a} = \frac{\left(\frac{^3He}{^4He} \right)_{sample}}{\left(\frac{^3He}{^4He} \right)_{atmosphere}}. \quad (17)$$

Where $R/R_a = 1$ indicates a water sample is in equilibrium with the atmosphere (Crossey et al., 2006). Short relative aquifer residence time or recent recharge may cause a spring water sample to be in equilibrium with the atmosphere (or close to equilibrium). When $1 < R/R_a \leq 7$, two explanations are possible: (1) tritiogenic helium is present; or (2) waters are a mixture of those in equilibrium with the atmosphere and those containing mantle-derived He (Crossey et al., 2006).

Strontium Isotopes of Water and Travertine to Identify Aquifer and Flow Paths

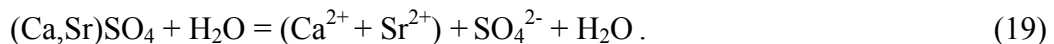
Strontium Substitution in Carbonate Rocks

Strontium isotopic analyses ($^{87}\text{Sr}/^{86}\text{Sr}$) of seventeen water and three travertine samples are used to identify the source of strontium ions in Cuatrociénegas Basin spring waters and to evaluate if the flow paths have changed over time using the approach discussed in Banner (2004). In carbonate rocks, strontium substitutes for calcium because

it has the same charge and a similar ionic radius (Banner, 1995). Weathering of calcium carbonate often entails incongruent recrystallization of calcium carbonate with the release of strontium into solution by the reaction (Salbu and Steinnes, 1995)



A similar reaction also takes place for gypsum to release strontium into solution (Salbu and Steinnes, 1995)



The ratio of strontium-87 to strontium-86 in seawater is known throughout the Cretaceous (Bralower et al., 1997). Also, strontium fractionation is negligible between water and travertine that forms from spring waters, so strontium isotopic ratios can be compared directly for water and travertine to infer the source of strontium ions in an aquifer (Banner, 2004, DeMott, 2007).

Collection of Water and Travertine Samples for Strontium Isotopic Analysis

Seventeen water samples were collected in August 2001 by Dean Hendrickson (The University of Texas at Austin Section of Integrative Biology) and in May 2002 by Suzanne Pierce (The University of Texas at Austin Department of Geological Sciences) from springs, canals, and marshes. The location of the water samples is shown on **Figure 21**. Three travertine samples were collected by the author in January 2005. Two travertine samples were collected at the travertine mine of inferred Pleistocene age on the Sierra San Marcos southwest flank (**Figure 22**). One travertine sample was collected from a stream at Los Hundidos. The travertine sample locations are shown on **Figure 23**.

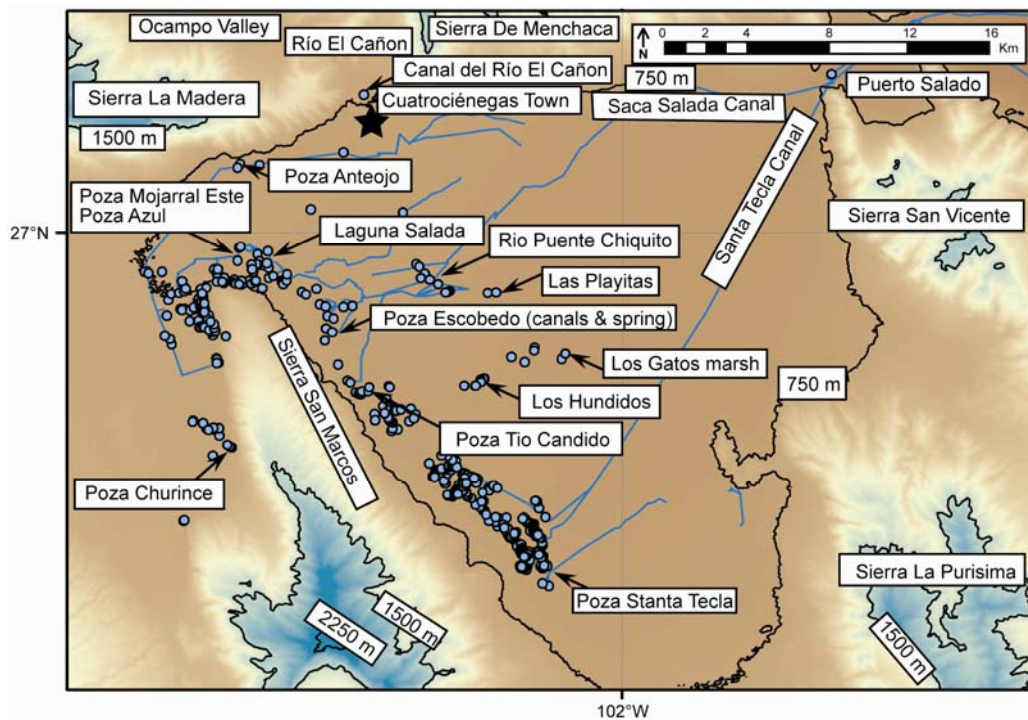


Figure 21. WATER SAMPLE LOCATIONS FOR STRONTIUM ISOTOPIC ANALYSES

Seventeen water samples were collected in August 2001 by Dean Hendrickson (The University of Texas at Austin Section of Integrative Biology) and in May 2002 by Suzanne Pierce (The University of Texas at Austin Department of Geological Sciences) from springs, canals, and marshes. The Town of Cuatrocienegas is indicated by the solid star. The open circles represent springs, but appear to be solid circles in areas of high spring density.

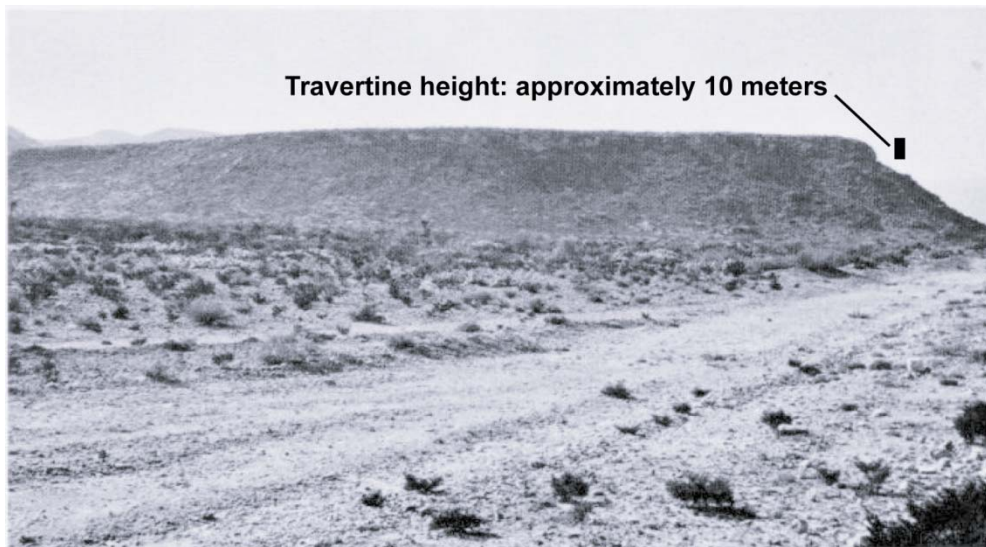


Figure 22. TRAVERTINE DEPOSIT ON THE WEST FLANK OF THE SIERRA SAN MARCOS

This travertine deposit is attributed to deposition in a lacustrine environment. The height of the vertical bar indicates an approximate travertine height of 10 meters. The travertine strata cap the hill and are roughly horizontal. The location of the travertine samples is shown on Figure 23. Photo by Minckley, 1969.

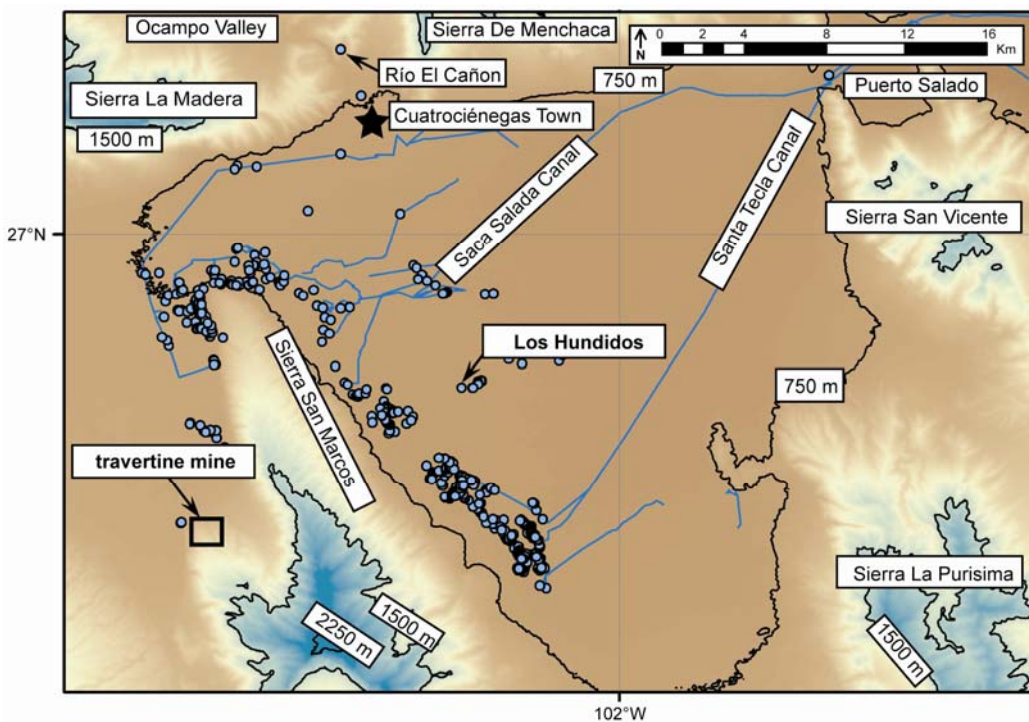


Figure 23. TRAVERTINE SAMPLE LOCATIONS FOR STRONTIUM ISOTOPIC ANALYSES

Three travertine samples were collected by the author in January 2006 for strontium isotopic analyses. Two travertine samples were collected from the travertine mine of inferred Pleistocene age on the southwest flank of the Sierra San Marcos (indicated by the open square). One modern travertine was collected from a flowing stream at Los Hundidos on the east flank of the Sierra San Marcos. The Town of Cuatrocienegas is indicated by the solid star. The open circles represent springs, but appear to be solid circles in areas of high spring density.

Rodríguez et al. (2005a) collected a travertine samples from the travertine of inferred Pleistocene age shown on **Figure 23** in 2004. Rodríguez et al. (2005a) calculated a carbon-14 relative age of approximately 17,000 years for analyses done on the travertine samples.

Laboratory Methods for Strontium Separation from Water and Travertine Samples

Strontium was separated from the water and travertine samples by ion exchange using strontium-specific resin in the Isotope Clean Laboratory in the Department of Geological Sciences at The University of Texas at Austin. Since strontium may be unintentionally introduced into the sample during all stages of sample preparation, blanks are analyzed to constrain the quantity of such introduced strontium. Blanks for the sample preparation and ion exchange process for this laboratory are typically five picograms for water samples and 20 picograms for carbonate samples (pers. com., Mack, 2008). These blank levels are negligible with respect to sample size. A flow chart for the analysis of strontium isotopes for water and travertine samples (DeMott, 2007) is shown on **Figure 24**.

Determination of Strontium Isotopic Composition of Water and Travertine Samples

Strontium isotopic composition of the water and travertine samples is determined using a Finnigan-MAT model 261 multi-collector thermal ionization mass spectrometer in dynamic multicollection mode following the method presented in Banner and Kaufman (1994) at The University of Texas at Austin Department of Geological Sciences. Two National Institute of Standards and Technology (NIST) Standard Reference Material (SRM) 987 strontium carbonate standards are run per turret of eleven samples for each sample run.

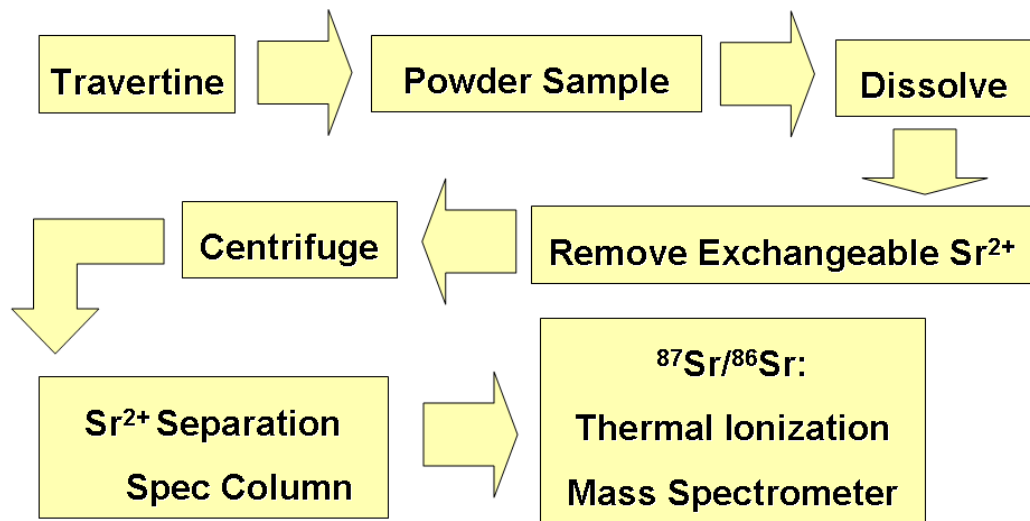


Figure 24. ANALYSIS FLOW CHART FOR STRONTIUM ISOTOPES IN WATER AND TRAVERTINE

This flow chart is modified from the analytical process described in DeMott (2007).

From approximately 1998 to 2008, the mean $^{87}\text{Sr}/^{86}\text{Sr}$ values of the NIST SRM 987 is 0.710266 ($n=422$, one standard deviation=0.000008). Based on the reproducibility for the standard, with a 95 percent confidence (equal to two times the standard error of the mean), the true value of a sample is within 2-sigma analytical precision, or 0.000016 of the value that is measured. Thus, the analytical uncertainty of the strontium isotopic analysis based on the analyses of laboratory standards and duplicate samples is ± 0.000016 (pers. com., Mack, 2008). The $^{87}\text{Sr}/^{86}\text{Sr}$ values reported for samples are normalized to an accepted NIST SRM 987 $^{87}\text{Sr}/^{86}\text{Sr}$ value of 0.710250 (Bralower et al., 1997). Because the long-term mean $^{87}\text{Sr}/^{86}\text{Sr}$ value of the NIST SRM 987 standard was 0.710266, 0.000016 has been subtracted from the $^{87}\text{Sr}/^{86}\text{Sr}$ ratio of each sample. The strontium concentration of the water and travertine samples is determined using a Micromass Platform inductively coupled plasma-mass spectrometer (now Thermo Fisher Scientific, Inc.) by John Lansdown at The University of Texas at Austin Department of Geological Sciences.

RESULTS

Tritium

The results of tritium in spring waters from Cuatrocienegas are shown in **Table 17** and on **Figure 25**. Most springs in the Cuatrocienegas Basin are under the detection limit of 0.1 tritium units, suggesting that most precipitation resulting in recharge to Cuatrocienegas Basin springs occurred at least 50 years ago (Solomon and Cook, 2000). Rodríguez et al. (2005a) present a value of 5.4 tritium units for a rain water sample collected in 2004 in the town of Cuatrocienegas.

Table 17. HYDROGEOLOGIC DATA

The presently dry spring from the Ocampo Valley is not included here because of the paucity of data in Minckley and Cole (1968). Data Sources: [1] Minckley and Cole (1968), [2] Johannesson et al. (2004) [3] Rodriguez et al. (2005a), [4] Wolaver and Sharp (2007), [5] Wolaver et al. (2008), [6] Wolaver unpublished. Locations of springs and other geographic features are shown on Figure 18. Geochemical and isotopic data are presented in Chapter 3.

Spring or Spring Group	Discharge [percent of total basin discharge]	Temperature [C]	Spring Temperature Response to Precipitation	Chloride Concentration [milligrams/liter]	Cl/Br Relationship	Tritium [Tritium Units]	Precipitation Elevation Inferred from $\delta^{18}\text{O}$ [m]	Recharge Elevation Inferred from Noble Gases [m]	R/Ra From Helium Isotopes	Water Table Elevation [m]
Reference:	[3]	[6]	[4]	[5] (unless noted)	[5]	[6]	[3] (unless noted)	[6]	[6]	[3]
Western Flank of the Sierra San Marcos (La Becerra)	~55	32.2 (cool vent), 34.2 (warm vent)	None	93.72 (cool vent) [6], 122.65 (warm vent) [6], 98.90 (undifferentiated)	Linear	0.3 (cool vent), <0.1 (warm vent)	1231 (fracture source undifferentiated), 1600 [2]	765 (cool vent), 768 (warm vent)	1.6 (cool vent), 1.8 (warm vent)	760
North Flank of the Sierra San Marcos	~30	33.0 (Azul), 35.0 (Escobedo)	--	98.76 (Azul) [2], 111.41 (Escobedo) [6], 48.74, 87.81, 8.84, 91.50, 100.30, 107.46 (various)	Linear	<0.1 (Azul), 0.4 (Escobedo)	1157, 1163, 1241 (Azul), 1245 (Orozco), 1237 (Escobedo)	730 (Azul), 703 (Escobedo)	1.8 (Azul), 1.8 (Escobedo)	702 (Escobedo)
Southeast Flank of the Sierra San Marcos	~15	30.0	Temp. decrease ~2°C	33.32 (Sta. Tecla) [6], 29.60, 29.75, 45.63 (various)	Linear	0.2 (Sta. Tecla)	1456, 1466	714 (Sta. Tecla)	1.5 (Sta. Tecla)	700 (well upgradient to Sta. Tecla)
Others	Low	29.9 (Anteojo), 31.1 (Churince), 28.5 (El Venado)	--	21.78 (Anteojo) [6], 103.95, 107.20, 79.74 (Churince) [2] 29.54 (El Venado) [6] 22.00 (Río Cañon) [1]	Linear	<0.1 (Anteojo), <0.1 (Churince), 1.1 (El Venado)	1585, 2350 (Anteojo) [2], 1337 (Churince), 1437 (El Venado)	735 (Anteojo), 745 (Churince), 722 (El Venado)	1.2 (Anteojo), 1.3 (Churince), 0.9 (El Venado)	749 (Churince)

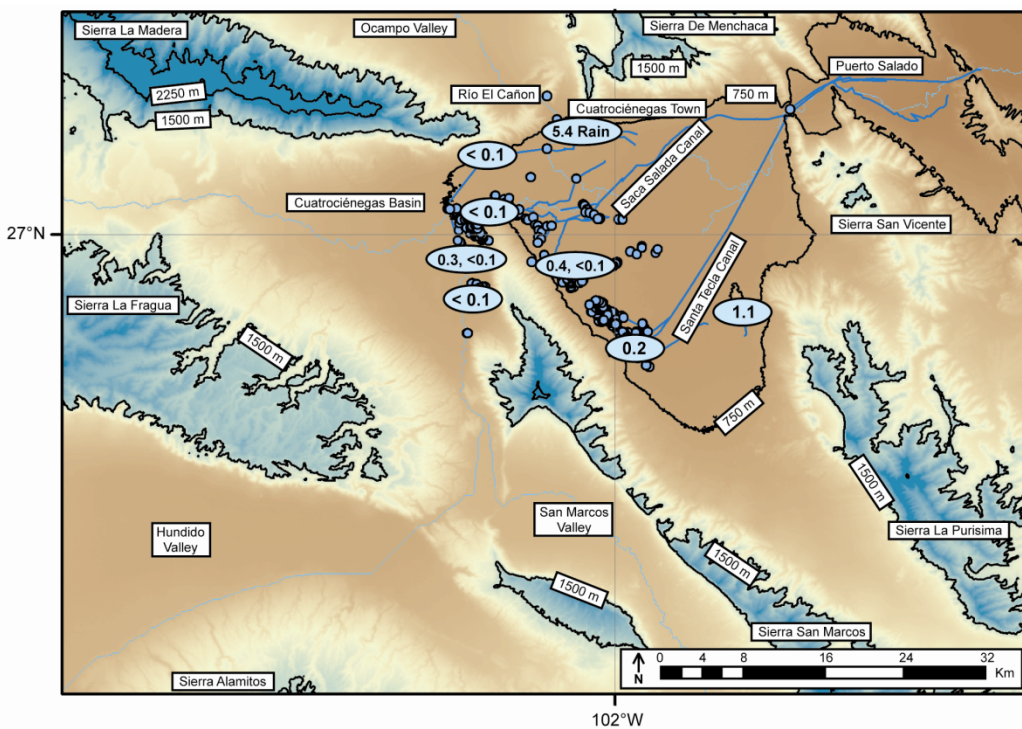


Figure 25. TRITIUM VALUES FOR SPRING WATER AND PRECIPITATION

The results of tritium analyses of water samples collected in July 2007 are shown in ellipses. The tritium concentration for a precipitation sample collected in spring 2004 was 5.4 tritium units (Rodríguez et al., 2005a). Thus, if springs were recharged by an aquifer with short, fast flow paths from recharge areas to springs, spring water tritium concentrations would be expected of approximately 5.0 tritium units. The cooler (32°C) spring vent of Poza La Becerra has a tritium concentration of 0.3 tritium units. The warmer (34°C) spring vent of Poza La Becerra has a tritium concentration of <0.1 tritium units. An inflow canal that travels several kilometers prior to discharge in Poza Escobedo has a tritium concentration of 0.4 tritium units. The tritium concentration of the Poza Escobedo spring is <0.1 tritium units. The detection limit for tritium analyses is approximately 0.1 tritium units. The names of the locations of water samples for tritium analyses are shown on Figure 18.

Thus, if locally-derived, rapid recharge from the mountains immediately surrounding the Cuatrocienegas Basin were the dominant recharge process, springs in the Cuatrocienegas Basin would have a tritium value of around five tritium units. The highest tritium reading is 1.1 tritium units at El Venado, which is also the coolest (28.5°C) and freshest water (551 microsiemens/centimeter at 25°C) in the Cuatrocienegas Basin region, suggesting this is the youngest water in the valley, but still with a probable mean residence time between 10 and 20 years. The plot of tritium versus chloride is shown on **Figure 26**. In general, chloride concentration increases with relative groundwater residence time, although some outliers exist (i.e., Poza Anteojo and Poza Azul).

Oxygen Isotopes

This research does not collect and interpret new stable oxygen isotopic data. The results of analyses of oxygen isotopes presented by Johannesson et al. (2004) are shown on **Figure 27** and in **Table 17**. The results of oxygen isotopic analyses by Johannesson et al. (2004) have a $\delta^{18}\text{O}$ value ranges from -8.2 to -5.7 ‰. The mean $\delta^{18}\text{O}$ value is -6.5 ± 0.82 ‰. The oxygen isotopic result suggests a precipitation elevation that ranges from 1,170 to 2,350 meters (using the relationship published by Cortés and Durazo, 2001). Additional results of oxygen isotopes are presented in Rodríguez et al. (2005a). The stable oxygen isotopic data presented by Johannesson et al. (2004) plot slightly below the local meteoric water line (Cortés et al., 1997) and a linear regression of the data (not including Poza Anteojo) has a slope of 4.9 for a postulated evaporation line of precipitation that originally had $\delta^{18}\text{O}$ and δD values of -8.1 and -54.5 ‰ respectively (Johannesson et al., 2004).

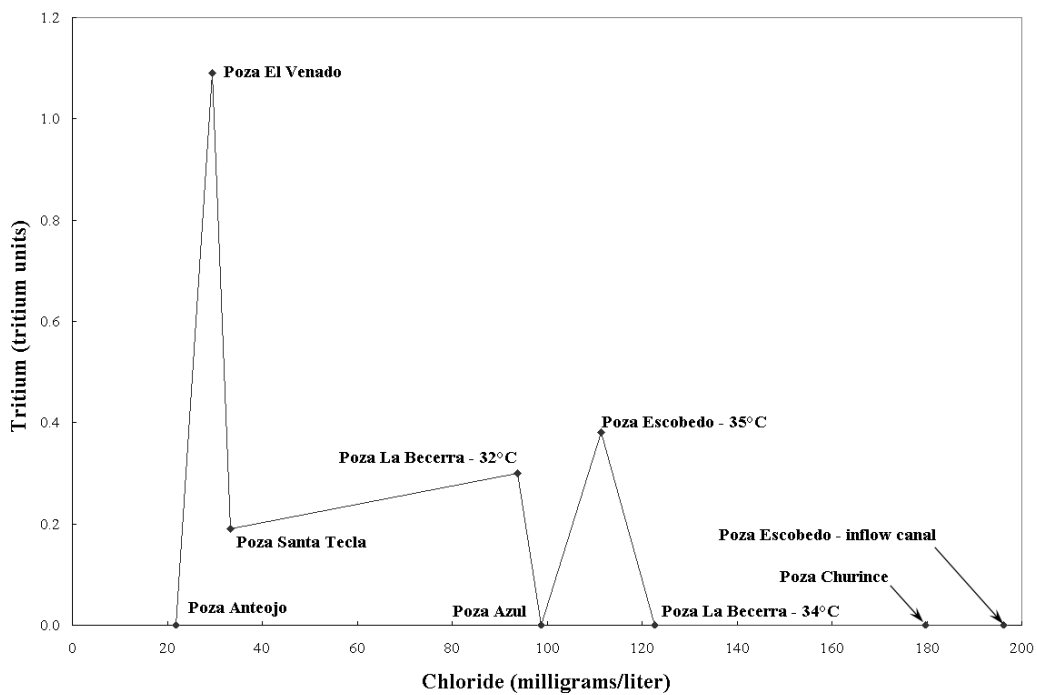


Figure 26. TRITIUM VERSUS CHLORIDE FOR CUATROCIÉNEGAS BASIN SPRINGS

This figure shows the results of tritium and chloride analyses for spring water collected in July 2007 by the author. The detection limit for the tritium analysis is 0.1 tritium units. Values below 0.1 tritium units are shown as 0.0 tritium units. The names of the locations of water samples for tritium analyses are shown on Figure 18. The results of tritium analyses also are shown on Figure 25.

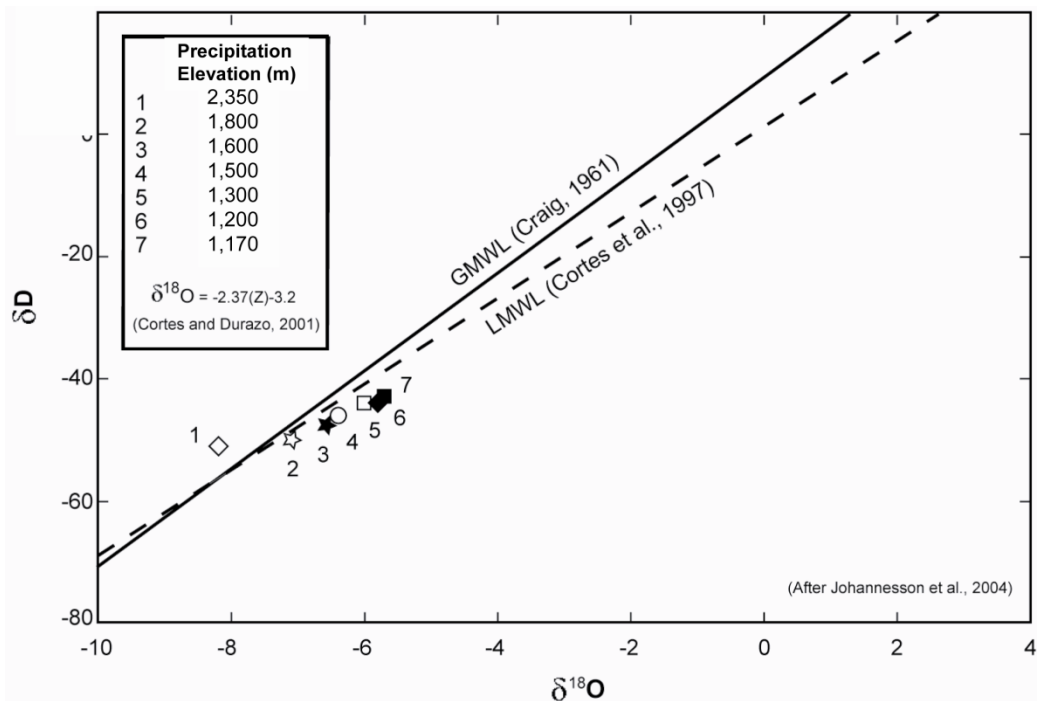


Figure 27. INFERRED PRECIPITATION ELEVATION FROM SPRING WATER STABLE ISOTOPES

Stable isotopic data are from Johannesson et al. (2004). The different symbol shapes refer to different sampling locations: (1) Poza Anteojo, (2) Poza Bonitos, (3) Poza La Becerra, (4) Poza Juan Santos, (5) Laguna de los Burros, (6) Saca del Fuente, and (7) Poza Caballo Cojo. GMWL is the global meteoric water line of Craig (1961). LMWL is the local meteoric water line presented by Cortés et al. (1997).

Dissolved Noble Gases in Spring Water

Using noble gas data for water collected from Cuatrocienegas Basin springs, the elevation at which groundwater enters the water table during recharge is 720–770 meters (indicated by recharge temperatures ranging from 17.0°–26.0°C). The results of the noble gas analyses are presented in **Table 18**. Terrigenic helium that is subtracted from the ${}^4\text{He}$ reading, excess air, and total dissolved gas concentration (a parameter that is measured along with temperature at the time dissolved gas samples are collected) is also shown in **Table 18**.

The results of helium isotopic analyses of Cuatrocienegas Basin spring waters are shown in **Table 18** and on **Figure 28**. The values of R/R_a range from a low of 0.9 at El Venado to 1.8 at the warm vent of Poza La Becerra, Poza Azul, and Poza Escobedo. Poza Anteojo has a low R/R_a value (1.2) relative to the other springs, which are 1.1 (Poza Escobedo surface water inlet canal), 1.3 (Poza Churince), 1.5 (Poza La Tecla), and 1.6 (the cool vent of Poza La Becerra).

Strontium Isotopes of Spring Water and Travertine

Strontium isotope results (${}^{87}\text{Sr}/{}^{86}\text{Sr}$) normalized to an accepted NIST SRM 987 of 0.710250 for seventeen water samples from the Cuatrocienegas Basin and three travertine samples (two samples of inferred Pleistocene age and one modern sample) are shown in **Table 19** and on **Figure 29**. Seventeen analyses of water give a mean ${}^{87}\text{Sr}/{}^{86}\text{Sr}$ value of 0.707443 with a standard deviation of 0.000011. The results of measured ${}^{87}\text{Sr}/{}^{86}\text{Sr}$ values for water samples give a range of 0.707429–0.707468. Three analyses of travertine give a range of 0.707428–0.707449, and a mean value of 0.707442 with a standard deviation of 0.000012. This standard deviation is within the analytical uncertainty of ± 0.000016 for a given analysis.

Table 18. RESULTS OF NOBLE GAS ANALYSES FOR WATER

Note: Dissolved gas data were processed at the University of Utah Dissolved Gas Laboratory. Samples were collected on July 24-July 26, 2007 by Wolaver.

Sample ID	^{40}Ar	^{84}Kr	^{129}Xe	^{20}Ne	^4He	Terri-genic He	Excess Air	Total Dissolved Gas	Recharge Temperature	Recharge Elevation
	[cm ³ /g at Standard Temperature and Pressure]						[atm]	[°C]	[m]	
Anteojo	3.43×10^{-4}	4.11×10^{-8}	2.46×10^{-9}	1.97×10^{-7}	2.30×10^{-7}	1.8×10^{-7}	0.0958	1.0920	22.1	735
Becerra-cool	3.92×10^{-4}	4.54×10^{-8}	2.83×10^{-9}	2.37×10^{-7}	7.61×10^{-7}	7.0×10^{-7}	0.0367	1.3150	17.3	765
Becerra-hot	3.61×10^{-4}	4.16×10^{-8}	2.61×10^{-9}	2.20×10^{-7}	9.46×10^{-7}	8.9×10^{-7}	0.0311	1.2580	19.3	768
Churince	3.01×10^{-4}	3.45×10^{-8}	2.13×10^{-9}	1.78×10^{-7}	3.01×10^{-7}	2.5×10^{-7}	0.0506	1.0580	25.6	745
El Venado	2.92×10^{-4}	3.51×10^{-8}	2.01×10^{-9}	1.63×10^{-7}	3.38×10^{-7}	2.9×10^{-7}	0.1035	0.9590	25.0	722
Escobedo-canal	2.86×10^{-4}	3.38×10^{-8}	2.07×10^{-9}	1.64×10^{-7}	5.11×10^{-8}	6.0×10^{-9}	0.1554	0.9720	26.2	703
Escobedo-hot-a	4.64×10^{-4}	5.57×10^{-8}	3.20×10^{-9}	2.76×10^{-7}	1.39×10^{-6}	1.3×10^{-6}	0.1020	1.6450	17.6	703
Azul	3.90×10^{-4}	4.65×10^{-8}	2.79×10^{-9}	2.41×10^{-7}	1.12×10^{-6}	1.1×10^{-6}	0.0346	1.4010	17.3	730
Santa Tecla	2.85×10^{-4}	3.32×10^{-8}	2.10×10^{-9}	1.70×10^{-7}	2.53×10^{-7}	2.1×10^{-7}	0.0221	0.9560	25.0	714

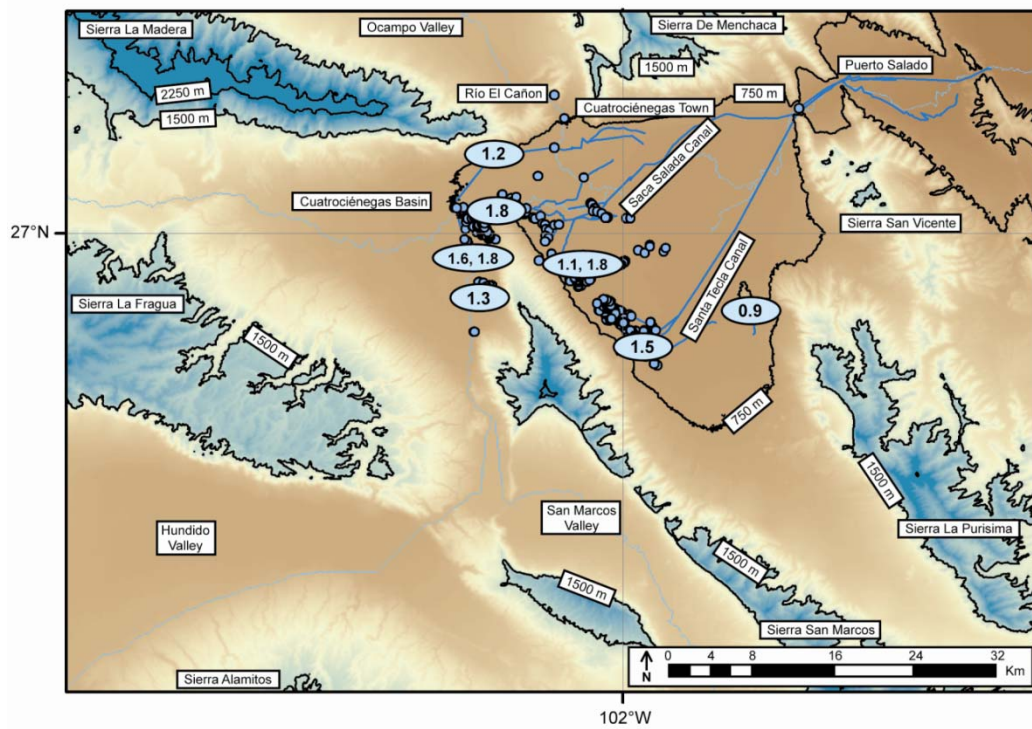


Figure 28. HELIUM ISOTOPE RESULTS FOR CUATROCIÉNEGAS SPRINGS

The results of helium isotopic analyses of water samples collected in July 2007 are shown in ellipses. Helium isotopic compositions are presented as R/Ra, where a water sample in equilibrium would have an R/Ra of 1.0. R/Ra values greater than 1.0 suggest that a component of helium from mantle degassing is present. The R/Ra of the cooler (32°C) spring vent of Poza La Becerra is 1.6. The warmer (34°C) spring vent of Poza La Becerra has a helium isotopic composition of 1.8. An inflow canal that travels several kilometers prior to discharge in Poza Escobedo has a helium composition of 1.1. Poza El Venado, the freshest spring in the valley (total dissolved solids ≈ 600 milligrams/liter), has a helium isotopic composition of 0.9, the spring closest to equilibrium with the atmosphere. The names of the locations of water samples for helium isotopic analyses are shown on Figure 18.

Table 19. RESULTS OF STRONTIUM ISOTOPIC ANALYSES FOR WATER AND TRAVERTINE

Sample locations for water are shown on Figure 21 and for travertine on Figure 23.

¹ Strontium isotope results are normalized to an accepted NIST SRM 987 value of 0.710250.

Sample Name	Sample Type	$\frac{^{87}Sr}{^{86}Sr}$ Measured Values	$\frac{^{87}Sr}{^{86}Sr}$ Corrected Values ¹	$\frac{1}{Sr}$ [1/parts/billion]
Poza Anteojo	water	0.707448	0.707432	0.0001437
Poza Mojarral Oeste	water	0.707470	0.707454	0.0000719
Poza Mojarral Este	water	0.707450	0.707434	0.0000718
Poza Churince	water	0.707484	0.707468	0.0000723
Poza Escobedo outflow canal	water	0.707462	0.707446	0.0000727
Poza Escobedo inflow canal	water	0.707454	0.707438	0.0000717
Poza Escobedo warm spring	water	0.707466	0.707450	0.0000711
Poza Azul	water	0.707452	0.707436	0.0000794
Poza Santa Tecla	water	0.707481	0.707465	0.0003860
Poza Tío Cándido	water	0.707467	0.707451	0.0000834
Los Gatos marsh 1	water	0.707455	0.707439	0.0000290
Los Gatos marsh 2	water	0.707451	0.707435	0.0000361
Los Hundidos	water	0.707453	0.707437	0.0000593
Las Playitas	water	0.707462	0.707446	0.0000440
Saca Salada Canal	water	0.707453	0.707437	0.0000735
Río Puente Chiquito	water	0.707448	0.707432	0.0000686
Laguna Salada	water	0.707445	0.707429	0.0000484
Canal del Río Cañon	water	--	--	0.0002148
mean	water	0.707459	0.707443	0.0000943
standard deviation	water	0.000011	0.000011	0.0000840
Los Hundidos travertine of modern age	travertine	0.707444	0.707428	0.0135
Travertine of inferred Pleistocene age	travertine	0.707465	0.707449	0.0689
Travertine of inferred Pleistocene age	travertine	0.707464	0.707448	0.0863
mean	travertine	0.707458	0.707442	0.0562
standard deviation	travertine	0.000012	0.000012	0.0380

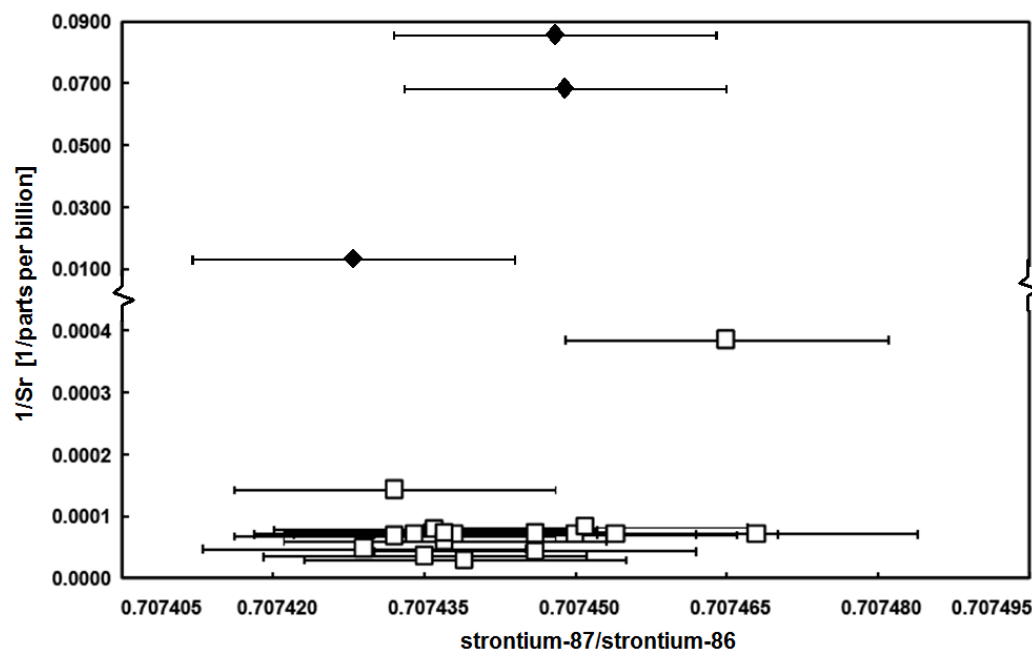


Figure 29. STRONTIUM ISOTOPIC ANALYSIS RESULTS FOR WATER AND TRAVERTINE

Strontium isotopes for water samples are shown as open squares and travertine samples are shown as solid diamonds. Strontium isotope results ($^{87}\text{Sr}/^{86}\text{Sr}$) are normalized to an accepted NIST SRM 987 of 0.710250 (Bralower et al., 1997). The range of strontium concentration for travertine samples is from 0.0135 to 0.0863 1/(parts/billion) and the range of strontium concentration for water samples is from 0.000029 to 0.000386 1/(parts/billion). The y-axis has a break in section so that $^{87}\text{Sr}/^{86}\text{Sr}$ results for travertine and water may be compared. The error bars indicate an analytical uncertainty of ± 0.000016 . The results of strontium isotopic analyses of water and travertine samples also are shown in Table 19. Water sample locations are shown on Figure 21. Travertine sample locations are shown on Figure 23.

The range of strontium isotopes shown in **Table 19** and presented on **Figure 29** is plotted with the strontium isotopic data from rock samples collected in northeast Mexico by Lehmann et al. (2000) and the secular seawater curve from the middle Cretaceous (Jenkyns et al., 1995; Bralower et al., 1997) in **Figure 30**. In this figure, the range of $^{87}\text{Sr}/^{86}\text{Sr}$ of Cuatrociénegas Basin water and travertine (indicated by the width of the gray rectangle) match the range of $^{87}\text{Sr}/^{86}\text{Sr}$ of rocks of the Barremian/Aptian Cupido formation and the Albian-age Aurora formation.

DISCUSSION

This section discusses the implications of the results of tritium, oxygen isotopic, noble gases, and strontium isotopic analyses.

Tritium

The results of tritium analyses of Cuatrociénegas Basin spring waters are shown in **Table 17** and on **Figure 25**. The tritium values range from a low of less than the detection limit of 0.1 tritium units at many springs to a high of 1.1 tritium units at El Venado. If an analysis has <0.1 tritium units, the water is at least 50–60 years old. However, for springs with tritium values below the detection limit, it is impossible to know the exact aquifer residence time. For instance, as Cuatrociénegas Basin spring water could have been recharged 500 or 5,000 years ago. Castiglia and Fawcett (2006) presented paleoclimate data from Chihuahua (approximately 500 kilometers to the northwest) that show multiple pluvial periods occurred in the last 5,000 years, complicating Cuatrociénegas Basin recharge timing. Goldman (1951) stated that now dry pluvial desert lakes existed within 100–200 km to the southeast (e.g., Laguna Mayrán) as late as 1926, suggesting recent past wetter climate.

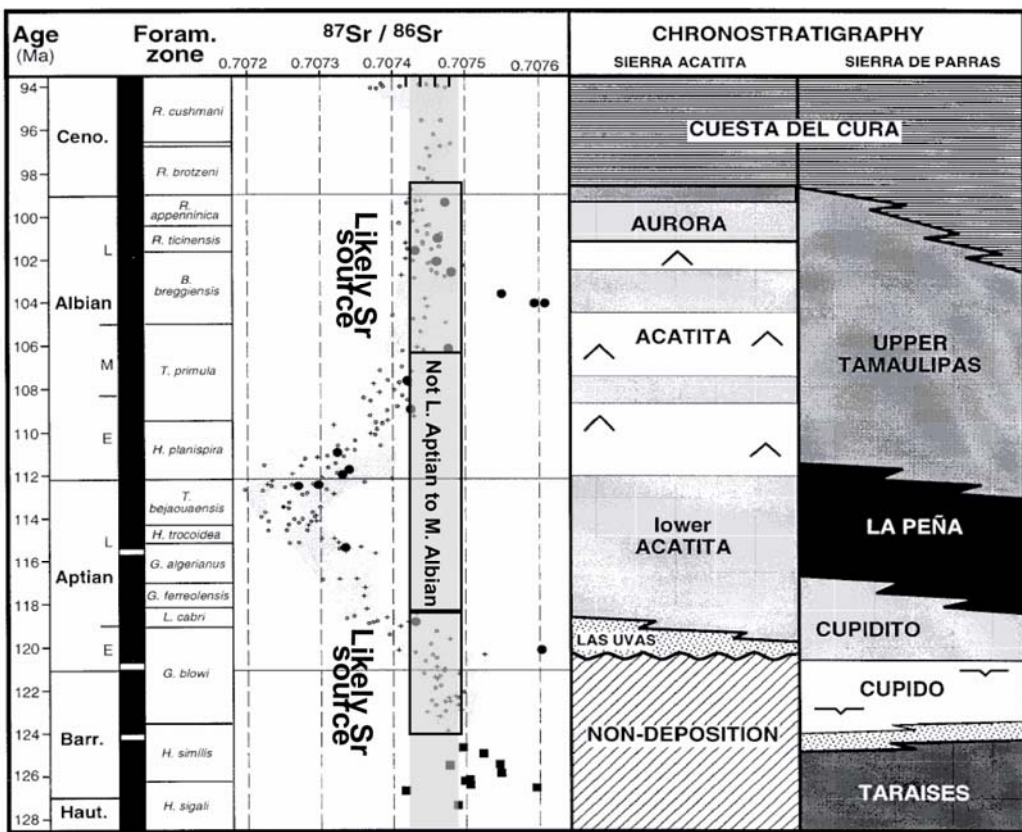


Figure 30. STRONTIUM ISOTOPIC VALUES OF CUATROCIÉNEGAS BASIN WATER AND TRAVERTINE, THE CRETACEOUS SECULAR SEAWATER CURVE, AND NORTHEAST MEXICO REGIONAL LITHOLOGY

Figure after Lehmann et al. (2000). The small crosses are $^{87}\text{Sr}/^{86}\text{Sr}$ values of Cretaceous shallow-water carbonates from guyots in the Mid-Pacific Mountains and also oysters and belemnites from England (Jenkyns et al., 1995). The small dots are $^{87}\text{Sr}/^{86}\text{Sr}$ values for Cretaceous foraminifera collected from Deep Sea Drilling Project-Ocean Drilling Program (DSDP-ODP) cores (Bralower et al., 1997). The solid circles are $^{87}\text{Sr}/^{86}\text{Sr}$ values for carbonate rocks collected by Lehmann in the Sierra Acatita (located approximately 75 kilometers west-southwest of the Cuatrocienegas Basin) and the solid squares are $^{87}\text{Sr}/^{86}\text{Sr}$ values for carbonate rocks collected by Lehmann in the Sierra Escondida (located approximately 175 kilometers south-southeast of the Cuatrocienegas Basin; Lehmann et al., 2000). Stratigraphy for the Sierra Acatita and the Sierra Escondida is shown on the two panels on the right side of the figure (Lehmann et al., 2000). The width of the gray box indicates the range of $^{87}\text{Sr}/^{86}\text{Sr}$ values for travertine and water in the Cuatrocienegas Basin. The areas where the gray box overlaps $^{87}\text{Sr}/^{86}\text{Sr}$ values from Jenkyns et al. (1995), Bralower et al. (1997) and Lehmann et al. (2000) show likely ages of the formation that is the source of strontium ions to Cuatrocienegas Basin travertine and water. Matches occur with the Aurora Formation, although Lehmann et al. (1999) state that Aurora Formation is relatively thin compared to the Cupido Formation in the Cuatrocienegas Basin region. Thus, the Cupido Formation is the likely source of strontium isotopes to Cuatrocienegas Basin travertine and spring water and that groundwater does not interact with siliciclastics of the San Marcos Formation.

Future research in the Cuatrocienegas region should focus on refining the paleo-hydrologic record to constrain better recharge timing. Analysis of tree ring growth bands (current and those in Cuatrocienegas homes), travertine and speleothem growth rates, and pollen and carbon-14 in valley sediment cores may be valid approaches to evaluate Cuatrocienegas regional paleo-hydrology.

A plot of tritium versus chloride is shown on **Figure 26**. In general, chloride concentration in spring water increases with decreasing tritium in spring water. Poza Anteojo and Poza Azul are the exceptions to this trend. Banner et al. (1989) commented that rock-water interaction of fluids with carbonate rocks is a possible mechanism to increase chloride in spring waters. Alternatively, evaporative concentration (as suggested by stable isotopic data of oxygen) may be a likely mechanism to produce chloride concentrations observed in Cuatrocienegas Basin spring waters. In addition, mixing of groundwaters of different tritium and chloride concentration may be an important process. Based on chloride-bromide ratios of Cuatrocienegas Basin spring waters, dissolution of halite does not occur.

Oxygen Isotopes

Rodríguez et al. (2005) and Johannesson et al. (2004) used stable isotopes ($\delta^{18}\text{O}$) to infer that recharge-causing precipitation to Cuatrocienegas Basin springs occurs at the elevation of mountains that surround the Basin (1,170–2,350 meters; **Figure 27**). However; the exact mountain range from which recharge occurs cannot be determined because mountain elevations are similar throughout northeast Mexico. Also, the $\delta^{18}\text{O}$ analyses show that valley floor precipitation (~770 meters) does not presently result in the majority of recharge flowing to Cuatrocienegas Basin springs. This is consistent with the findings of Darling (1997) and Scanlon et al. (1999) that found essentially no recharge presently occurs in analogous west Texas inter-drainage valley-floor settings.

The $\delta^{18}\text{O}$ analyses presented by Rodríguez et al. (2005) and Johannesson et al. (2004) also suggest that precipitation recharging springs on the western flank of the Sierra San Marcos occurs between approximately 1,250 meters (Rodríguez et al., 2005a) and 1,600 meters 2005 (Johannesson et al., 2004). It should be noted that any evaporation in the sample would cause the precipitation elevation signal to appear lower than it actually is. Precipitation feeding springs at the northern flank of the Sierra San Marcos occurs between approximately 1,150 and 1,250 meters (Rodríguez et al., 2005a). On the southeast flank of the Sierra San Marcos, precipitation to springs falls at approximately 1,450 meters (Rodríguez et al., 2005a).

Using oxygen isotopic analyses of Cuatrocienegas Basin spring waters, the inferred elevation at which precipitation occurs is shown on **Figure 27**. Because the data plot slightly below the local meteoric water line, some evaporation may occur prior to precipitation infiltration or after spring discharge (Cortés et al., 1997). Alternatively, interaction with the carbonate aquifer may also shift the $\delta^{18}\text{O}$ values, causing higher isotopic values. However, due to the linear trend in the $\delta^{18}\text{O}$ data presented by Johannesson et al. (2004), it is likely that evaporation is the dominant process. It is important to note that mixing of lower and higher elevation precipitation may also occur. One value from Poza Anteojo (interpreted as precipitation falling at approximately 2,350 meters—the highest elevation) is slightly higher in δD (or lower in $\delta^{18}\text{O}$) than the global meteoric water line (Craig, 1961). One explanation for this difference may be a different moisture source for precipitation feeding this spring (i.e., precipitation that has fallen, evaporated, and fallen again, causing the higher $\delta^{18}\text{O}$ value) or variations in the local precipitation. Johannesson et al. (2004) also commented that Poza Anteojo flows from the Sierra La Madera—while the other springs sampled are located on the flanks of the Sierra San Marcos—and may represent precipitation that fell at a different time of

the year, at a different elevation (the Sierra San Marcos is about 400 meters lower than the Sierra La Madera, that tops out at over 3,000 meters), or during different climatic conditions compared to Sierra San Marcos springs.

Dissolved Noble Gases in Spring Water

The difference between $\delta^{18}\text{O}$ precipitation elevation (approximately 1,170–2,350 meters) and noble gas recharge elevation (approximately 720–770 meters) suggests that a thick vadose zone exists (Heilweil et al., 2006). A thick vadose zone is consistent with other arid karst regions globally. The tallest mountains in the Cuatrocienegas Basin study area are approximately 3,000 meters and noble gas data suggest a recharge elevation (indicative of the water table) of approximately 750 meters. Thus, the vadose zone is approximately 2,250 meters thick. Previous researchers (Rodríguez et al., 2005a) suggested groundwater divides exist under the mountain ranges separating the Cuatrocienegas Basin from adjacent valleys, with no interbasin groundwater flow occurring. However, the results of the noble gas analyses support an important implication that interbasin flow does indeed occur and that topographic highs (i.e., mountains separating adjacent basins) do not necessarily represent groundwater divides. It should be noted that both the results of $\delta^{18}\text{O}$ and noble gases have uncertainties in the evaluation of the elevation at which precipitation falls and the elevation at which recharge enters the water table. However, the results of $\delta^{18}\text{O}$ and noble gases suggest that precipitation may fall at the elevation of mountains in the study area and that a thick vadose zone exists.

The results of helium isotopic analyses of Cuatrocienegas Basin spring waters are shown on **Figure 28**. The values of R/R_a range from a low of 0.9 at El Venado to 1.8 at the warm vent of Poza La Becerra, Poza Azul, and Poza Escobedo. Poza Anteojo has a low R/R_a value (1.2) relative to the other springs, which are 1.1 (Poza Escobedo surface

water inlet canal), 1.3 (Poza Churince), 1.5 (Poza La Tecla), and 1.6 (the cool vent of Poza La Becerra). The source of helium-3 that causes the R/R_a values to be greater than one is either from the decay of tritium in groundwater or from the decay of radiogenic elements in the mantle (Solomon, 2000; Crossey et al., 2006). Because tritium in Cuatrocienegas Basin springs is generally below the detection limit of 0.1 tritium units, mantle degassing is likely the source of helium-3 found in Cuatrocienegas Basin spring waters. Thus, mantle-sourced helium may be leaking up along basement-involved faults. Future research should focus on collecting additional helium isotope samples to constrain structural controls on groundwater evolution.

Strontium Isotopes of Spring Water and Travertine

Strontium isotopic data of waters and travertine are presented in **Table 19**, **Figure 29**, and **Figure 30**. The strontium data imply that carbonates and gypsum of the Aptian-age (approximately 124–119 million years) Cupido Formation is the most likely source of strontium ions and the predominant regional aquifer. While the range of strontium isotopic results ($^{87}\text{Sr}/^{86}\text{Sr} = 0.707429$ to 0.707468) also matches with the Albian-age (approximately 102–100 million years) Aurora Formation, Lehmann et al. (1999) noted that the Aurora Formation is largely absent in the Cuatrocienegas region. Thus, the Aptian-age Cupido Formation is likely the source of strontium ions in spring water and travertine. Results of strontium isotopes of water and travertine also suggest that the Cupido Formation is the regional carbonate aquifer feeding Cuatrocienegas Basin springs and that little flow occurs through the siliciclastics of the San Marcos Formation.

In addition, the homogeneous $^{87}\text{Sr}/^{86}\text{Sr}$ values for water and travertine also suggest that the source of strontium ions in Cuatrocienegas Basin spring water has not changed in approximately 17,000 years. $^{87}\text{Sr}/^{86}\text{Sr}$ for the two travertine samples of inferred Pleistocene age (or approximately 17,000 years, as presented by Rodríguez et al.,

2005a) is 0.707448 and 0.707449 and $^{87}\text{Sr}/^{86}\text{Sr}$ values for spring water ranges from 0.707429 to 0.707468. Poza Churince is located approximately four kilometers to the north of the location where the two travertine samples of inferred Pleistocene age were collected. A water sample from Poza Churince has a strontium isotopic ratio of 0.707468. The strontium isotopic ratio of the travertine of inferred Pleistocene age is just outside the lower range of uncertainty of the water sample from Poza Churince. However, the results suggest the source of strontium ions in the travertine of inferred Pleistocene age and nearby spring water has not changed appreciably in approximately 17,000 years, despite significant regional climatic changes.

Musgrove et al. (2001) evaluated growth rates of central Texas speleothems collected in caves located approximately 700 kilometers to the northeast of the Cuatrocienegas Basin. They determined that central Texas speleothem growth rates varied over two orders of magnitude. One period of rapid speleothem growth was from 24,000–12,000 years ago during the Last Glacial Maximum, a period of cooler and wetter climate than the present. Growth rates dropped from 15,000–12,000 years ago and had very slow growth rates until the present, indicating drier climatic conditions during the Holocene. Assuming the climate in northeast Mexico also was significantly cooler and wetter in the Pleistocene than present climatic conditions, the homogeneous results of strontium isotopes of travertine of inferred Pleistocene age and spring waters indicate that the Cupido Formation accommodated the elevated recharge that occurred during the Last Glacial Maximum. Noble gas analyses presented earlier infer a thick vadose zone under present climatic conditions. This thick vadose zone may have accommodated greater recharge and groundwater storage during past wetter climatic conditions.

Springs on the Southeast Flank of the Sierra San Marcos

Hydrogeologic data and environmental tracers infer that recharge to springs on the southeast flank of the Sierra San Marcos originates as precipitation on the Sierra San Marcos, but may also include a component of interbasin groundwater flow through the Cupido Formation aquifer. Tritium measured at Poza Santa Tecla in August 2007 was 0.2 tritium units, suggesting mostly older water, with a component of locally-derived mountain recharge. Oxygen isotopes suggest a precipitation elevation of approximately 1,450 meters, which is in the range of elevations in the Sierra San Marcos. Noble gas data indicate a recharge elevation (i.e., the elevation of the water table when recharge occurred) of approximately 714 meters—inferring that interbasin groundwater flow may occur. Thus, recharge calculations support a Sierra San Marcos source for springs feeding the Santa Tecla Canal, but the canal may also have mixing of groundwater from recharge on the Sierra San Marcos and interbasin flow from outside the Cuatrociénegas Basin.

Spring Discharging from the Ocampo Valley (Río Cañon)

Because the Río Cañon is presently dry, tritium and stable isotopic data and noble gas data are unavailable to evaluate recharge. However, a Sierra La Madera (and other mountains surrounding the Ocampo Valley) recharge source is likely for the formerly spring-fed Río Cañon flowing from the Ocampo Valley to the Cuatrociénegas Basin.

Springs on the West and North Flank of the Sierra San Marcos

Tritium measured in these springs ranged from <0.1–0.4 tritium units, indicating an aquifer residence time predominantly >50 years, which implies a regional flow system. Oxygen isotopes suggest a precipitation elevation ranging from approximately 1,150–1,250 meters (with an outlier of 1,600 meters), which agrees with generally lower mountain elevations. Noble gas data indicate a recharge elevation of approximately 700–

770 meters. Thus, topographic divides between adjacent basins do not have associated groundwater divides and that a regional flow system is possible.

CONCLUSIONS

The research finds that the Aptian-age (approximately 124–119 million years) Cupido Formation is likely a regional carbonate aquifer system discharging in Cuatrocienegas Basin springs (based on $^{87}\text{Sr}/^{86}\text{Sr}$ = approximately 0.707425–0.707505 for travertine and water). The research also suggests that the source of strontium ions in the travertine ($^{87}\text{Sr}/^{86}\text{Sr}$ = 0.707465 and 0.707464) of inferred Pleistocene age and nearby spring water ($^{87}\text{Sr}/^{86}\text{Sr}$ = 0.707487) is from the same source. Results of analyses of dissolved noble gases in Cuatrocienegas Basin spring water infer a maximum recharge elevation of approximately 768 meters — suggesting that groundwater mounds do not exist under mountains in the Cuatrocienegas Basin region and that inter basin flow is plausible. Tritium in springs on the southeast flank of the Sierra San Marcos (0.2 tritium units) suggests water mostly older than 50 years, with a component of locally-derived younger water (e.g., El Venado = 1.1 tritium units).

Tritium was not analyzed in the spring that fed the Río Cañon because groundwater no longer discharges from the Ocampo Valley. However, groundwater with a residence time >50 years likely recharged in the mountains on the western side of the Ocampo Valley (approximately 80 kilometers from the historic spring) may have also mixed with younger recharge water that discharged into the Río Cañon. Tritium in springs on the west and north flank of the Sierra San Marcos (<0.1–0.4 tritium units) suggests water mostly older than 50 years from a regional aquifer system, with a component of locally-derived younger water.

Oxygen isotopes in springs on the west and north flank of the Sierra San Marcos show an evaporative trend and also suggest a lower precipitation elevation (1,150–1,250 meters) compared to the other springs (e.g., Poza Anteojo, at the foot of the Sierra La Madera has an interpreted precipitation elevation of approximately 2,350 meters)—although many factors contribute to interpretation uncertainty.

Chapter 4: GIS-Based Chloride-Balance Modeling to Evaluate Recharge Areas and Understand Differences in Spring Discharge, Chloride Concentration, and Temperature in an Arid Karst Aquifer

A revised version of this chapter will be submitted for publication.

ABSTRACT

An integrated chloride and water-balance approach can delineate recharge catchments of arid karst aquifer systems with sparse hydrogeologic data such as the Cuatrocienegas Basin, Coahuila, Mexico. The Cuatrocienegas Basin is a UNESCO World Biosphere Reserve containing >500 springs that support groundwater-dependent ecosystems with >70 endemic species and irrigated agriculture. In circumstances in which a paucity of spatially- and temporally-distributed well data exists, aquifer characterization is hindered. This restricts development of effective water resource management policies in developing arid karst aquifer systems. To mitigate the paucity of data, an integrative data approach combining limited water quantity and quality data can minimize hydrogeologic conceptual model uncertainty. To facilitate the development of hydrogeologic conceptual models in the Cuatrocienegas Basin, initial aquifer contributing zones are delineated in a geographic information system environment using remotely sensed topographic data, geologic mapping, and permeability data.

Within the initial model domain, the integrative data modeling approach uses hydrogeologic data, environmental tracers, and selected groundwater levels (from springs, playa lakes, monitoring wells, and inferred from surface topography) to calculate recharge using water and chloride mass balance, groundwater flow between aquifer zones, and spring water temperature. Measured spring discharge is used to infer the minimum recharge volume. Spring water temperature is used to calculate the minimum

groundwater flow depth, which is used to infer deep interbasin flow versus shallow local recharge. Chloride concentrations of rain and spring water are used to estimate recharge using a chloride-balance approach. Chapter 2 used a fixed spatially-distributed recharge rate of approximately one percent. This analysis refines recharge with an elevation-depended recharge rate. Recharge is only applied on mountain recharge areas and does not occur on valleys, consistent with recharge in analogous regions. Noble gas, geochemistry, and isotopic data presented previously in Chapter 3 are consistent with a regional flow system, but of unknown extent. To reduce hydrogeologic conceptual model uncertainty, aquifer connectivity is adjusted until the error between measured and modeled spring discharge and chloride concentration is minimized. This approach is applied to understand the spatial extent of the regional aquifer system contributing to the springs of the Cuatrocienegas Basin. This research finds that springs with relatively low discharge, chloride concentration, and temperature on the southeast flank of the Sierra San Marcos are recharged in an approximately 450-square kilometer local catchment of exposed carbonate rock in the Sierra San Marcos. Historic spring discharge in the Río Cañon is recharged from an approximately 600-square kilometer recharge area of exposed carbonate rock of mountains surrounding the Ocampo Valley. Cuatrocienegas Basin springs on the west and north flank of the Sierra San Marcos with elevated discharge, chloride concentration, and temperature are recharged from an approximately 1,000-square kilometer recharge area of exposed carbonate rock of the mountains surrounding the Hundido, Sobaco, and San Marcos Valleys. In total, approximately a 18,000-square kilometer area provides recharge to springs in the Cuatrocienegas Basin through a combined local/regional flow system.

INTRODUCTION

It is difficult to estimate arid basin recharge because (1) subgrid scale precipitation estimates provide a large source of uncertainty in mountainous regions like the Cuatrocienegas Basin because of the lack of high elevation gages (Adam et al., 2006); (2) observation paucity hampers studies of the Mexico North American Monsoon that provides approximately 40 percent of the annual precipitation in northeast Mexico (Zhu and Lettenmaier (2007); Gochis et al., 2005); and (3) an appreciable amount of uncertainty in the rate and distribution of recharge (Sanford, 2002).

This research addresses the difficulty in estimating arid basin recharge rates. Other researchers have developed approaches to estimate recharge in arid basins with sparse hydrogeologic data. Maxey and Eakin (1949) used a water budget approach to estimate recharge that assumes negligible recharge at low elevations and the majority of recharge occurring in mountains in Nevada. Dettinger (1989) estimated recharge in the Great Basin of Nevada using a chloride balance approach, a method that is ideal for locations with little hydrogeologic data. This research extends the work of these researchers by considering spatially variable recharge rate to explain variations in spring chloride concentration, temperature, and flow rates and to delineate capture zones more accurately.

To demonstrate this approach, aquifer systems in the Cuatrocienegas Basin, Coahuila, Mexico, are evaluated. This system lacks long-term well data to support aquifer characterization and effective groundwater management. This research delineates catchments and maps recharge areas to Cuatrocienegas Basin springs. Previous research is expanded upon by using the spatial variability of chloride, and flow rate, in addition to other hydrogeologic data, to delineate the recharge areas. Wolaver et al. (2008) applied a uniform recharge rate (approximately one percent of annual precipitation) using a

chloride balance and integrative data approach to infer an approximately 18,000-square kilometer regional flow system, but did not explain variations in spring chloride concentration, flow rate, and temperature. New hydrogeologic data not available in Wolaver et al. (2008) refine the hydrogeologic conceptual model.

This research presents procedures to delineate arid karst aquifer systems with chloride balance recharge analysis and water budgets using a recharge conceptual model based upon Maxey and Eakin (1949). The approach also assesses groundwater flow rates, chloride and tritium concentrations, and temperature to minimize the hydrogeologic conceptual uncertainty of the spatial extent of regional arid karst aquifer systems. Associated hydraulic, geochemical, and temperature data presented previously are evaluated within the context of reducing hydrogeologic conceptual model uncertainty.

Because hydrogeologic data for the Cuatrocienegas Basin are limited in temporal and spatial extent, the use of distributed finite-difference or finite-element models to test hydrogeologic conceptual models is questionable—distributed models without effective distributed data can be at best expensive interpolation or hypothesis-generating tools (Beven, 1993; Fedra, 1993). Thus, the modeling framework presented herein is important for aquifer characterization in arid karst aquifer systems where population is expanding into previously under-utilized aquifer systems. The approach may be used to generate hydrogeologic conceptual models of arid karst aquifer systems that lack long-term well data, but may require more detailed numerical models to predict the effects of water development scenarios and projected climate change on temporal and spatial variations in groundwater levels and spring discharge. This approach builds upon previous arid karst aquifer delineation methods in the Great Basin (Maxey and Eakin, 1949; Eakin, 1966; Maxey, 1968; Winograd and Thordarson, 1975; Eakin et al., 1976; Mifflin, 1988; Dettinger, 1989; Anning and Konieczki, 2005).

BACKGROUND

The Cuatrocienegas Basin is located approximately 300 kilometers southeast of Big Bend National Park (located in the State of Texas, U.S.A), in the State of Coahuila, Mexico. The Cuatrocienegas Basin study area is located at the northern edge of the Sierra Madre Oriental in the Chihuahuan Desert (**Figure 31**). Historically, groundwater development in the region was limited. However, as high-quality groundwater suitable for agriculture was exhausted near the City of Torreón, Durango, farmers searched for new areas to grow crops (Brouste et al., 1997). In recent decades, large-scale irrigated agriculture has developed the Hundido and Ocampo Valleys adjacent to the Cuatrocienegas Basin. It is difficult to evaluate the effects of groundwater mining in surrounding valleys on Cuatrocienegas Basin springs because their recharge areas are yet uncertain. In the following section, the author discusses the water resources of the Cuatrocienegas Basin, the hydrogeology of the Cuatrocienegas Basin and surrounding region, and presents the chloride balance and water budget modeling approach. Wolaver et al. (2008) discussed details of the structural, tectonic, hydrostratigraphic, and the Cuatrocienegas Basin regional hydrogeologic setting.

Topography

Cuatrocienegas Basin regional elevation ranges from 770 meters in the valleys to over 3,000 meters in the Sierra La Madera at the north end of the Cuatrocienegas Basin, as shown on **Figure 32**. Elevation increases to the north, west, and south of the Cuatrocienegas Basin, providing a topographic gradient that may also represent a gradient for groundwater flow into the Cuatrocienegas Basin, based on the principals of regional flow of Tóth (1963). Vegetation in this LANDSAT image is indicated in red. Irrigated agriculture to the east of the Cuatrocienegas Basin (shown in the center of the image) relies on spring discharge. Thin pine forests are also present on the mountain tops.

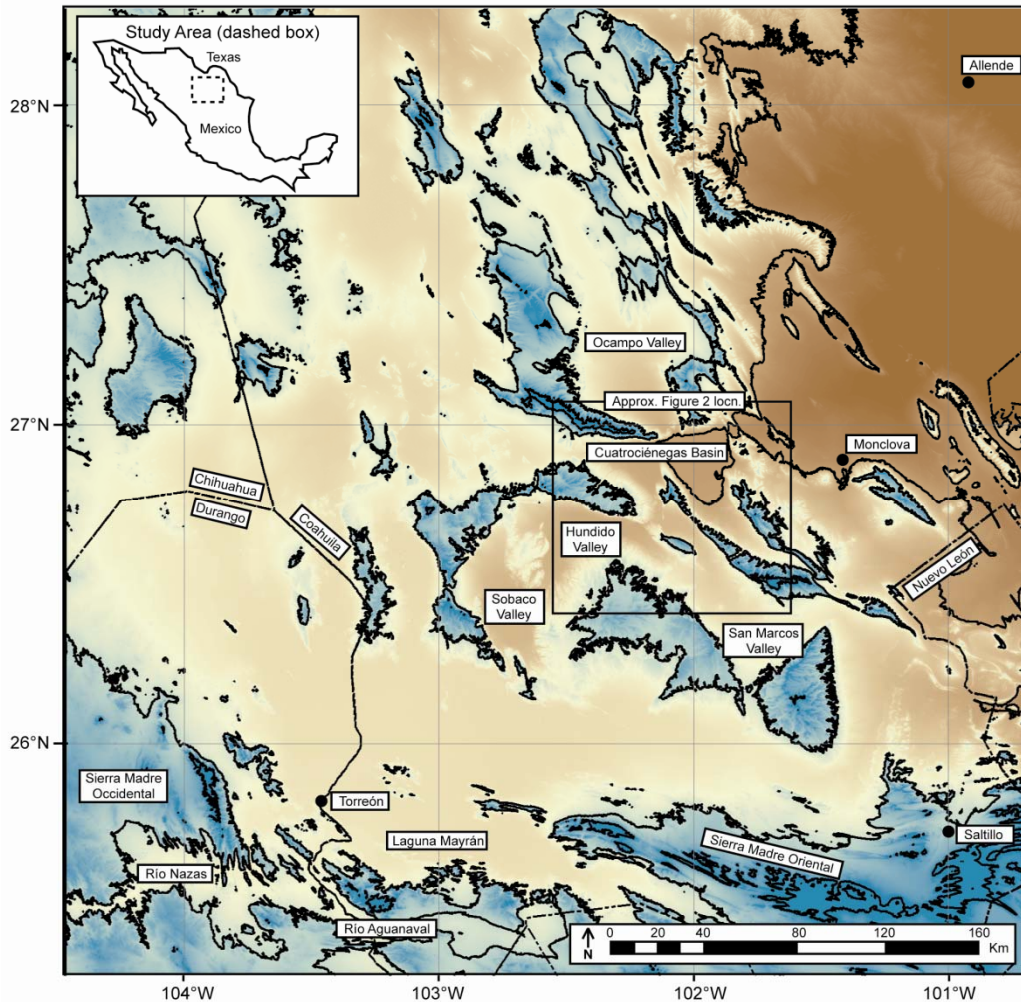


Figure 31. CUATROCIÉNEGAS BASIN STUDY AREA

Contour interval ranges from brown (750-meter)–green (1,500- and 2,250-meter). State boundaries are labeled with state names (e.g., Chihuahua, Coahuila, Durango, and Nuevo León).

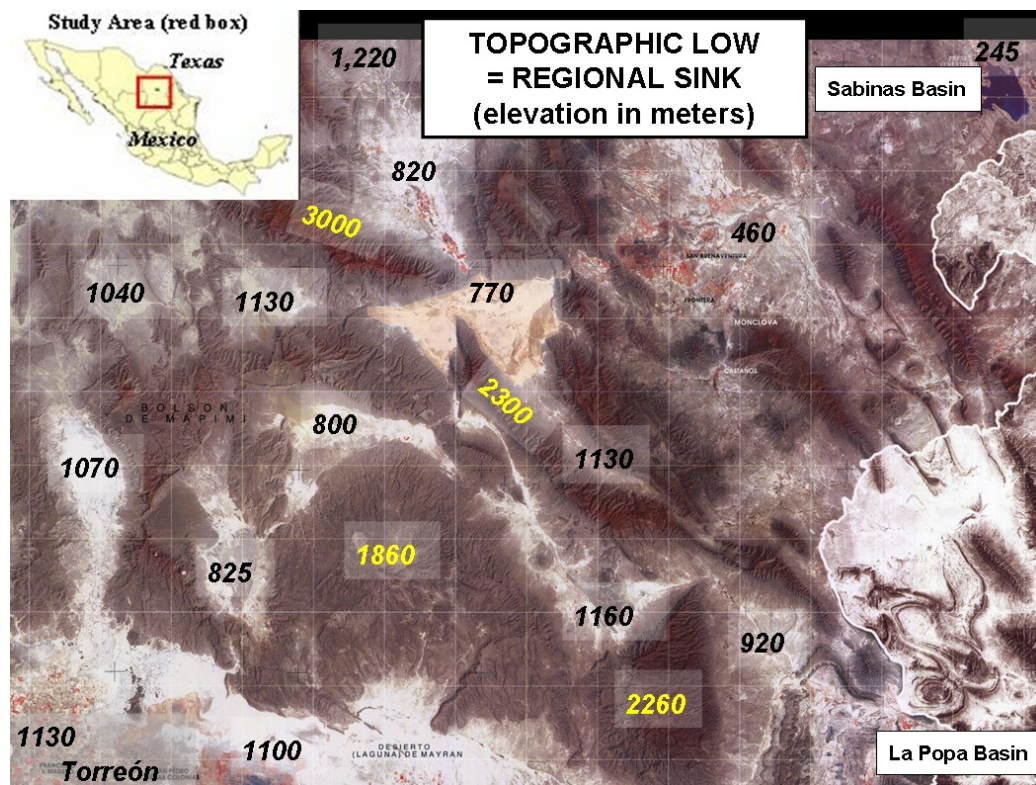


Figure 32. TOPOGRAPHY OF THE CUATROCIÉNEGAS BASIN REGION

Valley-floor elevation is shown in black. Mountain-top elevation is shown in yellow. Red indicates vegetation in this LANDSAT image with 10-kilometer grid marks. The Cuatrocienegas Basin is at a regional low elevation.

Water Resources

The springs of the Cuatrocienegas Basin have long been an important ecological and human resource. Prior to the intervention of man, the formerly closed basin included large playa lakes and extensive groundwater-dependent ecosystems (called ciénegas in Spanish). Natural discharge from the Cuatrocienegas Basin included evapotranspiration and possibly groundwater interbasin flow to the east, but interbasin groundwater flow out of Cuatrocienegas Basin has not been documented. Cuatrocienegas Basin place names are shown on **Figure 33**. Gilmore (1947) noted that a stream drained the Cuatrocienegas Basin through the Puerto Salado gap as late as the mid-1940s. Miller (1961) found that by 1961 this stream had dried completely due to canal construction and/or climatic effects. Carbon-14 dating of organic matter from cores in the valley-fill alluvium of the Cuatrocienegas Basin in the vicinity of present-day springs and groundwater-dependent ecosystems indicates that groundwater-dependent ecosystems have existed in the Cuatrocienegas Basin for at least 30,000 years (Meyer, 1973). Archeological remains in caves that do not include European domesticated animals or European trade goods suggest that humans lived around valley wetlands since at least pre-Spanish times (Gilmore, 1947).

Spaniards settled the Cuatrocienegas Basin in the 1760s, attracted by the spring-fed Río Cañon (**Figure 34**), which they used to irrigate gardens, orchards, and vineyards (Calegari, 1997). Now, canals convey spring discharge out of the formerly closed basin through the Puerto Salado gap to irrigate valleys to the east. French drains lowered shallow groundwater for grazing, while at the same time, reducing wetland size and drying unique freshwater stromatolites in the western Cuatrocienegas Basin as described by Winsborough (1990).

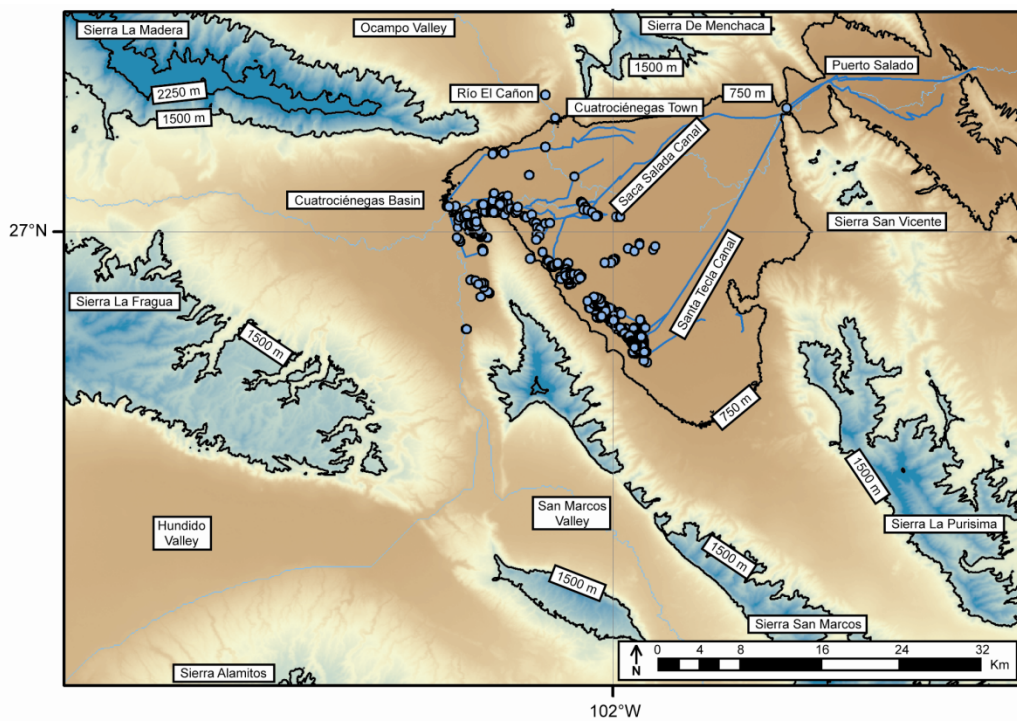


Figure 33. CUATROCIÉNEGAS BASIN FEATURES

Cuatrocienegas Basin features include springs (blue dots), canals (light blue lines), inferred surface drainage network (light blue dashed line, see Wolaver et al., 2008), and 750-meter contour intervals (low-high-elevation ranges from brown–green, respectively).



Figure 34. SPRING-FED RÍO CAÑON PRIOR TO OCAMPO VALLEY GROUNDWATER DEVELOPMENT

This photo was taken in 1964 by Minckley and Cole (1968). They estimated spring discharge in 1964 was 250 liters/second by visual inspection.

Groundwater level was close to the ground surface in the 1970s in upgradient valleys to the north (Ocampo Valley) and south (Hundido Valley; INEGI, 1975). Large-scale agricultural groundwater development (approximately 55,000,000 cubic meters/year; Lesser y Asociados, 2001) for alfalfa started in Ocampo Valley to the north in the mid-1980s, causing approximately one meter/year drawdown. As a result, the spring-fed Río Cañon that used to flow from the Ocampo Valley to the Cuatrociénegas Basin dried. The formerly spring-fed, now post-development Río Cañon is shown on **Figure 35**. In the 1960s, the Río Cañon flowed at approximately 0.25 cubic meters/second with a chloride concentration of approximately 20 milligrams/liter; now the Río Cañon rarely flows (Minckley and Cole, 1968). Thus, groundwater development for agriculture in the Cuatrociénegas Basin region has substantially reduced groundwater-dependent ecosystem size (Minckley, 1992).

Local managers at the Cuatrociénegas Reserve have observed the cause and effect relationship of Ocampo Valley groundwater pumping drying the Río Cañon. Reserve managers are concerned that more recent pumping for large-scale agriculture in the Hundido Valley will dry other springs in the Cuatrociénegas Basin. This research project addresses this question by refining the delineation of the aquifer system that discharges in Cuatrociénegas Basin springs.

Groundwater development for agriculture in the Hundido Valley to the south of the Cuatrociénegas Basin (approximately 21,900,000 cubic meters/year; Lesser y Asociados, 2001) commenced in the 1990s (Calegari, 1997). Historically, shallow groundwater in the Hundido Valley caused seeps that were used to provide water for horses in the earliest 1900s. Over 20 meters of drawdown has occurred since predevelopment conditions.



Figure 35. RÍO CAÑON AFTER OCAMPO VALLEY GROUNDWATER DEVELOPMENT

This photo was taken by the author in Fall 2005. Conditions prior to groundwater development are shown in Figure 34.

In light of the effects of water development projects on groundwater-dependent ecosystems in the Cuatrocienegas Basin, wetland restoration is occurring. Pronatura Noreste, a Mexican non-governmental conservation organization, recently purchased water rights from farmers to restore wetlands in Rancho Pozas Azules. This water rights transfer returns water that was previously used to irrigate crops to groundwater-dependent ecosystems. The water purchase is the first for instream (e.g., environmental) flows in Mexico. Reserve managers also are exploring the possibility of diverting canal flow to restore important spring-fed wetland habitat. Currently, continued groundwater over-exploitation in upgradient basins to the north, west, and south basins threatens spring-fed wildlife habitat in the Cuatrocienegas Basin. In light of the threat to Cuatrocienegas Basin spring flow from groundwater over exploitation, this paper presents an approach for evaluating arid karst aquifer systems in support of effective groundwater development.

Precipitation

The Cuatrocienegas Basin is in the Chihuahuan Desert. Average annual valley floor (~750 meters) precipitation is approximately 220 millimeters (Wolaver et al., 2008). Precipitation at the highest elevations in the study area (~3,000 meters) is estimated at approximately 400 millimeters (González, 2006, pers. com.). Annual valley floor precipitation since 1942 is shown on **Figure 36**. The drought of the 1950s is evident. Several dryer than normal years also occurred in the late 1990s and early 2000s. These dry years reflect a larger regional-scale drought that also occurred in the Southwest U.S. (Piechota et al., 2004), but they are not abnormal.

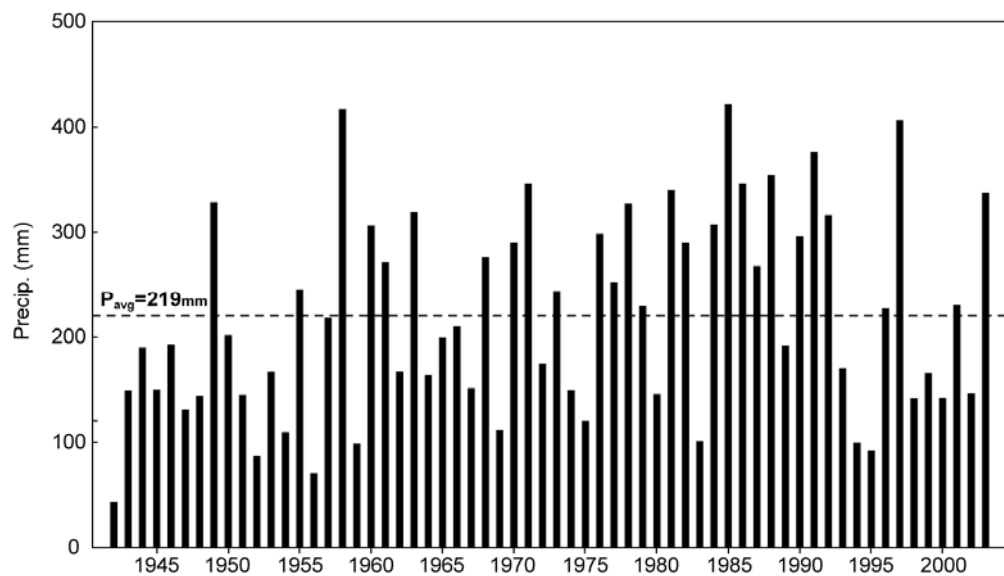


Figure 36. ANNUAL PRECIPITATION OF CUATROCIÉNEGAS BASIN VALLEY FLOOR

After Rodríguez et al., 2005a. 219 millimeters is the average valley floor precipitation value.

Satellite-derived precipitation using PERSIANN (Hsu et al., 1997; and Sorooshian et al., 2000) was evaluated by this research, but found to be inaccurate when compared to long-term Cuatrocienegas Basin gage precipitation. PERSIANN consistently over estimated precipitation compared to ground-truth data in the town of Cuatrocienegas. Therefore, only gage precipitation and inferred mountain precipitation based on vegetation requirements are used by this research.

Average monthly valley floor precipitation is shown on **Figure 37**. Total monthly precipitation data are calculated by summing daily precipitation for each month of the year using precipitation data collected at the Cuatrocienegas Town precipitation station (period of record: 1942–2004). Average monthly valley floor precipitation is calculated by taking the average of precipitation for each month in the record. The Cuatrocienegas Basin is located on the eastern edge of the North American Monsoon (Gochis et al., 2006). Approximately 75 percent of precipitation falls from May–October and approximately 40 percent occurs from June–August as intense, convective storms.

Hydrogeologic Setting and Conceptual Model

This paper considers a hydrogeologic conceptual model with a combination of local and regional flow systems. A cross section through the study area from southwest to northeast is shown on **Figure 38**; it includes the Sierra San Marcos and associated springs. Cretaceous carbonate rocks and terrigenous siliciclastics underlie Quaternary valley-fill alluvium throughout the study region. The regional basement is comprised of Triassic granodiorite. Arrows indicate the relative motion of multi-reactivated thrust faults that bound many of the anticlinal structures in the region. A cross section through the study area from north to south is shown on **Figure 39**.

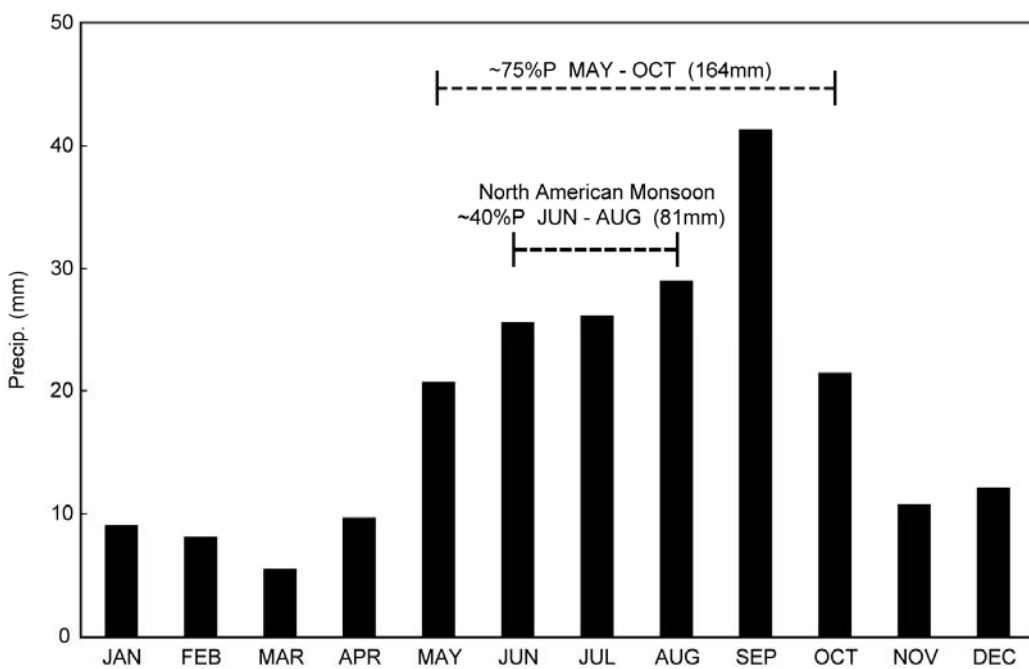


Figure 37. AVERAGE MONTHLY PRECIPITATION OF CUATROCIÉNEGAS BASIN VALLEY FLOOR
Precipitation data were presented in Rodríguez et al., 2005a.

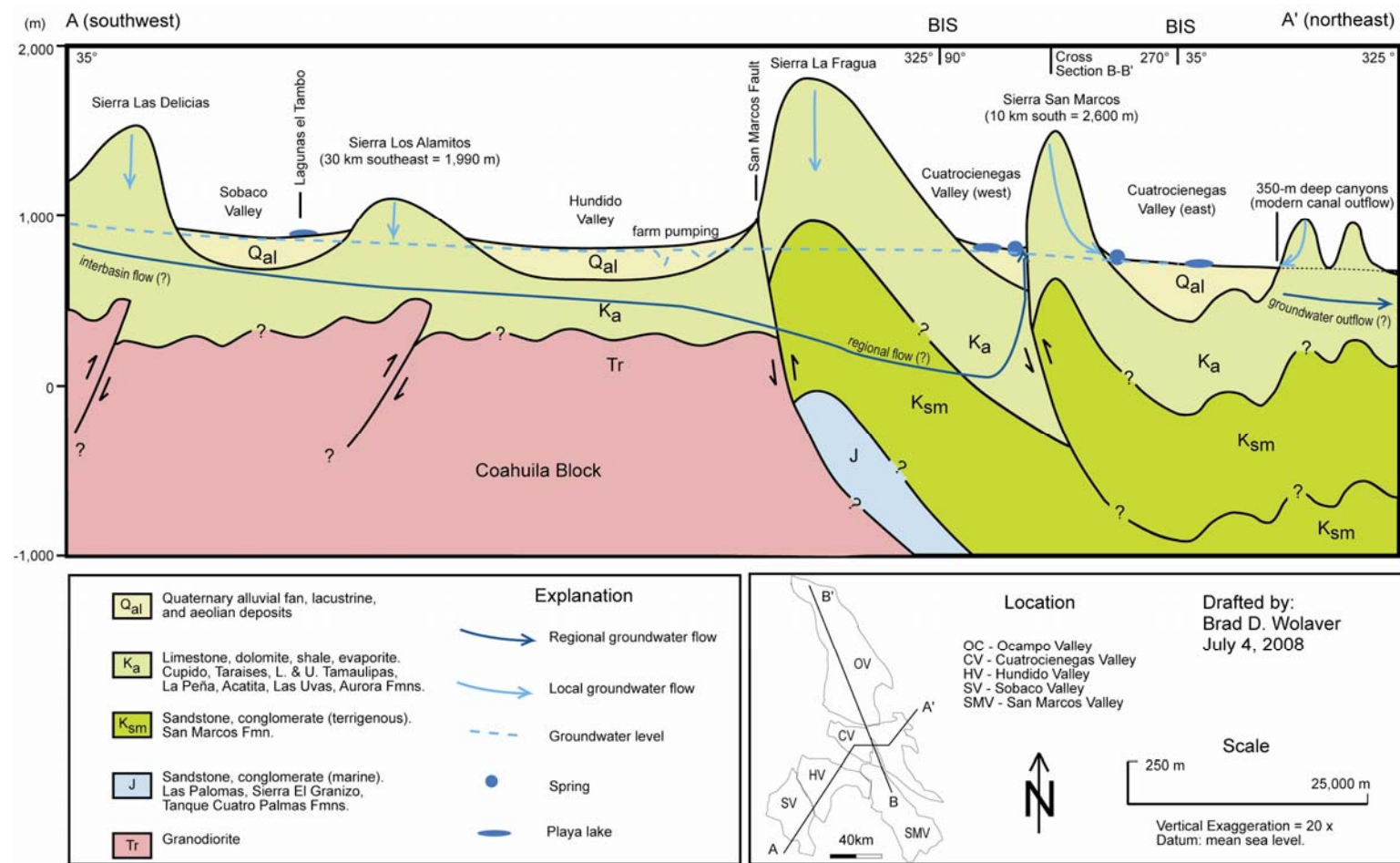


Figure 38. HYDROGEOLOGIC CONCEPTUAL CROSS-SECTION A-A' THROUGH THE CUATROCIÉNEGAS BASIN

Cross-section developed using data and analyses of Chávez-Cabello et al. (2005), Goldhammer (1999), McKee et al. (1984), Lehmann et al. (1999), McKee et al. (1990), and Rodríguez et al. (2005a).

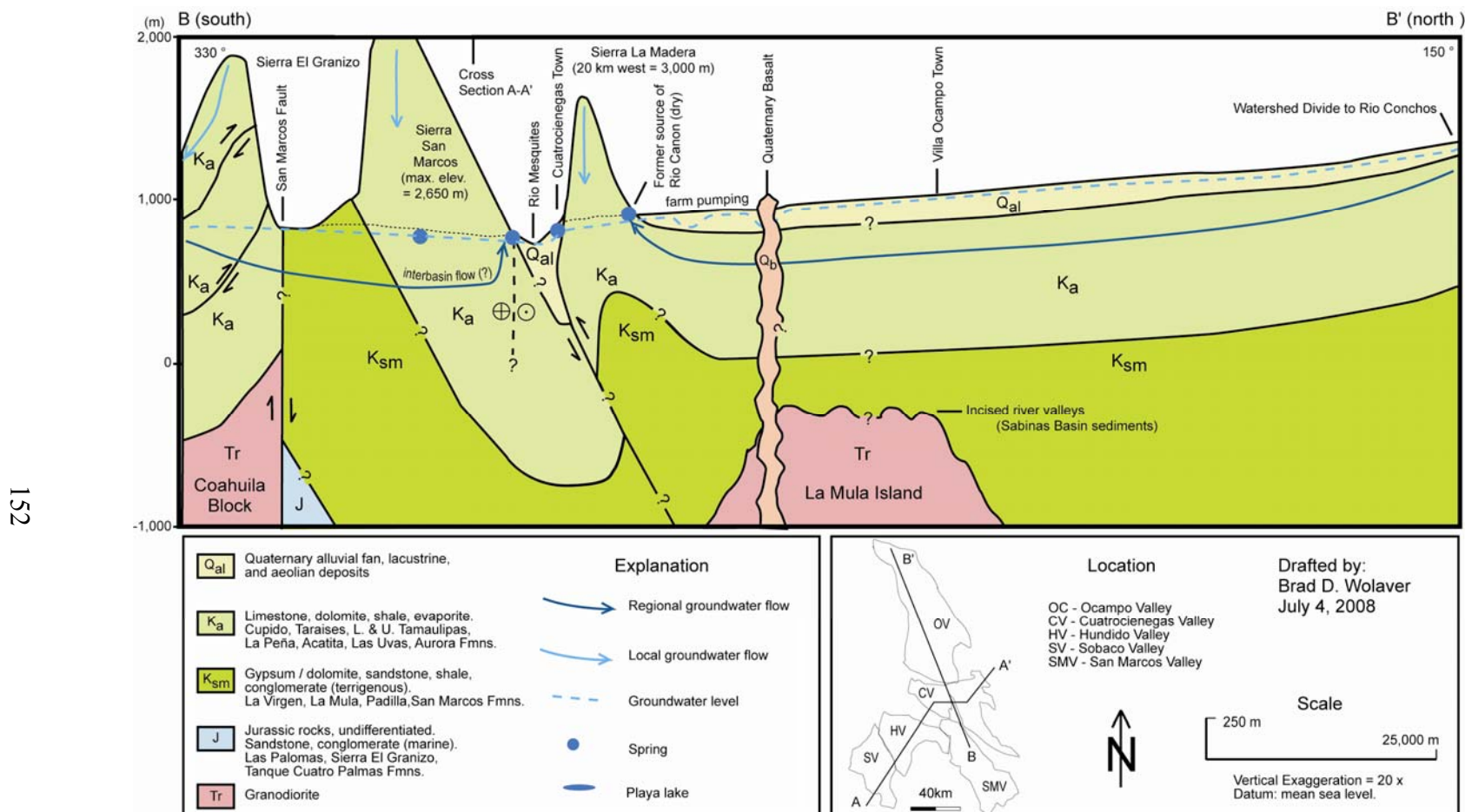


Figure 39. HYDROGEOLOGIC CONCEPTUAL CROSS-SECTION B-B' THROUGH THE CUATROCIÉNEGAS BASIN

Refer to Figure 38 for references cited.

Few pumping test data exist for the study area. Hydraulic conductivity values for analogous carbonate terranes are considered and are presented in **Table 20**. A hydrostratigraphic column is presented in **Table 21**.

METHODS

Wolaver et al. (2008) delineated catchments assuming a constant recharge rate using a chloride balance approach. However, that research leaves uncertainties in the delineation of local versus regional recharge areas. Also, Wolaver et al. (2008) do not explain spatial differences in chloride concentration, discharge, or temperature in springs. This research tests the hypothesis that differences in spring chloride concentration, discharge, and temperature are caused by recharge from different catchment areas. For example,

1. The low chloride concentration (22 milligrams/liter) of historic spring discharge from the Ocampo Valley to the Río Cañon is explained by high elevation precipitation in the mountains surrounding the Ocampo Valley with elevated recharge rates;
2. Elevated chloride concentrations of springs on the southeast flank of the Sierra San Marcos (approximately 30 milligrams/liter) are explained by precipitation on the lower elevation Sierra San Marcos (approximately 90 milligrams/liter) with a corresponding lower recharge rate; and
3. Overall lower elevation precipitation and evaporation from shallow water tables in Cuatrocienegas Basin spring recharge areas explains elevated chloride concentrations in springs on the western and northern flank of the Sierra San Marcos.

Table 20. PERMEABILITY FOR CARBONATE TERRAINS IN TEXAS, NEVADA, AND MEXICO

¹Hydraulic conductivity (meters/day) values from the literature are converted to transmissivity (shown in italics) assuming a saturated thickness of 22.5 meters, based on an average saturated thickness from analytical model inputs below. ²Belcher et al. (2002) reported hydraulic conductivity values as low as 10^{-4} meters/day for unfractured portions of the Lower Carbonate Aquifer of the Death Valley regional flow system. No data is indicated by -- .

Reference	Location & Rock Type	Hydraulic Conductivity [cm/sec]	Hydraulic Conductivity [m/sec]	Hydraulic Conductivity [m/day]	Transmissivity ¹ [m ² /day]
Nielson and Sharp (1985)	West Texas, U.S., Dell City, Bone Spring-Victorio Peak limestone	--	--	--	9×10^2 to 3×10^3
Bedinger et al. (1986)	Great Basin, Southwest U.S., Dense to mod. dense unfractured carbonate ²	6×10^{-7} to 9×10^{-4}	6×10^{-9} to 9×10^{-6}	5×10^{-4} to 8×10^{-1}	1×10^{-2} to 2×10^1
	Great Basin, Southwest U.S., Fractured, karst carbonate	1×10^{-4} to 1×10^1	1×10^{-6} to 1×10^{-1}	1×10^{-1} to 1×10^4	2×10^1 to 2×10^5
Uliana (2000)	West Texas, U.S., Apache Mts., Permian carbonate reef facies	--	--	--	2×10^2 to 2×10^3
Mace et al. (2004)	U.S. and Mexico Edwards-Trinity Aquifer	1×10^{-6} to 3×10^{-1}	1×10^{-8} to 3×10^{-3}	9×10^{-4} to 2×10^2	2×10^{-1} to 3×10^4
Rodríguez et al. (2005)	Cuatrociéneas Basin, Coahuila, México	2×10^{-2}	2×10^{-4}	2×10^1	4×10^2

Table 21. GENERALIZED HYDROSTRATIGRAPHIC COLUMN

Stratigraphic nomenclature is modified from McKee et al., 1990; Rodríguez and Sanchez, 2000; Lesser y Asociados, 2001; Evans, 2005.

Age	Formation	Description	Permeability
Quaternary	Alluvium	Sand, gravel, lake deposits, evaporate deposits, travertine	Variable
	Eagle Ford	Limestone, shale	Low
	Buda	Limestone, interbedded sand and gravel	Low
	Del Rio	Clay, sandy limestone	Low
	Georgetown (Cuesta del Cura)	Limestone	Moderate
	Washita Group	Limestone	Moderate
	Kiamichi	Limestone, shale	Low
	Aurora	Lime mudstones and wackestones, gypsum, dolomitized grainstones	High
	La Peña	Dark laminated shale, thin lime mudstone interbeds	Low
	Cupido	Lime mudstone	High
Cretaceous	La Virgen	Gypsum, dolomite, limestone, shale and clay	Low
	La Mula	Shale, sandstone, limestone, conglomerate	Low
	La Padilla	Massive dolomite, interbedded shale, sandstone, and evaporites	Low
	San Marcos	Sandstone, hematitic cement, interbedded conglomerate	Low–Moderate
	Triassic	Basement	Granodiorite
			Low

Spring discharge rates are a function of recharge rates and areas. Elevated temperatures correspond to deeper regional flow paths. To explain spatial differences in chloride concentration, discharge, and temperature, the following methods are used:

1. An evaluation of **hydrogeologic data**, including: spring discharge, spring water temperature, and chloride concentration of rain and spring water;
2. A **catchment delineation approach** (Wolaver et al., 2008) to determine the initial analysis domain of an approximately 18,000-square kilometer recharge area to Cuatrocienegas Basin springs;
3. Geographic information systems to create **elevation slices** from a digital elevation model to use in recharge analysis;
4. A **recharge approach** (Maxey and Eakin, 1949; Dettinger, 1989) that varies recharge rate with elevation to explain observed spring chloride concentration and flow rates; and
5. A **temperature model** to explain differences in spring temperature.

The hydrogeologic conceptual model is calibrated by varying recharge rate, chloride in precipitation, and recharge area until observed spring discharge rate, chloride concentration, and temperature are simulated. Below are discussed hydrogeologic data, environmental tracers, the catchment delineation approach (Wolaver et al., 2008), the geographic information systems elevation slice method, the Maxey and Eakin (1949) recharge approach, and the temperature model.

Hydrogeologic Data

This section discusses the methods used to evaluate hydrogeologic data for the Cuatrocienegas Basin, including: spring discharge, spring water temperature, and

chloride concentration of rain and spring water. The location of the Sierra San Marcos and major springs is shown on **Figure 40**.

Spring Discharge

Instantaneous spring discharge on the Saca Salada and Santa Tecla Canals was measured using a FlowTracker® hand-held acoustic Doppler velocimeter. U.S. Geological Survey standard methods for stream gaging are described in Carter and Davidian (1968) and for using acoustic velocity meter systems in Laenen (1985). Spring discharge is also measured at Poza La Becerra, the largest spring in the Cuatrocienegas Basin. Gaging locations are shown on **Figure 41**. The composite spring discharge is estimated by measuring the discharge of these two canals because gaging dozens of individual springs is impractical. A water-level pressure transducer records instantaneous stage in the Saca Salada Canal (Buchanan and Somers, 1982). These records are used to estimate average annual basin discharge using a stage-discharge relationship.

Spring Water Temperature

The author collected Cuatrocienegas Basin spring temperature data in the summer of 2006 using an iButton temperature logger (Wolaver and Sharp, 2007) and again in the summer of 2007 using an InSitu Troll 9500 multi-parameter water quality monitoring device. Evans (2005) collected spring water temperature data using an Ultrameter multi-parameter water quality meter manufactured by the Myron L Company. Rodríguez et al. (2005a) did not specify a spring water temperature method. For the collection of air temperature to understand spring temperatures in the Cuatrocienegas Basin, Rodríguez et al. (2005a) did not specify an air temperature collection method; however, a meteorological station with a solid-state precision linear thermistor like that used by the U.S. Geological Survey and described in Helm et al. (1995) was probably used.

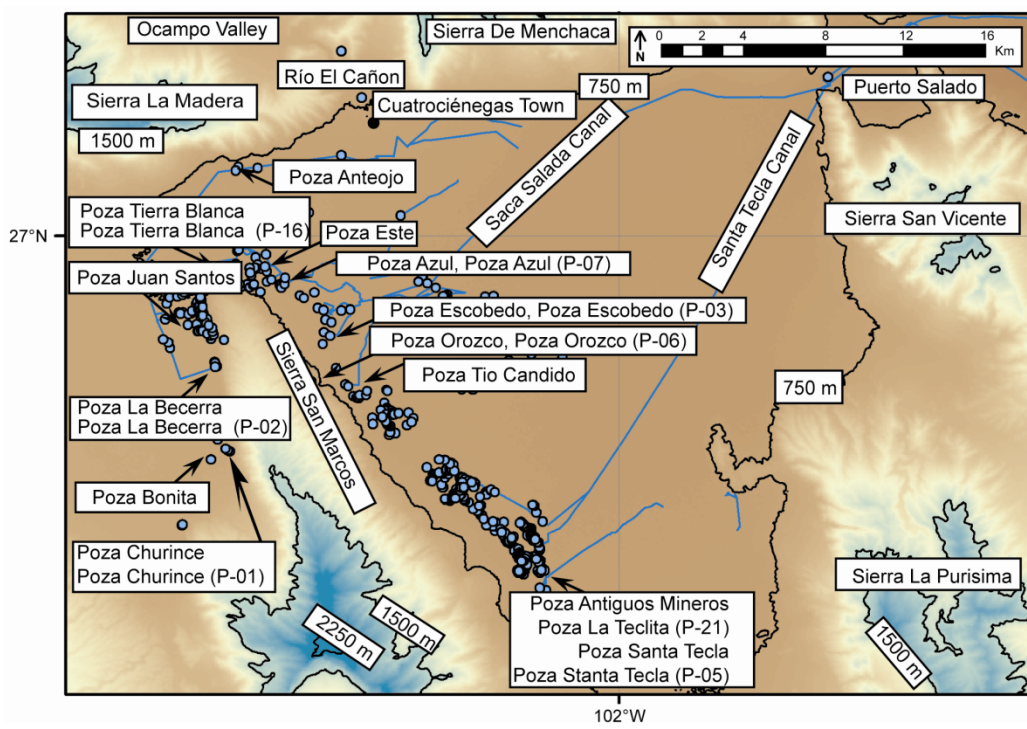


Figure 40. LOCATION OF THE SIERRA SAN MARCOS AND MAJOR SPRINGS

Springs described in Rodríguez et al. (2005a) have a name that includes “P-“.

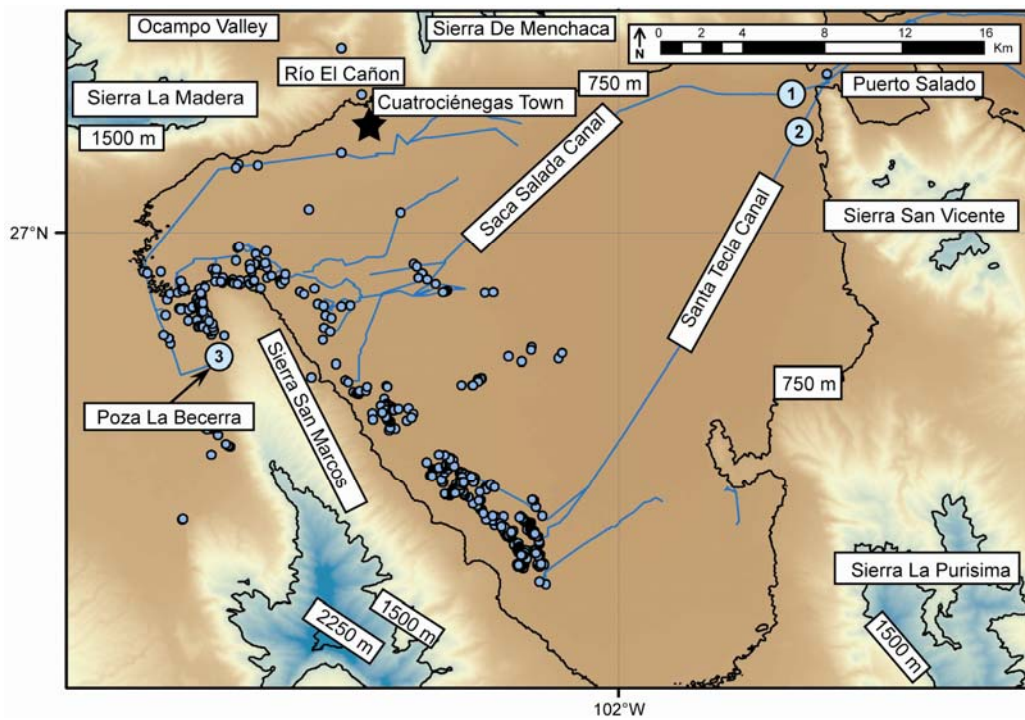


Figure 41. CANAL AND SPRING DISCHARGE MEASUREMENT LOCATIONS

The discharge of two canals and one spring were measured. The sample locations are indicated by large open circles. The locations are

- (1) Saca Salada Canal,
- (2) Santa Tecla Canal, and
- (3) Poza La Becerra.

The Town of Cuatrocienegas is indicated by the solid star. The open circles represent springs, but appear to be solid circles in areas of high spring density.

Chloride Concentration of Precipitation and Spring Water

This research tests the hypotheses that (1) lower spring water chloride concentration is caused by recharge that occurs at higher elevations, and (2) elevated spring water chloride concentrations is because of lower elevation recharge, evaporative concentration of chloride in playas of the Sobaco Valley and diffuse groundwater evaporation where the water table is close to the land surface (Allison and Barnes, 1985; Fontes et al., 1986). Johannesson et al. (2004), Evans (2005), and Rodríguez et al. (2005a) collected grab samples of spring water for chloride analysis. Rodríguez et al. (2005a) collected a rain water sample for oxygen isotope analysis using a sampling device similar to that described in Scholl et al. (1995). The author deployed four rain water samplers of this type during summer 2006. No rain water samples were collected because the samplers were either vandalized or blown over by high wind gusts. Chloride concentration of rain and spring water samples evaluated by this research project is analyzed using methods described in Chapter 2.

No chloride dry deposition data exists in the study area. As discussed previously in this dissertation (Chapter 2), the analysis assumes the dry deposition of chloride is negligible. Scanlon et al. (2007) assume a dry deposition of chloride equivalent to the chloride concentration in precipitation. As shown in Equation 24, if Cl_p (the chloride concentration of recharge water) is doubled and Cl_r (the chloride concentration in groundwater discharging in springs) is constant, the result of this assumption is a doubling of the recharge rate. The lack of chloride dry deposition data for the Cuatrocienegas Basin introduces a source of uncertainty in the recharge analysis. However, if dry deposition of chloride were occurring in addition to chloride input as precipitation, then the recharge area needed to produce observed spring discharge may be halved (if all else is equal). Also, the extent of dry-deposition chloride deflation is not

quantified. Thus, this analysis only considers chloride entering the system from precipitation.

Catchment Delineation Approach

Wolaver et al. (2008) described a catchment delineation approach that builds upon previous aquifer characterization approaches in the Great Basin. This approach, which is discussed in detail in Chapter 2, defines the initial model domain. In order to understand Cuatrocienegas Basin spring recharge sources, groundwater catchments are delineated based on surface topography using a geographic information system for an approximately 97,000-square kilometer upgradient area with a digital elevation model of 3-arc second resolution (digital elevation models, 700–3,025 meters; Tarboton, 1997; Maidment, 2002). However, the recharge analysis presented in Chapter 2 suggests a smaller (approximately 18,000 square kilometer) recharge area is likely. The research project tests the hypothesis that this 18,000 square kilometer area is the likely Cuatrocienegas Basin spring source (**Figure 42**).

Geographic Information System Elevation Slices

In order to understand spatial differences in spring chloride concentration, recharge can be varied as a function of elevation. A geographic information system approach is used to create elevation slices for the recharge evaluation so that different recharge rates can be applied to distinct elevation bands. Polygons of 200-meter wide elevation bands are created using a digital elevation model with a 3-arc second resolution for the area shown on **Figure 42** and described in **Table 22**.

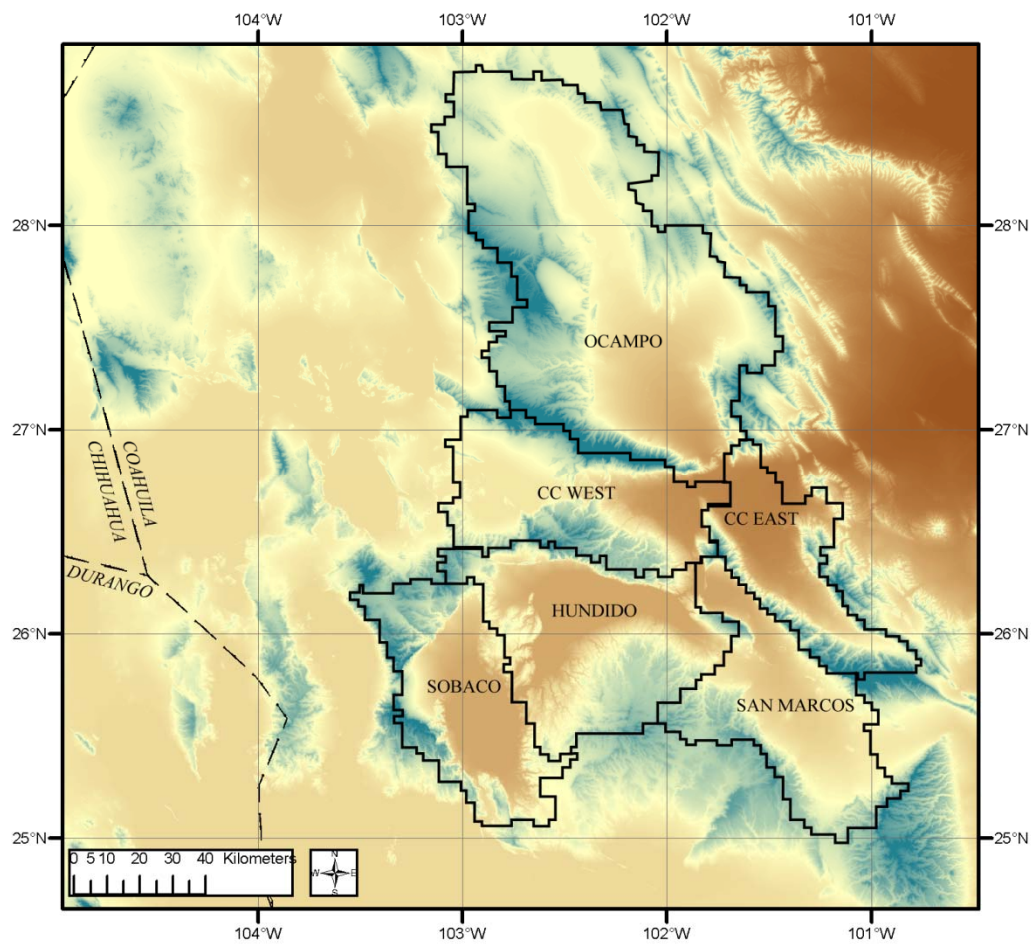


Figure 42. CATCHMENTS CHLORIDE BALANCE AND WATER BUDGET EVALUATION

The six catchments are delineated using a water budget and chloride balance approach. “CC” indicates the Cuatrocienegas Basin.

Table 22. GROUNDWATER CATCHMENT AREAS

This table presents areas for individual groundwater catchments in the approximately 18,000-square kilometer recharge area shown in Figure 42.

Groundwater Catchment	Area [square kilometers]
CC West	2,477
CC East	1,663
Ocampo	6,651
Sobaco	2,268
Hundido	3,036
San Marcos	2,430

The area and average elevation within each 200-meter slice are calculated throughout the range of elevation encountered in the study area (i.e., a minimum of 700–900 meters up to a maximum of 2,900–3,100 meters). These elevation bands are then used to assess the total annual chloride flux and recharge volume for the proposed recharge areas.

Recharge Using Maxey and Eakin and Chloride Balance Approaches

A Maxey and Eakin (1949) recharge analysis tests the hypothesis that spatial variability in spring chloride concentration in the Cuatrocienegas Basin is caused by two different flow systems: (1) recharge occurring in mountains adjacent to the Cuatrocienegas Basin that causes lower chloride springs and (2) recharge external to the basin that causes elevated chloride concentration springs. This research expands upon previous research (Wolaver et al., 2008) that mapped possible aquifer catchments to the Cuatrocienegas Basin based on surface topography, geologic maps, permeability data, and a chloride balance recharge approach.

A steady-state predevelopment condition is assumed (prior to groundwater pumping) for both the water and chloride budget, thus, the change in aquifer storage

$$dS/dt = R + GW_{in} - ET - GW_{out} - Q . \quad (20)$$

Where (all units are cubic meters)

S = aquifer storage,

R = recharge,

GW_{in} = groundwater inflow (i.e., interbasin flow from an upgradient catchment),

ET = evapotranspiration,

GW_{out} = groundwater outflow (i.e., interbasin flow to a downgradient catchment),

and

Q = spring discharged measured as canal flow.

Groundwater inflow and groundwater outflow are interbasin flow between groundwater catchments shown on **Figure 42**. In predevelopment conditions, a playa evaporation term would also be an outflow term in the system. When steady-state conditions are considered (i.e., $dS/dt = 0$) the water-balance equation is

$$R + GW_{in} = ET + GW_{out} + Q . \quad (21)$$

A numerical groundwater flow model was attempted using this equation with the system dynamics modeling approach of Tidwell et al. (2004) and Sehlke and Jacobson (2005), but was discontinued because of a lack of head and chloride data needed for calibration.

A steady-state condition is assumed for chloride flux in the aquifer system where the rate of chloride input into the aquifer system (kilogram/year) is

$$Cl_{in} = Cl_p P . \quad (22)$$

Where

Cl_{in} = chloride flux (kilograms/year),

Cl_p = average bulk precipitation chloride concentration (milligrams/liter), and

P = precipitation rate (cubic meters/year).

The precipitation rate is calculated as the product of precipitation depth (millimeter/year) and catchment area (in square meters, using groundwater catchments shown on **Figure 42**). Precipitation depth is calculated using a hypsometric relationship with elevation (meters) developed for the Cuatrociénegas Basin (Wolaver et al, 2008)

$$P = 0.000079 E + 0.16 . \quad (23)$$

Where

P = precipitation (meters/year), and

E = elevation (meters).

Valley floor (~750 meters) precipitation depth is approximately 220 millimeter/year and mountain top (~3,000 meters) precipitation depth is approximately 400 millimeter/year. Because of the highly fractured nature of the karst Cuatrociénegas Basin highlands,

surface water runoff (or “rejected recharge,” following the terminology of Dettinger, 1989) is presumed to be negligible. Few surface streams are observed in the highlands, which supports this assumption. This is also noted anecdotally by other researchers (Hendrickson, 2005, pers. com.). Thus, the chloride concentration of recharged groundwater (Cl_r) that eventually discharges as spring water is a function of the recharge rate (R%), where

$$R\% = \frac{Cl_p}{Cl_r} . \quad (24)$$

Spring discharge (R_{mf}) is calculated by multiplying precipitation (P; a product of precipitation depth and the catchment area) by the recharge rate (R%)

$$R_{mf} = P R\% . \quad (25)$$

For catchments in the Great Basin, an analogous arid karst region, Maxey and Eakin (1949) developed a relationship between recharge rate and elevation. In this mountainous region, precipitation depth is greatest and evapotranspiration is lowest at the highest elevations, resulting in high recharge rates and relatively low chloride concentration in recharged water. Conversely, at lower elevations, precipitation is lower and evapotranspiration dominates, resulting in low recharge rates and high recharge water chloride concentration. This recharge relationship (**Table 23**) is used as a starting point for estimating recharge as a function of elevation in the Cuatrociénegas region.

Table 23. MAXEY AND EAKIN (1949) PRECIPITATION DEPTH AND RECHARGE RATE RELATIONSHIP FOR THE GREAT BASIN, NEVADA

The recharge rates shown in this table are used as a starting point for the recharge analysis in this research project and are not necessarily the final recharge rates used.

Precipitation Range [mm/year]	Recharge Rate [Percent of Total Precipitation]
>500	25
400 to 500	15
300 to 400	7
200 to 300	3
<20	0 to minor

A vertically-integrated relationship of recharge volume and resulting chloride concentration is shown on **Figure 43**. Recharge volume summed over n elevation bands ($R_{mf\ i}$), such that the total recharge volume ($R_{mf\ tot}$) is calculated as:

$$R_{mf\ tot} = \sum_{i=1}^n R_{mf\ i} . \quad (26)$$

Similarly, the integrated chloride flux over n elevation bands ($Cl_{r\ tot}$) is:

$$Cl_{r\ tot} = \sum_{i=1}^n Cl_{r\ tot} . \quad (27)$$

Because the recharge analysis has two unknowns (recharge rate and precipitation chloride concentration) and one equation, an iterative approach is used. The recharge rate for discrete elevation bands and precipitation chloride concentration are varied to match the spring discharge and chloride concentration for relatively low chloride concentration springs in the southeast corner of the Cuatrocienegas Basin.

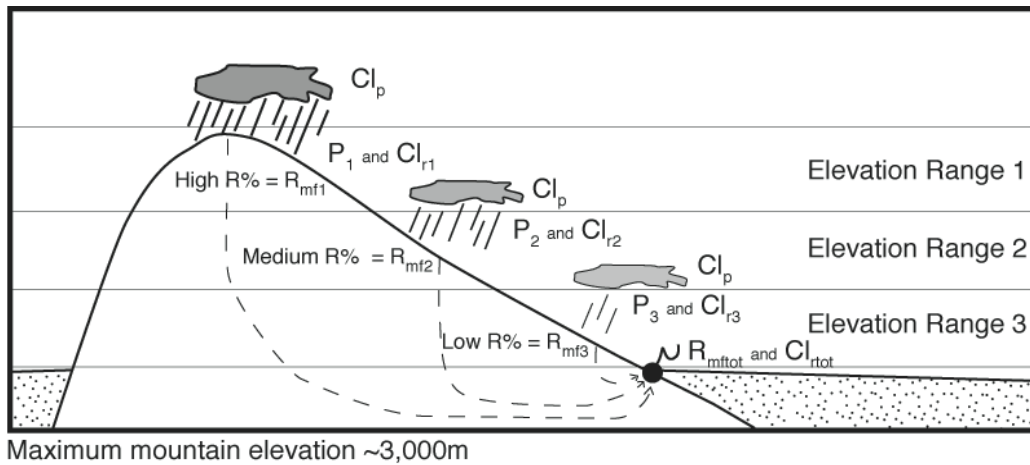


Figure 43. HYDROGEOLOGIC CONCEPTUAL MODEL FOR RECHARGE AND CHLORIDE FLUX

The vertical axis of the conceptual cross section is not to scale and the geology is generalized. The stippled pattern represents valley-fill alluvium. Cretaceous carbonate rocks are represented by the solid white that comprises the generic mountain recharge area. The closed shapes with diagonal lines below them represent clouds and associated precipitation with a chloride concentration, Cl_p . Precipitation increases with elevation and is represented by progressively darker cloud shading. Precipitation (P_n) is calculated for n elevation bands (indicated by horizontal lines and labeled as "Elevation Range n "). The recharge rate ($R\%$) also increases with elevation. Recharge volume for a given elevation band is calculated by multiplying the precipitation depth (P_n) by the recharge rate (R_{mf_n}) and the area of the elevation band. The chloride flux for a given elevation band is indicated by Cl_{rn} . The dashed lines inside the generic mountain represent inferred groundwater flow paths resulting from precipitation at different elevations. The solid dot and tail represents a Cuatrociéegas Basin spring with discharge volume indicated by R_{mftot} with a chloride concentration of Cl_{rtot} .

Using these spring discharge and chloride concentration values, upgradient catchments are sequentially summed until the discharge and chloride concentrations are matched for elevated discharge and chloride concentration springs on the west and north flanks of the Sierra San Marcos that bisects the Cuatrocienegas Basin, the east flank of the Sierra San Marcos, and the Río Cañon spring that flowed from the Ocampo Valley into the Cuatrocienegas Basin.

Temperature Model

The goal of the temperature model is to understand the depth of the groundwater system. Tóth (1963) showed that regional groundwater flow occurs at greater depths than local flow systems. Thus, elevated spring water temperatures would be expected for regional flow systems relative to local flow systems. In order to estimate the depth at which groundwater must circulate to obtain the observed water temperatures, the following equation is solved for depth (Blackwell et al., 1990)

$$T = (\partial T / \partial z) z . \quad (28)$$

Where

T = water temperature measured in springs ($^{\circ}\text{C}$),

$\partial T / \partial z$ = geothermal gradient ($0.025^{\circ}\text{C}/\text{meter}$), and

z = depth (meter) required to heat water to T .

This equation assumes a geothermal gradient of $0.025^{\circ}\text{C}/\text{meter}$ (Blackwell et al., 1990).

RESULTS

This section presents the results of the aquifer delineation. Recharge analysis results are presented and evaluated in the Discussion section of this chapter in the Recharge Using Maxey and Eakin and Chloride Balance Approaches subsection because of the large size of the accompanying data tables.

Hydrogeologic Data

To understand overall trends in Cuatrocienegas Basin springs, summary hydrogeologic data are considered. Hydrogeologic data for three different sets of springs, divided into groups based on similar average spring water chloride concentration, are presented in **Table 24**.

Table 24. SPRING DISCHARGE, CHLORIDE CONCENTRATION, AND TEMPERATURE

¹Minckley and Cole (1968) presented 1964 Ocampo Valley discharge and chloride concentration, but did not give temperature data. Wolaver et al. (2008) reported more recent canal discharge. Values for other springs are approximate and capture overall trends.

Spring Location	Discharge [m ³ /year]	Chloride Concentration [mg/L]	Temperature [°C]
Ocampo Valley	8,000,000	22	Unknown
Northern and Western Flank of the Sierra San Marcos	29,000,000	90	32.0°–35.0°
Southeast Flank of the Sierra San Marcos	6,000,000	30	30.0

The research project tests the hypothesis that longer flow paths with deeper circulation are likely for the springs on the west and north flank of the Sierra San Marcos. Historic spring flow from the Ocampo Valley (approximately 8,000,000 cubic meters/year) had the lowest chloride concentration in the valley (22 milligrams/liter). Springs on the northern and western flank of the Sierra San Marcos have elevated

discharge (approximately 29,000,000 cubic meters/year), chloride concentration (approximately 90 milligrams/liter), and temperature (approximately 32.0°–35.0°C). In the far southeast flank of the Sierra San Marcos, springs have lower discharge (approximately 6,000,000 cubic meters/year) and chloride concentration (approximately 30 milligrams/liter), and also elevated temperature (generally on the order of approximately 30.0°C). The chloride concentration of springs on southeast flank of the Sierra San Marcos is lower than that presented in Wolaver et al. (2008) to reflect an improved understanding of the canal discharge system (Pozas Escobedo, Orozco, and Tío Cándido drain to the Saca Salada canal). This chloride concentration is used to refine the hydrogeologic conceptual model.

Although hydrogeologic data in the Cuatrocienegas Basin are limited, a summary of hydrogeologic data is divided into four groups (Western, Northern, and Southeast Flanks of the Sierra San Marcos, and Others), as shown in **Table 17**. Because the spring feeding the Río Cañon that flowed from the Ocampo Valley to the Cuatrocienegas Basin is now dry, hydrogeologic data for the Ocampo Valley are not presented in **Table 17**. Disparate hydrogeologic data, including precipitation, spring discharge, spring geochemistry (including chloride concentration and environmental tracers of $\delta^{18}\text{O}$, ${}^3\text{H}$, and noble gases), and temperature are presented for the entire Cuatrocienegas Basin, because long-term data do not exist.

Spring Discharge

Spring discharge data show that approximately 35,000,000 cubic meters/year exits the basin in two canals (Wolaver et al., 2008). On the Western Flank of the Sierra San Marcos, Poza La Becerra is the largest spring in the valley with essentially stable discharge at approximately 19,000,000 cubic meters/year and represents approximately 55 percent of the total basin discharge (Wolaver et al., 2008). On the Southeast flank of

the Sierra San Marcos, approximately 6,000,000 cubic meters/year from dozens of seeps flows into the Santa Tecla Canal (Wolaver et al., 2008), representing approximately 15 percent of basin discharge. Spring discharge in the Santa Tecla Canal (which collects discharge from numerous springs in the east sub-basin) decreased during an approximately four-year period of record (discharge = 180–220 liters/second).

The remaining approximately 10,000,000 cubic meters/year in basin discharge originates in springs along the North flank of the Sierra San Marcos, representing approximately 30 percent of total basin discharge. Discharge from Pozas Azul and Escobedo, two such springs along the northern flank of the Sierra San Marcos, is approximately 100 liters/second each. Other smaller basin springs (e.g., Pozas Anteojo, Churince, and El Venado) discharge <25 liters/second each.

Spring Water Temperature

This section considers variations in basin spring temperature and average annual air temperature. Based on the literature, average annual Cuatrociénegas Basin valley floor air temperature is between 16.0°–21.0°C. Rodríguez el al. (2005a) reported the Cuatrociénegas Basin mean annual valley air temperature (1942–1998) is 16.3°C. Alternatively, Badino et al. (2004) integrated meteorological data from stations in Monclova and Saltillo, Coahuila, and Chihuahua, Chihuahua. These meteorological data are corrected for altitude differences to deduce mean annual temperatures of approximately 21.0°C at the valley floor, 16.0°C at 1,500 meters, and 13.0°C at 2,000 meters. Finally, Collins (1925) inferred a shallow groundwater temperature of 20.0°C (reflecting the average annual air temperature) for this part of northeast Mexico.

Temperature in the northern fracture orifice of Poza La Becerra, on the western flank of the Sierra San Marcos, remains stable at approximately 34.2°C during basin-wide precipitation events monitored over a six-week period during the summer

2006 North American Monsoon season (Wolaver and Sharp, 2007). Another fracture in Poza La Becerra is slightly cooler at 32.2°C, suggesting slightly shallower circulation or mixing with cooler waters.

During the same period of the 2006 monsoon, temperatures in Poza Santa Tecla, located on the southeast flank of the Sierra San Marcos vary diurnally by approximately 0.5°C. Its temperature decreased from approximately 30.0°C to approximately 28.0°C and 24.0°C, respectively, in response to two storms totaling approximately 2.0 centimeters of precipitation (Wolaver and Sharp, 2007).

On the northern flank of the Sierra San Marcos, Pozas Azul and Escobedo also have elevated temperature of approximately 33.0° and 35.0°C, respectively. Other smaller springs in the Cuatrocienegas Basin have temperatures that range from 28.5° at El Venado, to 29.9°C at Poza Anteojo, and to 31.1°C at Poza Churince.

Chloride Concentration of Precipitation and Spring Water

The source of chloride in Cuatrocienegas Basin springs is from precipitation evaporative concentration, halite dissolution, and/or dry deposition of chloride. Dissolution of halite was investigated, but discounted by Wolaver et al. (2008) because chloride is not enriched with respect to bromide in Cuatrocienegas Basin springs. The author assumes chloride dry deposition over the entire study area is negligible because Laguna Salada is the one evaporative pool in the Cuatrocienegas Basin with total dissolved solids >300,000 milligrams/liter and the dunes associated with Laguna Grande are >85 percent gypsum (Minckley and Cole, 1968). Precipitation chloride concentration data for northeast Mexico and Big Bend National Park, Texas range from 0.13 (National Atmospheric Deposition Program, 2008) to 2.00 milligrams/liter (Junge and Werby, 1958). In comparison, Maxey and Eakin (1949) assumed a precipitation chloride concentration of 1.00 milligrams/liter for rainfall in Nevada.

The chloride concentration of springs on the western and northern flanks of the Sierra San Marcos is approximately 90 milligrams/liter (**Table 24**). Springs on the southeast flank of the Sierra San Marcos are approximately 30 milligrams/liter. The grouping of spring chloride has been changed slightly here from that published in Wolaver et al. (2008) in order to capture spatial variations in chloride more accurately. Ocampo Valley historic spring discharge had a chloride concentration of approximately 22 milligrams/liter (Minckley and Cole, 1968). Other Cuatrocienegas Basin spring chloride concentration values range from 21.78 to 179.74 milligrams/liter.

Catchment Delineation Approach

The results of this analysis are described in detail in Wolaver et al. (2008). Hydrogeologic data, geophysical surveys, and geographic information system-delineated catchments are integrated to create a hydrogeologic conceptual model with springs of two distinct hydrogeologic characters: (1) primarily locally-derived (east sub-basin) and (2) regionally-derived (west sub-basin) recharge. The model domain considered in this paper includes catchments within the approximately 18,000-square kilometer inferred recharge area (Wolaver et al., 2008) shown on **Figure 44**. The edges of groundwater catchments are considered no-flow boundaries, except when groundwater flow is permitted between adjacent zones. Groundwater outflow is permitted as spring discharge or groundwater pumping. Recharge is applied to each cell as a percentage of precipitation.

Geographic Information System Elevation Slices

A geographic information system approach is used to create elevation bands for recharge analysis. These bands are used to evaluate the total annual chloride flux and recharge volume for springs on the southeast, west, and north flank of the Sierra San Marcos and the former Río Cañon draining the Ocampo Valley.

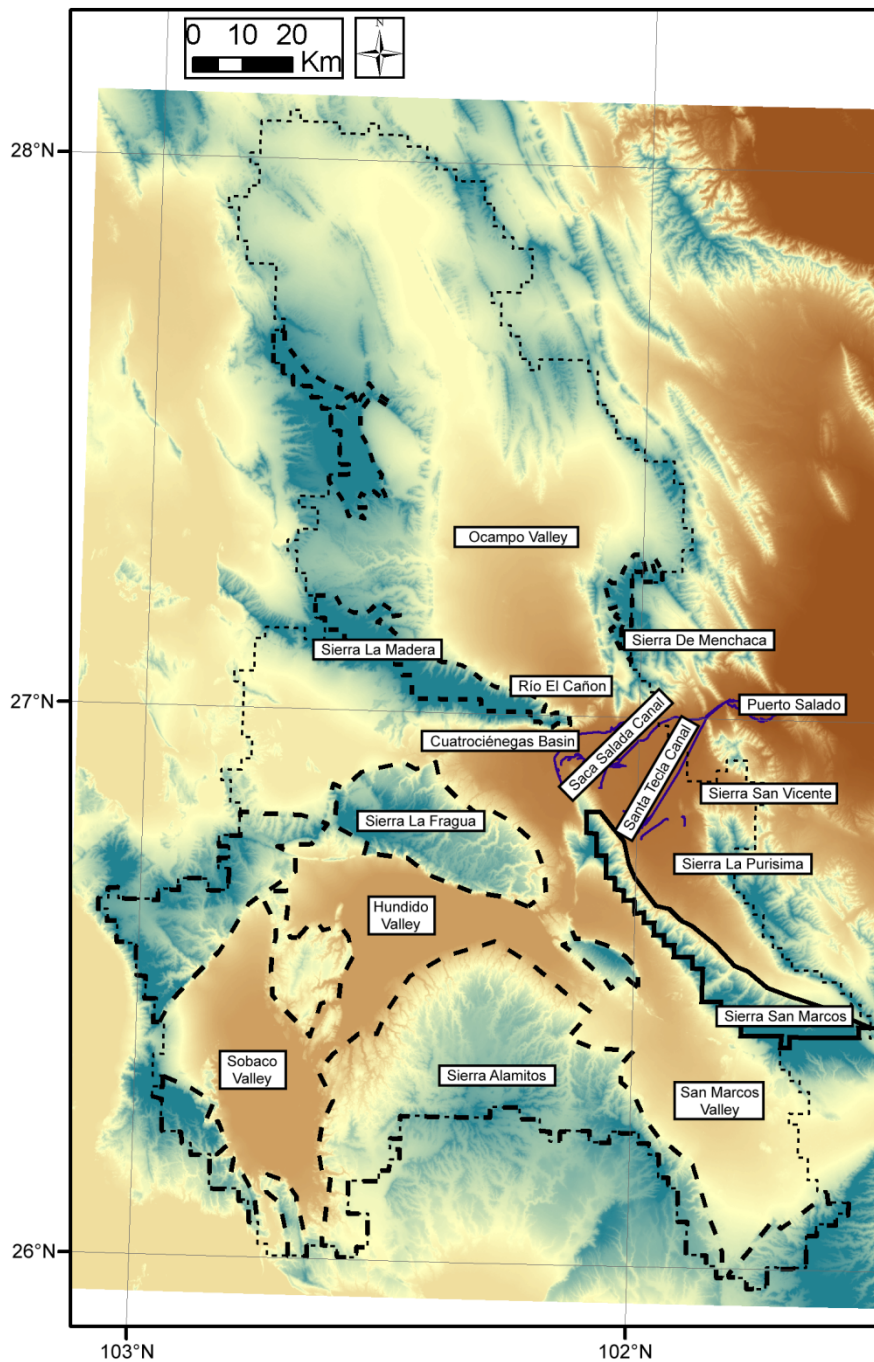


Figure 44. GROUNDWATER RECHARGE AREAS

The polygons represent Cuatrocienegas Basin spring recharge areas. Fine dash = 18,000-square kilometer initial recharge area. Solid line = East flank of the Sierra San Marcos. Short, thick dash = Ocampo Valley. Longer, thick dash = West and North flank of the Sierra San Marcos.

Recharge Using Maxey and Eakin and Chloride Balance Approaches

The results of the recharge analysis using a Maxey and Eakin (1949) and chloride balance approach are presented in three sub-section for springs on the southeast, west, and north flank of the Sierra San Marcos and the former Río Cañon draining the Ocampo Valley. Recharge analysis results are shown in **Table 25** to **Table 27**. Because of the length of the tables and the interpretation of the results, these tables are presented in the Discussion section of this chapter.

Recharge: Springs on the Southeast Flank of the Sierra San Marcos

For the area recharging springs on the southeast flank of the Sierra San Marcos, the majority of the area is from 700–2700 meters in elevation with only nine percent of the area >2,100 meters. The bands from 700–2,700 meters account for 82 percent of the precipitation and approximately 81 percent of the recharge, whereas elevations >1,700 meters account for approximately 65 percent of the recharge. The recharge rate is three percent (700–1700 meters) and seven percent (1700–2700 meters).

For the calculations, a precipitation chloride concentration of 1.4 milligrams/liter is assumed. From 700–1,700 meters, it is assumed that three percent of precipitation results in recharge and from 1,700–2,700 meters, seven percent of precipitation results in groundwater recharge (using Maxey and Eakin, 1949 as a starting point for recharge calculations). The result of this analysis generates a range of chloride concentration in groundwater. Groundwater chloride ranges from 0.01 milligrams/liter at 700–900 meters to 5.74 milligrams/liter at 1,500–1,700 meters. The resulting integrated spring water chloride concentration is 30 milligrams/liter with a target value of 30 milligrams/liter. Calculated spring discharge is approximately 6,150,000 cubic meters/year, with an observed value of approximately 6,000,000 cubic meters/year. Recharge rates for springs on the southeast of the Sierra San Marcos are shown in **Table 25**.

Recharge: Spring Discharging from the Ocampo Valley (Río Cañon)

The mountainous recharge area of the former Río Cañon falls within the 1,100–3100 meters elevation range. Approximately 78 percent of the recharge area is within 1,700–2,300 meters, with <13 percent >2,300 meters, and <10 percent <1,700 meters. From 1,700–2,300 meters, 77 percent of the precipitation occurs, and approximately 80 percent of the recharge occurs at these elevated mountain elevations. Approximately 15 percent of the recharge occurs >2,300 meters. Below 1,700 meters, only about five percent of recharge occurs. The recharge rate is three percent (700–1700 meters) and seven percent (1700–3100 meters).

This analysis assumes a precipitation chloride concentration of 1.4 milligrams/liter. The author assumes that from 1,100–1,700 meters, three percent of precipitation results in recharge, and from 1,700–3,100 meters, approximately seven percent of precipitation results in recharge. The resulting chloride concentration in groundwater ranges from 0.03 milligrams/liter at 2,900–3,100 meters up to 7.26 milligrams/liter at 1,900–2,100 meters. The resulting integrated spring water chloride concentration is 21 milligrams/liter with a target historic value of 22 milligrams/liter. Calculated spring discharge is 12,660,000 cubic meters/year, with an observed historic discharge value of approximately 8,000,000 cubic meters/year. Hendrickson (pers. com., 2005) suggests that Minckley estimated the 8,000,000 cubic meters/year discharge value from visual inspection, so a 12,000,000 cubic meters/year discharge value is plausible. Additionally, in order to preserve a (presumably more accurate) historic Río Cañon chloride concentration of 22 milligrams/liter, an elevated flow rate was necessary to dilute chloride from recharge. Recharge rates for the historic Río Cañon of the Ocampo Valley are shown in **Table 26**.

Recharge: Springs on the West and North Flank of the Sierra San Marcos

The recharge area for springs on the west and north flank of the Sierra San Marcos are somewhat different. Recharge likely ranges from 700–2,900 meters. However, approximately 92 percent of the area is from 700–1,700 meters, reflecting the lower overall mountains elevation. Only eight percent of the area is >1,700 meters. For Sierra San Marcos west and north flank springs, 91 percent of the precipitation occurs between 700–1,700 meters and results in 71 percent of annual recharge. Approximately 26 percent of the recharge occurs >1,700 meters, reflecting the lower elevation of these mountains compared to the Sierras San Marcos and La Madera. The recharge rate is zero percent (<1100 meters), one percent (1100–1500 meters), two percent (1500–1700 meters), three percent (1700–2100 meters), and four percent (2100–2900 meters).

For calculated discharge and spring chloride concentration to equal observed values, a precipitation chloride concentration of 1.0 milligrams/liter is assumed. The modeled integrated spring water chloride concentration is equal to 89 milligrams/liter, approaching the target value of 90 milligrams/liter. A spreadsheet-based numerical optimizer is used to vary recharge rates to model this chloride concentration and also calculate a spring discharge of 29,000,000 cubic meters/year (the observed Saca Salada Canal discharge). Thus, recharge rates range from essentially zero percent <1,100 meters up to four percent >2,100 meters. Recharge rates for springs on the west and north flank of the Sierra San Marcos are shown in **Table 27**.

Temperature Model

Table 17 shows spring temperature field analysis results. Most spring water temperatures range from approximately 30.0°–35.0°C. Exceptions include El Venado at 28.5°C (the coolest in the study area) and Poza Anteojo at 29.9°C. All other springs are greater than the average annual air temperature of approximately 16.0°–20.0°C.

If a geothermal gradient of 0.025°C/meter is assumed (Blackwell et al., 1990), spatial differences in spring temperature can be explained. For springs on the southeast flank of the Sierra San Marcos, a flow depth of at least 360–560 meters is required to generate an observed temperature of 30.0°C (considering an average air temperature range of approximately 16.0°–21.0°C). For springs on the west and north flank of the Sierra San Marcos, groundwater would need to circulate at a depth of at least 560–760 meters to attain 35.0°C, the highest temperature observed in a spring on the northern flank of the Sierra San Marcos (Poza Escobedo).

Elevated spring waters may be explained by deeper circulating groundwater of a regional flow system on the western and northern flank of the Sierra San Marcos. Postulated groundwater systems are shown in the conceptual hydrogeologic cross sections on **Figure 38** and **Figure 39**. The waters of this relatively deep flow system rise to the surface via fractures in the fault on the west side of the Sierra San Marcos. On the southeast flank of the Sierra San Marcos, less deeply circulating fluids flow from a smaller regional flow system predominantly recharged on the Sierra San Marcos. Temperature data from the presently dry Río Cañon are unavailable. However, it is plausible the temperature was at or around the average ambient temperature from shallow groundwater discharge from the Ocampo Valley.

DISCUSSION

Hydrogeologic Data

This section discusses the hydrogeologic data for Cuatrocienegas Basin springs. These data include spring discharge, spring water temperature, and chloride concentration of spring water and precipitation.

Spring Discharge

Spring discharge values are shown in **Table 17** and **Table 24**. Stable discharge of springs on the southeast, west, and northeast flanks of the Sierra San Marcos suggest a regional flow system. For example, stable discharge in Poza La Becerra (approximately 600 liters/second) suggests a regional aquifer source to this and other springs on the west flank of the Sierra San Marcos. The elevated discharge (approximately 10,000,000 cubic meters/year) and stable discharge of springs along the north flank of the Sierra San Marcos suggest a primarily regional flow system. Conversely, the spring feeding the former Río Cañon dried within 10–20 years after large-scale pumping commenced in the Ocampo Valley. Thus, the Ocampo Valley is likely recharged by a localized flow system with recharge occurring in the mountains surrounding the Ocampo Valley. The decrease of discharge in the Santa Tecla Canal (which collects discharge from numerous springs on the southeast flank of the Sierra San Marcos) during an approximately four-year period of record (discharge = 180–220 liters/second) suggests that springs on the southeast flank of the Sierra San Marcos (1) vary in response to a regional drought, and (2) could be decreasing in response to pumping in adjacent basins. However, the condition of leakage potential for the Santa Tecla Canal is unknown. The canal was closed for repairs in spring 2007, suggesting that the decrease in flow observed may be due to a leak in the concrete canal walls.

Spring Water Temperature

In other carbonate terranes, like those in Nevada and Texas, stable elevated spring temperatures indicate deep regional groundwater flow systems. For comparison, average ambient temperatures range between 16.0°C (air, Rodríguez et al., 2005a) and 20.0°C (shallow groundwater, Collins, 1925). In general, all Cuatrociénegas Basin spring water temperatures are greater than the average annual air temperature, which implies some

component of relatively deep circulation. Spring temperatures are shown in **Table 17**. For example, on the southeast flank of the Sierra San Marcos, the temperature in Poza Santa Tecla is approximately 30.0°C, which implies that a deeper regional flow dominates but local recharge processes are important during intense rainfall. Spring temperatures of approximately 31.0°–35.0°C on the west and north flank of the Sierra San Marcos suggest deeper regional groundwater flow relative to the southeast flank of the Sierra San Marcos. Historic temperature data are not available for the Río Cañon. However, historic spring discharge from the Ocampo Valley may have been close to ambient temperature (16.0°–21.0°C). Rodríguez et al. (2005a) reported Ocampo Valley well temperatures from 23.7°–27.4°C, but do not report the depth of the well screened interval (or any other well completion details, such as total depth or casing and screen materials), as deeper wells may reflect a higher groundwater temperature.

Chloride Concentration of Spring Water and Precipitation

Lower chloride concentration of springs on southeast flank of the Sierra San Marcos (approximately 30 milligrams/liter) suggests high elevation recharge with less evaporation. Chloride concentration of springs on west and north flank of the Sierra San Marcos (approximately 90 milligrams/liter) suggests lower elevation recharge dominates and/or evaporation from a shallow groundwater table or playa lakes occurs. Chloride concentration of the former Río Cañon (approximately 22 milligrams/liter) suggests higher elevation recharge occurs relative to other springs considered with less evaporative concentration of chloride in rain water. In fact, the elevation of the Sierra La Madera that surround the Ocampo Valley are the highest in the region (>3,000 meters).

Recharge Using Maxey and Eakin and Chloride Balance Approaches

For ease of understanding, the discussion of catchment delineation approach results and geographic information system elevation slices results also are integrated with the discussion of recharge results using the Maxey and Eakin (1949) and chloride balance approach. The results of the recharge analysis and chloride balance approach (**Table 25** to **Table 27**) are discussed for springs on the southeast, west, and north flanks of the Sierra San Marcos, in addition to the former Río Cañon that drained the Ocampo Valley. This research suggests that approximately 2,050 square kilometers — or approximately ten percent of the 18,000-square kilometer recharge area shown on **Figure 44** — contributes to recharge. Results of chloride-bromide and oxygen isotopic analyses suggest evaporative concentration is the dominant process causing concentration of chloride in spring waters. Alternatively, dissolution of evaporites may also contribute to increased chloride, but is considered less likely since halite is not mapped in the study area.

Recharge: Springs on the Southeast Flank of the Sierra San Marcos

The recharge analysis presented in this research suggests that springs on the southeast flank of the Sierra San Marcos feeding the Santa Tecla Canal are fed from an approximately 450-square kilometer recharge area of exposed carbonate rock in the Sierra San Marcos. The location of groundwater recharge areas are shown on **Figure 44**. Following Maxey and Eakin (1949), Eakin (1966), Tyler et al. (1996), and Darling (1997), who worked in analogous arid, karst regions, the author concludes that essentially no recharge occurs in the lower elevation valley fill alluvium.

Table 25. ANNUAL RECHARGE ANALYSIS FOR SOUTHEAST FLANK SIERRA SAN MARCOS SPRINGS

1. The recharge area for springs on the southeast flank of the Sierra San Marcos is between 700 and 2,700m (Figure 44).

2. The recharge rate and precipitation chloride concentration (Cl^-_p) are varied to minimize spring integrated chloride flux error (Cl^-_{spr}).

183

Elevation Zone ¹	Ave- rage Elev- ation [m]	Re- charge Area [km ²]	Re- charge [% of Total Area]	Precip- itation Depth [m/year]	Precip- itation Volume [m ³ /year]	Precip- itation Volume [% of Total]	Recharge Rate ² [%]	$\text{Cl}^-_p^2$ [mg/L]	Cl^-_{spr} [mg/L]	Re- charge Volume [m ³ /yr]	Re- charge Volume [% of Total]	Cl^- Flux per Zone [mg/yr]	Cl^-_{spr} Integrated Flux [mg/L]
700 to 900	890	<1	<1	0.23	3.0×10^4	<1	3	1.4	47	9.1×10^2	<1	4.2×10^7	<0.1
900 to 1,100	1,030	31	7	0.24	7.6×10^6	6	3	1.4	47	2.3×10^5	4	1.1×10^{10}	1.7
1,100 to 1,300	1,208	65	14	0.26	1.7×10^7	13	3	1.4	47	5.0×10^5	8	2.3×10^{10}	3.8
1,300 to 1,500	1,401	88	19	0.27	2.4×10^7	18	3	1.4	47	7.1×10^5	12	3.3×10^{10}	5.4
1,500 to 1,700	1,601	88	20	0.29	2.5×10^7	19	3	1.4	47	7.6×10^5	12	3.5×10^{10}	5.7
1,700 to 1,900	1,797	83	18	0.30	2.5×10^7	19	7	1.4	20	1.8×10^6	29	3.5×10^{10}	5.7
1,900 to 2,100	1,991	55	12	0.32	1.7×10^7	13	7	1.4	20	1.2×10^6	20	2.4×10^{10}	4.0
2,100 to 2,300	2,194	31	7	0.33	1.0×10^7	8	7	1.4	20	7.1×10^5	12	1.4×10^{10}	2.3
2,300 to 2,500	2,358	9	2	0.35	3.0×10^6	2	7	1.4	20	2.1×10^5	3	4.3×10^9	0.7
2,500 to 2,700	2,554	2	0	0.36	7.9×10^5	1	7	1.4	20	5.6×10^4	1	1.1×10^9	0.2
Total Recharge Area:	451				Total Precipitation Volume:	1.3×10^8			Total Recharge Volume:	6.2×10^6		Total Cl^-_{spr} Integrated Flux:	30

Table 26. ANNUAL RECHARGE ANALYSIS FOR HISTORIC OCAMPO VALLEY SPRING (RÍO CAÑON)

1. The recharge area for historical spring discharge to the Río Cañon is between 1,100 and 3,100m (Figure 44).

2. The recharge rate and precipitation chloride concentration (Cl^-_p) are varied to minimize spring integrated chloride flux error (Cl^-_{spr}).

184

Elev- ation Zone ¹	Ave- rage Elev- ation [m]	Re- charge Area [km ²]	Re- charge [% of Total Area]	Precip- itation Depth [m/year]	Precip- itation Volume [m ³ /year]	Precip- itation Volume [% of Total]	Recharge Rate ² [%]	Cl^-_p [mg/L]	Cl^-_{spr} [mg/L]	Re- charge Volume [m ³ /yr]	Re- charge Volume [% of Total]	Cl^- Flux per Zone [mg/yr]	Cl^-_{spr} Inte- grated Flux [mg/L]	
1,100 to 1,300	1,277	<1	<1	0.26	4.5×10^4	<1	3	1.4	47	1.3×10^3	<1	6.3×10^7	<0.1	
1,300 to 1,500	1,440	11	2	0.27	2.9×10^6	2	3	1.4	47	8.7×10^4	1	4.0×10^9	0.3	
1,500 to 1,700	1,614	47	8	0.29	1.4×10^7	7	3	1.4	47	4.1×10^5	3	1.9×10^{10}	1.5	
1,700 to 1,900	1,819	154	26	0.30	4.7×10^7	25	7	1.4	20	3.3×10^6	26	6.5×10^{10}	5.2	
1,900 to 2,100	1,998	206	35	0.32	6.6×10^7	34	7	1.4	20	4.6×10^6	36	9.2×10^{10}	7.3	
2,100 to 2,300	2,180	100	17	0.33	3.3×10^7	18	7	1.4	20	2.3×10^6	18	4.7×10^{10}	3.7	
2,300 to 2,500	2,390	42	7	0.35	1.5×10^7	8	7	1.4	20	1.0×10^6	8	2.1×10^{10}	1.6	
2,500 to 2,700	2,589	24	4	0.37	8.8×10^6	5	7	1.4	20	6.2×10^5	5	1.2×10^{10}	1.0	
2,700 to 2,900	2,770	11	2	0.38	4.1×10^6	2	7	1.4	20	2.9×10^5	2	5.8×10^9	0.5	
2,900 to 3,100	2,949	1	0	0.39	2.7×10^5	0	7	1.4	20	1.9×10^4	0	3.8×10^8	<0.1	
Total Recharge Area:	596				Total Precipitation Volume:	1.9×10^8				Total Recharge Volume:	1.3×10^7		Total Cl^-_{spr} Integrated Flux:	21

Table 27. ANNUAL RECHARGE ANALYSIS FOR WESTERN AND NORTHERN FLANK SIERRA SAN MARCOS SPRINGS

1. The recharge area for springs on the Western and Northern Flank of the Sierra San Marcos is between 700 and 2,900m (Figure 44).
 2. The recharge rate and precipitation chloride concentration (Cl_p^-) are varied to minimize spring integrated chloride flux error (Cl_{spr}^-).

Elevation Zone ¹	Ave- rage Elev- ation [m]	Re- charge Area [km ²]	Re- charge [% of Total Area]	Precip- itation Depth [m/year]	Precip- itation Volume [m ³ /year]	Precip- itation Volume [% of Total]	Recharge Rate ² [%]	Cl_p^- [mg/L]	Cl_{spr}^- [mg/L]	Re- charge Volume [m ³ /yr]	Re- charge Volume [% of Total]	Cl^- Flux per Zone [mg/yr]	Cl_{spr}^- Inte- grated Flux [mg/L]
700 to 900	874	1,521	15	0.23	3.5×10^8	14	0	1.0	270.	1.3×10^6	4	3.5×10^{11}	12.0
900 to 1,100	1008	1,864	19	0.24	4.5×10^8	17	0	1.0	301	1.5×10^6	5	4.5×10^{11}	15.4
1,100 to 1,300	1194	2,843	29	0.26	7.2×10^8	28	1	1.0	137	5.3×10^6	18	7.2×10^{11}	25.0
1,300 to 1,500	1396	1,588	16	0.27	4.3×10^8	17	1	1.0	75	5.8×10^6	20	4.3×10^{11}	14.8
1,500 to 1,700	1587	1,321	13	0.29	3.8×10^8	15	2	1.0	54	7.0×10^6	24	3.8×10^{11}	13.0
1,700 to 1,900	1788	539	5	0.30	1.6×10^8	6	3	1.0	34	4.8×10^6	16	1.6×10^{11}	5.6
1,900 to 2,100	1981	202	2	0.32	6.4×10^7	2	3	1.0	29	2.2×10^6	8	6.4×10^{10}	2.2
2,100 to 2,300	2172	53	1	0.33	1.8×10^7	1	4	1.0	25	7.1×10^5	2	1.8×10^{10}	0.6
2,300 to 2,500	2390	18	<1	0.35	6.3×10^6	<1	4	1.0	25	2.5×10^5	1	6.3×10^9	0.2
2,500 to 2,700	2589	10	<1	0.37	3.6×10^6	<1	4	1.0	25	1.5×10^5	1	3.6×10^9	0.1
2,700 to 2,900	2769	4	<1	0.38	1.6×10^6	<1	4	1.0	25	6.2×10^4	<0.1	1.6×10^9	<0.1
Total Recharge Area:	9,963				Total Precipitation Volume:	2.6×10^9			Total Recharge Volume:	2.9×10^7		Total Cl_{spr}^- Integrated Flux:	89

Recharge: Spring Discharging from the Ocampo Valley (Río Cañon)

This recharge analysis infers that the historically spring-fed Río Cañon (presently dry) flowing from the Ocampo Valley to the Cuatrocienegas Basin is fed by a ~600-square kilometer recharge area of exposed carbonate rock of mountains surrounding the Ocampo Valley, as shown on **Figure 44**. Again, the author assumes precipitation falling on lower elevation valley fill alluvium results in insignificant recharge because of evapotranspiration.

Recharge: Springs on the West and North Flank of the Sierra San Marcos

The evaluation of recharge area for springs on the west and north flank of the Sierra San Marcos that feed the Saca Salada Canal is slightly different than the previous two analyses. For this case, this research suggests a ~1,000-square kilometer recharge area of exposed carbonate rock comprising the generally lower overall elevation mountains surrounding the Hundido, Sobaco, and San Marcos Valleys as shown on **Figure 44**. Again, for this case, essentially no recharge occurs in the lower elevation valley fill alluvium.

This recharge regime is realistic because of the topography of the area. In the region southwest of the Cuatrocienegas Basin, lower elevation mountains with more gentle slopes are present. Here valleys are wider than other parts of the study area and have very shallow groundwater and playa lakes (**Figure 45**). This recharge scenario results in the observed spring discharge while still producing the necessary chloride concentration for present day recharge.

Alternatively, chloride concentration in spring discharge may have been generated from long-term diffuse evaporation from a shallow water table. The residence time in this aquifer is at least 50–60 years according to tritium values (Wolaver et al., 2009, *in*

preparation). Fontes et al. (1986) and Allison and Barnes (1985) presented a mechanism for long-term diffuse groundwater discharge because of evaporation or evapotranspiration from a shallow water table that could generate the observed spring chloride concentrations. Seasonal playa lakes exist in the Sobaco Valley that could serve as an evaporative concentrating mechanism. One such playa lake is shown on **Figure 45**. Also, prior to groundwater development in the Hundido Valley, groundwater was very near the surface. One former groundwater seep in the Hundido Valley was used to provide water for horses and is shown on **Figure 46**. This shallow groundwater in the Hundido Valley could have been subject to evaporative concentration in the manner described by Fontes et al. (1986).

Recharge: Estimate of Spatially-Distributed Recharge

Table 25, **Table 26**, and **Table 27** compile the results of the recharge analysis and chloride balance approach for three recharge areas: (1) springs in the southeast, and west and north flanks of the Sierra San Marcos (labeled as the Cuatrocienegas Basin, Hundido Valley, San Marcos Valley, and Sobaco Valley on **Figure 44**), and (2) the former Río Cañon that drained the Ocampo Valley (also labeled on **Figure 44**). The data show that recharge supporting springs in the Cuatrocienegas Basin primarily occurs in mountains above an elevation of approximately 1,000 meters and that valley-floor recharge is insignificant. Recharge is estimated to be up to seven percent of precipitation in mountainous recharge areas. Spatially-distributed recharge is typically less than or equal to one percent of precipitation in West Texas (Meyer, 1976; Gates et al., 1980; Nielson and Sharp, 1985; and Darling; 1997) and Nevada (Maxey and Eakin, 1949; Eakin, 1966; Eakin et al., 1976; and Tyler et al., 1996), two analogous, semi-arid regions.



Figure 45. PLAYA LAKE LOCATED IN THE SOBACO VALLEY

This photo was taken by the author in August 2006. The same playa lake was dry in February 2008. The playa lake is located near the lower right corner of the Sobaco Valley label on Figure 44.



Figure 46 GROUNDWATER SEEP LOCATED IN THE HUNDIDO VALLEY

Prior to groundwater development, horses were watered when this groundwater seep was located at the surface. As groundwater level declined >20 meters (as indicated in an adjacent well), a pit was dug so that livestock could still access the water. The groundwater seep is located near the northern-most flank of the Sierra Alamitos in the Hundido Valley (Figure 44). Megan Andring is standing in the foreground.

In order to compare spatially-distributed recharge rates of the Cuatrocienegas Basin with West Texas and Nevada, a geographic information system is used to calculate average elevation from the regional digital elevation model for (1) springs in the southeast, west, and north flanks of the Sierra San Marcos (labeled as the Cuatrocienegas Basin, Hundido Valley, San Marcos Valley, and Sobaco Valley on **Figure 44**), and (2) the former Río Cañon that drained the Ocampo Valley (also labeled on **Figure 44**). Precipitation volume for each of the two areas is estimated by using the average elevation described above. The resulting precipitation depth is multiplied by the recharge zone area. Wolaver et al. (2008) present discharge values for (1) springs in the southeast, west, and north flanks of the Sierra San Marcos at 35,000,000 cubic meters/year, and (2) the former Río Cañon at 8,000,000 cubic meters/year. The recharge rate is then varied until calculated recharge equals measured discharge.

Spatially-distributed recharge as a function of precipitation, as shown in **Table 28**, is approximately one percent for springs on the southeast, west, and north flanks of the Sierra San Marcos (labeled as the Cuatrocienegas Basin, Hundido Valley, San Marcos Valley, and Sobaco Valley on **Figure 44**). For the former Río Cañon, that drained the Ocampo Valley (**Figure 44**), spatially-distributed recharge is approximately 0.4 percent of precipitation. Spatially-distributed recharge rates for the Ocampo Valley may be slightly lower than the other springs in the Cuatrocienegas Basin because recharge is focused on a relatively smaller area with a high overall elevation compared to a larger area of lower elevation valley-floor. Alternatively, the published Río Cañon discharge value (8,000,000 cubic meters/year) was lower than the long-term average flow. If so, the recharge area for the Ocampo Valley may be >596 square kilometers.

Table 28. RESULTS OF SPATIALLY-DISTIBUTED RECHARGE ANALYSIS

Springs on the southeast, west, and north flanks of the Sierra San Marcos are recharged by five catchments: the Cuatrocienegas East and West Sub-Basins, the Hundido Valley, the San Marcos Valley, and the Sobaco Valley (Figure 44). The **spatially-distributed recharge rate is shown in bold** for springs on the southeast, west, and north flanks of the Sierra San Marcos is reported here for an aggregated catchment with a total area of approximately 11,900 square kilometers that is comprised of these five individual catchments. Wolaver et al. (2008) measured spring discharge for these catchments at approximately 35,000,000 cubic meters/year. The Ocampo Valley is comprised of only one catchment that drained to the former Río Cañon (Figure 44). Minckley and Cole (1968) estimated discharge for this approximately 6,700 square kilometer catchment at 8,000,000 cubic meters/year. Two precipitation extrapolation relationships (Equations 8 and 9) are used to account for uncertainties in spatially-distributed precipitation.

Catchment Name	Area [km ²]	Average Elevation [m]	Precip- itation Depth Eqn. 8	Precip- itation Depth Eqn. 9	Precip- itation Volume Eqn. 8 [1 x 10 ⁶ m ³]	Precip- itation Volume Eqn. 9 [1 x 10 ⁶ m ³]	Recharge Rate Eqn. 8 [%]	Recharge Rate Eqn. 9 [%]
			[m]	[m]				
Cuatrocienegas East Sub-Basin	1,663	1,143	0.251	0.258	417	429	--	--
Cuatrocienegas West Sub-Basin	2,477	1,307	0.264	0.274	653	678	--	--
Hundido Valley	3,036	1,193	0.255	0.263	773	798	--	--
San Marcos Valley	2,430	1,266	0.260	0.270	633	655	--	--
Sobaco Valley	2,268	1,282	0.262	0.271	593	615	--	--
Total for springs on the southeast, west, and north flanks of the Sierra San Marcos:							1.14	1.10
Ocampo Valley	6,651	1,371	0.269	0.280	1,787	1,862	0.45	0.43

Recharge: A Mixing Model to Evaluate Local versus Regional Flow

Recharge rate is varied based on elevation to explain spatial differences in Cuatrocienegas Basin spring chloride concentration and flow rates. Results of this analysis are shown in **Table 25**, **Table 26**, and **Table 27**. However, mixing of relatively fresh and saline waters can also cause observed chloride concentration differences.

A mixing model estimates the relative percent local versus regional flow to springs feeding the Santa Tecla Canal and also Poza Anteojo (**Figure 40**). Unfortunately, chloride concentration water endmembers for regional and local flow are poorly constrained, so the author assumes Poza La Becerra ($\text{Cl}^- = 90 \text{ milligrams/liter}$) represents discharge of deep, saline water from a regional aquifer system. Discharge from a shallow, fresh, local flow system is considered in a range from rain water ($\text{Cl}^- = 0.26 \text{ milligrams/liter}$, as discussed in Chapter 2) to El Venado ($\text{Cl}^- = 29 \text{ milligrams/liter}$). Because the Poza Anteojo chloride concentration is seventeen milligrams/liter, this value is considered the highest plausible local chloride concentration. Supporting hydrogeologic data are discussed earlier in this Chapter and in **Table 17**. The mixing model solves a system of two equations and two unknowns to find the relative discharge of a spring attributed to regional versus local flow systems. The first equation is

$$Q_{\text{spring}}C_{\text{spring}} = Q_{\text{regional}}C_{\text{regional}} + Q_{\text{local}}C_{\text{local}} . \quad (29)$$

Where

Q_{spring} = spring discharge,

C_{spring} = spring chloride concentration,

Q_{regional} = regional aquifer discharge contributing to spring discharge,

$C_{regional}$ = regional aquifer chloride concentration,

Q_{local} = local aquifer discharge contributing to spring discharge, and

C_{local} = local aquifer chloride concentration.

The second equation is

$$Q_{spring} = Q_{regional} + Q_{local}. \quad (30)$$

Where

Q_{spring} = spring discharge,

$Q_{regional}$ = regional aquifer discharge contributing to spring discharge, and

Q_{local} = local aquifer discharge contributing to spring discharge.

Local flow is found by rearranging Equation 30

$$Q_{local} = Q_{spring} - Q_{regional}. \quad (31)$$

Equation 31 is substituted into Equation 29 and is rearranged to solve for $Q_{regional}$ in the following series of equations

$$Q_{spring}C_{spring} = Q_{regional}C_{regional} + (Q_{spring} - Q_{regional})C_{local}, \quad (32)$$

$$Q_{spring}C_{spring} = Q_{regional}C_{regional} + Q_{spring}C_{local} - Q_{regional}C_{local}, \quad (33)$$

$$Q_{spring}C_{spring} = Q_{regional}(C_{regional} - C_{local}) + Q_{spring}C_{local}, \quad (34)$$

$$Q_{regional}(C_{regional} - C_{local}) = Q_{spring}C_{spring} - Q_{spring}C_{local}, \quad (35)$$

$$Q_{regional}(C_{regional} - C_{local}) = Q_{spring}(C_{spring} - C_{local}), \text{ and} \quad (36)$$

$$\frac{Q_{regional}}{Q_{spring}} = \frac{(C_{spring} - C_{local})}{(C_{regional} - C_{local})}. \quad (37)$$

$Q_{regional}$ is solved using Equation 37. Then Q_{local} is solved by substituting $Q_{regional}$ into Equation 31. The percent of total spring flow from the regional aquifer is given with this equation

$$\frac{Q_{regional}}{Q_{spring}} = \frac{(C_{spring} - C_{local})}{(C_{regional} - C_{local})}. \quad (38)$$

Mixing model inputs and results are shown in **Table 29**. The results for the Santa Tecla Canal show that for a low local chloride concentration (0.26 milligrams/liter, case 1) spring discharge is comprised of approximately nineteen percent regional flow and approximately 81 percent local flow. For a higher local chloride concentration (17 milligrams/liter, case 2) spring discharge is comprised of approximately one percent regional flow and approximately 99 percent local flow. The mixing model results for Poza Anteojo show that for a low local chloride concentration (0.26 milligrams/liter, case 1) spring discharge is comprised of approximately seventeen percent regional flow and approximately 83 percent local flow. For a higher local chloride concentration (17 milligrams/liter, case 2) spring discharge is comprised entirely of local flow.

Table 29. MIXING MODEL INPUTS AND RESULTS: LOCAL VERSUS REGIONAL FLOW

The results of the mixing model suggest separate flow paths converge and discharge into Cuatrocienegas Basin springs, as indicated by the geochemical modeling of Evans (2005) that suggested several geochemically unique flowpaths within the basin.

The **mixing model results are shown in bold** for Q_{regional} and Q_{local} (in terms of liters/second and percent of total spring discharge).

¹ Santa Tecla Canal Discharge \approx 190 liters/second. Poza Anteojo discharge 30 liters/second (or, approximately 1 cubic foot/second, Wolaver, unpublished).

² Santa Tecla Canal chloride concentration \approx 30 milligrams/liter (Wolaver and Tidwell, unpublished; Rodríguez et al., 2005a). Poza Anteojo chloride concentration \approx 12 milligrams/liter (Rodríguez et al., 2005a) and 22 milligrams/liter (Crossey, unpublished). The mixing model uses an average chloride concentration of 17 milligrams/liter.

³ The local chloride concentration is calculated for a range that includes (1) precipitation =0.26 milligrams/liter (from precipitation and dry deposition; National Atmospheric Deposition Program, 2008; Scanlon and Goldsmith, 1997; Scanlon et al., 2007), and (2) El Venado=29 milligrams/liter (Crossey, unpublished). A local flow chloride concentration up to 17 milligrams/liter is used because the Poza Anteojo chloride concentration is 17 milligrams/liter.

⁴ The regional flow chloride concentration \approx 90 milligrams/liter (Wolaver and Tidwell, unpublished; Rodríguez et al., 2005a).

⁵ The mixing model is solved for the regional flow component using Equation 37.

⁶ The local flow component is found by substituting Q_{regional} into Equation 31.

Case	Q_{spring} ¹ [L/sec]	C_{spring} ² [mg/L]	C_{local} ³ [mg/L]	C_{regional} ⁴ [mg/L]	Q_{regional} ⁵ [L/sec]	Q_{local} ⁶ [L/sec]	Q_{regional} [%]	Q_{local} [%]
	Model input parameters				Model results (bold text)			
Santa Tecla Canal case 1	190	17	0.26	90	36	154	19	81
Santa Tecla Canal case 2	190	17	29	90	1	189	1	99
Poza Anteojo case 1	30	17	0.26	90	5	25	17	83
Poza Anteojo case 2	30	17	17	90	0	30	0	100

Also, the results of the mixing model suggest that for the Santa Tecla Canal, a significant regional flow component is plausible only if the local chloride concentration is low (i.e., that of precipitation). The results suggest that local flow to the Santa Tecla Canal dominates with increasing local flow chloride concentration. For Poza Anteojo, local flow dominates spring discharge for both local chloride concentration scenarios. The results suggest that regional flow to the Santa Tecla Canal and Poza Anteojo is possible only with a local flow chloride concentration from rain. This scenario is improbable, because evapotranspiration increases rain chloride concentration during recharge processes.

Alternatively, it is possible that regional flow system endmember is different from Poza La Becerra. In fact, Evans (2005) suggested five separate flow systems within the Cuatrocienegas Basin based on geochemical modeling. Thus, it is possible that separate flow systems converge at the Cuatrocienegas Basin. It is possible that Poza Anteojo (10 kilometers east of the Río Cañon on the southern flank of the Sierra La Madera) and El Venado (located at the northern tip of the Sierra La Purísima) belong to unique flow systems. The results of the mixing model underscore the need for future research to refine the groundwater endmembers.

Recharge: Summary

A summary of the recharge analysis indicating local and regional flow systems is shown on **Figure 47**. The figure shows recharge areas delineated on **Figure 44** and also includes arrows showing inferred local and regional groundwater flow paths from recharge areas to Cuatrocienegas Basin springs.

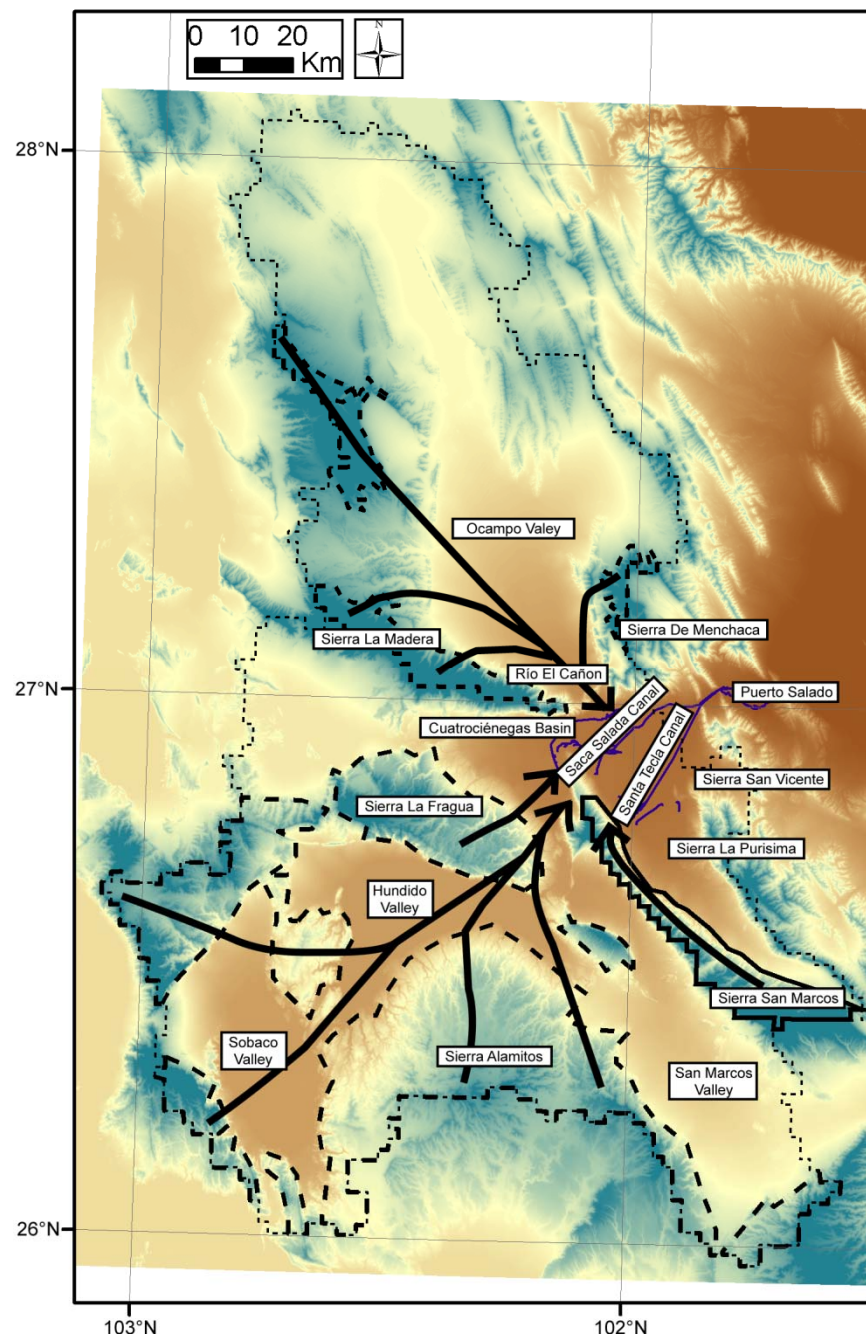


Figure 47. LOCAL AND REGIONAL GROUNDWATER FLOW PATHS

This figure includes the groundwater recharge areas (stippled and dashed lines, Figure 44). The bold lines and arrows indicate inferred local and regional groundwater flow paths from recharge areas to Cuatrocienegas Basin springs. The groundwater flow paths follow a topographic gradient shown on Figure 32. The Cuatrocienegas Basin likely represents a Tóth-style (1963) flow system with multiple flow paths converging at a regional low-elevation drain.

The three recharge areas shown on **Figure 47** include (1) the mountains surrounding the Ocampo Valley historically discharging in the now dry Río Cañon, (2) the Sierra San Marcos discharging into springs on the southeast flank of the Sierra San Marcos, and (3) mountains surrounding the Hundido, San Marcos, and Sobaco Valleys discharging into springs on the west and north flank of the Sierra San Marcos.

A summary geologic cross section that indicates the mechanisms to convey water from local and regional carbonate aquifers to Cuatrociénegas Basin springs is discussed in Chapter 5. The recharge rate in the mountainous areas surrounding the Cuatrociénegas Basin is up to seven percent of precipitation. Spatially-distributed recharge for the entire region is approximately one percent of precipitation. The mixing model suggests regional flow components to the Santa Tecla Canal and Poza Azul are significant only if local flow chloride concentration is close to that of precipitation (i.e., essentially no evapotranspiration occurs during recharge — an unlikely scenario). Alternatively, several separate flow systems converge and discharge into the Cuatrociénegas Basin. Ultimately, future research should constrain the geochemistry of local and regional flow endmembers to improve the delineation of flow systems.

Temperature Model

No recent igneous intrusions exist in the Cuatrociénegas Basin. Thus, the author infers that relatively deeply circulating groundwater causes warm spring water temperatures. Elevated temperatures (approximately 33.0° and 35.0°C, respectively) of Poza Azul and Poza Escobedo, two springs on the northern flank of the Sierra San Marcos, indicate deeper regional flow components. Of course, the geothermal gradient may be higher than assumed, which would slightly decrease the estimated depth of the flow system. Slightly lower temperatures of other smaller springs in the Cuatrociénegas

Basin (28.5°C , El Venado; 29.9°C , Poza Anteojo; and 31.1°C , Poza Churince) suggest shallower circulation indicative of more localized recharge processes.

Limitations of Analysis

Long-term hydrogeologic data do not exist for the Cuatrocienegas Basin region. Despite the hydrogeologic conceptual model and parameter uncertainty, the greatest utility of this research may well be as an interpretive model to test hydrogeologic conceptual models of the Cuatrocienegas Basin flow system. Specific hydrogeologic model conceptual uncertainties include (1) aquifer connectivity, (2) aquifer thicknesses, and (3) groundwater discharge out of the Cuatrocienegas Basin. Spring discharge in outlet canals can be measured, but no data exist to estimate the possibility of interbasin flows out of the Cuatrocienegas Basin to the east. Sources of hydrogeologic model parameter uncertainty include (1) precipitation and recharge rate (although reasonable estimates can be made, precipitation is the largest source of uncertainty in this model and is acknowledged as such in the literature, Adam et al., 2006; Zhu and Lettenmaier, 2007; Gochis et al., 2002); and (2) precipitation chloride concentration. Thus, this approach is limited by the fact that the solution is non-unique. However, this research presents a reasonable best-fit hydrogeologic conceptual model to explain spatial variations in spring chloride concentration, discharge, and temperature.

Summary

In the study area, chloride concentration and discharge balance under the following conditions:

1. Springs on the southeast flank of the Sierra San Marcos are largely recharged on the outcrop area of this mountain. This recharge area is shown on **Figure 44**.

2. Historical spring discharge (which may have been greater in past wetter, cooler climatic conditions) from the Ocampo Valley into the Cuatrocienegas Basin was recharged on the outcrop area of the mountains surrounding this basin (**Figure 44**,
4. Springs on the west and north flank of the Sierra San Marcos had recharge occur on the carbonate outcrop of mountains surrounding the Hundido, San Marcos, and Sobaco Valleys, as shown on **Figure 44**, and
5. Evaporative concentration from shallow water table and/or playa lakes in the Sobaco Valley and Hundido Valley likely increased chloride concentration in springs on the west and north flank of the Sierra San Marcos.

CONCLUSIONS

This research describes an approach to delineate recharge zones in arid karst aquifers based on spatial differences in spring discharge, chloride concentration, and temperature. This approach is tested in the Cuatrocienegas Basin of Coahuila, Mexico and improves upon a previous recharge area assessment (Wolaver et al., 2008) that applied a fixed recharge rate to delineate an approximately 18,000-square kilometer recharge area to basin springs. This research is important because it refines previous aquifer recharge area delineation for the Cuatrocienegas Basin and presents new hydrogeologic data. This research uses a water budget and chloride-balance approach to find that an approximately 2,050-square kilometer recharge area within an approximately 18,000-square kilometer area supports the springs of the Cuatrocienegas Basin.

A 450-square kilometer recharge area of exposed carbonate rock of the Sierra San Marcos feeds a local flow system flowing to springs on the southeast flank of the Sierra

San Marcos (discharge is approximately 6,200,000 cubic meters/year with an average chloride concentration of 30 milligrams/liter). Approximately 81 percent of recharge by volume occurs between 700–2,700 meters at a rate between three and seven percent of precipitation. A temperature model (with a spring temperature of approximately 30°C) suggests groundwater flows to a depth of approximately 360–560 meters.

An approximately 600-square kilometer recharge area of the Sierra La Madera and other mountains surrounding the Ocampo Valley fed the now dry Río Cañon. Historic discharge was approximately 12,600,000 cubic meters/year and chloride concentration of spring discharge was approximately 22 milligrams/liter. Approximately 80 percent of recharge by volume occurs between 1,700–2,300 meters, reflecting a higher overall mountain elevation — in fact, the Sierra La Madera has the highest elevation at over 3,000 meters, while the Sierra San Marcos is approximately 400 meters lower. The recharge rate is between three and seven percent of precipitation. A temperature model was not used because no historic spring temperature data exist. However, the historic spring discharge may have been close to ambient temperature (16°–21°C) because faults are not mapped in the immediate vicinity of the historic spring. However, historic spring discharge probably had a residence time under 50 years, given the relatively short flow paths (i.e., many of the recharge areas are within 20–30 kilometers) from the Sierra La Madera to the spring at the head of the Río Cañon.

An approximately 1,000-square kilometer recharge area of mountains surrounding the Hundido, Sobaco, and San Marcos Valleys feeds springs on the west and north flank of the Sierra San Marcos. These springs discharge approximately 29,000,000 cubic meters/year with an average chloride concentration of 90 milligrams/liter. Approximately 71 percent of recharge by volume occurs between 700–1,700 meters, with approximately 26 percent of recharge occurring above 1,700 meters — reflecting the overall lower

elevation of these mountains compared to the Sierra San Marcos and the Sierra La Madera. A recharge rate between zero and four percent of precipitation is required to generate the elevated spring chloride concentration. Evaporation off of a shallow water table or from playa lakes in the Sobaco and Hundido Valleys may also cause the elevated chloride concentration. Oxygen isotopes (discussed above in this dissertation) show an evaporative trend and also suggest a lower precipitation elevation (1,150–1,250 meters) compared to the other springs (Poza Anteojo, at the foot of the Sierra La Madera has an interpreted precipitation elevation of approximately 2,350 meters) — although many factors contribute to interpretation uncertainty. A temperature model (the highest spring temperature is approximately 35°C) suggests groundwater flows to a depth of approximately 560–760 meters.

Based on the results of this research, effective water management policies could be extended outside of the Cuatrociénegas Basin to include the irrigated agriculture in the Hundido, Sobaco, and San Marcos Valleys. Pumping in the Ocampo Valley should be managed to reduce drawdown and perhaps recover groundwater levels to predevelopment conditions to restore flow to the Río Cañon. Springs on the east flank of the Sierra San Marcos are probably not threatened as seriously by pumping in adjacent basins.

Future research may consider quantifying the effects of projected climate change on recharge in the Cuatrociénegas Basin and also the larger northeast Mexico region (with a population >6,000,000 people). The aquifer delineation presented here could be improved by adding samples from additional springs or wells and by including a time series analysis to capture any seasonal trends.

Chapter 5: Using Gravity Geophysics to Characterize Geologic Controls on Arid Karst Aquifer Spring Locations

A revised version of this chapter will be submitted to Environmental Geology

“Do not put the karst before the horst.”

—Or, structural controls on groundwater flow in karst aquifers.

*Dr. John M. Sharp, Jr.
Austin, Texas, April 22, 2008*

ABSTRACT

Land-based gravimetry is used to assess subsurface geologic controls on springs in the Cuatrocienegas Basin of Coahuila, Mexico. The Cuatrocienegas Basin is a National Biosphere Reserve that contains groundwater dependent ecosystems with high species endemism (>70 endemic species) in an arid climate. Groundwater from wells and dozens of springs supplies municipal water and irrigated agriculture requirements. Previous studies in the Cuatrocienegas Basin have investigated biologic resources and regional and local hydrogeology, but did not explain the controls on spring locations. Springs occur primarily in lines on either side of the Sierra San Marcos carbonate anticline. Hydrogeologic cross sections enable the use of classical models to understand controls on groundwater discharge in regional flow systems like the Cuatrocienegas Basin.

Land-based gravimetry is one way to test the hypothesis that spring locations are controlled by subsurface geology (e.g., buried anticlines, faulting, or permeability differences). Gravity surveys were conducted in January 2006 and March 2006 at four

selected Cuatrocienegas Basin locations. Results of these surveys suggest that springs on the west and north flank of the Sierra San Marcos are controlled by fractures associated with a reverse fault within the Sierra San Marcos that creates fracture permeability and permits discharge from a regional carbonate aquifer. On the east flank of the Sierra San Marcos, buried faults are not present. Here, springs are located at or near the base of alluvial fans.

INTRODUCTION

The Cuatrocienegas Basin is relatively well studied from a biological perspective (Minckley and Cole, 1968, Minckley, 1969; Hendrickson et al., 2005), but the geologic conditions that allowed these groundwater-dependent ecosystems to form are not well understood. This research uses land gravity geophysical surveys to characterize subsurface influences on spring locations in the Cuatrocienegas Basin, Coahuila, Mexico. The Cuatrocienegas Basin region is shown on **Figure 48**. The Cuatrocienegas Basin is shown on **Figure 49**.

Hypotheses, Objectives, and Importance

This study tests the hypothesis that subsurface geology, such as buried anticlines (**Figure 50a**) or faults (**Figure 50b**), controls spring locations. If anticlines or faults are not found, an alternative hypothesis is that permeability differences between valley-fill alluvium and underlying carbonate rocks is the controlling factor in spring locations (**Figure 50c**).

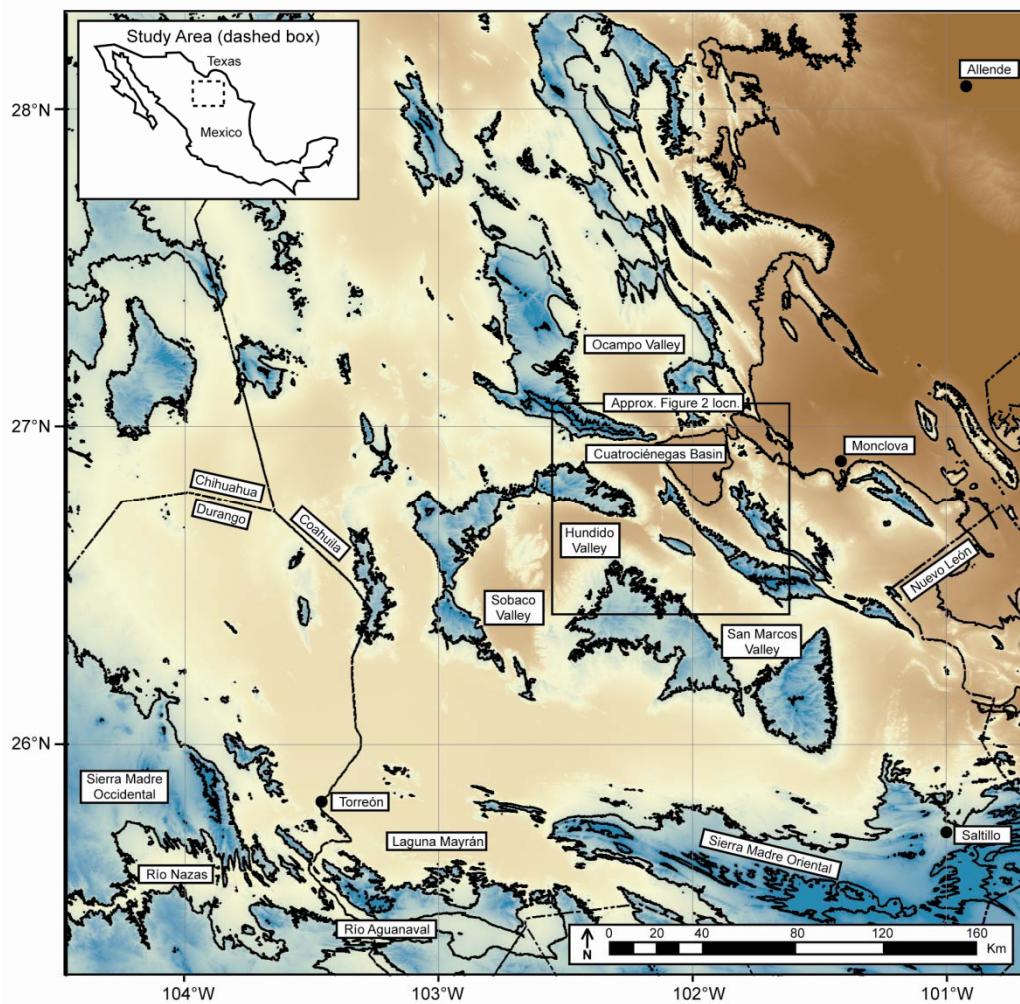


Figure 48. CUATROCIÉNEGAS BASIN STUDY AREA

Contour interval ranges from brown (750-meter)–green (1,500-meter and 2,250-meter). State boundaries are indicated by dashed lines. Study area is location in the black box (shown on Figure 49). Major topographic features, cities, and political boundaries are labeled. Inset: location of the figure within Mexico.

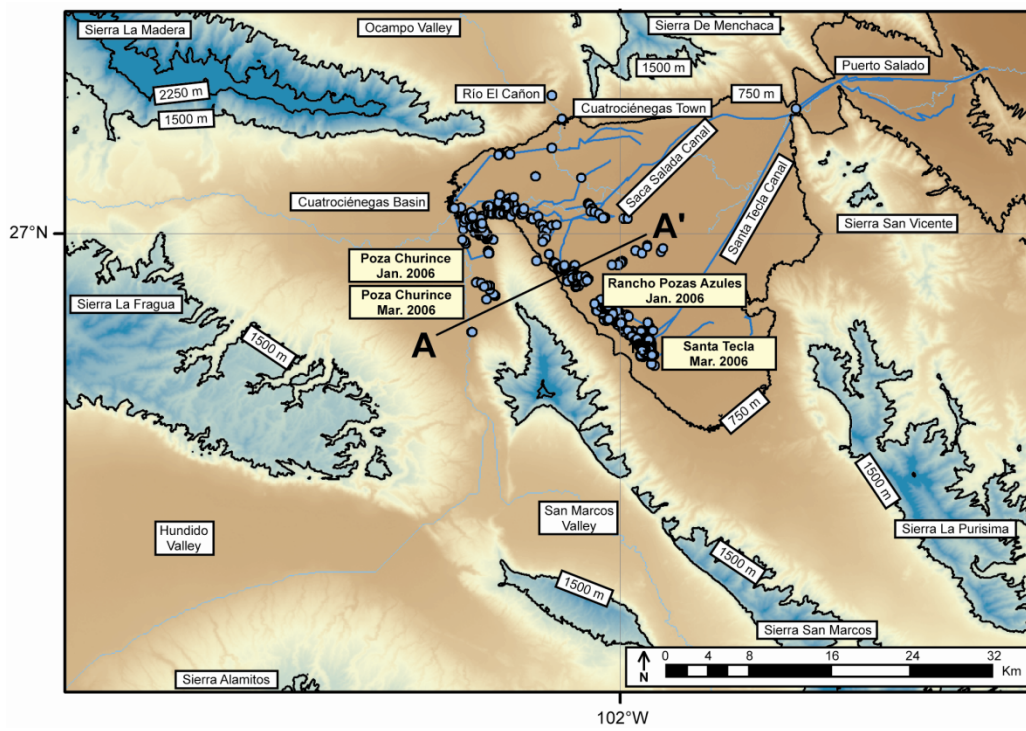


Figure 49. CUATROCIÉNEGAS BASIN

The general locations of the four gravity lines are labeled in bold text boxes (e.g., Poza Churince, Jan. 2006; Poza El Churince, Mar. 2006, Rancho Pozas Azules, Jan. 2006; and Santa Tecla, Mar. 2006). Cuatrocienegas Basin features include springs (blue open circles), canals (light blue lines), inferred surface drainage network (light blue dashed line, see Wolaver et al., 2008), and 750-meter contour intervals (low-high-elevation ranges from brown–green, respectively). The general location of Cuatrocienegas hydrogeologic conceptual cross section shown on Figure 50 is indicated by a line labeled A-A'.

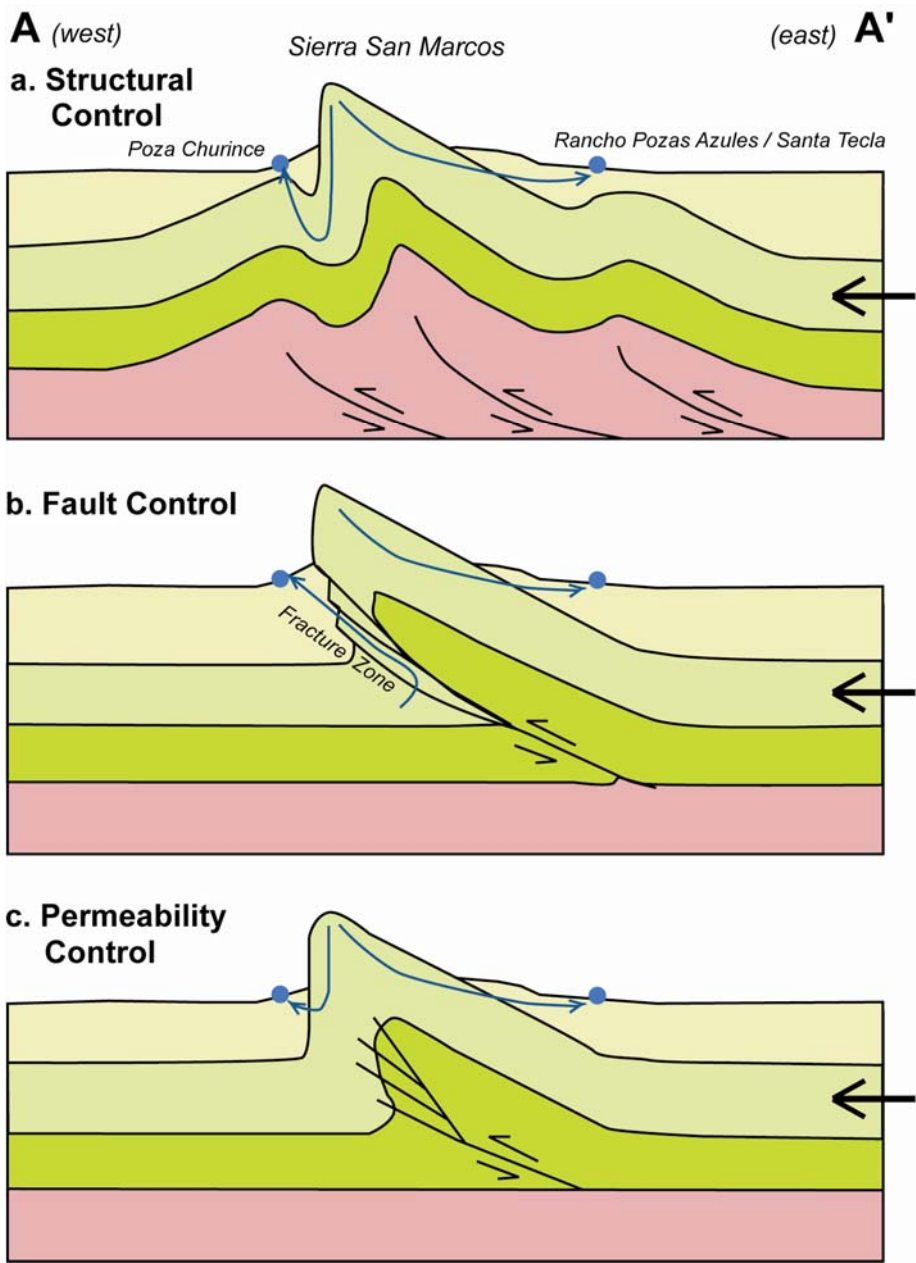


Figure 50. POSSIBLE CUATROCIÉNEGAS HYDROGEOLOGIC CROSS SECTIONS

Three hydrogeologic conceptual cross sections are tested by this research. Hydrogeologic conceptual cross sections (A-A'); hypotheses include structural, fault, and permeability controls on spring locations where low hydraulic conductivity valley-fill alluvium (yellow) overlies a high-permeability Cretaceous carbonate aquifer (light green) and low permeability granodiorite (pink). Cross sections b and c are based on the fault propagation and trishear zone models of Erslev and Mayborn (1997) and Mitra (2002). Solid blue circles indicate springs, curved arrows indicate groundwater flow paths, and light black arrows indicate relative fault motion.

The hypotheses are tested by conducting land gravimetry surveys in the vicinity of two locations of high spring density: two surveys on the west flank of the Sierra San Marcos around Poza El Churince, and two surveys on the east flank of the Sierra San Marcos around Rancho Pozas Azules and Poza Santa Tecla. The objective is to generate a conceptual hydrogeologic cross section in locations of high spring density. Four profiles were taken: (1) Poza El Churince (northerly line), (2) Poza El Churince (southerly line), (3) Rancho Pozas Azules, and (4) Poza Santa Tecla.

This study is important if the gravimetry surveys show that subsurface structures exist, then classic models (Tóth, 1963; Freeze and Witherspoon, 1967) can be used to infer controls on groundwater discharge in the Cuatrocienegas Basin as well as other regional arid karst aquifer systems where subsurface geology data are sparse.

Motivation for Gravity Surveys

Land gravimetry geophysical surveys are used instead of other geophysical methods because gravity surveys are relatively (1) inexpensive, (2) easy to implement, (3) non-intrusive, and (4) the resulting data can be processed and interpreted relatively easily compared to seismic surveys. Also, Jansen et al. (2004) used gravimetry surveys to determine subsurface influences on spring locations in similar carbonate terrains, while Langenheim et al. (2002) used gravity to determine alluvium-filled valley thickness. Seismic reflection or refraction may provide detailed information on subsurface geology influencing spring locations (Bushman et al., 2005). Exploratory borehole drilling would effectively determine alluvium thickness if drilled to carbonate rocks. However, these methods can be costly. Ground penetrating radar (GPR) also was tested in the vicinity of springs in the Cuatrocienegas Basin, but shallow groundwater with elevated salinity hindered collection of useful subsurface data.

BACKGROUND: SURVEY AREA SETTING

Previous workers have investigated springs in the Cuatrocienegas Basin and analogous locations. Adkins (1920) conducted the first hydrogeologic assessment of the Cuatrocienegas Basin and inferred that faulting causes springs to occur in the Cuatrocienegas Basin because of the linear trend of dozens of springs on either side of the Sierra San Marcos anticline (**Figure 49**). Minckley and Cole (1968) presented a preliminary description of Cuatrocienegas Basin spring water chemistry from an aquatic biology perspective, and Evans (2005) defined groundwater flow paths within the basin based on hydrochemical facies. Johannesson et al. (2004) and Rodríguez et al. (2005a) used oxygen isotopes to suggest that groundwater recharge occurs as mountain precipitation. Meyer (1973) used radiocarbon dating and pollen analyses, determining that basin springs have been active for >30,000 years. Wolaver et al. (2008) conducted an aquifer delineation using an integrative data approach and inferred that interbasin groundwater flow provides the majority of Cuatrocienegas Basin groundwater discharge, but did not investigate subsurface controls on spring locations.

In Ash Meadows, Nevada, an analogous arid region with an alluvial-fill valley aquifer overlying a carbonate aquifer, Bushman et al. (2005) used seismic reflection to show fault influences on spring locations. In Death Valley, Jansen et al. (2004) mapped the top of a carbonate aquifer using land gravity, an approach this research also uses.

In general, three different sets of springs are present in Cuatrocienegas: (1) historic spring flow from the Ocampo Valley to the Río Cañon, (2) springs on the northern and western flank of the Sierra San Marcos, and (3) springs on the southeastern flank of the Sierra San Marcos. First, historic spring flow from the Ocampo Valley to the Río Cañon had the lowest chloride concentration in the valley. However, this spring is now dry, and is not evaluated. Second, springs on the northern and western flank of the

Sierra San Marcos have elevated discharge (approximately 85 percent of the total discharge of 35,000,000 cubic meters/year), chloride concentration (with an average chloride concentration of approximately 90 milligrams/liter), and temperature (~31.0°–34.0°C). Poza La Becerra, the largest spring in this part of the basin is associated with fractures in carbonate rock (**Figure 51**).

In comparison, springs on the southeast flank of the Sierra San Marcos that have lower relative discharge (~15 percent of the total discharge), chloride concentration (with an average chloride concentration of approximately 30 milligrams/liter), and temperature (~28.0°–30.0°C). In this portion of the basin, springs are typically associated with the foot of alluvial fans (**Figure 52**). The author hypothesizes that long flow paths with deeper circulation are likely for springs flanking either side of the Sierra San Marcos. The author hypothesizes that lower chloride concentration in Ocampo Valley and southeastern Sierra San Marcos springs suggests elevated elevation recharge with less evaporation, while higher spring chloride concentrations for springs on the northern and western flanks of the Sierra San Marcos suggest lower elevation recharge or evaporative processes. A brief summary Cuatrociénegas Basin spring hydrogeologic data are shown in **Table 30**.

Northeast Mexico Stratigraphy and Tectonics

The Cuatrociénegas Basin is located at the northern edge of the folded and faulted Sierra Madre Oriental. Goldhammer (1999) described northeastern Mexico stratigraphy in the vicinity of the Cuatrociénegas Basin. Lehmann et al. (1999) correlated Cretaceous carbonate mountain anticlines surrounding the 1,200-square kilometer Cuatrociénegas Basin with coeval formations on the Gulf Coast. Lesser y Asociados (2001) presented a regional hydrogeologic conceptual model of parallel mountain anticlines and synclines filled with alluvium and lacustrine sediments.

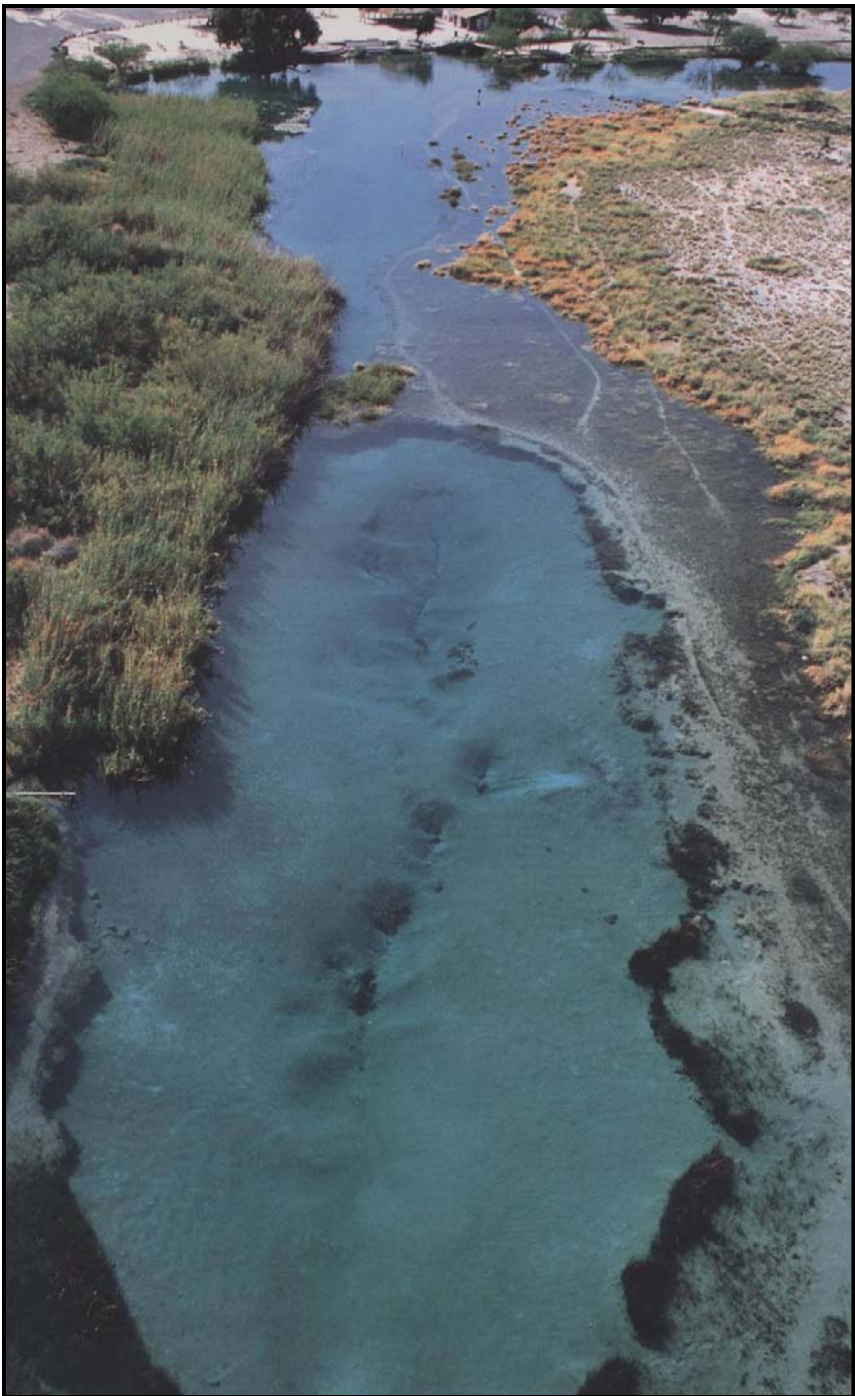


Figure 51. SPRING ON WEST FLANK OF SIERRA SAN MARCOS

Photo of Poza La Becerra (Badino et al., 2004). Carbonate fractures are visible in the spring bottom and trend north-south. Palapas (reed huts) in background indicate scale.



Figure 52. SPRING ON EAST FLANK OF SIERRA SAN MARCOS

Springs are generally associated with the foot of alluvial fans. Dirt road for scale. Photo by Badino et al. (2004).

Table 30. SUMMARY HYDROGEOLOGIC DATA FOR CUATROCIÉNEGAS SPRINGS

¹Minckley and Cole (1968) presented 1964 Ocampo Valley discharge and chloride concentration, but did not give temperature data. Wolaver et al. (2008) reported more recent canal discharge. Values for other springs are approximate and capture overall trends.

Spring Location	Discharge [m ³ /year]	Chloride Concentration [mg/L]	Temperature [°C]
Ocampo Valley	8,000,000	22	Unknown
Northern and Western Flank of the Sierra San Marcos	29,000,000	90	32.0°–35.0°
Southeast Flank of the Sierra San Marcos	6,000,000	30	30.0

Both the mountains surrounding the Cuatrocienegas Basin and the valley fill alluvium are highly karstified (Badino et al., 2004). Miele et al. (2000) used time domain electromagnetics to image buried carbonate anticlines for groundwater development in an adjacent basin and Rodríguez et al. (2005a) used time domain electromagnetics to estimate an average Cuatrocienegas Basin alluvium depth of approximately 200 meters. These sparse soundings and interpolation of results cover wide areas. However, these valley fill depths are used as a starting point for geologic modeling.

Hydrostratigraphy

Irrigation pumping of groundwater that started in the mid-1900s has caused groundwater level declines on the order of 10s of meters or more in neighboring valleys and dried up surface water that previously flowed into the Cuatrocienegas Basin (Minckley, 1992). Concerns exist that continued regional groundwater resource development may decrease Cuatrocienegas Basin spring discharge. Wolaver et al. (2008) described the hydrostratigraphy in the Cuatrocienegas Basin as primarily comprised of Cretaceous carbonates and evaporites overlying terrigenous siliciclastics and a Triassic

granodiorite basement. A generalized hydrostratigraphic column of the Cuatrocienegas Basin is shown in **Table 31**.

Structure of the Cuatrocienegas Basin

Goldhammer (1999) stated that northeast Mexico experienced rifting associated with the opening of the Gulf of Mexico in the Triassic and Jurassic. This rifting created basement highs (e.g., Coahuila Platform) and lows (e.g., Sabinas Basin). Chávez-Cabello et al. (2005) described the San Marcos Fault, a 300-kilometer long fault with reverse displacement that separates the Coahuila Block, shown as “BC” on from the Coahuila Fold Belt shown as “CPC” on **Figure 53**. Erosion of the Coahuila Block permitted accumulation of a 700–3,000-meter thick clastic sedimentary wedge that thickens towards the Sabinas Basin to the east of the study area (Chávez-Cabello et al., 2005). Chávez-Cabello et al. (2005) determined that the San Marcos Fault reactivated during the Laramide orogeny as a reverse fault, causing extensive folding of the clastic and carbonate package. These tectonic processes created anticlinal carbonate highlands and alluvial-filled synclinal valleys that characterize the structural style of northeast Mexico. For reference, the Cuatrocienegas Basin is located approximately 25 kilometers west of the Town of Monclova, Coahuila (**Figure 53**).

An approximately 18,000-square kilometer recharge area supports spring discharge in the Cuatrocienegas Basin, as shown on **Figure 42** and **Figure 44** (Wolaver et al., 2008, Wolaver and Tidwell, 2008). Chávez-Cabello et al. (2005) present generalized structure of the Cuatrocienegas Basin region shown on **Figure 53**. The Sierra San Marcos is an asymmetrical anticline of Cretaceous carbonate rocks (Cupido, La Pena, and Aurora Formations) and cored by the clastic San Marcos Formation. The Sierra San Marcos is shown as “ASSMP.”

Table 31. GENERALIZED HYDROSTRATIGRAPHIC COLUMN

Stratigraphic nomenclature is modified from McKee et al., 1990; Rodríguez and Sanchez, 2000; Lesser y Asociados, 2001; Evans, 2005.

Age	Formation	Description	Permeability
Quaternary	Alluvium	Sand, gravel, lake deposits, evaporate deposits, travertine	Variable
	Eagle Ford	Limestone, shale	Low
	Buda	Limestone, interbedded sand and gravel	Low
	Del Rio	Clay, sandy limestone	Low
	Georgetown (Cuesta del Cura)	Limestone	Moderate
	Washita Group	Limestone	Moderate
	Kiamichi	Limestone, shale	Low
	Aurora	Lime mudstones and wackestones, gypsum, dolomitized grainstones	High
	La Peña	Dark laminated shale, thin lime mudstone interbeds	Low
	Cupido	Lime mudstone	High
Cretaceous	La Virgen	Gypsum, dolomite, limestone, shale and clay	Low
	La Mula	Shale, sandstone, limestone, conglomerate	Low
	La Padilla	Massive dolomite, interbedded shale, sandstone, and evaporites	Low
	San Marcos	Sandstone, hematitic cement, interbedded conglomerate	Low–Moderate
	Triassic	Basement	Granodiorite
			Low

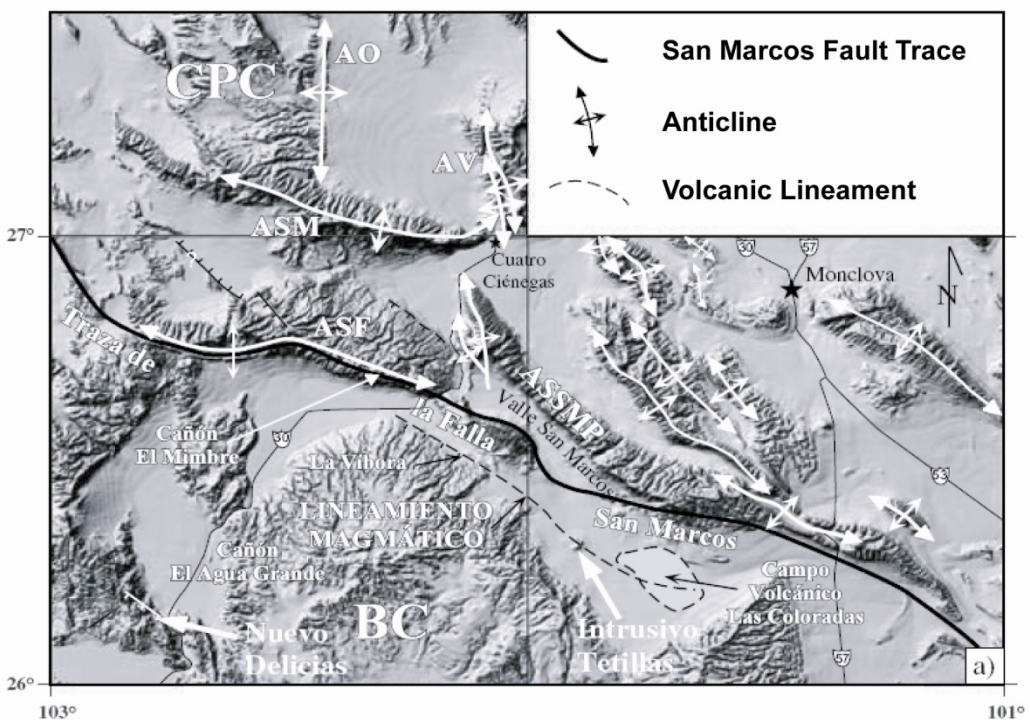


Figure 53. GENERALIZED STRUCTURE OF THE CUATROCIÉNEGAS BASIN REGION

The Cuatrocienegas Basin study area (after Chávez-Cabello et al., 2005). BC is the Coahuila Block, CPC is the Coahuila Fold Belt, ASSMP is the Sierra San Marcos, and la Falla San Marcos is the San Marcos Fault.

An approximately 7,700-square kilometer recharge area is located to the south and southwest of the Cuatrocienegas Basin (e.g., the Hundido, San Marcos, and Sobaco Valleys). These three valleys are located on the Coahuila Block. Because the Coahuila Block is comprised of granodiorite—a stronger material relative to the sedimentary rocks of the Sabinas Basin to the east—high-frequency folds, such as those that comprise the Sierra Madre near Monterrey have not developed (Marrett and Bentham, 1997; Marrett and Aranda-García, 2001). Instead, the Cretaceous carbonate rocks that overlie the Triassic granodiorite of the Coahuila Block have been gently folded into broad anticlines with relatively shallow dips, as shown on **Figure 53**. The regional structural style changes dramatically at the San Marcos Fault (labeled as “la Falla San Marcos” on **Figure 53**). This basement-involved reverse fault of Laramide age forms the northeast boundary of the Coahuila Block. To the east of the San Marcos Fault, higher-frequency basement involved folds characterize the regional structural style.

General groundwater flow paths are discussed in Chapter 4 (**Figure 54**). Groundwater flows into the Cuatrocienegas Basin from the southwest from the upgradient Sobaco and Hundido Valleys. The regional dip in these valleys is gentle because the granodiorite of the Coahuila Block precluded the formation of steep anticline mountains. However, as groundwater flows into the Cuatrocienegas Basin, it crosses the San Marcos Fault, a basement-involved fault that separates the Hundido Valley from the Cuatrocienegas Basin. To the east of the San Marcos Fault, steep anticline mountains that may be associated with additional faults are present. Fractures associated with these faults may permit groundwater flow to the springs of the Cuatrocienegas Basin. Springs are located in the Cuatrocienegas Basin because this is the location that fault-associated fractures create the secondary permeability needed to generate discharge from the regional carbonate aquifer as it flows off of the Coahuila Block.

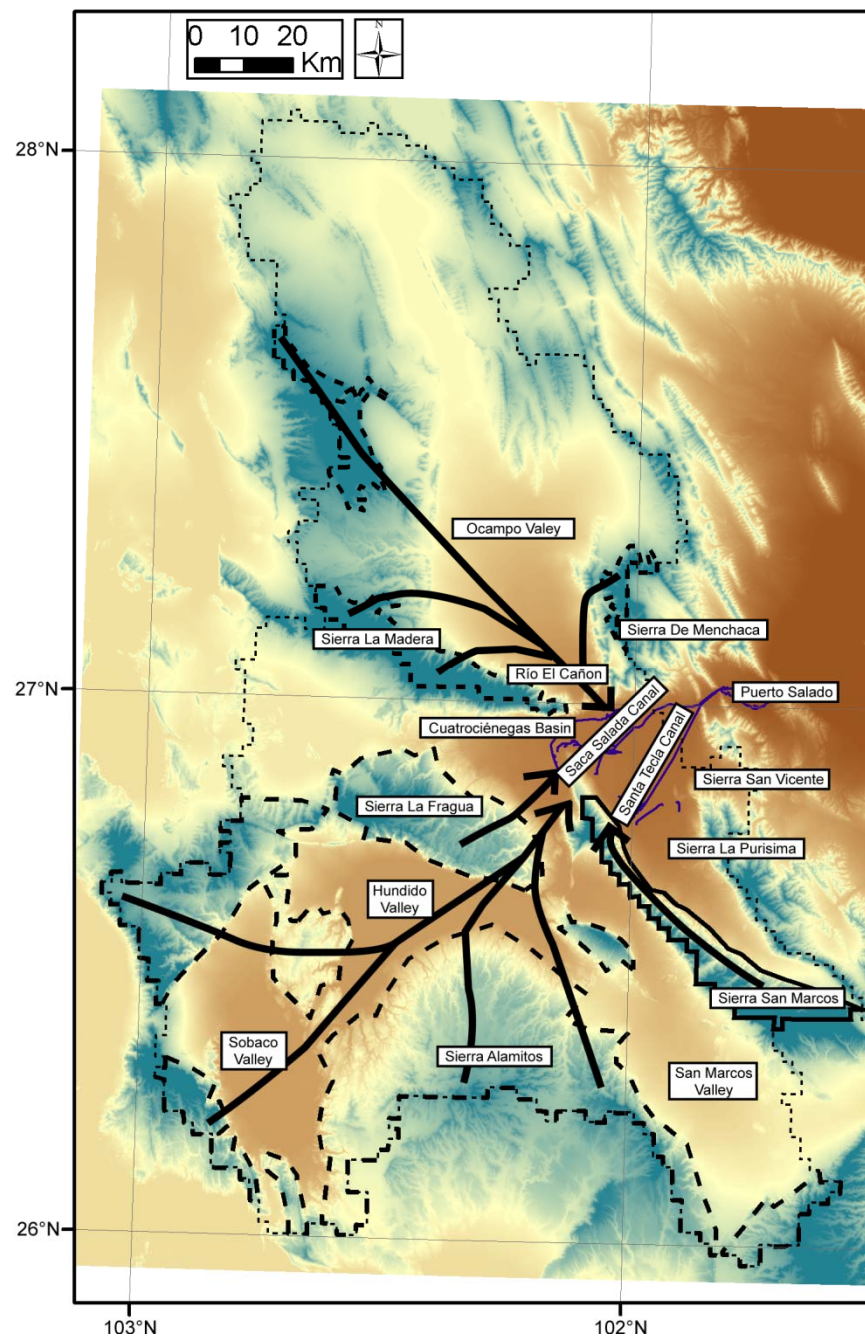


Figure 54. LOCAL AND REGIONAL GROUNDWATER FLOW PATHS

The bold arrows indicate general regional and local groundwater flow paths from recharge areas to Cuatrocienegas Basin springs described in Chapter 4.

Dips of Cretaceous carbonate strata on the west side of the Sierra San Marcos range from 50 to >90 degrees; the Sierra San Marcos anticline is slightly overturned in its farthest south exposure. On the east flank of the Sierra San Marcos, the strata dip more gently at approximately 30 degrees to the east. The entire Sierra San Marcos anticline plunges approximately 5–10 degrees to the north. Springs flank either side of the Sierra San Marcos anticline; however, the largest springs are on the west and north flank of the anticline.

Chávez-Cabello et al. (2005) indicated that the Sierra San Marcos anticline is actually two parallel anticlines and a closed syncline and has been truncated by Laramide reverse reactivation of Jurassic normal faulting. As a result, the San Marcos Fault has cut the Sierra San Marcos anticline and created a spectacular outcrop >1,300 meters high exposed in the San Marcos Valley to the south of the Cuatrociénegas Basin. Chávez-Cabello et al. (2005) commented that a restraining bend in the San Marcos Fault may be the cause of the Sierra San Marcos, which trends roughly north-south. The San Marcos Fault and most mountain ranges in the study area have a roughly east-west orientation.

Eguiluz de Antunano (2001) discussed the structural style in the Cuatrociénegas Basin region and commented that Jurassic evaporites are absent here because of the presence of the paleogeographic high created by the Coahuila Block. Thus, faults are emergent and form anticlinal mountains of exceptionally high relief—the distance from the valley floor (approximately 750 meters) to the highest mountains (>3,000 meters) is as little as five kilometers. Chávez-Cabello et al. (2005) presented a conceptual cross section for the formation of high-elevation anticlines like the Sierra San Marcos. This structural mechanism is shown on **Figure 55**.

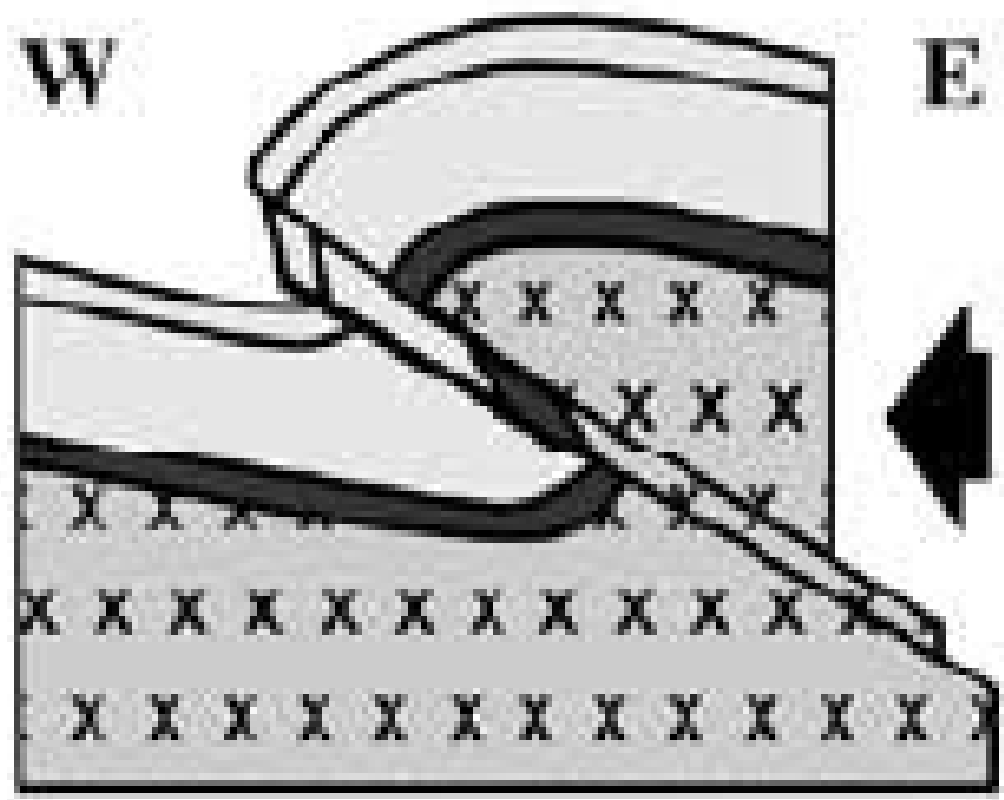


Figure 55. GENERALIZED SIERRA SAN MARCOS STRUCTURAL CROSS SECTION
Showing Laramide reactivated reverse fault (After Chávez-Cabello et al., 2005).

The structural style of this model is based on the fault-propagation model of the trishear zone described in the following section (Mitra, 2002; Erslev and Mayborn, 1997), although deep basement-involved faults described by Eguiluz de Antunano (2001) may be present. This model is one of the hypotheses this research tests.

Structural and Fracture Models

Mitra (2002) and Mitra and Mount (1998) discussed the trishear zone originally proposed by Erslev and Mayborn (1997) to explain observed fracture patterns in asymmetrical anticlines similar to the Sierra San Marcos. This evolution of a fault-propagation fold by the trishear mechanism is shown on **Figure 56**. The trishear zone, when viewed in cross section, is a triangular zone of deformation formed during fault-propagation fold (i.e., when a fold is cored with a fault, in the case of the Cuatrocienegas Basin, a reverse fault under Laramide compressive forces) where the basement is undeformed and the overlying sedimentary cover is highly deformed. Mitra and Mount (1998) present the trishear model for foreland basement-involved structures.

Hennings et al. (2000) combined outcrop data from folded structures in Wyoming (a folded region similar to the Cuatrocienegas Basin region) and evaluate them with three-dimensional structural models to characterize the distribution of fractures associated with these structures. Whereas Hennings et al. (2000) were interested in fracture-related permeability of oil reservoirs, this study investigates if modeled fracture distributions are associated with Cuatrocienegas Basin spring distribution. Hennings et al. (2000) found that predicted fracture intensity associated with an asymmetrical plunging anticline in Wyoming is highest along the steeply plunging limb of the anticline —analogous to the west flank of the Sierra San Marcos.

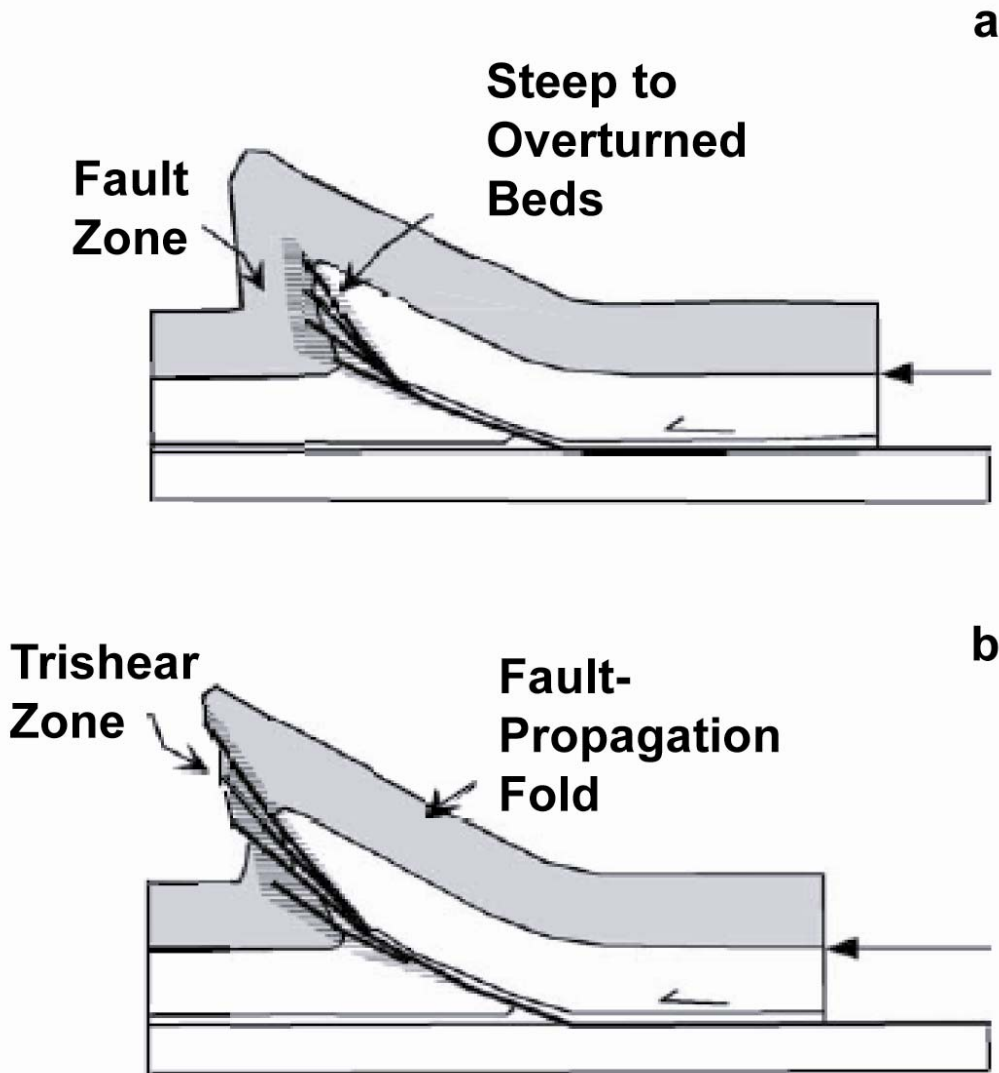


Figure 56. FAULT-PROPAGATION FOLD EVOLUTION BY THE TRISHEAR MECHANISM

The figure is oriented to match the structural style of a west to east cross-section (left to right, respectively) through the Sierra San Marcos (after Mitra, 2002). The labels “b” and “c” presented in Mitra (2002) are presented as “a” and “b” to present an example of the structural style observed in the Cuatrocienegas Basin. The northern Sierra San Marcos is represented by “a” and the southernmost Sierra San Marcos is represented by “b.”

The highest fracture intensity is associated with the trishear zone (Mitra, 2002) on the steeply-dipping side of the Wyoming anticline studied by Hennings et al. (2000). Additional stress is accommodated in a series of fold accommodation strike slip faults off the nose of the anticline in Wyoming. Similarly, fold accommodation faults may be the cause of springs located off the northeast nose of the Sierra San Marcos anticline, such as Poza Azul, Poza Escobedo, and Poza Tío Cándido.

METHODS

Data Collection

Field methods

Survey lines are established roughly perpendicular to the Sierra San Marcos mountain front through regions of high spring density towards the valley center. Gravity data were collected during two field campaigns: January 2006 and March 2006. The location of gravity stations is initially laid out along strike using a 100-meter measuring tape with a station spacing of approximately 100 meters for Poza El Churince and 200 meters for Rancho Pozas Azules, as shown on **Figure 57**. This station spacing is equal to, or less than, the anticipated alluvium depth (Langenheim, pers. comm., 2005). In January 2006, total survey line lengths were approximately one and three kilometers. In March 2006, survey lines totaled approximately fifteen kilometers.

Accurately determining the position of gravity survey stations is essential for later data processing. During the January 2006 survey, a Sokkia SET610 total station is used to determine the coordinates of gravity stations. A Garmin eTrex Vista hand-held GPS unit is used to determine the northing, easting, and elevation averaged using the 1984 World Geodetic System datum and Universal Transverse Mercator zone 13 projection.



Figure 57. SURVEYING GRAVITY STATION LOCATIONS

January 2006 surveys were conducted with a total station. March 2006 gravity station coordinates were determined using a differentially-corrected global positioning system. Kim Nguyen is in the foreground with a Sokkia SET610 total station and Dr. John M. Sharp, Jr. is in the background.

A different method was used to determine the location of March 2006 gravity survey stations. Because the gravity surveys were longer lengths during the March 2006 field campaign compared to January 2006, a Trimble 4000SSI global positioning system was used. The data were post-processed using the Scripps Orbit and Permanent Array Center (SOPAC) website to complete differential corrections (Ghoddousi-Fard and Dare, 2006; Jamason et al., 2004).

The collection of gravity data is accomplished using a LaCoste & Romberg Model G (#G-399; Fett, 1992) gravimeter owned by The University of Texas at Austin Department of Geological Sciences to measure (relative) gravity at survey stations. The four gravity geophysical survey lines are shown on **Figure 58**. A photo of a typical gravity station is shown on **Figure 59**. To evaluate gravity meter performance and identify possible meter drift or tare (i.e., an abrupt change in the readings often caused by the gravity meter being jarred or bumped), base station data are collected twice daily. The base station is approximately 2 kilometers north of the Town of Cuatrocienegas (**Figure 49**) and is shown on **Figure 60**. Relative gravity data were tied to absolute gravity by measuring gravity before and after the survey at the Austin AA International Gravity Standardization Net 1971 absolute gravity reference site located on the campus of The University of Texas at Austin in the basement of Robert Lee Moore Hall (Peter et al., 1991). The site is located at latitude $30^{\circ} 17' 30.5''$ N and longitude $97^{\circ} 44' 10.9''$ W at an elevation of 162 meters and has an absolute gravity value of $979,277.614 \pm 0.005$ milligals.

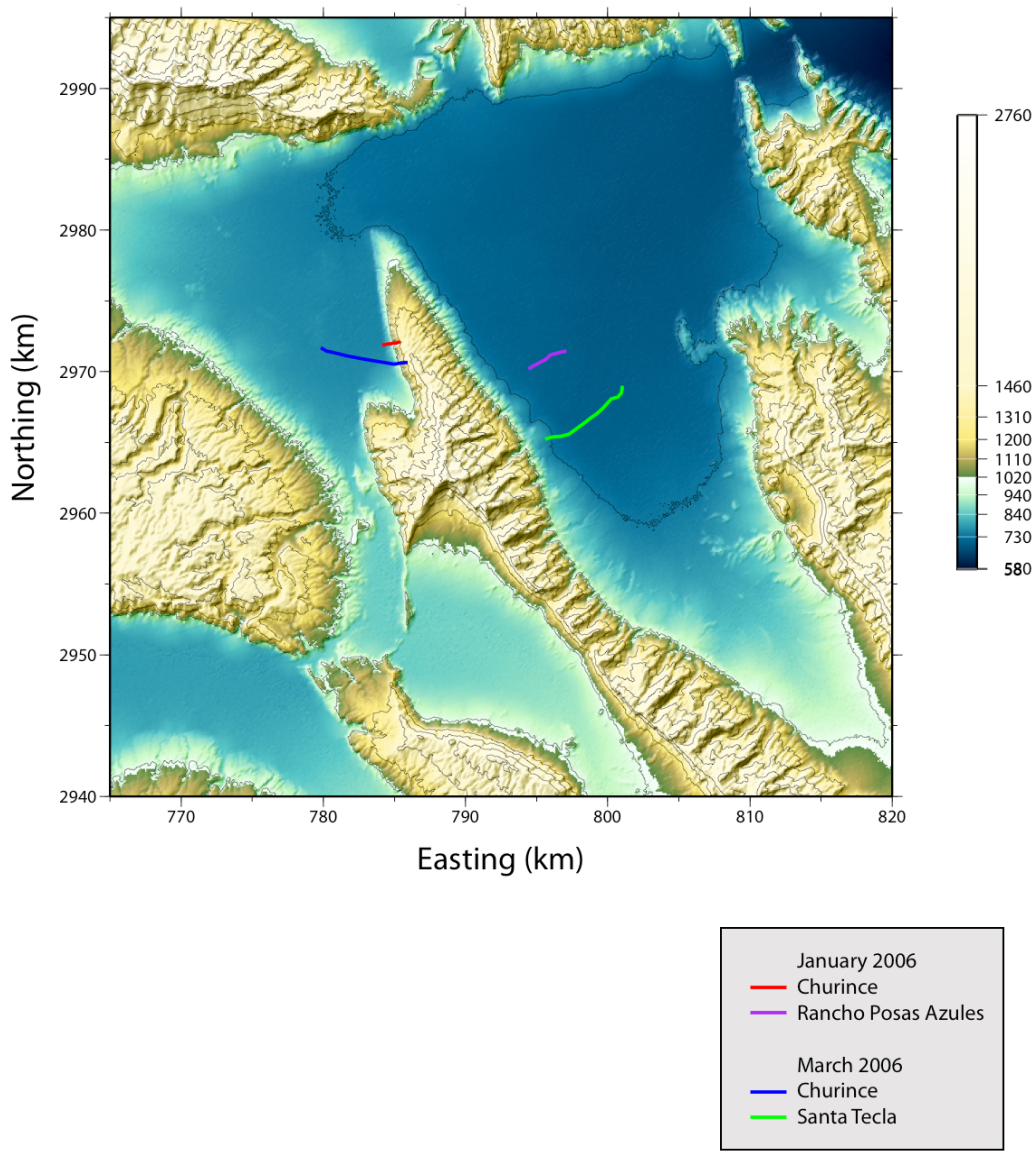


Figure 58. GRAVITY SURVEY LOCATIONS WITH SHADED DIGITAL ELEVATION MODEL

The mountain range in the center of the figure is the Sierra San Marcos. The figure generated by Theresa Diehl.



Figure 59. COLLECTING GRAVITY DATA

Theresa Diehl collects gravity data using a LaCoste and Romberg G-meter set up beneath a total station tripod on the Rancho Pozas Azules line on the east flank of the Sierra San Marcos (background). The Rancho Pozas Azules survey area is indicated by the northern-most line on the east flank of the Sierra San Marcos Figure 58.



Figure 60. MEASURING BASE STATION GRAVITY

Base station data are collected twice daily to evaluate gravity meter performance. The base station is located approximately 2 kilometers north of the Town of Cuatrocienegas (Figure 49).

Error

The primary source of error in gravity surveys is caused by the gravity meter operator and uncertainties in elevation. To reduce error introduced by inaccuracies because of the operator, at least three gravity measurements are conducted at each station. Fournier et al. (2004) stated that the effects of uncertainty in the digital elevation model used for terrain correction (described in the subsequent section) were a large source of error. Survey elevations are determined using a total station and DGPS to minimize elevation errors.

Elevation uncertainty, for both Total Station and DGPS, is probably in the order of a few centimeters. A one-centimeter change in elevation creates a 0.003086-milligal difference in the Bouguer Anomaly (Nettleton, 1971). Because the gravity meter precision is approximately \pm one milligal, an elevation error of a few centimeters is negligible.

Data Reduction

Relative gravity measured by a meter is a function of factors that include gravitational pull of Sun and Moon on the shape of the Earth, gravity meter drift, latitude, and elevation. Gravity data processing applies corrections for known topography so that only the effects of density differences remain. The result of processing is a complete, terrain-corrected Bouguer gravity anomaly. A summary of the primary corrections used herein were described in detail by Telford et al. (1990) and Nettleton (1971).

Instrument Scale Factor

The spring of a gravimeter varies between devices (Fett, 1992). As a result, each device has unique calibration factor, called an instrument scale factor, that converts the unique counter units of a meter into relative gravity (measured in milligals).

The instrument scale factor is

$$r_c = rS(r) . \quad (39)$$

Where

r_c = corrected reading in milligals

r = instrument reading in counter units

$S(r)$ = scale factor (milligal/counter units)

Tide Correction

The gravitational pull of sun and moon distorts the shape of the Earth (known as an Earth tide) and causes an approximately 0.3 milligal variation in gravity. This error is corrected knowing the location of the sun and moon (at 2-hour, 24-hour, 14-day, and 6-month cycles) with

$$r_t = r_c + g_{tide} . \quad (40)$$

Where

r_t = tide corrected reading,

r_c = scale corrected reading, and

g_{tide} = tide correction.

As the precision of the gravity meter used in this study is approximately one milligal (Wilson, 2005, pers. com.), the tide correction is insignificant and an explicit correction was not applied.

Instrument Height

The elevation of gravimeter above the station causes an approximately 0.3 milligal error/meter. This error is subtracted from the data using

$$r_h = r_t + 0.308596h_i . \quad (41)$$

Where

r_h = instrument height corrected reading,

r_t = tide corrected reading, and

h_i = instrument height in meters.

Absolute Gravity

The relative gravity reading from the gravity meter is converted to absolute gravity value for a station using

$$g_a = g_{B1} + (r_h - r_{B1}) - (t - t_{B1})d . \quad (42)$$

Where

g_a = absolute gravity in milligals,

g_{B1} = base 1 absolute gravity in milligals,

r_h = instrument height corrected reading,

r_{B1} = base 1 reading,

t = reading time,

t_{B1} = base 1 time, and

d = drift (milligals/hour).

In this study, the Austin AA reference site is used for absolute gravity calculations (see Peter et al., 1991 for additional information).

Drift Correction

Gravity meters are subject to an elastic spring creep that may cause an apparent change of gravity at a given location with time. To identify and remove this error, repeated measurements are taken at one station (referred to as a base station). Drift varies from a fraction of a milligal to 10s of milligals and is removed using the formula

$$d = \frac{(r_{B2} - r_{B1}) - (g_{B2} - g_{B1})}{t_{B2} - t_{B1}}. \quad (43)$$

Where

d = drift in milligals/hour,

r_{B1} = base 1 reading,

t_{B1} = base 1 time,

g_{B1} = base 1 absolute gravity in milligals,

r_{B2} = base 2 reading,

t_{B2} = base 2 time, and

g_{B2} = base 2 absolute gravity in milligals.

Meter drift is quantified by taking repeat measurements at a base station. In this survey, the base station is a field research station located at approximately 27.00°north latitude and 102.07°west longitude.

Latitude Correction

The shape of the Earth and centrifugal acceleration are a function of latitude (Reynolds, 1997). These differences cause a maximum error of approximately 0.01 milligal/13 meters at 45° latitude. This error decreases towards the poles. The latitude correction is done using the formula (Telford et al., 1990)

$$g_l = 9780327 [1 + 0.0053024 \sin^2(l) - 0.0000058 \sin^2(2l)] . \quad (44)$$

Where

g_l = theoretical gravity in milligals (latitude correction), and

l = latitude of station.

Free Air Anomaly

Nettleton (1976) accounted for the fact that gravity measurement are not made at sea level. Thus, the gravity field is influenced by elevation and gravity decreases at a rate of the inverse square of distance. Telford et al. (1990) added gravity if a station above a datum and subtracts gravity if a station is below a datum at 0.3086 milligal/meter using the formula

$$g_{fa} = g_a - g_l + 0.308596h_s . \quad (45)$$

Where

g_{fa} = free air anomaly in milligals,

g_a = absolute gravity,

g_l = latitude correction, and

h_s = station elevation in meters.

Thus, small elevation differences can cause relatively large deviations in gravity compared to the anomaly of interest.

Digital Elevation Model

Terrain corrections are done using a high resolution (3-arc second) digital elevation model produced by the National Aeronautics and Space Administration shuttle radar topography mission described by Hall et al. (2005). Null data points in the digital elevation model are filled using a spline interpolation routine. The digital elevation model extends approximately 10 kilometers outside of the survey area. The digital elevation

model is projected to Universal Transverse Mercator Projection (North America Zone 13) and resampled to 100-square meter resolution for the Bouguer correction.

Bouguer Anomaly

A Bouguer anomaly is calculated by filling in “air” between sea level and station elevation with an infinite slab of rock with a known density (Nettleton, 1976). The gravitational pull because of this rock (or water or ice) mass is calculated by

$$g_{ba} = g_{fa} - 0.0419088 [\rho h_s + (\rho_w - \rho)h_w + (\rho_i - \rho_w)h_i] + g_{curv}. \quad (46)$$

Where

g_{ba} = Bouguer anomaly in milligals,

g_{fa} = free air anomaly,

ρ = Bouguer density of rock in grams/cubic centimeter,

ρ_w = Bouguer density of water in grams/cubic centimeter,

ρ_i = Bouguer density of ice in grams/cubic centimeter,

h_s = station elevation in meters,

h_w = water depth in meters,

h_i = ice thickness in meters, and

g_{curv} = curvature correction (infinite slab to spherical cap, LaFehr, 1991).

A rock density of 2.67 grams/cubic centimeter is assumed for this calculation. The Bouguer Anomaly is approximately equal to 0.4193 milligal/meter.

Complete Bouguer Anomaly

The assumption of an infinite slab is made more realistic by adding bumps (extra mass) and pits (missing mass) to a horizontal slab based on the topography described in the digital elevation model section. Hammer (1939) developed a graphical method to calculate this correction. This research uses the Gaussian-Legendre Quadrature method to calculate both the slab and terrain corrections for a complete Bouguer correction (von Frese et al., 1981).

Data Modeling

Conceptual geologic cross sections are generated by calculating the Bouguer gravity anomaly and fitting the data with a simple geologic model that is comprised of alluvium overlying carbonate. The hypothetical cross sections are tested by visual inspection of the profiles to infer which of the three hypotheses most closely matches the inverse geologic model created from field data.

The GM-SYS software geophysical processing and analysis module of the Geosoft Oasis Montage software package (Geosoft Inc., 2001) is used to create an inverse geologic model that best fits the measured data. GM-SYS uses the Talwani algorithm to calculate a curve of the residual Bouguer gravity anomaly using a line integration method that represents the gravitational response because of modeled subsurface geology (Northwest Geophysical Associates, Inc., 2004; Talwani et al., 1959). The Bouguer anomaly of the model is a function of (1) density differences between background and body (e.g., alluvium and carbonate rock), (2) geometry of body defined by vertices, and (3) location at which gravitational response is calculated (Telford et al., 1990; Nettleton, 1971).

Alluvial and carbonate thickness, density, and geometry are changed manually to create a geologically-plausible, non-unique, best-fit model with a resulting gravity

anomaly that most closely matches observed data and honors expected structural style. This study uses typical rock density values presented in Telford et al. (1990).

RESULTS

No reference station is located near the Cuatrocienegas Basin. Furthermore, The University of Texas at Austin Department of Geological Sciences building does not have a reference station. The closest reference station is the Austin (Texas) AA reference station at The University of Texas at Austin. Therefore, gravity data collected at the Austin (Texas) AA reference station are used to calibrate the gravity meter to absolute gravity (**Table 32**). Base station drift measurements are summarized in **Table 33** to **Table 35**.

Raw and Processed Gravity Data

Raw and processed gravity survey data are shown in **Table 36** to **Table 39**. Raw gravity data are shown in counter units (CU). The instrument scale factor is applied to calculate raw gravity (milligals). The raw gravity value is converted to absolute gravity in milligals. Drift and latitude corrections are applied to the absolute gravity value, yielding the free air anomaly. The Bouguer correction is calculated to subtract terrain effects and the Bouguer anomaly is used for data modeling.

Best Fit Geological Models

This section presents the best fit geological models for the four land gravimetry surveys. The first set of two surveys is for springs on the west and north flank of the Sierra San Marcos conducted in January 2006 and March 2006 in the vicinity of Poza Churince. The second set of two surveys is for springs on the east flank of the Sierra San Marcos conducted in January 2006 at Rancho Pozas Azules and March 2006 at Santa Tecla.

Table 32. GRAVITY METER CALIBRATION TO ABSOLUTE GRAVITY

The LaCoste Romberg gravity meter used in this survey is calibrated to absolute gravity using the Austin AA reference site located at The University of Texas at Austin campus in the basement of Robert Lee Moore Hall (Peter et al., 1991). The Absolute Gravity Correction is added to relative gravity (milligals) data collected during the survey to convert the values to absolute gravity (milligals). The two correction values (Jan. 6 and Jan. 17, 2006) are approximately 0.5 milligals different (within the approximately one milligal error of the meter). The January 6, 2006 correction is used in this survey. The Austin AA reference site value for absolute gravity is 979277.614 milligals (Peter et al., 1991).

Date	Relative Gravity Measured at Austin AA Reference Site [CU]	Relative Gravity Measured at Austin AA Reference Site [mGals]
January 6, 2006	2,779.14	2,896.55
	2,778.48	2,895.86
	2,778.16	2,895.53
	Average:	2,895.98
Absolute Gravity Correction:		976,381.64
January 17, 2006	2,779.17	2,896.58
	2,778.74	2,896.13
	2,778.92	2,896.32
	Average:	2,896.34
Absolute Gravity Correction:		976,381.27

Table 33. BASE STATION DRIFT MEASUREMENTS, JANUARY 2006 SURVEY

Base station drift measurements and daily averages are shown. The meter drift is within the approximately one-milligal error of the meter.

Date	Relative Gravity [CU]	Relative Gravity [mGals]	Absolute Gravity [mGals]
January 8, 2006 PM	2,358.48	2,457.76	978,839.40
	2,358.42	2,457.70	978,839.34
	2,358.18	2,457.45	978,839.09
	Average:	2,358.36	2,457.64
January 9, 2006 AM	2,358.88	2,458.18	978,839.82
	2,358.42	2,457.70	978,839.34
	2,358.43	2,457.71	978,839.35
	Average:	2,358.58	2,457.86
January 9, 2006 PM	2,358.59	2,457.88	978,839.52
	2,358.62	2,457.91	978,839.55
	2,358.01	2,457.27	978,838.91
	Average:	2,358.41	2,457.69
January 10, 2006 AM	2,358.79	2,458.09	978,839.72
	2,358.69	2,457.98	978,839.62
	2,358.58	2,457.87	978,839.50
	Average:	2,358.69	2,457.98
All measurements	Average:	2,358.51	2,457.79
			978,839.43

Table 34. BASE STATION DRIFT MEASUREMENTS, MARCH 2006 SURVEY, PART 1 OF 2
 (Table is continued on subsequent page)

Date	Relative Gravity [CU]	Relative Gravity [mGals]	Absolute Gravity [mGals]
January 12, 2006 AM	2,359.28	2,458.60	978,840.23
	2,359.26	2,458.58	978,840.21
	2,359.35	2,458.67	978,840.31
	Average:	2,359.30	2,458.62
January 12, 2006 PM	2,359.15	2,458.46	978,840.10
	2,359.09	2,458.40	978,840.04
	2,359.10	2,458.41	978,840.05
	Average:	2,359.11	2,458.42
January 13, 2006 AM	2,359.78	2,459.12	978,840.76
	2,359.87	2,459.21	978,840.85
	2,359.88	2,459.22	978,840.86
	Average:	2,359.84	2,459.19
January 13, 2006 PM	2,359.18	2,458.49	978,840.13
	2,359.47	2,458.80	978,840.43
	2,359.01	2,458.32	978,839.95
	Average:	2,359.22	2,458.54
January 14, 2006 AM	2,359.69	2,459.03	978,840.66
	2,358.87	2,458.17	978,839.81
	2,358.85	2,458.15	978,839.79
	Average:	2,359.14	2,458.45
January 14, 2006 PM	2,359.63	2,458.96	978,840.60
	2,359.74	2,459.08	978,840.71
	2,359.65	2,458.98	978,840.62
	Average:	2,359.67	2,459.01

Table 35. BASE STATION DRIFT MEASUREMENTS, MARCH 2006 SURVEY, PART 2 OF 2
(Continued)

The gravity meter experiences a minor (approximately 1.50 milligals) positive drift some time after the March 17 PM reading was taken. Only point C204 was affected and this correction is applied to the data.

Field House	Relative Gravity [CU]	Relative Gravity [mGals]	Absolute Gravity [mGals]
January 15, 2006 AM	2,359.71	2,459.05	978,840.68
	2,359.71	2,459.05	978,840.68
	2,359.83	2,459.17	978,840.81
	2,359.54	2,458.87	978,840.51
Average:		2,459.03	978,840.67
January 15, 2006 PM	2,359.84	2,459.18	978,840.82
	2,359.95	2,459.30	978,840.93
	2,359.91	2,459.25	978,840.89
	Average:		978,840.88
January 16, 2006 AM	2,359.76	2,459.10	978,840.74
	2,359.92	2,459.27	978,840.90
	2,359.65	2,458.98	978,840.62
	Average:		978,840.75
January 17, 2006 AM	2,359.74	2,459.08	978,840.71
	2,359.76	2,459.10	978,840.74
	2,359.77	2,459.11	978,840.75
	Average:		978,840.73
January 18, 2006 AM	2,361.08	2,460.47	978,842.11
	2,361.18	2,460.58	978,842.22
	2,360.80	2,460.18	978,841.82
	Average:		978,842.05
All measurements	Average:	2,359.68	2,459.01
			978,840.65

Table 36. RAW AND PROCESSED GRAVITY SURVEY DATA, RANCHO POZAS AZULES, JANUARY 2006

Station ID	UTM Northing [m]	UTM Easting [m]	Elevation [m]	Raw Gravity [CU]	Raw Gravity [mGals]	Absolute Gravity [mGals]	Free Air Anomaly [mGals]	Bouguer Correction [mGals]	Bouguer Anomaly [mGals]
RPA106	2,970,185	794,410	727.39	2,359.06	2,458.36	978,840.00	-20.37	18.92	-39.29
RPA108	2,970,291	794,585	725.31	2,359.43	2,458.75	978,840.39	-20.69	18.62	-39.31
RPA110	2,970,392	794,760	724.60	2,361.26	2,460.67	978,842.30	-19.06	18.36	-37.42
RPA112	2,970,493	794,935	724.25	2,359.54	2,458.87	978,840.51	-21.03	18.11	-39.14
RPA114	2,970,579	795,118	724.13	2,358.96	2,458.26	978,839.90	-21.73	17.89	-39.62
RPA116	2,970,682	795,293	723.35	2,359.25	2,458.57	978,840.20	-21.73	17.68	-39.41
RPA118	2,970,773	795,472	721.43	2,359.45	2,458.78	978,840.42	-22.17	17.49	-39.66
RPA120	2,970,867	795,648	720.95	2,358.95	2,458.25	978,839.89	-22.90	17.32	-40.22
RPA122	2,971,004	795,793	719.16	2,359.42	2,458.75	978,840.38	-23.04	17.16	-40.21
RPA124	2,971,145	795,936	719.54	2,359.00	2,458.31	978,839.94	-23.46	17.02	-40.48
RPA126	2,971,223	796,120	719.59	2,358.83	2,458.13	978,839.76	-23.67	16.90	-40.57
RPA128	2,971,271	796,314	718.69	2,359.12	2,458.43	978,840.07	-23.67	16.79	-40.45
RPA130	2,971,320	796,509	717.88	2,359.33	2,458.65	978,840.29	-23.73	16.69	-40.42
RPA132	2,971,371	796,703	717.29	2,359.03	2,458.34	978,839.97	-24.26	16.60	-40.85
RPA134	2,971,416	796,899	716.44	2,359.04	2,458.35	978,839.99	-24.53	16.52	-41.05
RPA136	2,971,471	797,090	716.65	2,358.91	2,458.21	978,839.85	-24.64	16.44	-41.08

Table 37. RAW AND PROCESSED GRAVITY SURVEY DATA, SANTA TECLA, MARCH 2006

Station ID	UTM Northing [m]	UTM Easting [m]	Elevation [m]	Raw Gravity [CU]	Raw Gravity [mGals]	Absolute Gravity [mGals]	Free Air Anomaly [mGals]	Bouguer Correction [mGals]	Bouguer Anomaly [mGals]	
ST201	2,965,241	795,600	841.07	2,326.98	2,424.92	978,805.48	-16.55	22.82	-39.38	
ST202	2,965,399	796,142	797.86	2,336.09	2,434.41	978,814.97	-20.49	21.38	-41.87	
ST203	2,965,426	796,654	765.58	2,342.35	2,440.94	978,821.50	-23.93	20.35	-44.29	
ST204	2,965,572	797,271	726.18	2,350.09	2,449.01	978,829.57	-28.11	19.24	-47.35	
ST206	2,966,434	798,430	688.40	2,356.14	2,455.32	978,835.88	-34.01	17.48	-51.49	
ST207	2,966,641	798,724	688.14	2,355.92	2,455.09	978,835.65	-34.46	17.19	-51.65	
243	ST208	2,967,017	799,295	685.94	2,356.32	2,455.51	978,836.07	-34.97	16.77	-51.74
	ST209	2,967,305	799,621	685.25	2,356.25	2,455.44	978,836.00	-35.45	16.57	-52.02
	ST210	2,967,672	799,945	685.31	2,356.00	2,455.17	978,835.73	-35.95	16.39	-52.34
	ST211	2,967,996	800,271	685.01	2,356.24	2,455.42	978,835.98	-36.01	16.27	-52.27
	ST212	2,968,077	800,719	685.10	2,356.37	2,455.57	978,836.13	-35.89	16.18	-52.07
	ST213	2,968,366	800,976	685.09	2,356.55	2,455.75	978,836.31	-35.91	16.12	-52.03
	ST214	2,968,869	801,013	684.87	2,356.78	2,455.99	978,836.55	-36.07	16.07	-52.14

Table 38. RAW AND PROCESSED GRAVITY SURVEY DATA, CHURINCE, JANUARY 2006

Station ID	UTM Northing [m]	UTM Easting [m]	Elevation [m]	Raw Gravity [CU]	Raw Gravity [mGals]	Absolute Gravity [mGals]	Free Air Anomaly [mGals]	Bouguer Correction [mGals]	Bouguer Anomaly [mGals]	
CHU101	2,972,123	785,407	858.49	2,319.46	2,417.07	978,798.71	-22.61	22.84	-45.45	
CHU102	2,972,089	785,325	835.82	2,324.50	2,422.33	978,803.97	-24.33	22.70	-47.03	
CHU103	2,972,062	785,222	813.62	2,329.01	2,427.03	978,808.67	-26.47	22.53	-48.99	
CHU104	2,972,032	785,127	798.42	2,332.33	2,430.50	978,812.13	-27.67	22.36	-50.03	
CHU105	2,972,019	785,026	786.57	2,335.08	2,433.37	978,815.00	-28.45	22.19	-50.64	
CHU106	2,972,010	784,927	775.15	2,337.45	2,435.83	978,817.47	-29.51	22.01	-51.52	
244	CHU107	2,971,994	784,826	770.58	2,338.30	2,436.72	978,818.35	-30.02	21.84	-51.86
	CHU108	2,971,975	784,727	769.96	2,337.77	2,436.16	978,817.80	-30.75	21.68	-52.44
	CHU109	2,971,960	784,628	770.36	2,337.44	2,435.82	978,817.46	-30.97	21.52	-52.49
	CHU110	2,971,947	784,529	770.00	2,337.48	2,435.86	978,817.50	-31.03	21.37	-52.39
	CHU111	2,971,926	784,432	769.88	2,337.19	2,435.57	978,817.20	-31.35	21.22	-52.57
	CHU112	2,971,909	784,333	769.75	2,337.47	2,435.85	978,817.49	-31.09	21.07	-52.16
	CHU113	2,971,888	784,234	769.96	2,337.31	2,435.69	978,817.33	-31.18	20.93	-52.11
	CHU114	2,971,868	784,134	769.72	2,337.44	2,435.83	978,817.46	-31.11	20.80	-51.90

Table 39. RAW AND PROCESSED GRAVITY SURVEY DATA, CHURINCE, MARCH 2006

Station ID	UTM Northing [m]	UTM Easting [m]	Elevation [m]	Raw Gravity [CU]	Raw Gravity [mGals]	Absolute Gravity [mGals]	Free Air Anomaly [mGals]	Bouguer Correction [mGals]	Bouguer Anomaly [mGals]
CHU201	2,970,661	785,935	864.61	2,309.04	2,406.21	978,786.77	-31.70	24.44	-56.14
CHU202	2,970,624	785,460	777.48	2,331.94	2,430.09	978,810.65	-34.69	23.48	-58.16
CHU203	2,970,507	784,995	764.87	2,335.44	2,433.74	978,814.30	-34.86	22.63	-57.49
CHU207	2,970,914	782,626	748.31	2,336.82	2,435.18	978,815.74	-38.83	19.42	-58.25
CHU208	2,971,015	782,161	747.57	2,335.66	2,433.96	978,814.52	-40.35	19.05	-59.40
CHU209	2,971,123	781,669	748.82	2,335.26	2,433.55	978,814.11	-40.45	18.73	-59.19
245	CHU210	2,971,226	781,202	748.93	2,334.07	978,812.87	-41.73	18.51	-60.24
	CHU212	2,971,338	780,693	748.16	2,333.01	978,811.76	-43.16	18.33	-61.49
	CHU213	2,971,441	780,250	749.64	2,332.59	978,811.33	-43.21	18.22	-61.43
	CHU214	2,971,683	779,817	749.46	2,332.69	978,811.43	-43.33	18.11	-61.44

The best fit geologic models for each of the four gravity surveys (**Table 36** to **Table 39**) are shown on **Figure 61** to **Figure 64**. In each of these figures, the dots in the upper panel are Bouguer gravity anomalies calculated from data collected in the field. The line in the upper panel is the best fit determined by visual inspection by the analyst of the geologic model shown in the lower panel. Gravity-based geologic models are non-unique because different variations in the number of model layers, density values, and orientations produce an identical residual Bouguer anomaly. The best fit is an informed decision based upon the known hydrogeology, structure, and lithology of the area that generates Bouguer anomaly consistent with the data.

Springs on the West and North Flank of the Sierra San Marcos

This section presents the results of gravity surveys for springs on the west and north flank of the Sierra San Marcos.

January 2006 Churince Survey

The residual Bouguer gravity anomaly and best-fit inverse geologic model for the January 2006 Churince results from a two layer valley fill alluvium on the west and east flank of the Sierra San Marcos with a total depth of approximately 400 meters divided into two layers of approximately 200 meters each. The best fit geologic model for the January 2006 Churince gravity data is shown on **Figure 61**. The upper layer has a density of 1.8 grams/cubic centimeter and the slightly more consolidated lower layer has a density of 2.0 grams/cubic centimeter. A 200 meter-thick wedge-shaped alluvial fan has a density of 1.9 grams/cubic centimeter. A granodiorite with a density of 2.67 grams/cubic centimeter forms the basement. All density values follow Telford et al. (1990).

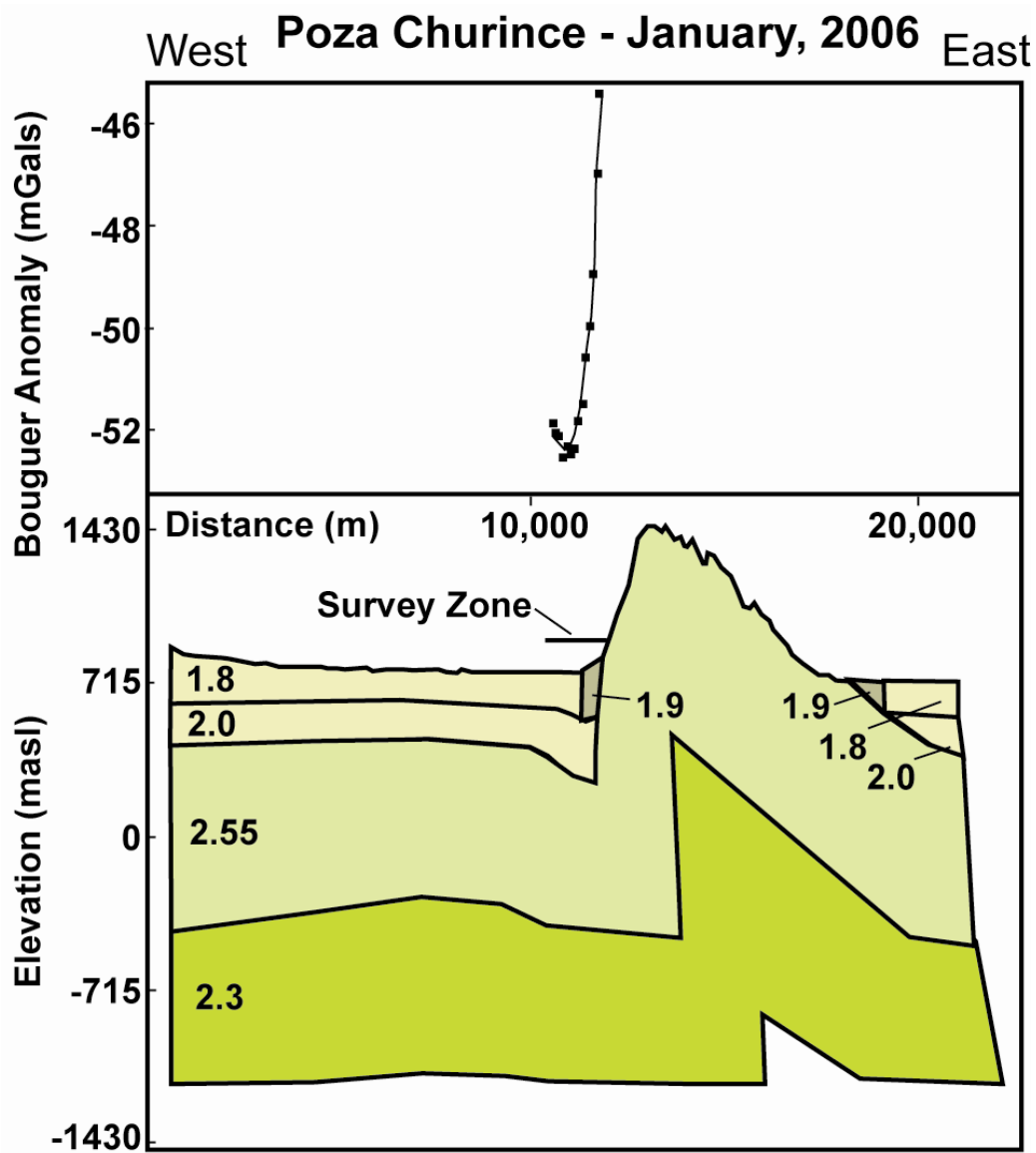


Figure 61. BEST FIT GEOLOGIC MODEL AND JANUARY 2006 CHURINCE GRAVITY DATA

In the bottom panel, the geologic formations are (from bottom–top): granodiorite (not shown), conglomerate, carbonate, two layers of valley fill alluvium, and alluvial fan. Rock density values are labeled in grams/cubic centimeter, based on typical rock densities presented in Telford et al. (1990). The granodiorite layer in all cases is assumed to have a density of 2.67 grams/cubic centimeter. In the top panel, residual Bouguer gravity anomalies are shown as small solid squares and best fit inverse model results are shown as a solid line. The triangular geometry in the conglomerate represents the fracture zone associated with reverse faulting.

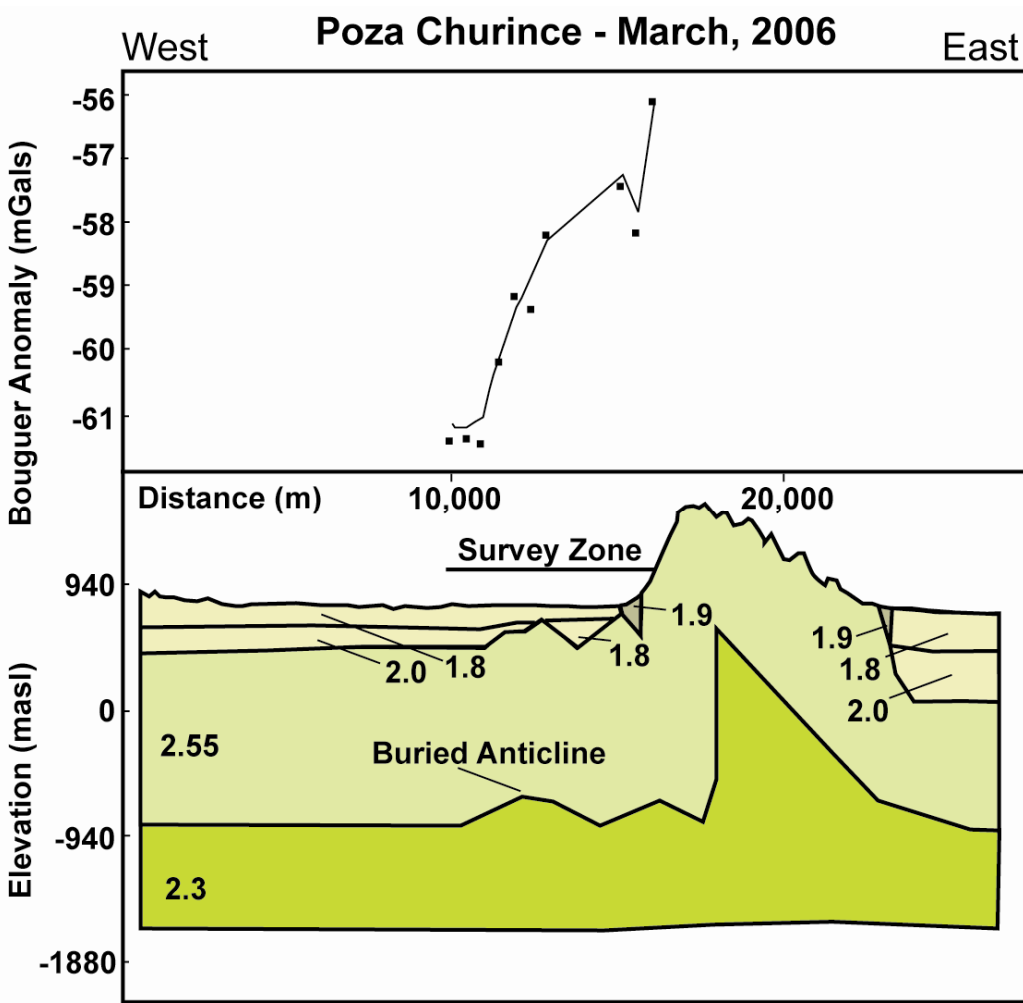


Figure 62. BEST FIT GEOLOGIC MODEL AND MARCH 2006 CHURINCE GRAVITY DATA

In the bottom panel, the geologic formations are (from bottom–top): granodiorite (not shown), conglomerate, carbonate, two layers of valley fill alluvium, and alluvial fan. Rock density values are labeled in grams/cubic centimeter, based on typical rock densities presented in Telford et al. (1990). The granodiorite layer in all cases is assumed to have a density of 2.67 grams/cubic centimeter. In the top panel, residual Bouguer gravity anomalies are shown as small solid squares and best fit inverse model results are shown as a solid line. The triangular geometry in the conglomerate represents the fracture zone associated with reverse faulting. A buried anticline is present to the west of the Sierra San Marcos. This feature is a northern extension of an anticline that crops out to the west of the Sierra San Marcos that is south of this survey line, as shown on Figure 58. This anticline does not have springs directly above it.

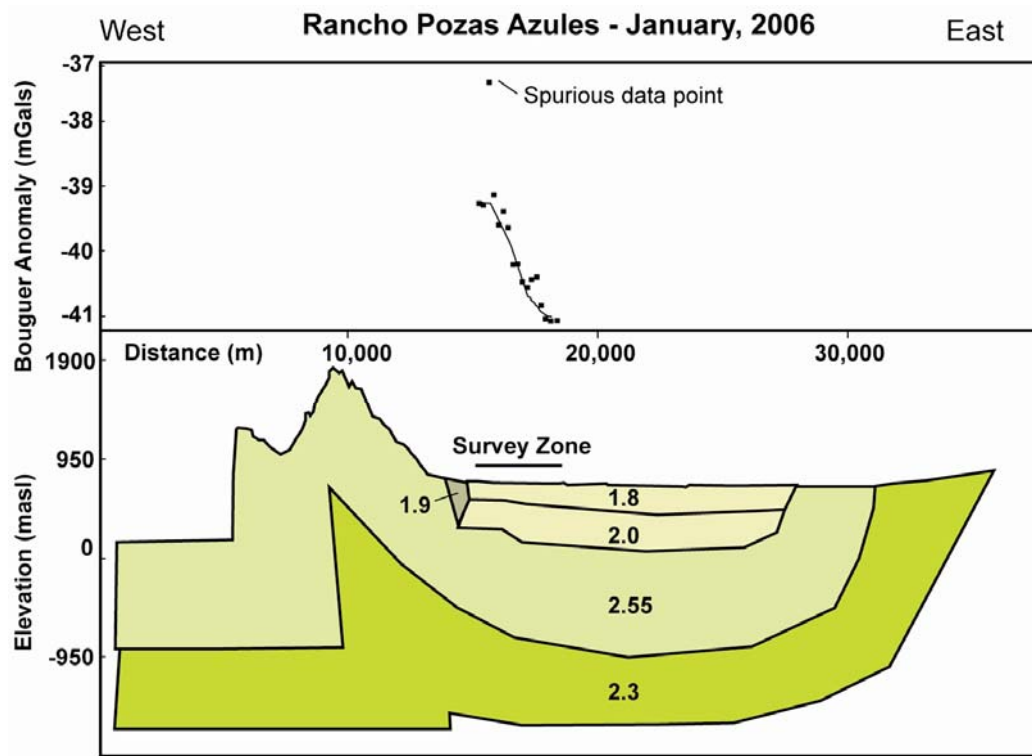


Figure 63. BEST FIT GEOLOGIC MODEL AND JANUARY 2006 RANCHO POZAS AZULES GRAVITY DATA

In the bottom panel, the geologic formations are (from bottom–top): granodiorite (not shown), conglomerate, carbonate, two layers of valley fill alluvium, and alluvial fan. Rock density values are labeled in grams/cubic centimeter, based on typical rock densities presented in Telford et al. (1990). The granodiorite layer in all cases is assumed to have a density of 2.67 grams/cubic centimeter. In the top panel, residual Bouguer gravity anomalies are shown as small solid squares and best fit inverse model results are shown as a solid line. The triangular geometry in the conglomerate represents the fracture zone associated with reverse faulting. The valley to the east of the Sierra San Marcos is a synclinal structure. Survey data do not show the presence of faulting to the east of the Sierra San Marcos.

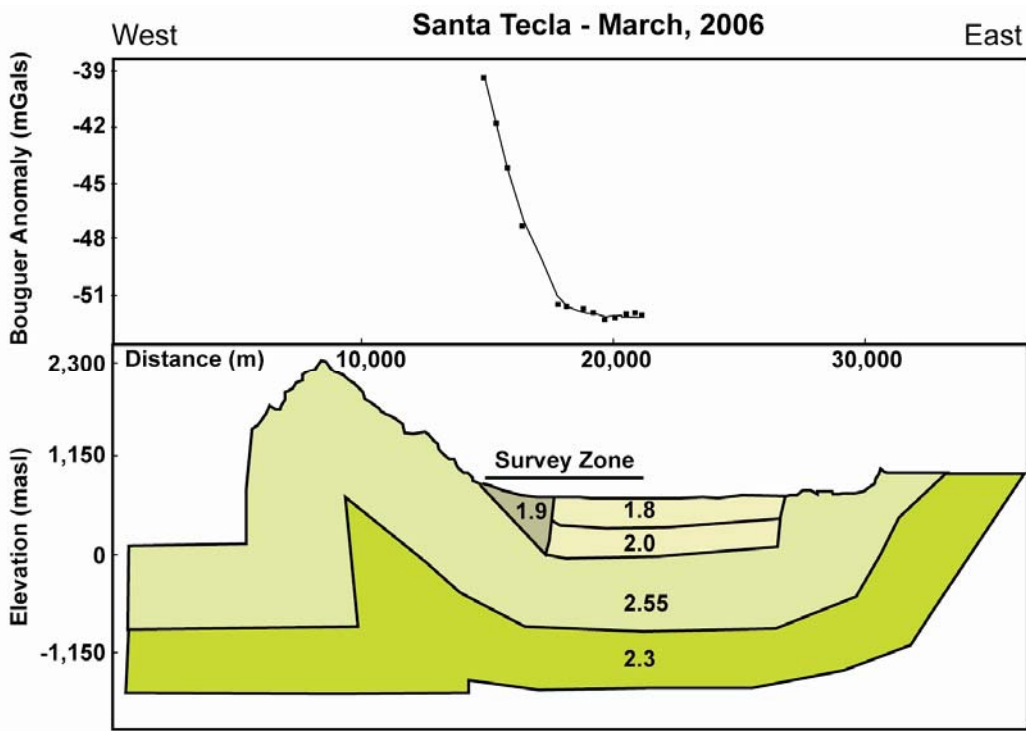


Figure 64. BEST FIT GEOLOGIC MODEL AND MARCH 2006 SANTA TECLA GRAVITY DATA

In the bottom panel, the geologic formations are (from bottom–top): granodiorite (not shown), conglomerate, carbonate, two layers of valley fill alluvium, and alluvial fan. Rock density values are labeled in grams/cubic centimeter, based on typical rock densities presented in Telford et al. (1990). The granodiorite layer in all cases is assumed to have a density of 2.67 grams/cubic centimeter. In the top panel, residual Bouguer gravity anomalies are shown as small solid squares and best fit inverse model results are shown as a solid line. The triangular geometry in the conglomerate represents the fracture zone associated with reverse faulting. The valley to the east of the Sierra San Marcos is a synclinal structure. Survey data do not show the presence of faulting to the east of the Sierra San Marcos.

The residual Bouguer gravity anomaly for Poza El Churince and the best-fit model varies from approximately -46 to -52 milligals. The structure of the best-fit model in all cases honors field observations and also expected structure at depth based on the literature presented in the Introduction. In the case of Poza Churince, the best-fit model agrees with the data only when a slightly thicker valley fill alluvium layer is present next the west flank of the Sierra San Marcos.

March 2006 Churince Survey

The residual Bouguer gravity anomaly and best-fit inverse geologic model for the March 2006 Churince results from a two-layer valley fill alluvium on the west flank of the Sierra San Marcos with a total depth of approximately 400 meters divided into two layers of approximately 200 meters each. Note that this is thicker than the 200-meter valley-fill alluvium depth suggested by Rodríguez et al. (2005a). The best fit geologic model for the March 2006 Churince gravity data is shown on **Figure 62**.

The upper layer has a density of 1.8 grams/cubic centimeter and the slightly more consolidated lower layer has a density of 2.0 grams/cubic centimeter. An approximately 300-meter thick, wedge-shaped, alluvial fan has a density of 1.9 grams/cubic centimeter. A granodiorite with a density of 2.67 grams/cubic centimeter forms the basement. An approximately 700-meter thick clastic package and approximately 1000-meter thick carbonate units with densities of 2.3 grams/cubic centimeter and 2.55 grams/cubic centimeter, respectively, overly the granodiorite. The residual Bouguer gravity anomaly for Poza El Churince and the best-fit model varies from approximately -56 to -61 milligal. The structure of the best-fit model for the March 2006 Churince survey is very similar to that of January 2006.

Springs on the East Flank of the Sierra San Marcos

Two different gravity lines were conducted on the east flank of the Sierra San Marcos, one at Rancho Pozas Azules and one at Santa Tecla (**Figure 58**).

Rancho Pozas Azules

The residual Bouguer gravity anomaly and best-fit inverse geologic model for the January 2006 Rancho Pozas Azules survey results differ from west flank of the Sierra San Marcos surveys. A synclinal structure controls the model with two layers of valley fill alluvium (a total depth of approximately 700 meters, comprised of two layers approximately 350-meter thick with upper and lower layer densities of 1.8 grams/cubic centimeter and 2.0 grams/cubic centimeter, respectively). Note the valley fill alluvium is thicker than the 200-meter alluvium depth suggested by Rodríguez et al. (2005a).

The best fit geologic model for the January 2006 Rancho Pozas Azules gravity data is shown on **Figure 63**. An approximately 700-meter thick, wedge-shaped, alluvial fan has a density of 1.9 grams/cubic centimeter. The alluvial fans that form on the east flank of the Sierra San Marcos can be seen on the shaded topographic relief map on **Figure 58**. The basement is granodiorite with a density of 2.67 grams/cubic centimeter and is overlain by an approximately 700-meter thick clastic package and approximately 1000-meter thick carbonate units with densities of 2.3 grams/cubic centimeter and 2.55 grams/cubic centimeter, respectively.

The residual Bouguer gravity anomaly for the January 2006 Rancho Pozas Azules survey and the best-fit model varies from approximately -39 to -41 milligal. A spurious data point with a residual Bouguer gravity anomaly of approximately -37.5 milligals is not included in the model.

Santa Tecla

The residual Bouguer gravity anomaly and best-fit inverse geologic model for the March 2006 Santa Tecla survey has a similar structural style to the Rancho Pozas Azules line. A synclinal structure controls the model. Two layers of valley fill alluvium occur with a total depth is approximately 700 meters. Two layers with a total thickness of approximately 350-meters with upper and lower layer densities of 1.8 grams/cubic centimeter and 2.0 grams/cubic centimeter, respectively, are found. The best fit geologic model for the March 2006 Santa Tecla gravity data is shown on **Figure 64**. An approximately 700-meter thick, wedge-shaped, alluvial fan has a density of 1.9 grams/cubic centimeter. The size of this fan is controlled by sediment deposition at the mouth of one of the largest canyons on the east flank of the Sierra San Marcos, as shown on **Figure 57**. The basement is granodiorite with a density of 2.67 grams/cubic centimeter and is overlain by an approximately 700-meter thick clastic package and approximately 1,000-meter thick carbonate units with densities of 2.3 grams/cubic centimeter and 2.55 grams/cubic centimeter, respectively.

The residual Bouguer gravity anomaly for Santa Tecla varies from approximately -39 to -51 milligals, as shown on **Figure 64**. The best fit geologic model includes the same syncline valley identified in the Rancho Pozas Azules section located to the north. Neither a buried anticline nor large-scale faulting appears to be present in the Santa Tecla line. The increase in surface topography on the east side of the best fit geologic model for the Santa Tecla gravity data is comprised of an anticline mountain in the eastern basin.

DISCUSSION

This section evaluates modeled geologic cross sections (**Figure 61** to **Figure 64**) and compares them to the three hypothesized subsurface geologic controls on spring locations presented on **Figure 50**. Hydrogeologic data are constrained by the geologic

models. This section also presents a summary geologic cross section of the subsurface geologic controls on springs in the Cuatrocienegas Basin showing that two distinct geologic mechanisms influence spring locations: a reverse fault on the west flank, and permeability differences on the east flank of the Sierra San Marcos.

Geologic Evaluation: Springs on the West and North Flank of the Sierra San Marcos

In this part of the Basin, springs are inferred to be controlled by fractures associated with reverse faulting that provide a conduit to a regional carbonate aquifer. On the west flank, the Sierra San Marcos anticline dips steeply to the west from approximately 50 to >90 degrees. The mountain crops out in nearly a straight line for approximately 10 kilometers, and the linear orifice of Poza La Becerra suggests the presence of fault-associated fractures instead of a buried anticline or permeability differences. Similarly, in Ash Meadows, Nevada, springs discharge from a 16-kilometer long fault (Winograd and Pearson, 1976). The model of Hennings et al. (2000) suggested that the highest fracture density should be along the west flank of the Sierra San Marcos —precisely where the largest springs occur.

The wedge-shaped alluvial fan of the March 2006 survey is thicker than the alluvial fan in the January 2006 Churince survey. The difference in alluvial fan thickness reflects its position at the mouth of a small canyon separating the Sierra San Marcos with a smaller anticline to the west, as shown on the shaded relief map on **Figure 57**.

The difference between the residual Bouguer anomalies between the January and March 2006 Churince surveys is explained best by the presence of an approximately 300-meter high buried anticline at depth. Field observation of the small, north-plunging anticline mountain to the west of the Sierra San Marcos just south of this line supports this model. Models of Freeze and Witherspoon (1967) implied that such high hydraulic conductivity carbonate layers in the subsurface could cause springs or seeps. However,

springs are located closer to the west flank of the mountain, suggesting fractures determine spring locations here instead of a buried highly permeable anticline.

In order to constrain results of the gravity geophysical analyses, additional hydrogeologic data are considered. Wolaver et al. (2008) measured spring discharge of spring-fed canals in the Cuatrocienegas Basin. Springs located on the west side of the basin contribute approximately 85 percent of the total basin discharge of approximately 35,000,000 cubic meters/year, suggesting high-volume spring discharge occurs along a linear zone of fault-associated fractures from a deeper carbonate aquifer. Spring water temperatures on west side of the basin range between 32.0°–35°C, approximately 2.0°–5.0°C warmer than on the east flank of the mountain. This also suggests deeper circulation occurs in the west flank springs. Tritium data (Wolaver et al., 2009, *in preparation*) suggest aquifer residence times of >50 years indicative of longer flow paths and a regional aquifer system.

The observation of the spatial distribution of springs on the west and north flank of the Sierra San Marcos agrees with predicted fracture distribution in structural models. Following the trishear zone model of Erslev and Mayborn (1997) and Mitra (2002), a reverse fault and associated fractures are expected in the core of the anticline on the western side of the Sierra San Marcos following the trishear mechanism shown on **Figure 56**. Similarly, according to the analytical model of fracture density presented by Hennings et al. (2000), the highest fracture intensity is predicted on the western side of the Sierra San Marcos anticline, precisely where the highest discharge springs are found. In fact, spring discharge emanates from fractures in Cretaceous carbonates in the bottom of Poza La Becerra that are parallel to the strike of the Sierra San Marcos (shown on **Figure 51**). Also, fold accommodation faults may explain elevated temperature springs

(e.g., Poza Escobedo) located off the northeast nose of the Sierra San Marcos. Faults of this type for an analogous anticline in Wyoming were studied by Hennings et al. (2000).

Geologic Evaluation: Springs on the East Flank of the Sierra San Marcos

Springs on the east flank of the Sierra San Marcos, have stratigraphically controlled springs where incised ancestral stream canyons intersect the piezometric surface of a regional and local aquifer system that drains through the base of alluvial fans. The best fit model for the east flank of the Sierra San Marcos does not have a buried anticline at depth. Instead, a broad syncline valley appears to be present in the subsurface. Field observations of mountains comprised of anticlines surrounding the valley on the east flank of the Sierra San Marcos supports this assumption.

On the eastern flank of the Sierra San Marcos, springs contribute approximately fifteen percent of total basin spring discharge (Wolaver et al., 2008). Here, permeability differences between highly permeable carbonate rocks and lower permeability valley fill alluvium controls spring location. The potentiometric surface of a shallower carbonate aquifer is intersected by down-cut stream channels. Veni (2005) noted this occurs in Central Texas karst springs as well. The channels associated with alluvial fans permit relatively low-discharge springs from a regional carbonate-aquifer flow system with a component of local mountain runoff. Groundwater flows in permeable layers of the alluvial fans beneath observed low hydraulic conductivity caliche layers, as also occurs on alluvial fans in West Texas (Darling, 1997). Springs form at the base of the alluvial fans because groundwater cannot infiltrate into lower permeability lacustrine alluvial valley-fill.

CONCLUSIONS

The best-fit hydrogeologic conceptual model for the subsurface geologic controls on springs in the Cuatrocienegas Basin is presented on **Figure 65**. Springs on the west and north flank of the Sierra San Marcos are controlled by fractures associated with a reverse fault within the Sierra San Marcos that creates fracture permeability. Gravity surveys suggest the presence of an anticline at depth on the west side of the Sierra San Marcos, but this structure does not correlate with spring locations.

On the east flank of the Sierra San Marcos, buried anticlines or faults are not present. Here, springs are located at the base of alluvial fans. The source of spring discharge is a combination of regionally and locally derived water. The results of land gravimetry surveys in the Cuatrocienegas Basin generate hydrogeologic cross sections that allow a general interpretation of subsurface geologic controls on spring location where additional hydrogeologic data, including groundwater quality, spring discharge rates, field observation of spring location, and strike and dip of exposed bedrock are considered. Future research may wish to consider higher-resolution geophysical methods (such as seismic reflection) and exploratory boreholes to refine the hydrogeologic conceptual model.

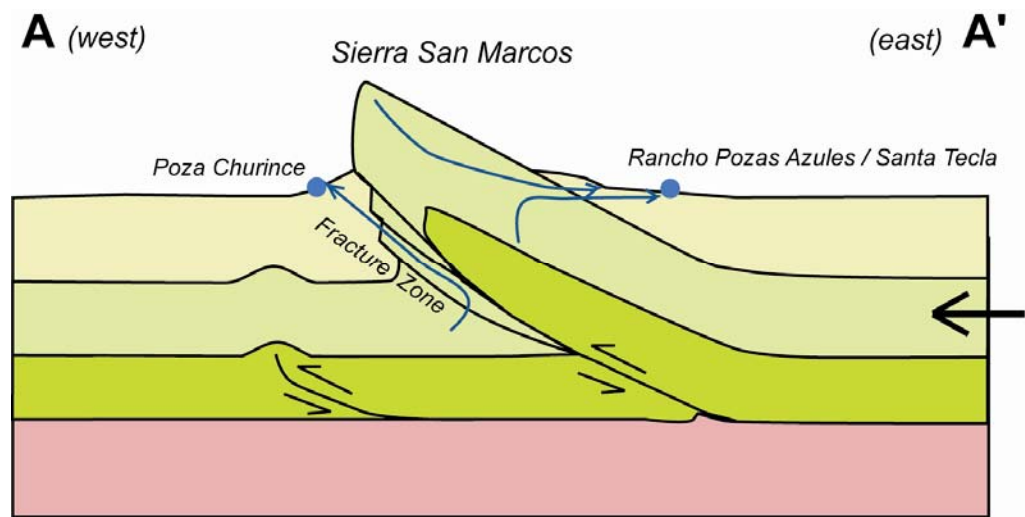


Figure 65. SUMMARY GEOLOGIC CROSS SECTION BASED ON LAND GRAVIMETRY

This summary geologic cross section honors the hydrology and geology of the Cuatrocienegas Basin. Light, straight arrows show relative fault movement. The dark, straight arrow shows direction of relative stress. The curved, light arrows show groundwater flow.

Chapter 6: A Systematic Approach for Characterization of Arid Aquifer Systems

A revised version of this chapter will be submitted for publication.

ABSTRACT

This research describes a systematic approach for the characterization of developing arid karst aquifer systems where long-term well data typically used to generate hydrogeologic conceptual models are sparse or even nonexistent. The objective of this research is to infer the location of recharge areas and recharge volume, groundwater flow paths and flow rates, discharge volume and water quality, and understand the primary uses of the aquifer's water resources.

The aquifer characterization approach combines a human narrative (anecdotal evidence) aspect that includes an evaluation of anecdotal evidence gained by "talking to the locals" and groundwater-related data shared through interdisciplinary collaboration. The approach assesses data acquired through remote sensing tools, including satellite or aerial photos, the analysis of digital elevation models often generated through satellite-derived radar altimetry, and geophysical methods. The approach also integrates physical observations, including field observations, evaluation of geologic maps, measurement of groundwater head in wells and springs, and measurement of spring discharge. The interpretation of geochemistry and isotopic data, including chloride in precipitation and groundwater, dissolved noble gases, strontium isotopes, tritium, and oxygen isotopes is also included in the approach. In addition, land gravity surveys are used to infer subsurface controls on spring locations.

The application of this approach (portions of which are described in Wolaver et al., 2008) in northeast Mexico indicates than an approximately 18,000-square kilometer aquifer system discharges to Cuatrocienegas Basin springs based on chloride mass balance recharge calculations and a regional low-elevation sink identified from digital elevation data. Oxygen isotopes suggest mountain recharge in the surrounding five valleys dominates. Noble gas data indicate topographic divides are not groundwater divides. Strontium isotopes of spring water and travertine samples indicate the regional carbonate aquifer is likely the Aptian Cupido Formation. Stable discharge, temperature, and chloride data of some springs corroborate the existence of a regional flow system. Gravity surveys suggest fault-associated fractures permit regional aquifer discharge in some springs and stratigraphic controls influence the location of other springs.

INTRODUCTION

Motivation for, objectives of, hypotheses of, and importance of this research in the specific study area are discussed below.

Motivation for Research

Population growth and economic expansion in Mexico is stressing limited groundwater resources, particularly in the northeast Mexico state of Coahuila. For example, Brouste et al. (1997) investigated the effects of water resource development for agriculture that started in the 1800s around Torreón, Coahuila, one of the most important dairy farming areas in Mexico (Rosas et al., 1999). Unsustainable surface water diversions of the Río Nazas and Río Aguanaval and groundwater overdraft by farms near Torreón on a Quaternary alluvial aquifer has made groundwater quality unsuitable for irrigated agriculture. Total dissolved solids in well water ranges from 140 to 5,100 milligrams/liter (mean=1,180 milligrams/liter) and arsenic ranges from

7 to 740 micrograms/liter (Brouste et al., 1997; Rosas et al., 1999). Groundwater withdrawals also caused increased pumping lifts (groundwater was at the surface in the 1890s and is now up to 100 meters below ground surface around pumping centers) because of groundwater drawdown in excess of one meter/year (Brouste et al., 1997). Because alfalfa used for dairy cow fodder is irrigated with well water with elevated arsenic, arsenic is found in cow's milk (up to 27.40 nanograms arsenic/gram of milk). As high-quality groundwater suitable for agriculture was exhausted near the City of Torreón, Durango, farmers searched for new areas to grow crops (Brouste et al., 1997). Areas that have received new agricultural development since the 1980s in response to this regional change in land use are the Hundido and Ocampo Valleys adjacent to the Cuatrocienegas Basin, Coahuila (**Figure 66**).

Cuatrocienegas Basin: Background

The Cuatrocienegas Basin is located approximately 300 kilometers southeast of Big Bend National Park (located in the State of Texas, U.S.A), in the State of Coahuila, Mexico and is shown on **Figure 66**. It is located at the northern edge of the Sierra Madre Oriental in the Chihuahuan Desert. Historically, groundwater development in the region was limited. However, in recent decades, large-scale irrigated agriculture has developed in the Hundido and Ocampo Valleys adjacent to the Cuatrocienegas Basin.

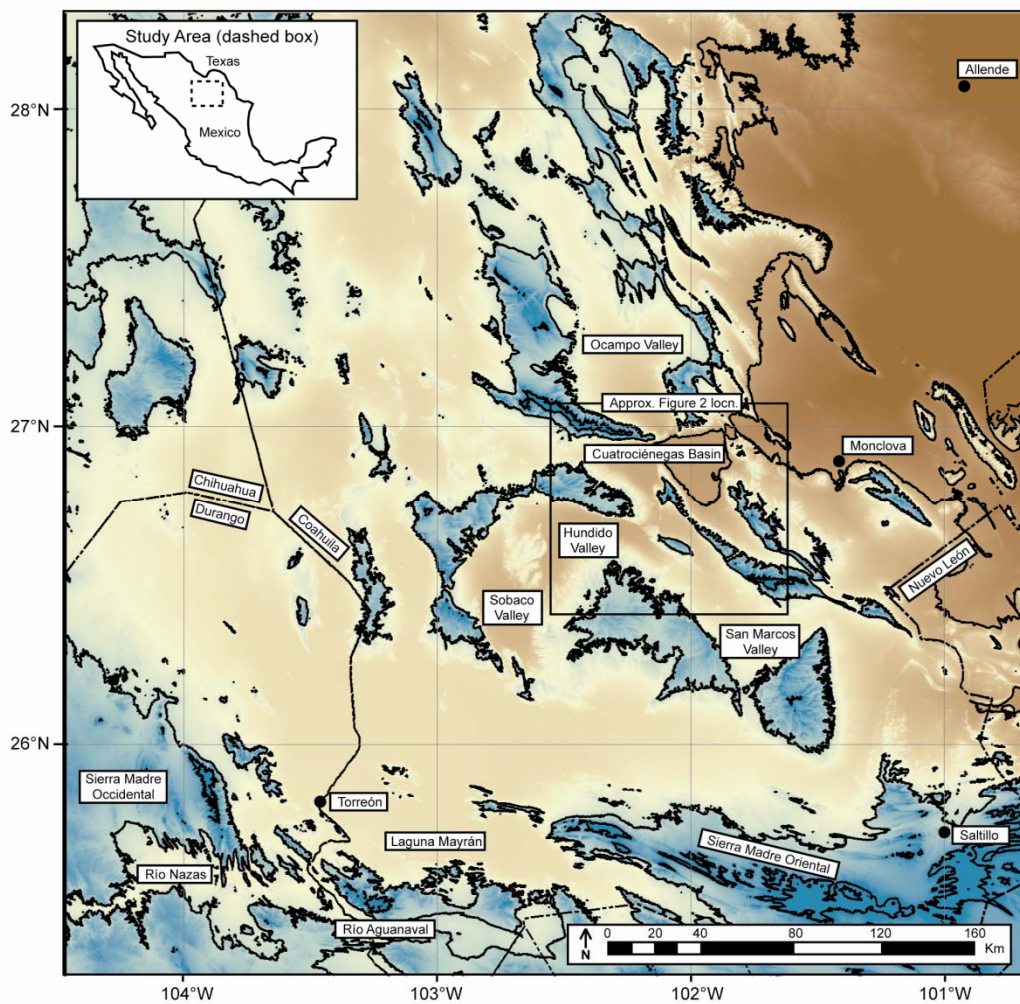


Figure 66. CUATROCIÉNEGAS BASIN STUDY AREA

Contour interval ranges from brown (750-meter) to green (1,500-meter and 2,250-meter). State boundaries are indicated by dashed lines.

Research Questions

It is difficult to evaluate the effects of groundwater mining in surrounding valleys on Cuatrocienegas Basin spring discharge for several reasons. Groundwater development in the Hundido and Ocampo Valleys is relatively recent (starting in the 1980s). Thus, long-term well data, which is typically used to generate a hydrogeologic conceptual model of an aquifer system, do not exist. Complicating the paucity of hydrogeologic data in the Cuatrocienegas Basin is the fact that farmers often do not openly share data like well depth (and lithology encountered during drilling), pumping rate, and water quality. As a result of sparse hydrogeologic data in the Cuatrocienegas Basin region, several research questions are at the root of understanding groundwater pumping effects on springs:

1. Where are the recharge areas;
2. What is the recharge volume;
3. What are the groundwater flow paths;
4. What are the flow rates;
5. What is the discharge volume;
6. What is the water quality;
7. What are the uses of the wells;
8. What are the uses of the springs; and
9. What are the environmental requirements of groundwater-dependent ecosystems?

Objectives

The goal of this research is to develop a systematic approach for the characterization of this and similar developing arid-zone karst aquifer systems. The objective of this research is to provide an approach that answers the fundamental questions described above and characterizes an arid karst aquifer system's recharge areas and recharge volume, groundwater flow paths and flow rates, discharge volume and water quality, and understands the primary uses of the aquifer's water resources.

Hypothesis

The author hypothesizes that a systematic approach for the characterization of developing arid karst aquifer systems can be developed. This aquifer characterization approach can integrate a wide variety of data sources, including: geologic maps, satellite images and aerial photos, anecdotal evidence and physical observations in the field, and topographic analysis of digital elevation models to generate a hydrogeologic conceptual model. The model can be refined with selected use of geophysical methods to make inferences into subsurface geology, head and discharge, and geochemistry of both precipitation and groundwater. The author applies this aquifer characterization approach to the Cuatrocienegas Basin, Mexico and postulates that this approach may be applicable to understanding developing arid karst aquifer systems elsewhere.

Importance of Study

As population growth continues in northeast Mexico and similar arid regions globally, previously undeveloped aquifer systems will be exploited. As a result, techniques are required to evaluate and effectively manage groundwater resources despite limited hydrogeologic data. For example, in the Great Basin of Nevada, the City of Las Vegas is considering the development of 60,000 acre-feet/year of groundwater in the previously undeveloped Spring Valley of White Pine County (Gillespie et al., 2007). A

lack of long-term well data in the Cuatrociénegas Basin complicates recharge area delineation, the focus of this research. Procedures are developed for the delineation of regional groundwater flow systems in arid aquifers with sparse hydrogeologic data with application in the Cuatrociénegas Basin. The approach developed by this research also shows promise as a means to characterize developing aquifers such as that of the Spring Valley, Nevada and similar aquifers.

AN APPLICATION OF THE APPROACH IN NORTHEAST MEXICO

This section discusses how this approach is applied to the arid karst aquifer system that supports springs in the Cuatrociénegas Basin, Coahuila, Mexico. The scientific questions this research addresses and the different tools of this approach are presented in **Table 40**.

Human Narratives

In the author's research in the Cuatrociénegas Basin, human narratives (anecdotal evidence) form the foundation of the research. From the start of the research, the aquifer characterization is facilitated by gathering anecdotal evidence by "talking with the locals." In the author's case, much of this research was conducted in Spanish and fluency in the local language was invaluable in doing this successfully. Building working research relationships through interdisciplinary collaboration is essential for work in developing aquifer systems such as the Cuatrociénegas Basin.

Table 40. A TOOLBOX FOR CHARACTERIZATION OF A DEVELOPING ARID KARST AQUIFER SYSTEM

Scientific Question	Human Narratives		Remote Sensing			Physical Observations				Geochemistry and Isotopes					
	Anec-dotal Evi-dence	Inter-Disc. Collab-oration	Sat-ellite/Aerial Photo	Digital Elev-ation Model	Geo-physics	Field Ob-serva-tions	Geo-logic Maps	Head	Meas-ure Spring Dis-charge	Cl ⁻ In Precipi-tation, Ground-water	An-ions and Cat-ions	Noble Gases	$\frac{^{87}\text{Sr}}{^{86}\text{Sr}}$	³ H	$\delta^{18}\text{O}$
Where are the recharge areas?			✓	✓		✓	✓	✓		✓				✓	
What is the recharge?									✓	✓					
What are the groundwater flow paths?				✓		✓	✓	✓				✓	✓	✓	
What are the flow rates?									✓	✓	✓				
What is the amount of water in storage?					✓	✓		✓				✓			
What is the discharge?	✓	✓	✓			✓	✓			✓					
What is the water quality?	✓	✓				✓		✓			✓	✓			
What are the preferred well locations?	✓		✓				✓	✓	✓						
What are the effects on springs?	✓	✓	✓				✓		✓	✓		✓			
What are environmental requirements?	✓	✓					✓		✓	✓					

Anecdotal Evidence

Gathering anecdotal evidence of hydrologic and hydrogeologic conditions was critical for the hydrogeologic characterization of the Cuatrocienegas Basin. In this area, long-term well data are nonexistent. A preliminary hydrogeologic conceptual model can be constructed by talking with a variety of people. In my research, I visited with non-profit agency members who organized environmental tours, national park employees, ranchers, economic geologists, federal government anthropologists, a doctoral student in anthropology working on the water issues, vineyard operators, casual conversations with people on the town plaza, business owners who rely on local orchard production, farmers who work in alfalfa production, state government geologists working on a regional well survey, and anyone willing to discuss water resources.

Anecdotal evidence is used to understand the historic spring discharge of the formerly spring-fed Río Cañon that drained into the Cuatrocienegas Basin. Prior to groundwater development in the Ocampo Valley, discharge from the Río Cañon was sufficient to operate two wheat mills and irrigate orchards in the Town of Cuatrocienegas. Minckley and Cole (1968) estimated Río Cañon discharge to be 250 liters/second. Anecdotal evidence also suggests that Río Cañon water was of relatively high quality (i.e., low total dissolved salts) so it could be used for irrigation. Minckley and Cole (1968) measured Río Cañon chloride concentration at approximately 22 milligrams/liter, but did not measure total dissolved solids.

In the Cuatrocienegas Basin, anecdotal evidence suggests the effects of groundwater pumping for agriculture in the Hundido Valley, in addition to the Ocampo Valley (both adjacent to the Cuatrocienegas Basin) has decreased spring discharge. Therefore, it might be preferable to locate future well sites in the Cuatrocienegas Basin region relatively far away from key springs to minimize the effects of drawdown on

spring discharge. Alternatively, agricultural operations should rely on spring discharge and be located entirely down gradient of the Cuatrociénegas Basin.

Finally, anecdotal evidence can provide insight into the environmental requirements of groundwater-dependent ecosystems. For example, in the Cuatrociénegas Basin, anecdotal evidence suggests that wetlands were much more extensive prior to the construction of French drains to lower the water table for grazing and the installation of canals to convey water out of the basin for agriculture starting in the early 1900s (Calegari, 1997). In fact, much of the eastern portion of the Cuatrociénegas Basin was a shallow wetland, now greatly reduced. This was the preferred habitat for a species of aquatic box turtle found only in the valley (Webb et al., 1963).

Interdisciplinary Collaboration

In developing aquifer systems, such as the Cuatrociénegas Basin, hydrogeologic characterization can be facilitated by interdisciplinary collaboration with other scientists working on water-related subjects. In the author's research, collaboration with aquatic biologists and geophysicists has been beneficial. In the Cuatrociénegas Basin, research was started in the late 1950s and early 1960s by biologists interested in aquatic species found in the groundwater-dependent ecosystems of the valley (Minckley, 1962). These researchers, in addition to collecting biologic samples, also collected preliminary hydrologic data (such as the historic discharge and water quality of Minckley and Cole, 1968). More recently, the author has coordinated field work with biologists actively conducting research in the Cuatrociénegas Basin. Hydrologic observations by biologists led to a refinement of the hydrogeologic conceptual model of the Cuatrociénegas Basin (Hendrickson et al., 2005). Finally, the effects of water resource development on Cuatrociénegas Basin springs and associated groundwater-dependent ecosystems is well documented with comparative photos in Minckley (1992) and continued more recently in

Hendrickson et al. (2008). In considering the environmental flow requirement for groundwater-dependent ecosystems, collaboration with biologists can be instrumental in determining target flow rates.

Remote Sensing

The characterization of the hydrogeology of the Cuatrocienegas Basin by the author has relied extensively on remotely-sensed data, including satellite and aerial photos, topographic analysis of digital elevation models, and geophysics.

Satellite/Aerial Photos

Remotely sensed images from satellites and aerial photos are a useful tool for preliminary reconnaissance of developing arid regional aquifer systems, as well as a tool to confirm relationships observed in the field. In the early stages of this aquifer characterization project, the author used satellite images available at the Google Earth website (Lisle, 2006) to gain insight into regional structure and topography. Google Earth images can also be used to locate recharge areas. Furthermore, in the arid Chihuahuan Desert, annual valley-floor precipitation is approximately 220 millimeters/year (Rodríguez et al., 2005a). Recharge is focused in the mountains, where average annual rainfall is >400 millimeters/year (at an elevation >3,000 meters, Rodríguez et al., 2005a). Google Earth images of the Cuatrocienegas Basin region confirm this where vegetation (i.e., pine trees, Meyer, 1973) grow and the images can be manipulated to show topography, providing a means to identify mountain recharge. Similarly, discharge areas can be identified from Google Earth images. Vegetation also grows around springs, making springs easily identifiable against the otherwise brown desert vegetation. In addition to Google Earth, geo-referenced aerial photos are also used to identify springs.

Remotely sensed images can also be used to evaluate preferred well locations and the potential effects of pumping on springs. Ideally, municipal or agricultural supply wells should be located away from springs to preserve discharge. For instance, Bedinger and Harrill (2006) used the Theis analytical solution for drawdown to evaluate water table declines in the vicinity Devils Hole, Death Valley National Park, Nevada, due to pumping. Remotely sensed images can provide the distances between pumping centers and springs needed for the Theis analysis.

Digital Elevation Model

The author used digital elevation models to provide insight into regional aquifer behavior. Hall et al. (2005) described the first global (60° north– 50° south) high resolution (3-arc second) digital elevation model produced by the Shuttle Radar Topography Mission for 80 percent of the Earth's surface. The data set is particularly valuable for developing regions where accurate elevation surveys may not have been available previously. Wolaver et al. (2008) described the use of ArcHydro, a geographic information system topographic analysis tool developed by Tarboton (1997) and Maidment (2002), to evaluate the Cuatrociénegas Basin aquifer system. The ArcHydro topographic analysis is performed on an approximately 100,000 square kilometer area to generate catchments located at higher elevations than the Cuatrociénegas Basin. Inferences on regional groundwater flow can be made based on topographic gradient. In conjunction with the Google Earth image analysis described above, high-elevation recharge areas can be identified with the topographic analysis of a digital elevation model. Groundwater flow paths can also be inferred from the terrain data. For example, Eakin (1966) delineated an aquifer system of thirteen interconnected valley-fill basins overlying Paleozoic carbonates in the White River Valley of Nevada based on recharge/discharge relationships, a regional groundwater gradient, uniformity of spring

discharge, and geochemical characteristics. Wolaver et al. (2008) used digital topographic analysis, in conjunction with other data, to identify five basins (totaling approximately 18,000 square kilometers) that likely discharge in the Cuatrocienegas Basin springs.

Geophysics

Geophysics is another remote sensing tool used to characterize the hydrogeology of the Cuatrocienegas Basin aquifer system, including estimating the amount of water in storage and the evaluation of geologic controls on discharge areas. The author evaluated data collected by Miele et al. (2000) using time domain electromagnetics to image buried carbonate anticlines for groundwater development in an adjacent basin to understand Cuatrocienegas Basin structural style. The author also assessed a time domain electromagnetics survey by Rodríguez et al. (2005a) to estimate an average Cuatrocienegas Basin alluvium depth of approximately 200 meters. These data can be used to create a hydrogeologic conceptual model and estimate the amount of groundwater in storage.

Wolaver and Diehl (2008) used land gravimetry surveys to evaluate subsurface controls on spring locations — an important Cuatrocienegas Basin aquifer system discharge component. Land gravity surveys are used instead of other geophysical methods because land gravimetry is relatively (1) inexpensive, (2) easy to implement, and (3) non-intrusive, and (4) the resulting data are relatively simple to process and interpret compared to other geophysical survey data.

Ground penetrating radar was tested in the vicinity of Cuatrocienegas Basin springs to evaluate subsurface geologic controls on spring locations. However, a shallow valley-fill alluvium water table (<1m), relatively saline groundwater

(>2,000 milligrams/liter total dissolved solids), and soil mineralization hindered useful subsurface data collection. Thus, ground penetrating radar was not useful in this study.

Physical Observations

Talking with people and using remotely sensed images provide initial data in support of characterization of arid regional aquifer systems. However, a complete understanding of an aquifer system cannot be obtained without hydrogeologic data. Thus, field observations, geologic maps, and measurements of head and spring discharge are a critical component of the characterization of the Cuatrocienegas Basin region.

Field Observations

In the Cuatrocienegas Basin, observations refine the hydrogeologic conceptual model after conducting initial site reconnaissance using remotely sensed images on Google Earth. Adkins (1920) conducted the first hydrogeologic assessment of the Cuatrocienegas Basin in support of water resource development and well siting. He observed that the linear trend of springs that flank the Sierra San Marcos may be caused by faulting – an idea tested by Wolaver and Diehl (2008) using land gravimetry surveys. Chávez-Cabello (2005) investigated the structural style of the Cuatrocienegas Basin region and finds that gently-dipping anticlines are located in adjacent valleys located to the south and southwest of the Cuatrocienegas Basin. Topographic analysis of the regional digital elevation model shows these areas of gently-dipping anticlines and gently-dipping strata are located at higher elevations than the Cuatrocienegas Basin (Wolaver et al., 2008). The structural style changes to the northeast, with decreasing elevation towards the Cuatrocienegas Basin, as the gently-dipping strata change to faulted rocks associated with steeply-dipping anticlines that first occur in the Cuatrocienegas Basin. Steeply-dipping anticline mountains like those bordering the Cuatrocienegas Basin

are typically associated with basement-involved faults (Erslev and Mayborn, 1997; Mitra and Mount, 1998; Mitra, 2002). Faults associated with these mountains, like the Sierra San Marcos, probably influence the distribution of springs in the Cuatrocienegas Basin.

Although pumping has altered the predevelopment hydrogeologic condition of the Cuatrocienegas Basin region, the author makes field observations of these changes. The formerly spring-fed Rio Canon used to drain from springs at the southern end of the Ocampo Valley. Although dry, a canyon has been eroded by flow into the Cuatrocienegas Basin, which suggests that historic spring discharge was considerable. In 1964 Minckley and Cole (1968) estimated spring discharge at approximately 250 liters/second. The author also observed the carbonate rocks exposed by erosion of the Rio Canon. Secondary permeability features can be observed in Cuatrocienegas Basin rocks: (1) dissolution along bedding plane partings, (2) locally spectacular caves, and (3) fractures associated with localized structures that all increase permeability in the subsurface.

To the south, in the Hundido Valley, the water table used to be close to ground level. In the northeastern Hundido Valley, it was possible in the early 1900s for horses to drink from a groundwater seep without pumping groundwater. As agricultural development occurred, and the water table dropped, residents dug down, following the water table for approximately 20 meters, providing a direct observation of the drawdown caused by groundwater pumping.

The author also makes inferences into the paleo-hydrology of the Cuatrocienegas Basin from field observations. Miller (1961) presented a photograph of an outlet canyon several 100s of meters deep on the eastern side of the valley. While the canyon was dry in the 1960s, the deep outlet canyon suggests a watershed of considerable size once drained the region here. As climate dried, possibly in the Holocene (Castiglia and Fawcett, 2006),

the surface water system became truncated, but a regional groundwater flow system continued to exist.

Geologic Maps

In addition to field observations, published geologic maps provide insight into regional hydrogeologic conditions. INEGI (1975), the branch of the Mexican government responsible for geologic mapping, produced a geologic map of the Cuatrocienegas Basin region. The author initially consulted this map to infer the effects of regional geology on hydrogeology. Of particular interest is the distribution of Cretaceous carbonate rocks throughout the study area. In similar carbonate terrains, such as the Great Basin of Nevada, researchers recognize that carbonate rocks typically support regional, interbasin flow systems because of high secondary permeability (Maxey and Eakin, 1949; Snyder, 1962; Eakin, 1966; Maxey, 1968; Eakin et al., 1976; Winograd and Thordarson, 1975; Mifflin, 1988; Anning and Konieczki, 2005). Based on geologic maps, the author infers that the regionally extensive Cretaceous carbonate rocks support a regional flow system.

Head

Carbonate rocks commonly have elevated permeability that enables regional flow systems, but for this to occur, a regional head gradient must also exist. In the Cuatrocienegas Basin, long-term water level data in wells typically used to characterize aquifer systems are non-existent. Thus, the author infers groundwater head based on playa lake elevations in the Sobaco Valley in the far southwest portion of the study area. In the Ocampo Valley and Hundido Valley, groundwater head is inferred from historic shallow groundwater and playa lakes. In the Cuatrocienegas Basin, spring elevation is used, in absence of well water level data, to determine a regional groundwater gradient

(9.52×10^{-4} to 1.75×10^{-2} ; Wolaver et al., 2008). Tóth (1963) presented a conceptual model for regional flow systems with regional discharge occurring at the lowest elevation. The Cuatrocienegas Basin is located at a regional low elevation in high-permeability media. This implies that spring discharge is from a regional system.

Measure Spring Discharge

In addition to evaluating groundwater head, the author also measures discharge of selected springs as well as two canals that integrate discharge of dozens of springs too small to measure individually. The author measures spring discharge with a FlowTracker acoustic Doppler velocimeter profiler and the author also evaluates discharge data collected by Mexican technicians using a Pygmy flow meter to generate an approximately five-year record of the Cuatrocienegas Basin. Spring discharge in Poza La Becerra, the largest spring in the valley (approximately 600 liters/second, or approximately 19,000,000 cubic meters/year) has essentially been stable for the period of record. Eakin (1966) uses the stability of discharge of Muddy River spring in southern Nevada to infer a regional flow system. Similarly, Wolaver et al. (2008) suggested the stability of discharge of Poza La Becerra is due to a regional aquifer system ($>10,000$ square kilometers) that dampens out fluctuations due to drought or wet periods. Conversely, Canal Santa Tecla, a canal that drains springs on the southeastern flank of the Sierra San Marcos, shows a decrease in discharge over the period of record. The pattern may be due to drought, pumping in adjacent basins, or a leak that closed the canal for repairs in the spring of 2007. It is difficult to infer the cause of the decrease in discharge of Canal Santa Tecla. However, the stability of discharge of Poza La Becerra reflects a regional flow system.

Geochemistry and Isotopes

In addition to physical measurements and observations, geochemistry and isotopes in spring water can provide insight into the regional hydrogeologic conceptual model. The author uses chloride in precipitation and spring water to estimate recharge rates, in addition to evaluating anions and cations for basin water quality parameters. Noble gases are used to infer recharge elevation and oxygen isotopes are evaluated to estimate the elevation at which precipitation occurs. Tritium provides insight into aquifer residence time and strontium isotopes in spring water and travertine elucidate the regional aquifer.

Chloride in Precipitation and Groundwater

The author uses chloride in precipitation and groundwater to estimate recharge in the Cuatrocienegas Basin region using the chloride mass-balance approach (Dettinger, 1989; Wood, 1999; Anderholm, 2000). Rodríguez et al. (2005a) collected rain samples for oxygen isotope analysis, but did not measure chloride concentration. The author installed several precipitation samplers in the summer of 2006. However, no rain samples were retrieved due to vandalism or strong wind gusts blowing over the samplers. Thus, the author uses previously published rain chloride data (Junge and Werby, 1958; Lamb and Bowersox, 2000; Gay et al., 2008; National Atmospheric Deposition Program, 2008) and spring water chloride concentration from a variety of sources (Wolaver et al., 2008) to estimate recharge in the Cuatrocienegas Basin region. Wolaver and Tidwell (2008, *in preparation*) use the chloride mass balance approach with variable recharge rates by elevation (following Maxey and Eakin, 1949) to find that an approximately 18,000 square kilometer recharge area provides spring discharge. Of this larger area, approximately 600 square kilometers of exposed carbonate rock provided recharge for the historic Rio Canon (approximately 8,000,000 cubic meters/year at

approximately 22 milligrams/liter chloride, Minckley and Cole, 1968). Approximately 450 square kilometers of the exposed Sierra San Marcos likely recharges springs on the southeast flank of the same mountain (approximately 6,000,000 cubic meters/year at approximately 30 milligrams/liter chloride). Higher flow rates (approximately 29,000,000 cubic meters/year) and elevated chloride concentration (approximately 90 milligrams/year) are explained by lower-elevation recharge on approximately 10,000 square kilometers of mountains surrounding the Hundido, San Marcos, and Sobaco Valleys.

Anions and Cations: Water Quality Parameters

The author evaluates the results of water quality analyses for anions and cations for springs and wells in the Cuatrocienegas Basin area presented by Rodríguez et al. (2005a) and other authors (Winsborough, 1990, Johannesson et al., 2004; Evans, 2005) to understand groundwater evolution and hydrogeochemical facies (Back, 1966). The author also collected water samples from springs during the summer of 2007 for water quality analyses by Crossey (2008). Anions are analyzed using ion chromatography and cations are analyzed using an inductively coupled plasma mass spectrometer. The results of anion and cation analysis are plotted on a Piper Plot (Piper, 1944) to understand groundwater evolution. As would be expected for groundwater flowing through carbonate rocks with evaporite layers, the hydrochemical facies are predominantly calcium-sulfate and also calcium-bicarbonate. Results of analyses for water samples collected in springs at the head of the Canal Santa Tecla (that experience a decrease in discharge) plot on a linear trend with the results of a precipitation sample, suggesting that regional flow and also locally-derived, less-evolved water contribute to spring flow here.

The results of water quality analyses can also be used to validate the chloride mass balance model to assure that the only source of chloride is from precipitation and

that dissolution of halite is not contributing chloride. By plotting chloride and sodium and chloride and bromide, following the approach of Davis (1998), the author finds the linear trend in chloride and sodium is due to evaporation. If dissolution of halite were occurring, the waters would be enriched with chloride with respect to bromide and this does not occur.

Noble Gases

The author uses noble gases dissolved in spring water to infer the elevation at which recharge water enters the water table. The author also uses noble gas data to investigate if groundwater divides exist under mountain recharge zones — providing insight into groundwater flow paths in the Cuatrocienegas Basin. The author collected noble gas samples from springs July 2008 that were analyzed at the University of Utah Dissolved Gas Laboratory. Manning and Solomon (2003) and Heilweil et al. (2006) used noble gases (i.e., Ar, Ne, Xe, etc.) to infer groundwater recharge elevation. While oxygen isotopes provide insight into the elevation at which precipitation occurs, the temperature dependency of noble gases by Henry's Law can be used as a recharge thermometer, with an assumption of lapse rate. The results of noble gases show the elevation at which recharge water enters the water table is between approximately 722 and 768 meters. From the digital elevation model, valley floor elevation is approximately 770 meters. Thus, groundwater does not appear to mound under the mountains that separate valleys adjacent to the Cuatrocienegas Basin and serve as recharge areas, indicating that interbasin groundwater flow likely occurs.

Strontium Isotopes

The author uses strontium isotopes in spring water and travertine to infer the source of strontium ions to evaluate through which formation groundwater is flowing.

The author also uses strontium isotopes to evaluate if groundwater flow paths have evolved from the time travertine of inferred Pleistocene age was deposited. Banner and Kaufman (1994) described the method for analyzing strontium isotopes (i.e., $^{87}\text{Sr}/^{86}\text{Sr}$). Since strontium has a similar ionic radius and the same charge as calcium, strontium substitutes in calcium carbonate in carbonate rock and gypsum. Also, the strontium isotopic ratio has changed through the Cretaceous and is well known (Bralower et al., 1997). Thus, strontium ions in spring water and travertine of the Cuatrocienegas Basin have the same isotopic ratio as the aquifer matrix through which the water flows. The author measures strontium isotopes from seventeen water samples and three travertine samples. Strontium isotope results ($^{87}\text{Sr}/^{86}\text{Sr}$) for seventeen water samples and three travertine samples range from 0.707428 to 0.707468. A comparison the secular Cretaceous seawater curve (Bralower et al., 1997) with Cuatrocienegas strontium isotopic results matches with the Aptian Cupido Formation and the Albian Aurora Formation (Lehmann et al., 1999). Because the Aurora Formation is not as extensive as the Cupido Formation in this part of northeast Mexico (Lehmann et al., 1999), it is most likely that the Cupido Formation is the regional carbonate aquifer.

Tritium

The author evaluates aquifer residence time using tritium in spring water to investigate if Cuatrocienegas Basin springs are derived from a regional or local aquifer system. The author collected water samples from springs July 2008 for tritium analysis at the University of Utah Dissolved Gas Laboratory using the tritium in-growth method (Clark et al., 1976). Five of the nine samples had tritium under 0.1 tritium units (the method detection limit). A precipitation sample collected by Rodríguez et al. (2004) had a tritium concentration of 5.4 tritium units. Rapid recharge of a local flow system would have a similar tritium concentration. Tritium has a half-life of approximately 12 years, so

tritium concentrations under 0.1 tritium units suggest aquifer residence times of at least 50 years (and possibly much longer). Thus, many springs in the Cuatrocienegas Basin appear to be due to discharge from an aquifer system that is comprised of groundwater recharged from outside of the Cuatrocienegas Basin.

Oxygen Isotopes

The author evaluates oxygen isotopic data of water samples collected by other researchers (Johannesson et al., 2004; Rodríguez et al., 2005a) to evaluate recharge areas. Oxygen isotopes in water are affected by many factors, one of which is an elevation dependency. Cortés et al. (1997) showed an equation explaining the elevation dependency of oxygen isotopes for the Cuenca de Mexico. Johannesson et al. (2004) used this relationship to infer that Cuatrocienegas Basin spring discharge originated as precipitation at the elevation of mountains surrounding the valley. However, mountains throughout the study area are the same elevation of mountains surrounding the Cuatrocienegas Basin. Thus, the recharge areas for Cuatrocienegas Basin springs appear to be predominantly the high mountains and that valley-floor precipitation, where evapotranspiration is large, does not contribute appreciably to recharge.

CONCLUSIONS

Human narratives (anecdotal evidence), remote sensing, physical observations, and geochemistry and isotopes are applied to characterize the hydrogeology of the developing arid karst aquifer system of the Cuatrocienegas Basin, Coahuila, Mexico. The approach builds upon aquifer evaluation techniques developed in the Great Basin of Nevada, U.S. (Maxey and Eakin, 1949; Snyder, 1962; Eakin, 1966; Maxey, 1968; Eakin et al., 1976; Winograd and Thordarson, 1975; Mifflin, 1988; Anning and Konieczki, 2005). Wolaver and Sharp (2007), Wolaver et al. (2008), Diehl and

Wolaver (2008) apply the approach in the Cuatrocienegas Basin to characterize an approximately 18,000 square kilometer regional carbonate aquifer system.

This research provides a template for aquifer characterization in other developing arid karst aquifers globally to answer questions of interest when conducting a groundwater resource assessment. The questions this approach addresses are

1. What is the water balance for the aquifer,
2. Where is water recharged,
3. Where is water discharged,
4. What are recharge and discharge volumes (both natural and anthropogenic), and
5. What is the volume of water in storage?

All aquifers are different and existing data, budget, and time available dictate which of the methods shown in **Table 40** are applicable to answer these key questions for any given project.

In general, building human relationships to obtain anecdotal evidence takes time, particularly when working in a new project location or internationally. In the Cuatrocienegas Basin, initial trips to the project site primarily involved meeting with local water resource managers and stakeholders. In each of approximately one dozen subsequent trips, the first day of a field trip and often the first hour or two of many days typically involves meeting with project participants to provide project updates and coordinate field activities. Human relationships were strengthened by several project presentations in Spanish to audiences at the local, regional, and federal levels, as well as publishing results in peer-reviewed publications with Mexican co-authors.

Remote sensing is a valuable tool for aquifer characterization. For satellite imagery, aerial photos, and digital elevation models, the initial data acquisition phase can progress rapidly. However, costs vary substantially, particularly if the project includes imagery with high spatial or temporal resolution. The acquisition of geophysical data also can be costly in both the acquisition and data processing phase. Thus, for aquifer characterization projects, the value of geophysics may be in hypothesis testing to refine a hydrogeologic conceptual model. For example, in the Cuatrocienegas Basin, remotely sensed imagery was used to identify vegetation typical of mountain recharge areas, as well as vegetation associated with springs discharge areas. Time domain electromagnetics was used to estimate alluvial fill thickness. Land gravimetry was used to evaluate the influence of fractures associated with faulting on spring locations.

Remotely sensed data can provide a wide outlook on a project and geophysics can refine local hydrogeologic understanding. However, physical observations in the field are essential to understand the hydrogeology of a region. Thus, it is important to plan for the time required to observe in the field the influence of stratigraphy and structure on hydrogeology. Prior to visiting the Cuatrocienegas Basin, the author thoroughly reviewed published geologic maps. Observations in the field early on the Cuatrocienegas Basin project guided measurement of head and spring discharge in select locations during subsequent field trips. Despite costs associated with visiting the field, hands-on observations are essential in understanding the hydrogeology of a site prior to any data analysis or modeling efforts.

Initial site visits also can be used to guide the collection of geochemical and isotopic data. Both the collection and analysis of water samples can add significant labor and budgetary demands on a regional aquifer characterization project, so they should be planned and managed carefully. In the Cuatrocienegas Basin, chloride concentration in

spring water was used for a chloride-balance approach recharge calculation to delineate upgradient recharge areas and is relatively inexpensive to analyze.

Water-quality data were used to assess basin water quality, including the hydrochemical facies, and changes in water quality because of groundwater management practices. Noble gas, strontium isotopic, and tritium data were used to evaluate the flow paths and estimate the amount of water in storage in the Cuatrocienegas Basin. Oxygen isotopes were useful in refining recharge areas and showed that most water is recharged in mountain highlands.

Human narratives are the focus at the start of a project and are important on a continuing basis. Remote sensing and physical observations in the field provide wide initial perspective for regional hydrogeologic characterization and can be used to guide the collection of more labor and cost intensive data, such as head, discharge, geochemical, and isotopic data.

Ultimately, budgetary constraints dictate the extent and type of data that can be acquired for aquifer characterization. The approach developed for the Cuatrocienegas Basin, Mexico shows promise for the hydrogeologic characterization of other similar arid aquifer systems where available data are sparse and budgets constrain the extent of data collection and analysis that can be undertaken.

Chapter 7: Conclusions

This chapter summarizes the primary results of this doctoral research project. Also included in this chapter are recommendations for research that builds upon the body of knowledge presented in this dissertation.

SCIENCE QUESTIONS

The principle scientific questions addressed by this research project are

1. What groundwater catchment(s) recharge rainwater and contribute to Cuatrocienegas Basin spring flow,
2. What are the components of the regional water budget, and
3. What subsurface geologic structures influence the spring locations?

HYPOTHESES

To investigate the science questions, the following hypotheses were formulated:

1. Cuatrocienegas Basin spring outflow originates as precipitation in both local and regional groundwater catchments. Thus, groundwater development in adjacent basins will affect spring discharge.
2. An integrative data approach can delineate recharge zones.
3. Regional low elevation, faults, and stratigraphy controls spring locations.

KEY FINDINGS

The key findings of this study, discussed in detail in previous chapters, are

1. Recharge from local mountain precipitation (i.e., falling on the Sierra San Marcos, Sierra La Fragua, and Sierra La Madera) cannot generate observed spring discharge;
2. Tritium values <0.1 tritium units indicate regional flow and aquifer residence times >50 years indicative of a regional flow system;
3. Dissolved noble gases in spring water suggest that recharge from mountain precipitation enters the water table at an elevation of approximately 750 meters, suggesting that groundwater divides do not exist under topographic highs and that interbasin flow occurs;
4. West sub-basin fault fractures tap a >10,000-square kilometer regional carbonate aquifer. Thus, effective groundwater management should be extended outside the Cuatrociénegas Basin;
5. East sub-basin canyons intersect the potentiometric surface of a stratigraphically controlled (local/regional) aquifer recharged in the 500-square kilometer Sierra San Marcos;
6. Sierra La Madera recharge accounts for Ocampo Valley predevelopment flow and chloride concentration; and
7. The integrative data approach for arid karst aquifer system delineation tested for the Cuatrociénegas Basin and can delineate recharge zones in similar developing arid aquifers.

The following four sections summarize the results of the groundwater catchment delineation, water budget estimation, and surface geophysics evaluation, as well as make recommendations for future work.

GROUNDWATER CATCHMENT DELINEATION

This section summarizes the results of groundwater catchment delineation in the arid Cuatrocienegas Basin karst aquifer system using sparse hydrogeologic data, geologic mapping, and remotely sensed topographic data to create maps of regional groundwater flow. Geographic information system catchment delineation routines are used in conjunction with field geomorphology observations (i.e., basin outlet canyons 100s of meters deep) and fish fauna (Echelle and Echelle, 1998) to delineate surface drainages in past pluvial periods. These occurred during one of many Holocene wet periods (Castiglia and Fawcett, 2006). This evidence suggest a river system flowed from the Sierra Madre Occidental (the Continental Divide with the Pacific Ocean) through a series of now dry desert lakes, through the Cuatrocienegas Basin, and out to the Río Grande. The author maps an approximately 91,000-square kilometer basin upgradient of the Cuatrocienegas Basin that drained the Sierra Madre Occidental and linked Río Nazas and Río Aguanaval with the Río Grande through the Cuatrocienegas Basin. The chloride balance recharge approach indicates that approximately 18,000 square kilometers of this 91,000-square kilometer upgradient area contributes to the flow system that discharges in the Cuatrocienegas Basin today. Within the approximately 18,000 square kilometer recharge area, a water-balance and chloride-balance recharge evaluation with a variable recharge rate by elevation shows that approximately 11,000 square kilometers of exposed carbonate mountains comprise the recharge area — recharge on the remaining approximately 7,000 square kilometers of valleys is essentially zero.

As the northeast Mexico regional climate dried (Castiglia and Fawcett, 2006), surface water drainages became truncated and retreated to the subsurface. In the present hydrologic conditions, regional carbonate aquifers exist and take advantage of the regional topographic gradient to flow towards the Cuatrocienegas Basin, which is a regional topographic sink. An analytical model and noble gas recharge elevation estimation show that interbasin groundwater flow is plausible under topographic divides between valleys (e.g., the Hundido and Sobaco Valleys). The Cuatrocienegas Basin represents a low elevation discharge zone to this regional aquifer system.

Results of synoptic spring water sampling event during summer 2007 indicate most Cuatrocienegas Basin spring water has <0.1 tritium units, which suggests that spring water has an aquifer residence time of at least 50 years, and perhaps much longer. Thus, the majority of Cuatrocienegas Basin spring discharge is likely recharged from regional catchments outside the Cuatrocienegas Basin, with minor local flow components. Regional flow provides groundwater to nearly constant-discharge, elevated total dissolved solids, and elevated temperature springs in the Cuatrocienegas Basin on the west and northern flanks of the Sierra San Marcos that do not respond to localized rainfall. Recharge on the Sierra San Marcos explains lower chloride concentrations, discharge rates, and temperatures observed in springs on the southeast flank of the Sierra San Marcos that feed the Santa Tecla Canal.

Stable isotopic data (i.e., $\delta^{18}\text{O}$) suggest that spring discharge originates as mountain precipitation falling above approximately 1,200 meters. Precipitation below this elevation is lost to evapotranspiration and does not result in appreciable groundwater recharge. Low permeability late-stage calcic soils limit recharge on Cuatrocienegas Basin alluvial fans. Noble gas data collected in spring water during summer 2007 suggest groundwater recharge occurs between 703–768 meters, consistent with a thick vadose

zone in a karstified carbonate aquifer. These relatively low recharge elevations support analytical model results that topographic divides do not represent groundwater divides and that interbasin groundwater flow occurs under the mountains separating the basins of the Cuatrociénegas Basin region.

WATER BUDGET ESTIMATION

This section summarizes the results of the regional water budget estimation. The author measured discharge of the Saca Salada and Santa Tecla Canal discharge during the study period (January 2005–February 2008) with a Flow Tracker acoustic Doppler velocimeter, an integrated tool for discharge measurement. This section also addresses the question “What components comprise the regional water budget?”

The author finds the water budget includes approximately 35,000,000 cubic meters/year leaving the Cuatrociénegas Basin through the two basin outlet canals. Thus, recharge to Cuatrociénegas Basin springs must be at least this volume. The recharge zones delineated by this research are probably conservatively sized. The discharge of Poza La Becerra, the largest spring in the basin (located in the west sub-basin), was also measured. This spring also was gaged by this study and has relatively constant discharge of approximately 580 liters/second (approximately 18,300,000 cubic meters/year) over the study period. Flow from Poza La Becerra eventually flows into the Saca Salada Canal.

In addition to discharge, spring temperature and precipitation during a summer monsoon period of six weeks was measured. Poza La Becerra (32.0° – 34.0°C) and Poza Escobedo (35.0°C) have elevated temperatures indicative of regional groundwater flow at a depth of up to 760 meters. Poza Santa Tecla, at the head of the Santa Tecla Canal, has lower temperature ($\sim 30.0^{\circ}\text{C}$) that decreases ($\sim 2.0^{\circ}$ – 6.0°C) in response to local precipitation. Thus, east basin springs also have elevated temperature indicative of a

deeper flow component up to a depth of 560 meters in addition to a minor local precipitation contribution to spring flow. As part of the temperature monitoring component of the research project, Wolaver and Sharp (2007) find that current models of the Thermochron iButton temperature loggers are susceptible to complete data loss because of leakage previously unreported in the literature (Johnson et al., 2005).

SURFACE GEOPHYSICS EVALUATION

This section summarizes the evaluation of subsurface controls on spring location with gravity geophysical surveys. The study finds that fractures associated with a reverse fault on the west flank of the Sierra San Marcos permits high-discharge flow from a deep regional Cretaceous carbonate aquifer. Gravity surveys discounted the presence of major faults and subsurface structures on the east flank of the Sierra San Marcos. Instead, in the east sub-basin, ancestral stream-incised canyons intersect the potentiometric surface permitting relatively low groundwater discharge to the base of permeable alluvial fans. Here, spring discharge is caused by precipitation falling on the Sierra San Marcos.

CONCLUSIONS

For this research project, an integrative data approach is developed that provides a framework for the evaluation of recharge areas in developing arid karst aquifer systems. The author tests this approach in the Cuatrocienegas Basin and confirms it can be applied to other developing aquifers with sparse hydrogeologic data globally. To this end, disparate geologic data are integrated, including field observations, historical hydrologic data that may be anecdotal human narratives, and all other available data, including geologic maps, digital elevation models, geographic information systems, analytical models, water quality parameters, environmental isotopes, spring discharge data, and land

gravimetry surveys to evaluate recharge areas to support development of effective groundwater management policies.

In the Cuatrocienegas Basin, this research refutes the hypothesis that all spring discharge is locally derived (Rodríguez et al., 2005a). Instead, spring discharge originates from a predominantly regional flow system. Because a regional flow system supports Cuatrocienegas Basin springs, the author recommends that groundwater policy should also include provisions for the effective management of basins upgradient to the Cuatrocienegas Basin.

RECOMMENDATIONS FOR FUTURE WORK

This research improves the understanding of the hydrogeology of the Cuatrocienegas Basin region. The research project also develops an integrative data approach for delineation of arid karst aquifer systems that may be applied globally. This doctoral research project sets the stage for additional post graduation research. A partial list of journal articles (with the proposed title shown in italics) that expands upon this doctoral research project is provided below.

1. **Projected climate change effects on groundwater recharge in semi-arid northeast Mexico.** This research project would expand upon the author's presentation at the 2007 Meeting of the American Geophysical Union in San Francisco, California (Wolaver, 2007) to assess the effects of projected climate change on northeast Mexico recharge with implications for other semi-arid mountainous regions.

2. **Hydrologic system along the Sonora-Mojave Megashear: deeply derived fluids of the San Marcos Fault Zone, northeast Mexico.** Preliminary noble gas sampling for this research project to infer recharge elevation also generated helium isotopic data. These helium isotopic data suggest the presence of deeply derived fluids influenced by mantle degassing. This proposed research would use additional helium isotopic data to refine the conceptual understanding of basement-involved faults along the San Marcos Fault Zone that runs through the study area of this doctoral research project.
3. **Hydrogeology of a unique groundwater-dependent ecosystem: Cuatrocienegas Basin, Mexico.** The author would like to publish a summary “case-study” type article that documents the current hydrogeologic conceptual understanding of the Cuatrocienegas Basin in one article that can be used as a key reference for future researchers in the area.
4. **Using digital elevation models to identify paleodrainage networks: northern Mexico flow from the Continental Divide to the Río Grande.** Topography upgradient to the Cuatrocienegas Basin leads to the Río Nazas, a river draining a portion of the Sierra Madre Occidental. Surface water discharge to the east of the Cuatrocienegas Basin would flow to the Río Grande. The author would like to publish an article on a now dry surface water system that flowed from the Sierra Madre Occidental, through the Cuatrocienegas Basin, to the Gulf of Mexico using this surface water delineation, field observations of outlet canyons downstream and upstream of the Cuatrocienegas Basin and fish fauna from Mexico and Texas.

5. **Insights into past climate change from modern stromatolites.** The author would like to research the possibility of using trace elements in stromatolites to make inferences on past climatic conditions using modern day Cuatrociénegas Basin stromatolites.
6. **On an integrated paleoclimate record in northeast Mexico.** The author would like to conduct research on a multi-temporal and multi-frequency paleoclimate record of northeast Mexico. The paleoclimate research project would use tree rings, uranium-series dates of travertine and speleothems, pollen, and carbon-14 analyses of sediment cores to develop insights into paleoclimate and future water resources for this arid region of Mexico.
7. **On using satellite-derived precipitation to estimate groundwater recharge.** Precipitation gages are often preferentially installed at lower elevations near population centers in semi-arid, mountainous regions, such as northeast Mexico. However, mountain recharge dominates and sparse mountain gages complicate recharge estimation. PERSIANN satellite precipitation estimates (Hsu et al., 1997; Sorooshian et al., 2000) do not effectively estimate Cuatrociénegas Basin precipitation. The author would like to refine spatially-distributed precipitation estimates with other satellite precipitation products to improve recharge calculations for enhanced water resource management in northeast Mexico. Long-term precipitation gage records need to be evaluated for a larger area and for a greater elevation range. In addition, more precipitation gages need to be installed in the mountain areas where recharge dominates to augment the existing network of gages that is preferentially located at low elevations.

SIGNIFICANCE OF STUDY AND APPLICABILITY TO OTHER AREAS GLOBALLY

This study makes a fundamental contribution to the field of hydrogeology by developing and applying an integrative data approach to characterize arid, karst aquifers. As global population expands into undeveloped arid regions, this approach can be used to develop hydrogeologic conceptual models in support of effective groundwater management.

UN PUNTO DE PARTIDO (A POINT OF DEPARTURE)

As population expands globally, particularly in arid and semi-arid regions, the need for effective water resource management will be ever increasing. Whereas this study focuses on the Cuatrocienegas Basin of northeaster Mexico, the problems addressed by this research pertain to analogous regions globally. How can society effectively manage scarce water resources for municipal, agricultural, and industrial needs and simultaneously provide adequate water to preserve healthy ecosystems and enhance recreational opportunities? The research included in this dissertation augments and expands upon previous research in arid region karst hydrogeology. Hopefully this research project will serve as a point of departure upon which future research benefiting humanity will continue...

Appendix A

Thermochron iButton: Limitation of this inexpensive and small-diameter temperature-logger

This section is based primarily upon Wolaver and Sharp (2007).

Introduction

The purpose of this Technical Note is to inform the reader of an important limitation of the Thermochron iButton that may lead to data loss because of water leakage. Johnson et al. (2005) evaluate the performance of the Thermochron iButton, an inexpensive, small-diameter temperature logger manufactured by Dallas Semiconductor (a subsidiary of Maxim Integrated Products, Sunnyvale, California). The Thermochron iButton is traditionally used to track fresh food shipping temperature and recently used for hydrogeology applications. The Thermochron iButton is an attractive new tool for hydrogeologists because it collects high-resolution shallow water temperature data for a fraction of the cost and size of traditional temperature loggers, permitting multiple-logger deployment in tight areas like small-diameter monitoring wells. Recent field testing of the Thermochron iButton in fresh water springs at ambient temperatures and water depths less than six meters for a period of seven weeks resulted in the loss of data in some temperature loggers because of water leakage. Johnson et al. (2005) did not encounter this problem with earlier Thermochron iButtons.

Field Deployment: Successes and Failures

We installed eight high-resolution Thermochron iButtons at water depths of approximately two–six meters in freshwater springs of the Cuatrocienegas Basin, Coahuila, Mexico in mid-June 2006 (temperatures 30.0°–34.0°C, specific conductance 2,300–2,500 microsiemens/centimeter at 25°C). When we attempted to retrieve temperature data from the loggers after seven weeks, communication was not possible with three (3) loggers, and an error message was displayed (“Invalid CRC16 read from device”).

Our findings are contrary to those of Johnson et al. (2005), who suggest successful deployment and data retrieval from iButton Thermochrons (without iButton capsules) installed at depths of up to five meters for a time period as long as 12 months (and depths perhaps as great as 15 meters) without any waterproof protection.

Thermochron iButton: Design Updates

Dallas Semiconductor recently has made available a waterproof iButton Capsule (Model DS9107, approximately \$30, Figure 1) that corrects for this design limitation. In addition, the waterproof iButton Capsule increases the size of the device from 17.35 by six millimeters (Johnson et al. 2005) to approximately 35 by 25 millimeters (Dallas Semiconductor 2006). However, the iButton Capsule has two (2) stainless steel screws that may facilitate deployment in small-diameter monitoring wells.

Summary

iButton Thermochron temperature loggers offer a low-cost, small-diameter solution for high-resolution temperature measurement. However; a water leakage problem in current models may result in complete logger failure in installations as shallow as two meters in fresh water at ambient temperatures. In the summer of 2006, Dallas Semiconductor began offering the previously unavailable waterproof iButton Capsule (model DS9107) that facilitates deployment of iButton Thermochron loggers for hydrogeology applications. The waterproof iButton Capsule adds approximately \$30 to the base price of an iButton Thermochron (\$15–\$40, depending on temperature range and resolution). The size of the iButton Thermochron also is increased by approximately eight times (from a volume standpoint) by the waterproof capsule, making it nearly the same size as other temperature loggers Johnson et al. (2005). Ultimately, price, size, and application requirements should guide the purchase of an appropriate temperature logger.

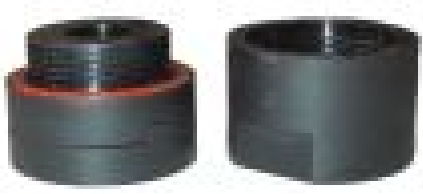


Figure 1. iButton capsule. Diameter = 25.4 millimeters.

References

- Activation Laboratories, 2008, Code Ultratrace-3 [Online]
http://www.actlabs.com/methsub_codeut3.htm [accessed on May 12, 2008].
- Adam, J.C., Clark, E.A., Lettenmaier, D.P., and Wood, E.F., 2006, Correction of global precipitation products for orographic effects: *Journal of Climate*, v. 19, p. 15–38.
- Adkins, W.S., 1920, Cuatrocienegas, Coahuila — water resources: Walter Scott Adkins Collection, Center for American History, The University of Texas at Austin, Austin, Texas, COL2/M329, AR89–194, 19 p.
- Aeschbach-Hertig, W., Peeters, F., Beyerle, U., and Kipfer, R., 2000, Palaeotemperature [sic] reconstruction from noble gases in ground water taking into account equilibrium with entrapped air: *Nature*, v. 405, p. 1040–1044.
- Allison, G.B., and Barnes, C.J., 1985, Estimation of evaporation from the normally “dry” Lake Frome in South Australia: *Journal of Hydrology*, v. 78, p. 229–242.
- American Water Works Association, 1998, 4500-Cl⁻ B. Argentometric Method, *in* Clesceri, L.S., Greenberg, A.E., Eaton, A.D., eds., Standard methods for the examination of water and wastewater, 20th Edition: Washington, D.C., p. 4-67–4-68.
- Anderholm, S.K., 2000, Mountain-front recharge along the eastern side of the Middle Río Grande Basin, central New Mexico: U.S. Geological Survey Water-Resource Investigations Report 00-4010, 44 p.
- Andring, M.J., Wolaver, B.D., Sharp J.M., Jr., and Banner, J.L., 2006, Analyzing groundwater flowpaths in a karstic basin using cross-plots of major ions: Cuatrocienegas Basin, Coahuila, Mexico: *Geological Society of America Abstracts with Programs* v. 38, p. 288.
- Anning, D.W., and Konieczki, A.D., 2005, Classification of hydrogeologic areas and hydrogeologic flow systems in the Basin and Range physiographic province, southwestern U.S.: U. S. Geological Survey Professional Paper 501-D, 37 p.
- Back, W., 1966, Hydrochemical facies and groundwater flow patterns in northern part of Atlantic Coastal Plain: U. S. Geological Survey Professional Paper 498-A, 42 p.
- Badino, G., Bernabei, T., De Vivo., A., Giulivio, I., and Savino, G., 2004, Under the Desert: the mysterious waters of Cuatrocienegas: Treviso, Italy, Associazione Geografica La Venta, 272 p.
- Banner, J.L., Wasserburg, G.J., Dobson, P.F., Carpenter, A.B., and Moore, C.H., 1989, Isotopic and trace element constraints on the origin and evolution of saline

- groundwaters from central Missouri: *Geochimica et Cosmochimica Acta*, v. 53, p. 383–398.
- Banner, J.L., and Kaufman, J., 1994, The isotopic record of ocean chemistry and diagenesis preserved in non-luminescent brachiopods from Mississippian carbonate rocks, Illinois and Missouri: *Geological Society of America Bulletin*, v. 106, p. 1074–1082.
- Banner, J.L., 1995, Application of the trace element and isotope geochemistry of strontium to studies of carbonate diagenesis: *Sedimentology*, v. 42, p. 805–824.
- Banner, J.L., 2004, Radiogenic isotopes: systematics and applications to earth surface processes and chemical stratigraphy: *Earth-science reviews*, v. 65, p. 141–194.
- Bedinger, M.S., Langer, W.H., and Reed, J.E., 1986, Synthesis of hydraulic properties of rocks with reference to the basin and range province, southwestern United States, in *Selected papers in the hydrologic sciences*: U.S. Geological Survey Water-Supply Paper 2310, 142 p.
- Bedinger, M.S., and Harrill, J.R., 2006, Analytical regression stage analysis for Devils Hole, Death Valley National Park, Nevada: *Journal of the American Water Resources Association*, v. 42, p. 827–839.
- Belcher, W.R., Sweetkind, D.S., Elliott, P.E., 2002, Probability distributions of hydraulic conductivity for the hydrogeologic units of the Death Valley regional ground-water flow system, Nevada and California: U.S. Geological Survey Water-Resources Investigations Report 02-4212, 18 p.
- Beven, K., 1993, Prophecy, reality and uncertainty in distributed hydrologic modelling: *Advances in Water Resources*, v. 16, p. 41–51.
- Bigeleisen, J., Perlman, M.L., and Prosser, H.C., 1952, Conversion of hydrogenic materials for isotopic analysis: *Analytical Chemistry*, v. 24, p. 1356–1357.
- Blackwell, D.D., Steele, J.L., Carter, L.C., 1990, Heat flow patterns of the North American continent: A discussion of the DNAG geothermal map of North America, in Slemmons, D.B., Engdahl, E.R., Zoback, M.D., and Blackwell, D.D., eds., *Neotectonics of North America*: Boulder, Colorado: Geological Society of America, Decade Map v. 1.
- Bralower, T.J., Fullagar, P.D., Paull, C.K., Dwyer, G.S., and Leckie, R.M., 1997, Mid-Cretaceous strontium-isotope stratigraphy of deep-sea section: *Geological Society of America Bulletin*, v. 109, p. 1421–1442.
- Brouste, L., Marlin, C., and Drever, L., 1997, Geochemistry and residence time estimation of groundwater from the upper aquifer of the Chihuahua desert (Comarca Lagunera, Northern Mexico): *Applied Geochemistry*, v. 12, p. 775–786.

- Buchanan, T.J., and Somers, W.P., 1982, Stage measurement at gaging stations: U.S. Geological Survey, Techniques for Water-Resource Investigations, Book 3, Chapter A7, 28 p.
- Bushman, M., McBride, J.H., Nelson, S.T., and Mayo, A.L., 2005, Preliminary results from a shallow, high-resolution seismic survey and potential field data filtering near Devil's Hole at Ash Meadows, Nevada: Geological Society of America Abstract with Programs, v. 37, p. 373.
- Calegari, V., 1997, Environmental perceptions and local conservation efforts in Cuatrocienegas, Coahuila, Mexico [M.S. thesis]: The University of Texas at Austin, 133 p.
- Carter, R.W., and Davidian, J., 1968, General procedure for gaging streams: U.S. Geological Survey, Techniques for Water-Resource Investigations, Book 3, Chapter A6, 13 p.
- Castiglia, P.J., and Fawcett, P.J., 2006, Large Holocene lakes and climate change in the Chihuahuan Desert: Geology; v. 34, p. 113–116.
- Castro, M.C., Hall, C.M., Patriarche, D., Goblet, P., and Ellis, B.R., 2007, A new noble gas paleoclimate record in Texas — Basic assumptions revisited: Earth and Planetary Science Letters; v. 257, p. 170–187.
- Cey, B.D., 2008, Dissolved noble gases in groundwater [Ph.D. dissertation]: The University of Texas at Austin, 255 p.
- Chávez-Cabello, G., Aranda-Gómez, J.J., Molina-Garza, R.S., Cossío-Torres, T., Arvizu-Gutiérrez, I.R., González-Naranjo, G.A., 2005, La Falla San Marcos: una estructura Jurásica de basamento multirreactivada del noreste de México: Boletín de la Sociedad Geológica Mexicana, Volumen Commemorativo Del Centenario, Grandes Fronteras Tectónicas De México, Tomo Lvii, Núm. 1, p. 27–52.
- Clark, W.B., Jenkins, W.J., and Top, Z., 1976, Determination of tritium by mass spectrometric measurements of ${}^3\text{He}$: International Journal of Applied Radioactive Isotopes, v. 27, p. 515–522.
- Collins, D., 1925, Temperature of water available for industrial use in the United States: U.S. Geological Survey Water-Supply Paper 520-F, p. 97–104.
- Coplen, T.B., 1996, New guidelines for reporting stable hydrogen, carbon, and oxygen isotope-ratio data: Geochimica et Cosmochimica Acta, v. 60, p. 3359–3360.
- Cortés, A., Durazo, J., and Farvolden, R.N., 1997, Studies of isotopic hydrology of the basin of Mexico and vicinity: annotated bibliography and interpretation: Journal of Hydrology, v. 198, p. 346–376.
- Cortés, A., Durazo, J., 2001, Tendencia del Oxígeno-18 en la precipitación del centro de México: Revista Ingeniería Hidráulica en México, v. 26, p. 93–102.
- Craig, H., 1961, Isotopic variations in meteoric waters: Science, v. 133, p. 1702–1703.

- Crossey, L.J., Fischer, T.P., Patchett, P.J., Hilton, D.R., Newell, D.L., Huntoon, P., Reynolds, A.C., Leeuw, G.A.M., 2006, Dissected hydrologic system at the Grand Canyon: Interaction between deeply derived fluids and plateau aquifer waters in modern springs and travertine: *Geology*, v. 34, p. 25–28.
- Crossey, L.J., 2008, Personal Communication, Professor, Department of Earth and Planetary Sciences, The University of New Mexico, Albuquerque.
- Dallas Semiconductor 2006. DS9107 iButton Capsule Data Sheet [Online]: <http://datasheets.maxim-ic.com/en/ds/DS9107.pdf>.
- Darling, B. K., Hibbs, B. J., and Dutton, A. R., 1994, Ground-water hydrology and hydrochemistry of Eagle Flat and surrounding area: The University of Texas at Austin, Bureau of Economic Geology contract report, prepared for the Texas Low-Level Radioactive Waste Disposal Authority under Interagency Contract IAC (92-93)-0910, 137 p.
- Darling, B.K., 1997, Delineation of the ground-water flow systems of the Eagle Flat and Red Light Basins of Trans-Pecos Texas [Ph.D. dissertation]: The University of Texas at Austin, 179 p.
- Davis, S.N., Whittemore, D.O., Fabryka-Martin, J., 1998, Use of chloride/bromide ratios in studies of potable water: *Ground Water*, v. 36, p. 338–350.
- De Gregorio, S., Gurrieri, S., and Valenza, M., 2005, A PTFE membrane for the in situ extraction of dissolved gases in natural waters: Theory and application: *Geochemistry, Geophysics, Geosystems*, v. 6, p. 1–13.
- DeMott, L.M., 2007, Travertine deposits as records of groundwater evolution in urbanizing environments [M.S. thesis]: The University of Texas at Austin, 269 p.
- Dettinger, M.D., 1989, Reconnaissance estimates of natural recharge to desert basins in Nevada, U.S.A. by using chloride-balance calculations: *Journal of Hydrology* v. 106, p. 55–78.
- Dionex, 2003, Determination of anions in acid rain by ion chromatography: Application Update 146, 5 p.
- Drever, J.I., 1997, The geochemistry of natural waters: surface and groundwater environment: Princeton, New Jersey, Prentice Hall, 436 p.
- Eakin, T.E., and Moore, D.O., 1964, Uniformity of Discharge of Muddy River Springs, Southeastern Nevada, and Relation to Interbasin Movement of Ground Water: U.S. Geological Survey Professional Paper 501-D, p. D171–D176.
- Eakin, T.E., 1966, A regional interbasin groundwater system in the White River area, southeastern Nevada: *Water Resources Research*, v. 2, p. 251–271.
- Eakin, T.E., Price, D., and Harrill, J.R., 1976, Summary appraisals of the nation's ground-water resources — Great Basin region. U.S. Geological Survey Professional Paper 813-G, 36 p.

- Echelle, A.A., and Echelle, A.F., 1998, Evolutionary Relationships of Pupfishes in the *Cyprinodon eximius* Complex (Atherinomorpha: Cyprinodontiformes): Copeia, v. 1998, p. 752–865.
- Edmonston, K. 2006. Personal Communication. Software Developer, Dallas Semiconductor, Maxim Integrated Products, Sunnyvale, California.
- Eguiluz de Antuñano, S. 2001, Geologic evolution and gas resources of the Sabinas Basin in northeastern Mexico, in Bartolini, C., Buffler, R.T., and Cantú-Chapa, A., eds., The western Gulf of Mexico Basin: Tectonics, sedimentary basins, and petroleum systems: American Association of Petroleum Geologists Memoir 75, p. 241–270.
- Erslev, E.A., and Mayborn, K.R., 1997, Multiple geometries and modes of fault-propagation folding in the Canadian thrust belt: Journal of Structural Geology, v. 19, p. 321–335.
- Epstein, S., and Mayeda, T., 1953, Variations of O¹⁸ content of waters from natural sources: *Geochimica et Cosmochimica Acta*, v. 4, p. 213–224.
- Evans, S.B., 2005, Using geochemical data to define flow systems in Cuatrocienegas, Coahuila, Mexico [M.S. thesis]: The University of Texas at Austin, 114 p.
- Fedra, K., 1993, GIS and environmental modeling, in Goodchild, M.F., Parks, B.O., and Steyaert, L.T., Environmental Modeling with GIS: New York, p. 35–50.
- Fett, J., 1992, Instructional manual: Model G and D gravity meters: LaCoste and Romberg Gravity Meters, Inc., Austin, Texas, 127 p.
- Fontes, J.C., Yousfi, M., and Allison, G.B., 1986, Estimation of long-term, diffuse groundwater discharge in the Northern Sahara using stable isotope profiles in Soil Water: *Journal of Hydrology*, v. 86, p. 315–327.
- Fournier, N., Rymer, H., Williams-Jones, G., and Brenes, J., 2004, High-resolution gravity survey: Investigation of subsurface structures at Poás volcano, Costa Rica: *Geophysical Research Letters*, v. 31, p. L15602–L15606.
- Freeze, R.A., and Witherspoon, P.A., 1967, Theoretical analysis of regional groundwater flow; [Part] 2, Effect of water-table configuration and subsurface permeability variation: *Water Resources Research*, v. 3, p. 623–634.
- Gallardo, P.A. 2006. Email interview, July 3, Mexico City, Mexico.
- Gates, J.S., White, D.E., Stanley, W.D., and Ackerman, H.D., 1980, Availability of fresh and slightly saline ground water in the basins of westernmost Texas: Texas Department of Water Resources, Report no. 256, 108 p.
- Gay, D., C. Lehmann, J. Rothert, M. Rhodes, 2008, Quality assurance plan, Central Analytical Laboratory: National Atmospheric Deposition Program, NADP QA Plan 2008-01, 59 p.
- Geosoft Inc., 2001, Oasis Montaj 5.1.2 quick start tutorials: Toronto, Ontario, Geosoft Inc., 245 p.

- Ghoddousi-Fard, R., and Dare, P., 2006, Online GPS processing services: An initial study: *GPS Solutions*, v. 10, p. 12–20.
- Gillespie, J.M., Stephen, T., Mayo, A.L. and Parks, E., 2007, Preliminary analysis of groundwater residence and aquifer segmentation in the Central Great Basin: Geological Society of America Abstracts with Programs v. 39, p. 46.
- Gilmore, R.M., 1947, Report on a collection of mammal bones from archeologic cave-sites in Coahuila, Mexico: *Journal of Mammalogy*, v. 28, p. 147–165.
- Gladney, E.S., Burns, C.E., and Roelandts, I., 1984, 1982 compilation of elemental concentration data for the United States Geological Survey's Geochemical Exploration Reference Samples GXR-1 to GXR-6, *Geostandards and Geoanalytical Research*, v. 8, p. 119–154.
- Gochis, D.J., Shuttleworth, W.J., and Yang, Z.L., 2005, Sensitivity of the modeled North American monsoon regional climate to convective parameterization: *Monthly Weather Review*, v. 130, p. 1282–1298.
- Gochis, D.J., Brito-Castillo, L., and Shuttleworth, J., 2006, Hydroclimatology of the North American monsoon region in northwest Mexico: *Journal of Hydrology*, v. 316, p. 53–70.
- Goldhammer, R.K., 1999, Mesozoic sequence stratigraphy and paleogeographic evolution of northeast Mexico: *Geological Society of America Special Paper* 340, 54 p.
- Goldman, E.A., 1951, Biological investigations in Mexico: *Smithsonian Miscellaneous Collection* 115, 476 p.
- Gonzalez-Partida, E., and Carrillo-Chávez, A., 2001, Petroleum-rich fluid inclusions in fluorite, Coahuila, Mexico; implications for sources of oil and fluorine: *Geological Society of America Abstract with Programs*, v. 33, p. 420.
- González, M., 2006, Personal Communication, Cuatrocienegas, Mexico.
- Hall, O., Falorni, G., and Bras, R.L., 2005, Characterization and quantification of data voids in the Shuttle Radar Topography Mission data: *Geoscience and Remote Sensing Letters* v. 2, p. 177–181.
- Hammer, S., 1939, Terrain corrections for gravimeter stations: *Geophysics*, v. 4, p. 184–194.
- Hawley, J.W., 1993, Geomorphic setting and late quaternary history of pluvial-lake basins in the southern New Mexico region: *New Mexico Bureau of Mines and Mineral Resources Open-File Report* 391, 28 p.
- Heilweil, V.M., Earle, J.D., Cederberg, J.R., Messer, M.M., Jorgensen, B.E., Verstraeten, I.M., Moura, M.A., Querido, A., Spencer, F., and Osório, T., 2006, Evaluation of baseline ground-water conditions in the Mosteiros, Ribeira Paul, and Ribeira Faja

- Basins, Republic of Cape Verde, West Africa, 2005-06 Survey: U.S. Geological Survey Scientific Investigations Report 2006-5207, 42 p.
- Helm, P.J., Breed, C.S., Tigges, R., and Garcia, P.A., 1995, Geometeorological data collected by the USGS Desert Winds Project at Gold Spring, Great Basin Desert, northeastern Arizona, 1979–1992: U.S. Geological Survey Open-File Report 95-361.
- Hendrickson, D.A., 2005, Personal Communication. Teaching Faculty, Section of Integrative Biology, and Curator of Ichthyology at the Texas Memorial Museum, The University of Texas at Austin.
- Hendrickson, D.A., García de León, F.J., and Souza, V., 2005, Proceedings of the First Meeting of Cuatrocienegas Researchers; Memorias de la Primera Junta de Investigadores de Cuatrocienegas, 49 p.
- Hendrickson, D.A., Marks, J.C., Moline, A.B., Dinger, E.C., and Cohen, A.E., 2008, Combining ecological research and conservation: a case study in Cuatro Ciénegas, Mexico, *in* Stevens, L., and Meretsky, V. J., eds., Aridland Springs in North America, Tucson, 432 p.
- Hennings, P.H., Olson, J.E., and Thompson, L.B., 2000, Combining outcrop data and three-dimensional structural models to characterize fractured reservoirs: an example from Wyoming: American Association of Petroleum Geologists Bulletin, v. 84, p. 830–849.
- Hermance, J.F., 1998, A mathematical primer on groundwater flow: An introduction to the mathematical and physical concepts of saturated flow in the subsurface: Princeton, New Jersey, Prentice Hall, 230 p.
- Hibbs, B.J., and Darling, B.K., 2005, Revisiting a classification scheme for U.S.-Mexico alluvial basin-fill aquifers: Groundwater v. 43, p. 750–763.
- Hubbert, M.K., 1940, The theory of groundwater motion: Journal of Geology, v. 48, p. 785–944.
- Hsu, K., Gao, X., Sorooshian, S., and Gupta, H.V., 1997, Precipitation estimation from remotely sensed information using artificial neural networks: Journal of Applied Meteorology, v. 36, p. 1176–1190.
- Instituto Nacional de Estadística Geografía e Informática (INEGI), 1975, Carta Geológica, Cuatro Ciénegas: Instituto Nacional de Estadística Geografía e Informática Mapa G13B59, scale 1:50,000, 1 sheet.
- Jacob, C.E., 1943, Correlation of ground-water levels and precipitation on Long Island, New York: Part 1, Theory: Transactions, American Geophysical Union v. 24, p. 564–573.
- Jamason, P., Bock, Y., Fang, P., Gilmore, B., Malveaux, D., Prawirodirdjo, L., and Scharber, M., 2004, SOPAC Web site (<http://sopac.ucsd.edu>): GPS solutions, v. 8, p. 272–277.

- Jansen, J.; King, M.J.; Loughry, J.; Powell, T.; and Laymon, D., 2004, An overview of Inyo County's 2003 Death Valley California area geophysical program: *in* Proceedings of the Symposium on the Application of Geophysics to Environmental and Engineering Problems SAGEEP, v. 2004, p. 981–991.
- Jenkyns, H.C., Paull, C.K., Cummins, D.I., and Fullagar, P.D., 1995, Strontium-isotope stratigraphy of Lower Cretaceous atoll carbonates in the Mid-Pacific Mountains, *in* Winterer, E.L., Sager, W.W., Firth, J.V., and Sinton, J.M., eds., Proceedings of the Ocean Drilling Program: Ocean Drilling Program Scientific Results, v. 143, p. 89–97.
- Johannesson K.H., Cortés, A., and Kilroy, K.C., 2004, Reconnaissance isotopic and hydrochemical study of Cuatro Ciénelas groundwater, Coahuila, México: Journal of South American Earth Sciences, v. 17, p. 171–180.
- Johnson, A.N., Boer, B.R., Woessner, W.W., Stanford, J.A., Poole, G.C., Thomas, S.A., and O'Daniel, S.J., 2005, Evaluation of an inexpensive small-diameter temperature logger for documenting groundwater-river interactions: Groundwater Monitoring & Remediation, v. 25, p. 68–74.
- Junge, C.E., and Werby, R.T., 1958, The concentration of chloride, sodium, potassium, calcium, and sulfate in rain water over the United States: Journal of Meteorology, v. 15, p. 417–425.
- Kolb, T. 2005. Email Interview. February 7, Flagstaff, Arizona.
- Krueger, D. 2008, Personal Communication, President, Geochron Laboratories, Cambridge, Massachusetts.
- Kushnir, J., 1980, The coprecipitation of strontium, magnesium, sodium, potassium and chloride with gypsum, an experimental study: *Geochimica et Cosmochimica Acta*, v. 44, p. 1471–1482.
- Laenen, A., 1985, Acoustic velocity meter systems: U.S. Geological Survey, Techniques for Water-Resource Investigations, Book 3, Chapter A17, 38 p.
- LaFehr, T.R., 1991, Standardization in gravity reduction: *Geophysics*, v. 56, p. 1170–1178.
- Lamb, D., Bowersox, V., 2000, The national atmospheric deposition program: an overview: *Atmospheric Environment*, v. 34, p. 1661–1663.
- Langenheim, V.E., Hoffmann, J.P., Blasch, K.W., Dewitt, E., and Wirt, L., 2002, Preliminary report on geophysical data in Yavapai County, Arizona: U.S. Geological Survey Open-File Report 02-352, 19 p.
- Langenheim, V., 2005, Personal Communication, Geophysicist, U.S. Geological Survey, Menlo Park, California.
- Lehmann, C., Osleger, D.A., Montanez, I.P., Sliter, W.V., Arnaud-Vanneau, A., and Banner, J.L., 1999, Evolution of Cupido and Coahuila carbonate platforms, early

- Cretaceous, northeastern Mexico: Geological Society of America Bulletin, v. 111, p. 1010–1029.
- Lehmann, C., Osleger, D.A., Montanez, I.P., 2000, Sequence stratigraphy of Lower Cretaceous (Barremian–Aptian) carbonate platforms of northeastern Mexico: regional and global correlations: Journal of Sedimentary Research, v. 70, p. 373–391.
- Lesser y Asociados, 2001, Sinopsis del estudio de evaluación hidrogeológica e isotópica en el Valle del Hundido, Coahuila: Comisión Nacional del Agua, Subdirección General Técnica, Gerencia de Aguas Subterráneas, 125 p.
- Lisle, R.J., 2006, Google Earth: a new geological resource: Geology Today, v. 22, p. 29–32.
- Lu, F.H., Meyers, W.J., Schoonen, M.A.A., 1997, Minor and tracer element analyses on gypsum: an experimental study: Chemical Geology, v. 142, p. 1–10.
- Mace, R.E., Angle, E.S., and Mullican, W.F., 2004, Aquifers of the Edwards Plateau: Texas Water Development Board Report 360, 366 p.
- Mack, L., 2008, Personal Communication, Austin, Texas.
- Mahlknecht, J., Schneider, J.F., Merkel, B.J., Navarro de León, I., and Bernasconi, S.M., 2004, Recharge in a sedimentary basin in semi-arid Mexico: Hydrogeology Journal, v. 12, p. 511–530.
- Maidment, D.R., 2002, Arc Hydro: GIS for Water Resources: Redlands, California, ESRI Press.
- Mamyrin, B.A., and Tolstikhin, I.N., 1984, Helium Isotopes in Nature: New York, Elsevier, 273 p.
- Manning, A.H., and Solomon, D.K., 2003, Using noble gases to investigate mountain-front recharge: Journal of Hydrology, v. 275, p. 194–2007.
- Marrett, R., and Bentham, P.A., 1997, Geometric analysis of hybrid fault-propagation/detachment folds: Journal of Structural Geology, v. 19, p. 243–248.
- Marrett, R., and Aranda-García, M., 2001, Regional structure of the Sierra Madre Oriental fold-thrust belt, Mexico, in Marrett, R., ed., Genesis and controls of reservoir-scale carbonate deformation, Monterrey Salient, Mexico: Bureau of Economic Geology, Guidebook 28, p. 31–56.
- Maxey, G.B., and T.E. Eakin, 1949, Groundwater in White Valley, White Pine, Nye, and Lincoln counties, Nevada: Nevada State Engineer's Office, Water Resource Bulletin 8, 59 p.
- Maxey, G.B., 1968, Hydrogeology of desert basins: Groundwater v. 6, p. 1–22.

- Mazor, E., 1972, Paleotemperatures and other hydrological parameters deduced from noble gases dissolved in groundwaters, Jordan Rift Valley Israel: *Geochimica et Cosmochimica Acta*, v. 36, p. 1321–1336.
- McKee, J.W., Jones, N.W., and Long, L.E., 1984, History of recurrent activity along a major fault in northeastern Mexico: *Geology*, v. 12, p. 103–107.
- McKee, J.W., Jones, N.W., and Long, L.E., 1990, Stratigraphy and provenance of strata along the San Marcos fault, central Coahuila, Mexico: *Geological Society of America Bulletin*, v. 102, p. 593–614.
- Meyer, E.R., 1973, Late-Quaternary paleoecology of the Cuatro Ciénegas Basin, Coahuila, México: *Ecology*, v. 54, p. 982–995.
- Meyer, W.R., 1976, Digital model for simulated effects of ground-water pumping in the Hueco Bolson, El Paso area, Texas, New Mexico, and Mexico: U.S. Geological Survey Water Resources Investigation 58-75, 31 p.
- Miele, M.J., Jansen, J., Davila Arizpe, J.E., and Magallanes Mercado, M.A., 2000, A regional groundwater evaluation using magnetotelluric soundings for Monclova, Mexico: *In Proceedings of the Symposium on the Application of Geophysics to Environmental and Engineering Problems SAGEEP*, v. 2000, p. 699–708.
- Mifflin, M.D., 1988, Region 5, Great Basin, *in* Back, W., Rosenschein, J.S., and Seaber, P.R., eds., *Hydrogeology, The Geology of North America: Geological Society of America, Decade of North American Geology*, v. O-2, p. 69–78.
- Miller, R.R., 1961, Man and the changing fish fauna of the American Southwest: *Papers of the Michigan Academy of Science, Arts and Letters* v. 46, p. 365–404.
- Miller, N., 2008, Personal Communication, Austin, Texas.
- Minckley, W.L., 1962, Two new species of fishes of the genus *Gambusia* (Poeciliidae) from Northeastern Mexico: *Copeia*, v. 1962, p. 391–396.
- Minckley, W.L., and Cole, G.A., 1968, Preliminary limnologic information on waters of the Cuatrociénegas Basin, Coahuila, Mexico: *The Southwestern Naturalist*, v. 13, p. 421–431.
- Minckley, W.L., 1969, Environments of the Bolson of Cuatrociénegas, Coahuila, Mexico, with special reference to the aquatic biota: *The University of Texas at El Paso Science Series*, v. 2, p. 1–65.
- Minckley, W.L., 1992, Three decades near Cuatro Ciénegas, México: photographic documentation and a plea for area conservation: *Proceedings of the Arizona-Nevada Academy of Science*, v. 26, p. 89–119.
- Mitra, S., and Mount, V.S., 1998, Foreland basement-involved structures: *American Association of Petroleum Geologists Bulletin*, v. 82, p. 70–109.
- Mitra, S., 2002, Structural models of faulted detachment folds: *American Association of Petroleum Geologists Bulletin*, v. 86, p. 1673–1694.

- Murillo, G., 1997, Sequence stratigraphy and diagenesis of the lower Cretaceous Cupido carbonate platform margin, northeastern Mexico: American Association of Petroleum Geologists Foundation Grants-In-Aid Abstracts, v. 81, p. 1779.
- Münnich, K.O., 1957, Messungen des C 14 gehaltes von hartem grundwasser: Naturwissenschaften, v. 44, p. 32–33.
- Musgrove, M., Banner, J.L., Mack, L.E., Combs, D.M., James, E.W., Cheng, H., Edwards, R.L., 2001, Geochronology of late Pleistocene to Holocene speleothems from central Texas: implications for regional paleoclimate, Bulletin of the Geological Society of America, v. 113, p. 1532–1543.
- National Atmospheric Deposition Program, 2008, NADP/NTN Monitoring Location TX04 [Online] <http://nadp.sws.uiuc.edu/sites/siteinfo.asp?net=NTN&id=TX04> [accessed on March 9 2008].
- Nettleton, L.L., 1971, Elementary gravity and magnetics for geologists and seismologists: Society of Exploration Geophysicists Geophysical Monograph Series, no. 1, 121 p.
- Nielson, P.D., and J.M. Sharp, Jr., 1985, Tectonic controls on the hydrogeology of the Salt Basin, Trans-Pecos, Texas, in Dickerson, P.W. and Muehlberger, W.R., eds., Structure and Tectonics of Trans-Pecos Texas: West Texas Geological Society Publication 85-81, p. 231–234.
- Northwest Geophysical Associates, Inc., 2004, GM-SYS Gravity/Magnetic modeling software user's guide: Northwest Geophysical Associates, Inc, Corvallis, Oregon, 101 p.
- Orion, 1977, Analytical Methods Guide: Cambridge, Massachusetts, Orion Research Incorporated.
- Ozima, M., and Podosek, F.A., 1983, Noble Gas Geochemistry: Cambridge, United Kingdom, Cambridge University Press, 367 p.
- Payne, B.R., 1972, Isotope hydrology: Advances in Hydroscience, v. 8, p. 95–138.
- Peter, G., Klopp, F.J., Carter, W.E., and Dewhurst, W.T., 1991, Absolute gravity reference sites in the United States: Geophysics: The Leading Edge of Exploration, v. 10, p. 43–45.
- Piechota, T., Timilsena, J., Tootle, G., and Hidalgo, H., 2004, The Western U.S. drought: how bad is it: EOS: Transactions of the American Geophysical Union, v. 85, p. 301–308.
- Piper, A.M., 1944, A graphic procedure in the geochemical interpretation of water analyses: Transactions, American Geophysical Union, v. 25, p. 914–923.
- Poole, J.C., McNeill, G.W., Langman, S.R., and Dennis, F., 1997, Analysis of noble gases in water using a quadrapole mass spectrometer in static mode: Applied Geochemistry, v. 12, p. 707–714.

- Reynolds, J.M., 1997, An introduction to applied and environmental geophysics: Chichester, United Kingdom, John Wiley and Sons, 796 p.
- Rodríguez, J.M., and Sánchez, J.A.V., 2000, Disponibilidad de recursos hídricos en el Cañon de las Calaveras como una alternativa de abastecimiento de agua para el municipio de Cuatrociénegas, Coahuila: Universidad Autónoma de Coahuila, Facultad de Ciencias Químicas, Departamento de Biotecnología, 12 p.
- Rodríguez, J.M., 2005, Personal Communication, Department Chairman, The Department of Geophysics and Geohydrology, Universidad Autónoma de Nuevo León, Monterrey.
- Rodríguez, A.A.A., Mijares, F.J.A., Ojeda, C.G., Morales, M.M., Hita, L.G., Zamarrón, G.H., Arellano, I.M., González, M.A.M., Flores, G.O., Almanza, P.G., Sánchez, R.L., López, J.L.P., Arzate, G.R., Fritz, P., and Espinoza, J.R., 2005a, Estudio hidrogeológico de los acuíferos el Hundido y Cuatrociénegas, Coahuila: Secretaría de Medio Ambiente y Recursos Naturales, Instituto Mexicano de Tecnología del Agua, Comisión Nacional del Agua, Instituto Nacional de Ecología, 292 p.
- Rodríguez, J.M., Souza, S.V., and Arriaga Diaz de Leon, L.E., 2005b, The overexploitation of the aquifer of the Hundido Valley and the corresponding ecological impact on the reserves of Cuatrociénegas Valley of Coahuila, Mexico, in Stevanović, Z., and Milanović, P., eds., Proceedings of the international conference and field seminars, Water resources and environmental problems in karst: International Association of Hydrogeologists, Belgrade, Serbia and Montenegro, p. 303–310.
- Rosas, I., Belmont, R., Armienta, A., Baez, A., 1999, Arsenic concentrations in water, soil, milk and forage in Comarca Lagunera, Mexico: Water, Air, and Soil Pollution, v. 112, p. 113–149.
- Salbu, B., and Steinnes, E., 1995. Trace elements in natural waters: Boca Raton, Florida, CRC Press, 302 p.
- Salem, O., Visser, J.H., Dray, M., and Gonfiantini, R., 1980, Environmental isotopes used in a hydrogeological study of north-eastern Brazil, in Arid-zone hydrology: investigations with isotope techniques: International Atomic Energy Agency, Vienna, p. 165–197.
- Sanford, W., 2002, Recharge and groundwater models: an overview: Hydrogeology Journal, v. 10, p. 110–120.
- Scanlon, B.R., and Goldsmith, R.S., 1997, Field study of spatial variability in unsaturated flow beneath and adjacent to playas: Water Resources Research, v. 33, p. 2239–2252.
- Scanlon, B.R., Langford, R.P., and Goldsmith, R.S., 1999, Relationship between geomorphic settings and unsaturated flow in an arid setting: Water Resources Research, v. 35, p. 983–999.

- Scanlon, B.R., Reedy, R.C., Tachovsky, J.A., 2007, Semiarid unsaturated zone chloride profiles: archives of past land use change impacts on water resources in the southern High Plains, United States: Water Resources Research, v. 43, p. W0643.1–W0643.23.
- Scholl, M.A., Ingebritsen, S.E., Janik, C.J., Kauahikaua, J.P., 1996, Use of precipitation and ground water isotopes to interpret regional hydrology on a tropical volcanic island: Kilauea volcano area, Hawaii: Water Resources Research, v. 32, p. 3525–3537.
- Secretaría de Medio Ambiente y Recursos Naturales (SEMARNAT). 2003. Diario Oficial de la Federación, Tomo DCII., no. 1, Mexico City, Mexico.
- Sehlke, G., and Jacobson, J., 2005, System dynamics modeling of transboundary systems: The Bear River Basin Model: Ground Water v. 43, p. 722–730.
- Sharp, J.M., Jr., 1989, Regional ground-water systems in northern Trans-Pecos Texas, in Dickerson, P.W., and Muehlberger, W.R., eds., Structure and stratigraphy of Trans-Pecos Texas: American Geophysical Union Field Trip Guidebook T317, p. 123–130.
- Sharp, J. M., Jr., 1998, Sustainable groundwater supplies—an evolving issue: examples from major carbonate aquifers of Texas, U.S.A., in Weaver, T.R., and Lawrence, C.R., eds., Groundwater — sustainable solutions: International Association of Hydrogeologists, Melbourne, Australia, p. 1–12.
- Shreve, F., 1944, Rainfall in northern Mexico: Ecology v. 25, p. 105–111.
- Snyder, C.T., 1962, A hydrologic classification of valleys in the Great Basin, western United States: Bulletin of the International Association of Scientific Hydrology, v. 7, p. 53–59.
- Solomon, K., 2000, ^4He in Groundwater, in Cook, P.G., and Herczeg, A.L., eds., Environmental tracers in subsurface hydrology: Dordrecht, The Netherlands, Kluwer Academic Publishers, 529 p.
- Solomon, K., and Cook, P.G., 2000, ^3H and ^4He , in Cook, P.G., and Herczeg, A.L., eds., Environmental tracers in subsurface hydrology: Dordrecht, The Netherlands, Kluwer Academic Publishers, 529 p.
- Sorooshian, S., Hsu, K.L., Gao, X., Gupta, H.V., Imam, B., and Braithwaite, D., 2000, Evaluation of PERSIANN system satellite-based estimates of tropical rainfall: Bulletin of the American Meteorological Society, v. 81, p. 2035–2046.
- Stute, M., Schlosser, P., Clark, J.F., and Broecker, W.S., 1992, Paleotemperatures in Southwestern United States derived from noble gases in ground water: Science, v. 256, p. 1000–1001.
- Stute, M., and Schlosser, P., 1993, Principles and applications of the noble gas paleothermometer, in Swart, P.K., Lohmann, K.C., McKenzie, J.A., and Savin, S.,

- eds., Climate change in continental isotopic records: American Geophysical Union, Geophysical Monograph, v. 78, p. 89–100
- Stute, M., and Schlosser, P., 2000, Atmospheric Noble Gases, *in* Cook, P.G., and Herczeg, A.L., eds., Environmental tracers in subsurface hydrology: Dordrecht, The Netherlands, Kluwer Academic Publishers, 529 p.
- Talwani, M., Worzel, J.L., and Landisman, M, 1959, Rapid gravity computations for two-dimensional bodies with application to the Mendocino Submarine Fracture Zone: *Journal of Geophysical Research*, v. 64, p. 49–59.
- Tamers, M.A., 1975, Validity of radiocarbon dates on ground water: *Geophysical Surveys*, v. 2, p. 217–239.
- Tarboton, D. G., 1997, A new method for the determination of flow directions and upslope areas in grid digital elevation models: *Water Resources Research*, v. 33, p. 309–319.
- Telford, W.M., Geldart, L.P., and Sheriff, R.E., 1990, Applied geophysics: Cambridge, United Kingdom, Cambridge University Press, 770 p.
- Tidwell, V.C., Passell, H.D., Conrad, S.H., and Thomas, R.P., 2004, System dynamics modeling for community-based planning: Application to the Middle Rio Grande: *Aquatic Sciences*, v. 66, p. 357–372.
- Tóth, J.A. 1963, A theoretical analysis of ground-water flow in small drainage basins: *Journal of Geophysical Research*, v. 68, p. 4795–4811.
- Tyler, S.W., Chapman, J.B., Conrad, S.H., Hammermeister, D.P., Blout, D.O., Miller, J.J., Sully, M.J. and Gianni, J.M., 1996, Soil-water flux in the southern Great Basin, United States; temporal and spatial variations over the last 120,000 years: *Water Resources Research*, v. 32, p. 1481–1499.
- Uliana, M.M., 2000, Delineation of regional groundwater flow paths and their relation to structural features in the Salt and Toyah Basins, Trans-Pecos, Texas [Ph.D. dissertation]: The University of Texas at Austin, 215 p.
- Uliana, M. M., and Sharp, J.M., Jr., 2001, Tracing regional flow paths to major springs in Trans-Pecos Texas using geochemical data and geochemical models: *Chemical Geology*, v. 179, p. 53–72.
- University of Utah Dissolved Gas Laboratory (2008), Service and pricing list [Online] <http://www.insec.utah.edu/~ksolomon/> [accessed on May 15, 2008].
- Van Broekhoven, N.G., 2002, Recharge in a semi-arid basin aquifer: Ryan Flat and Lobo Flat, Trans-Pecos, Texas [M.S. thesis] The University of Texas at Austin, 257 p.
- Veni, G., 2005, Declaration of Dr. George Veni: United States District Court for the Western District of Texas, San Antonio Division, no. Civ. SA-05-CA-1170-XR, 15 p.

- Vivó Escoto, J.A., 1964, Weather and climate of Mexico and Central America, in West, R.C., ed., *Handbook of Middle American Indians*: University of Texas Press, Austin, v. I, p. 187–215.
- Von Frese, R.R.B., Hinze, W.J., Braile, L.W., and Luca, A.J., 1981, Spherical-earth gravity and magnetic anomaly modeling by Gauss-Legendre quadrature integration: *Journal of Geophysics — Zeitschrift fuer Geophysik*, v. 49, p. 234–242.
- Webb, R.G., Minckley, W.L., and Craddock, J.E., 1963, Remarks on the Coahuilan Box turtle, *Terrapene coahuila* (Testudines, Emydidae): *The Southwestern Naturalist*, v. 8, p. 89–99.
- Wilson, C.R., 2005, Personal Communication, Austin, Texas.
- Wilkes, S.M., Clement, T.P. and Otto, C.J., 2004, Characterization of the hydrogeology of the Augustus River catchment, Western Australia: *Hydrogeology Journal*, v. 12, p. 209–223.
- Winograd, I.J., and Thordarson, W., 1975, Hydrologic and hydrogeochemical framework, south-central Great Basin, Nevada-California, with special reference to the Nevada Test Sites: U.S. Geological Survey Professional Paper 712-C, 126 p.
- Winograd, I.J. and Pearson, F.J., Jr., 1976, Major carbon-14 anomaly in a regional carbonate aquifer: Possible evidence for megascale channeling, South Central Great Basin: *Water Resources Research*, v. 12, p. 1125–1143.
- Winsborough, B.M., and Golubić, S., 1987, The role of diatoms in stromatolites growth: two examples from modern freshwater settings: *Journal of Phycology*, v. 23, p. 195–201.
- Winsborough, B.M., 1990, Some ecological aspects of modern fresh-water stromatolites in lakes and streams of the Cuatrocienegas Basin, Coahuila, Mexico [Ph.D. dissertation]: The University of Texas at Austin, 341 p.
- Wolaver, B.D., Banner, J.L., and Sharp, J.M. Jr., 2005, Groundwater recharge in the Cuatrocienegas Basin, Mexico: Insights from strontium isotope and trace element analyses: *Geological Society of America Abstract with Programs*, v. 37, p. 361.
- Wolaver, B.D., 2007, Ground water recharge evaluation in semi-arid northeast Mexico in response to projected climate change: *EOS*, v. 88, p. 52.
- Wolaver, B.D., and Sharp, J.M., Jr., 2007, Thermochron iButton: limitation of this inexpensive and small-diameter temperature logger: *Ground Water Monitoring and Remediation*, v. 27, p. 127–128.
- Wolaver, B.D., and Diehl, T.M., 2008, Using Gravity Geophysics to Characterize Geologic Controls on Arid Karst Aquifer Spring Locations: *Environmental Geology (in preparation)*.

- Wolaver, B.D., Sharp, J.M., Jr., Rodríguez, J.M., and Ibarra Flores, J.C., 2008, Delineation of regional arid karstic aquifers: an integrative data approach: *Ground Water*, v. 46, p. 396–413.
- Wolaver, B.D., and Tidwell, V.C., 2008, GIS based chloride balance modeling to evaluate recharge areas and understand differences in spring discharge, chloride concentration, and temperature in an arid karst aquifer: *Hydrogeology Journal* (*in preparation*).
- Wolaver, B.D., Sharp, J.M., Jr., Banner, J.L., 2009, Using tritium, oxygen isotopes, noble gases, and strontium isotopes to evaluate residence time and recharge processes in an arid karst aquifer: *Hydrogeology Journal* (*in preparation*).
- Wood, W.W., 1999, Use and misuse of the chloride-mass balance method in estimating ground water recharge: *Ground Water*, v. 37, p. 2–3
- Zhu, C., and Lettenmaier, D.P., 2007, Long-term climate and derived surface hydrology and energy flux data for Mexico: 1925–2004: *Journal of Climate*, v. 20, p. 1936–1946.

Vita

Brad David Wolaver was born in Boston, Massachusetts at the Boston Lying-In Hospital on November 6, 1972 to Peggy Schmitt Wolaver and John Anthony Wolaver. I spent my first 10 years learning geology on the trails of the Town of Weston Conservation land (see the Weston Forest & Trail Association at www.westonforesttrail.org) behind my house — a former dairy farm that my parents rebuild over a period of five years. My early outdoor rambles also included hikes in the Presidential Range in New Hampshire with my father (see the Appalachian Mountain Club at www.outdoors.org), and walking the coast at my grandparents house near Cundy's Harbor, Maine (where the Trust for Public Land has preserved nearby property).

In 1983, a family move brought me to Austin, Texas where I continued my outdoor exploration in the Barton Creek Greenbelt. I graduated from Westlake High School in 1990. After starting school at The University of Texas at Austin, I spent a summer in Yellowstone National Park in 1991 scooping ice cream and serving coffee to tourists with a huge window looking out at the Old Faithful geyser! I spent every weekend hiking the trails of Yellowstone and Grand Teton National Parks. That summer in Yellowstone cemented my decision to pursue a geology degree at The University of Texas at Austin, where I received a B.S. in Geology in 1995. In the summer of 1992, I served as an intern at the Geophysical Institute at the University of Alaska, Fairbanks working under Dr. Max Wyss on earthquake prediction methods. During the spring of 1993, I participated on a marine geology and geophysics research cruise to Antarctica with Dr. Lawrence Lawver of The University of Texas at Austin Institute for Geophysics. After the cruise, I spent about two weeks in Chile and Argentina, where I fell in love with the Andes. This trip initiated my desire to work in Latin America.

After graduation from The University of Texas, I worked for a year as a geophysical survey assistant for Western Geophysical (now WesternGeco) about 125 miles offshore of Louisiana. One seismic survey was done in the vicinity of British Petroleum's highly successful Gulf of Mexico Thunder Horse platform. On another survey, I served as the informal Spanish translator for a PEMEX project off of the City of Coatzacoalcos, Veracruz, Mexico. In July 1996, I moved to Santiago, Chile as a Fulbright Scholar, where I started my M.S. research in alpine snow hydrology in the Chilean Andes collaborating with government hydrologists from the Ministerio de Obras Públicas. I completed this research project at the Department of Hydrology and Water Resources at The University of Arizona, where I was awarded a M.S. in Hydrology and Water Resources under Dr. Roger Bales in 1999. I also participated in the Entrepreneurship Program of the Eller School of Management, developing a business plan for a water resource management company I eventually want to found.

After moving from Tucson, Arizona, I worked five years in Southern California, where I am a Registered Geologist (no. 7494). From 1999–2002, I worked with Montgomery Watson Harza, Inc. in Pasadena. From 2002–2004, I was hydrogeologist at Geoscience Support Services, Inc. of Claremont with Dr. Dennis Williams (also a professor at The University of Southern California). I first visited Cuatrociénegas in January 2004. I started this Ph.D. under Dr. John M. Sharp, Jr. in August 2004.

I will start a three-year appointment as a Research Fellow at Flinders University in Adelaide, Australia in late October, 2008. I will collaborate with Dr. Andrew Love, Dr. Craig Simmons, and others on an aquifer management project for the Great Artesian Basin — an aquifer that covers 20 percent of Australia. In particular, we will evaluate South Australian Great Artesian Basin spring hydrogeology in the context of allocating water for people while maintaining spring discharge. I look forward to you visiting!

A common theme throughout my life has been the importance of both formal and informal outdoor education. I encourage you to donate your time and money to actively conserve land in your home town, write your state legislators to fund State parks, and demand that Congress continue to fund and set aside wild spaces at a national level so future generations can learn from and study nature.

Brad Wolaver's permanent address and contact information is

1731 Spyglass Drive, No. 75, Austin, Texas 78746,

wolaver.brad@gmail.com , and

brad_wolaver@yahoo.com .

This dissertation was typed by Brad David Wolaver.